1521-0081/68/3/701–787$25.00
PHARMACOLOGICAL REVIEWS

http://dx.doi.org/10.1124/pr.115.012070
Pharmacol Rev 68:701–787, July 2016

ASSOCIATE EDITOR: ERIC L. BARKER

# Lipid-Based Drug Delivery Systems in Cancer Therapy: What Is Available and What Is Yet to Come

Phatsapong Yingchoncharoen, Danuta S. Kalinowski, and Des R. Richardson

*Molecular Pharmacology and Pathology Program, Department of Pathology, Faculty of Medicine, Bosch Institute, The University of Sydney, Sydney, NSW, Australia*



Des R. Richardson is the recipient of a National Health and Medical Research Council (NHMRC) Senior Principal Research Fellowship [1062607] and Project Grant [1060482]. Danuta S. Kalinowski is the recipient of an NHMRC RD Wright Career Development Fellowship [1083057] and NHMRC Project Grant [1048972].

**Address correspondence to:** Dr. Des R. Richardson, Molecular Pharmacology and Pathology Program, Department of Pathology and Bosch Institute, The University of Sydney, Blackburn Building D06, Sydney, NSW 2006, Australia. E-mail: d.richardson@med.usyd.edu.au
dx.doi.org/10.1124/pr.115.012070.

**ABBREVIATIONS:** ABV, doxorubicin, bleomycin, and vincristine; AUC, area under the curve; $A_v/A_p$ ratio, lipid vesicle to polymeric nanoparticle ratio; CHEMS, 3$\beta$-hydroxy-5-cholestene 3-hemisuccinate; CMC, critical micelle concentration; cryo-TEM, cryo-transmission electron microscope; CSF, cerebrospinal fluid; DC-cholesterol, 3$\beta$-[*N*-(*N*′,*N*′-dimethylaminoethane)-carbomoyl] cholesterol; DOPC, 1,2-dioleoyl-*sn*-glycero-3-phosphocholine; DOPE, 1,2-dioleoyl-*sn*-glycero-3-phosphoethanolamine; DOTAP, dioleoyl-trimethylammonium propane; DOX, doxorubicin; DOX-NLC, doxorubicin encapsulated nanostructured lipid carrier; DPPC, 1,2-dipalmitoyl phosphatidylcholine; DPPE, dipalmitoyl phosphoethanolamine; DSPC, 1,2-distearoyl-*sn*-glycerol-3-phosphocholine; DSPE, 1,2-distearoyl-*sn*-glycerol-3-phosphoethanolamine; DSPE-$PEG_{2000Da}$, 1,2-distearoyl-*sn*-glycerol-3-phosphoethanolamine-*N*-[methoxy(polyethylene glycol)-2000]; DTX, docetaxel; DTX-NLC, docetaxel encapsulated nanostructured lipid carrier; EGFR, epidermal growth factor receptor; EMA, European Medicines Agency; EPR, enhanced permeability and retention; ESE, emulsification-solvent-evaporation; FDA, U.S. Food and Drug Administration; FITC, fluorescein isothiocyanate; HA-NLC, hyaluronic acid coated nanostructured lipid carrier; HCPT, 10-hydroxycamptothecin; HCPT-NLC, 10-hydroxycamptothecin encapsulated nanostructured lipid carrier; HIFU, high-intensity focused ultrasound; KSP, kinesin spindle protein; LCST, low critical solution temperature; LFUS, low-frequency ultrasound; LLC, Lewis lung carcinoma; L/P ratio, lipid-to-polymer mass ratio; LPN, lipid-polymer hybrid nanoparticle; LUV, large unilamellar vesicle; MDR, multidrug resistant; MLV, multilamellar vesicle; MMP, matrix metalloproteinase; MMP-2, matrix metalloproteinase-2; MMP-9, matrix metalloproteinase-9; MPPC, 1-palmitoyl-2-hydroxy-*sn*-glycero-3-phosphocholine; MR-HIFU, magnetic resonance guided high-intensity focused ultrasound; MSPC, 1-steroyl-2-hydroxy-*sn*-glycero-3-phosphocholine; MT1-MMP, membrane type 1 matrix metalloproteinase; MTD, maximum tolerated dose; MVL, multivesicular liposome; NGR, Asn-Gly-Arg; NLC, nanostructured lipid carrier; NM, neoplastic meningitis; NTA, nitrilotriacetic acid; o/w, oil-in-water; OLV-DOX, egg-derived phosphatidylcholine/egg-derived phosphatidylglycerol/cholesterol liposomal doxorubicin formulation; PC, phosphatidylcholine; PDT, photodynamic therapy; PE, phosphatidylethanolamine; PEG, polyethylene glycol; PEG-DTP-DSPE, PEG-$\alpha$-aminocarbonylethyl-dithiopropionyl-DSPE; PEG-PE, polyethylene glycol-phosphatidylethanolamine conjugate; PG, phosphatidylglycerol; PI, phosphatidylinositol; PLGA, poly(lactic-*co*-glycolic acid); PPE, palmar plantar erythrodysthesia; PS, phosphatidylserine; PTT, phase transition temperature; PTX, Paclitaxel; PTX-NLC, paclitaxel encapsulated nanostructured lipid carrier; RES, reticuloendothelial system; Rf, Flory dimension; RGD, Arg-Gly-Asp; SLN, solid lipid nanoparticle; SUV, small unilamellar vesicle; TATp, transactivator of transcription peptide; Tf, transferrin; TfR, transferrin receptor; ULV, unilamellar vesicle; VCAM-1, vascular cell adhesion molecule-1; VEGF, vascular endothelial growth factor; w/o, water-in-oil; w/o/w, water-in-oil-in-water.

*Abstract*——**Cancer is a leading cause of death in many countries around the world. However, the efficacy of current standard treatments for a variety of cancers is suboptimal. First, most cancer treatments lack specificity, meaning that these treatments affect both cancer cells and their normal counterparts. Second, many anticancer agents are highly toxic, and thus, limit their use in treatment. Third, a number of cytotoxic chemotherapeutics are highly hydrophobic, which limits their utility in cancer therapy. Finally,**

**many chemotherapeutic agents exhibit short half-lives that curtail their efficacy. As a result of these deficiencies, many current treatments lead to side effects, noncompliance, and patient inconvenience due to difficulties in administration. However, the application of nanotechnology has led to the development of effective nanosized drug delivery systems known commonly as nanoparticles. Among these delivery systems, lipid-based nanoparticles, particularly liposomes, have shown to be quite effective at exhibiting the ability to: 1) improve the selectivity of cancer chemotherapeutic agents; 2) lower the cytotoxicity of anticancer drugs to normal tissues, and thus, reduce their toxic side effects; 3) increase the solubility of hydrophobic drugs; and 4) offer a prolonged and controlled release of agents. This review will discuss the current state of lipid-based nanoparticle research, including the development of liposomes for cancer therapy, different strategies for tumor targeting, liposomal formulation of various anticancer drugs that are commercially available, recent progress in liposome technology for the treatment of cancer, and the next generation of lipid-based nanoparticles.**

## I. Introduction

The application of nanotechnology in cancer, also known as Cancer Nanotechnology, is an emerging field of research involving collaborations between various disciplines, including biology, chemistry, engineering, and medicine. Its main goal is to develop novel technologies for more advanced cancer detection, diagnosis, and treatment (Srinivas et al., 2002; Ferrari, 2005; Nie et al., 2007; Wang et al., 2007b; Wang and Thanou, 2010). The field has gained a strong support over the years because of its potential as a solution for improving cancer therapy.

The second half of the last century was characterized by a tremendous advancement in the pharmaceutical industry, with much attention being given to the development of biopharmaceutics and enhanced pharmacokinetics (Kreuter, 2007). As a result, the idea of a controlled and targeted drug delivery system was introduced for the first time. With nanotechnology becoming more involved in the medicinal field, such a delivery system was made possible in the form of submicron particles called nanoparticles (also known as nanocarriers or nanospheres) (Kreuter, 2007). Typically, nanoparticles are found in a size range between 100 to 1000 nm, are often composed of different matrix materials, and have varying surface characteristics as well as mechanical and physicochemical properties. The application of nanoparticles in drug therapy has been increasingly studied in various diseases. However, many studies have focused on the use of nanoparticles in the field of oncology. This is because nanoparticles can be designed to be highly selective for tumors and allow a slow release of active anticancer agents, both of which reduce systemic toxicity and improve the distribution and circulation time of these agents in the body.

Among the available colloidal drug delivery systems, nanoparticles prepared from natural polymers, such as phospholipids, polysaccharides, proteins, and peptides, represent the most promising formulations. Such systems were proven to be more efficient than synthetic polymers in terms of better drug loading capacity, biocompatibility, and generate less opsonization by the reticuloendothelial system (Liu et al., 2008). Moreover, natural polymers have been proven to be more advantageous than synthetic polymers, because they are readily absorbed by the human body as well as producing less toxic end products after degradation (Vandelli et al., 2001; Sahin et al., 2002). Therefore, nanoparticles prepared from naturally occurring polymers may represent the most suitable colloidal drug delivery systems for human use, because they are relatively safe and can be prepared efficiently (Rubino et al., 1993; Langer et al., 2003; Kommareddy and Amiji, 2005; Azarmi et al., 2006).

Liposomes, initially known as spherules, are spherical lipid vesicles with a bilayered structure composed of phospholipids (Gregoriadis, 1976a; Sharma and Sharma, 1997; Torchilin, 2005; Wacker, 2013). They were one of the first nanosized drug delivery systems ever to be produced and also represent the first generation of lipid-based nanoparticle drug carriers. The long history of these particles started in 1965 when Alec D. Bangham and his colleagues published a paper on liquid crystals of lecithin (Bangham et al., 1965). It was demonstrated for the first time that univalent cations and anions were able to diffuse out of spontaneously formed liquid crystals of lecithin in a similar manner as the diffusion of ions across a biologic membrane (Bangham et al., 1965). The ability of these lecithin liquid crystals or spherules (later called liposomes) to encapsulate solutes and selectively release them made such systems a suitable model for cell membrane studies. This finding led to numerous investigations in cell membrane physiology, including its structure and function (Sessa and Weissmann, 1968; Bangham et al., 1974; Klausner et al., 1980). Apart from their use in cellular membrane research, the ability of these liquid crystals to encapsulate solutes also formed the basis of liposomal drug delivery systems. This concept was first explored by Gregoriadis and colleagues (Gregoriadis, 1976a,b, 1995) when they demonstrated the potential use of liposomes for the delivery of enzymes and anticancer and antimicrobial drugs to cells and tissues. Since these initial studies, liposomes have emerged as an attractive drug carrier system that could potentially improve the treatment of disease.

In cancer therapy, liposomes have been demonstrated to be particularly useful. This is because liposomes are capable of reducing the toxic side effects of chemotherapeutic agents while enhancing their antitumor efficacy. Generally, antitumor chemotherapeutics are quite toxic to both cancer and normal cells, which represent a

major problem as their use can be limited by their toxicity. However, by implementing different strategies, such as passive and active targeting (Table 1), the incorporation of chemotherapeutic agents into liposomes can help improve their specificity to cancer cells and tumor tissue. Consequently, the unwanted side-effects of anticancer drugs toward normal cells and tissues can be minimized, whereas the increased accumulation of liposomes within tumors results in enhanced anticancer efficacy. Furthermore, because many chemotherapeutics require a certain concentration to be efficacious, the clearance of these molecules by the immune system and by bodily excretion can limit their bioavailibility and activity. Liposomal encapsulation can help reduce drug clearance by the immune and renal systems, and thus, extend the circulation time of anticancer drugs and increase their availability to the tumor. Additionally, due to the amphiphilic properties of phospholipids, liposomes are considered to be a versatile drug carrier that can encapsulate both hydrophobic and hydrophilic drugs, improving their solubility and stability. The encapsulation of lipophilic anticancer drugs (e.g., anthracyclines; Fig. 1, A and B) can be achieved by the hydrophobic interaction of these molecules with the liposomal lipid membrane bilayer (Allen, 1998) or by active loading (Gubernator, 2011). In contrast, the encapsulation of hydrophilic chemotherapeutics (e.g., cytarabine; Fig. 1, A and B) can be achieved by entrapping these drugs within the aqueous interior of the liposome (Allen, 1998). A number of existing chemotherapeutics have been incorporated into liposomal formulations. The chemical structures of these chemotherapeutics and a summary of their log *P* and indications are shown in Fig. 1.

Over the past few years, a number of liposomal chemotherapeutic formulations have been approved by the European Medicines Agency (EMA) and the U.S. Food and Drug Administration (FDA) for the treatment of various cancers because of the positive outcomes observed during clinical studies. These formulations include Doxil (Johnson & Johnson, Piscataway, NJ) (Gabizon et al., 2003b), Myocet (Teva Pharmaceutical Industries Limited, Petah Tikva, Israel) (Swenson et al., 2001), DaunoXome (Galen Limited, Craigavon, U.K.) (Forssen, 1997), Marqibo (Spectrum Pharmaceuticals, Henderson, NV) (Silverman and Deitcher, 2013), and DepoCyt (Sigma-Tau Pharmaceuticals, Gaithersburg, MD) (Angst and Drover, 2006). Moreover, there are several other anticancer drug encapsulated liposome formulations currently undergoing different stages of clinical trials (Tables 2–4) or awaiting approval. The growing number of liposomal drug formulations available represents the enormous potential for the application of lipid-based nanoparticles in the treatment of cancer. This is further evident by the recent development of different types of liposome technology, such as pH-sensitive liposomes, temperature-sensitive liposomes, magnetic liposomes, multifunctional liposomes, etc. Innovations in liposome technology have also seen the emergence of the next generation of lipid-based nanoparticles, including solid lipid nanoparticles, nanostructured lipid carriers, and lipid-polymer hybrid nanoparticles, which will hopefully overcome current drawbacks presented by liposomes.

In this review, various liposomal characteristics and types will be discussed, including their methods of preparation. Additionally, important properties of lipid-based nanoparticles for cancer treatment, their routes of cellular uptake, fate within the body, and their toxicity will be reviewed. Moreover, various strategies for tumor targeting, different types of stimuli-sensitive liposomes for cancer therapy, and the next generation of lipid-based nanoparticles drug delivery systems will be discussed.

## II. Liposomal Drug Delivery Systems

### *A. Liposome Composition*

Liposomes are composed mainly of natural and/or synthetic phospho- and sphingo-lipids with other membrane bilayer constituents, such as cholesterol and hydrophilic polymer conjugated lipids positioned randomly around each liposomal vesicle (Sharma and Sharma, 1997). Phosphatidylcholine (PC; also known as lecithin) and phosphatidylethanolamine (PE) are the most common phospholipid found in both plants and animals and constitute the major structural parts of biologic membranes (Vemuri and Rhodes, 1995). In contrast, the membranes of liposomes and other lipid-based drug delivery systems consist mostly of PC with little PE present (Vemuri and Rhodes, 1995). This is because PE has the ability to form nonbilayer structures under physiologic conditions, destabilize membranes, and induce membrane fusion (Ellens et al., 1986). Other phospholipids, such as phosphatidylserine (PS), phosphatidylglycerol (PG), and phosphatidylinositol (PI), can also be used in the preparation of liposomes, depending on the desired liposomal characteristics (Vemuri and Rhodes, 1995).

Cholesterol is also an important component in the preparation of liposomes. Once it is incorporated into the liposomal membrane bilayer, cholesterol arranges itself among the phospholipid molecules with its hydroxyl group facing toward the water phase, whereas its tetracyclic ring inserts itself between the first few carbons of the fatty acyl chains into the hydrocarbon core of the membrane bilayer (Vemuri and Rhodes, 1995). The incorporation of cholesterol into liposomes helps to decrease the fluidity of the liposomal membrane bilayer, reduce the permeability of water soluble molecules through the liposomal membrane, and improve the stability of the liposomal membrane in biologic fluids, such as blood and plasma (Vemuri and Rhodes, 1995). In the absence of cholesterol, liposomes often interact with blood proteins, such as albumin,

TABLE 1
Specific cell surface moieties targeted by lipid-based drug delivery systems for use in cancer therapy

| Specific Cell Surface Moieties | Targeting Ligands | Cancer Types | Competing Tissues (in order of high to low accumulation) | Comments | Reference |
|---|---|---|---|---|---|
| Transferrin receptor (TfR) | Holo-transferrin (Tf) | Hepatocellular carcinoma (HepG2) | Liver > spleen > tumor > lung > kidney > heart | In vitro, at the equivalent dose of DOX, the $IC_{50}$ of Tf-liposomes was significantly lower than that of PEG-liposomes and free DOX.<br>In vivo, the average tumor weights were: 0.33, 1.17, and 1.38 g for Tf-liposomes, PEG-liposomes, and free DOX, respectively. Tumor AUC after 96 hours was Tf-liposomes > PEG-liposomes > free DOX. | Li et al. (2009) |
| | Transferrin | Human small cell lung cancer (SBC-3) and its DOX-resistant variant (SBC-3/ADM) | n/a | In vitro, using SBC-3 cells, DOX accumulation after 90 min was ~3-fold higher for Tf-liposomes than conventional liposomes. The $IC_{50}$ was lower for Tf-liposomes compared with conventional liposomes and free DOX.<br>Furthermore, using the SBC-3/ADM cell line, the DOX accumulation after 90 min was ~2.5-fold higher for Tf-liposomes than conventional liposomes. The $IC_{50}$ was lower for Tf-liposomes compared with conventional liposomes and free DOX. | Kobayashi et al. (2007) |
| | Murine IgG1 antihuman TfR scFv (5E9) compared with transferrin | Human head and neck cancer (JSQ-3), human breast cancer (MDA-MB-435), human lung cancer (H358), human liver cancer (Hep3B), and human prostate cancer (DU145) | n/a | In vitro, higher transfection of either luciferase or $\beta$-gal was achieved when TfR scFv-liposomes were used in comparison with conventional liposomes or Tf-liposomes in all cancer cell lines, but not in normal human fibroblast cells.<br>In vivo, higher expression of *p53* was observed when it was delivered by TfR scFv-liposomes compared with nontargeted liposomes. The coadministration of either TfR scFv-liposomes-p53 or Tf-liposome-p53 with DTX into mice bearing tumors resulted in improved antitumor effects and survival time than a nontargeted liposomal formulation with DTX. | Xu et al. (2001, 2002) |
| | Holo-transferrin (Tf) | Human gastric cancer (MKN45P) | Spleen > liver > tumor > kidney | In vivo, the levels of cisplatin in tumor cells increased significantly when treated with Tf-PEG-liposomes compared to nontargeted liposomes, and free cisplatin. The treatment of mice bearing tumor xenografts with TfR-targeted formulation significantly prolonged the survival time of these animals compared to nontargeted liposomes, and free cisplatin. | Iinuma et al. (2002) |
| Folate receptor (FR) | Folate (F) | Murine lung carcinoma (M109-HiFR) and its multi-drug resistant variant (M109R-HiFR) | n/a | In vitro, the level of DOX in M109R-HiFR cells was 4- to 6-fold greater when treated with F-liposomal DOX compared with free DOX. The $IC_{50}$ of F-liposomal DOX was comparable to free DOX, which were both lower than Doxil.<br>In vivo, the incidence of tumor growth in mice bearing M109R-HiFR tumors was much lower when treated with F-liposomal DOX (10%) compared with Doxil (53%) or free DOX (42%). The tumor weights after treatment with F-liposomes, Doxil, and free DOX were 57, 397, and 239 mg, respectively. | Goren et al. (2000) |
| | F | Mouse lymphoma expressing FR (J6456-FR) | n/a | In vitro, F-liposomes demonstrated a 50- to 70-fold increase in cell-associated fluorescence compared with nontargeted liposomes.<br>In vivo, the DOX level in J6456-FR tumors was 17-fold higher for F-liposomes compared with PEG-liposomes. The DOX level was also lower in ascitic | Shmeeda et al. (2006) |

(*continued*)

TABLE 1—*Continued*

| Specific Cell Surface Moieties | Targeting Ligands | Cancer Types | Competing Tissues (in order of high to low accumulation) | Comments | Reference |
|---|---|---|---|---|---|
| | | | | fluid (~2.25-fold) and plasma fluid (14-fold) when DOX was delivered by F-liposomes compared to PEG-liposomes. | |
| | F | Human squamous cell oral carcinoma (KB) | n/a | In vivo, the circulation time of F-PEG-liposomal DOX ≈ PEG-liposomal DOX >> free DOX. Treatment with F-PEG-liposomal DOX showed a significantly higher tumor growth inhibition and greater increase in lifespan of mice bearing tumor xenografts than PEG-liposomal DOX or free DOX. | Pan et al. (2003) |
| | F | Human squamous cell oral carcinoma (KB) | n/a | In vitro, F-PEG-liposomal ursolic acid (UA) showed ~3-fold lower $IC_{50}$ and higher apoptosis than PEG-liposomal UA.<br>In vivo, F-PEG-liposomal UA exhibited greater AUC and half-life than free UA by 6-fold and 9.8-fold, respectively. F-PEG-liposomal UA reduced tumor volume by 55% compared with the control. Animal lifespan was 56, 47, and 42 days for F-PEG-liposomal UA, PEG-liposomal UA, or free UA, respectively. | Yang et al. (2014b) |
| | F | Murine lung carcinoma (M109), human oral carcinoma (KB), and mouse lymphoma (J6456) | Empty: liver > tumor > spleen<br>DOX loaded: spleen > tumor > liver | For empty liposomes, F-PEG- and PEG-liposomes demonstrated similar tumor localization. However, the liver uptake of FR-targeting liposomes was significantly higher than nontargeted liposomes.<br>For DOX loaded liposomes, the liver uptake of both formulations decreased, whereas the spleen uptake increased. The uptake of F-PEG-liposomes by these two organs was higher than nontargeted liposomes. Tumor localization of F-PEG-liposomes increased, but was not significant. | Gabizon et al. (2003a) |
| CD44 receptor | Hyaluronic acid (HA) | Mouse colon carcinoma (C-26), mouse melanoma (B16F10.9), highly metastatic Lewis lung carcinoma (D122), human adenocarcinoma (PANC-1) | Tumor > liver > spleen > kidney | In vitro, the $IC_{50}$ of mitomycin C (MMC) against cancer cells expressing HA receptors was 50- to 200-fold lower when delivered by HA-liposomes compared with nontargeted liposomes or free MMC. A high $IC_{50}$ was observed in cells lacking HA receptors, suggesting low cytotoxicity.<br>In vivo, significantly higher accumulation of MMC in tumors occurred when delivered by HA-liposomes (20%) compared to nontargeted liposomes (4%), or free MMC (0.6%). HA-liposomal MMC significantly reduced tumor growth and prolonged the lifespan of mice bearing tumor xenografts compared with a nontargeted formulation and free MMC. | Peer and Margalit (2004a) |
| | HA | Mouse melanoma (B16F10.9), DOX-resistant murine leukemia (P388/ADR), mouse colon carcinoma (C-26), human adenocarcinoma (PANC-1) | Liver > tumor > spleen > kidney | In vivo, the order of DOX tumor accumulation was HA-liposomes > Doxil > nontargeted liposomes > free DOX. The order was reversed in tumor- free organs. A significant decrease in tumor growth and a marked increase in animal lifespan were observed across different tumor-types when treated with HA-liposomal DOX compared with the other 3 treatments. 4 of 10 mice treated with HA-liposomal DOX were free of tumor after 32 days of treatment. | Peer and Margalit (2004b) |
| EGFR | Anti-EGFR antibody | Human breast cancer (MDA-MB-468), human glioblastoma (U87) | After 24 h: spleen > blood > tumor ≈ liver ≈ skin<br>After 72 h: Spleen > tumor skin > liver > blood | In vivo, both anti-EGFR-liposomes and nontargeted liposomes showed comparable circulation half-life (~21 h) and tumor accumulation (up to 15%). However, anti-EGFR-liposomes were internalized more efficiently than nontargeted liposomes (92 | Mamot et al. (2005) |

(*continued*)

TABLE 1—*Continued*

| Specific Cell Surface Moieties | Targeting Ligands | Cancer Types | Competing Tissues (in order of high to low accumulation) | Comments | Reference |
|---|---|---|---|---|---|
| | | | | versus 5%). Anti-EGFR-liposomes were able to improve the anticancer efficacy of various drugs in mice bearing tumors compared with nontargeted liposomes and free drugs. | |
| HER2 (a member of EGFR family) | Anti-HER2 scFv antibody | J6456 lymphoma, human gastric carcinoma (N87), human breast carcinoma (SKBR-3) | n/a | In vitro, the binding of anti-HER2-liposomes to HER2 expressing cancer cells was 10- to 20-fold greater than PEG-liposomes. The $IC_{50}$ of DOX was much lower when delivered by anti-HER2-liposomes compared with PEG-liposomes (~2.8 versus ~25 $\mu$M).<br>In vivo, the binding of anti-HER2-liposomes to HER2 expressing cancer cells was ~20- fold higher than PEG-liposomes. Significant tumor growth inhibition was also observed with anti-HER2-liposomal DOX, whereas PEG-liposomal DOX showed no inhibition. | Shmeeda et al. (2009) |
| VCAM-1 | Anti-VCAM monoclonal antibody | Human ovarian cancer (A2780), and human multiple myeloma (Colo 677) | Liver > spleen ≈ kidney > tumor > lung | In vitro, the binding of anti-VCAM-PEG-liposomes to TNF-$\alpha$ activated murine endothelial cells expressing VCAM-1 was significantly higher than non-VCAM-targeted liposomes.<br>In vivo, the tumor accumulation of anti-VCAM-PEG-liposomes was slightly higher than nontargeted liposomes in mice bearing human Colo 677 tumor. However, intratumoral localization between these liposomes was different. Anti-VCAM-PEG-liposomes localized to tumor blood vessels, while nontargeted liposomes accumulated within tumor tissue by passive diffusion. | Gosk et al. (2008) |
| Protein tyrosine kinase 7 (PTK7) | Sgc8 aptamer | T-cell acute lymphoblastic leukemia (CCRF-CEM) | n/a | In vitro, sgc8-liposomes were able to selectively bind to target cells, while showing no binding to cells without the targeted surface moieties. The fluorescence from fluorescein-isothiocyanato-dextran encapsulated within sgc8-liposomes was also observed inside target cells, but not in nontarget cells. Sgc8-liposomes bind to the specific receptor, PTK7, which is not present on the surface of nontarget cells. | Kang et al. (2010) |
| Nucleolin | AS1411 DNA aptamer | Human breast cancer (MCF-7) | n/a | In vitro, a 6.6-fold increase in the fluorescence of MCF-7 cells was observed after incubation with AS1411-liposomes containing uranin (that bind nucleolin) compared with nontargeted liposomes, suggesting enhanced binding and internalization. The cytotoxicity of DOX was comparable when delivered as AS1411-liposomes or free drug, and was higher than nontargeted liposomes.<br>In vivo, the tumor growth inhibition was higher for AS1411-liposomal DOX compared with a nontargeted formulation due to improved binding and internalization. Early onset of tumor inhibition by AS1411-liposomal DOX was also observed. | Xing et al. (2013) |
| VEGF | siRNA targeting VEGF and/or siRNA targeting kinesin spindle protein (KSP) | Liver cancer and liver metastases | Liver and spleen > tumor | In vivo, liposomes containing siRNA targeting VEGF reduced tumor hemorrhage and tumor microvascular density to the same extent as anti-VEGF antibody, bevacizumab. Liposomes containing both *VEGF* and *KSP* siRNA could reduce the expression of these two genes by 50% within 24 h in mice bearing Hep3B tumor and prolonged the animal survival by 50% compared with control liposomes. | Tabernero et al. (2013) |

(*continued*)

TABLE 1—*Continued*

| Specific Cell Surface Moieties | Targeting Ligands | Cancer Types | Competing Tissues (in order of high to low accumulation) | Comments | Reference |
|---|---|---|---|---|---|
| | | | | In human clinical trials, liposomes containing siRNA for VEGF and KSP were detected in tumor biopsies. siRNA-mediated mRNA cleavage in liver, target downregulation, and anti-tumor activity (including complete regression of liver metastases) were also observed. These liposomes were well tolerated. | |
| $\alpha_v\beta_3$ integrin | Arg-Gly-Asp peptide (RGD peptide) | Mouse melanoma (B16F10) and its lung metastasis | After 2 h: liver > spleen ≈ tumor > lung ≈ kidney<br>After 6 and 24 h: liver ≈ tumor > spleen > lung ≈ kidney | In vitro, RGD-PEG-liposomes demonstrated 7-fold higher binding to human umbilical vein endothelial cells compared with nontargeted liposomes.<br>In vivo, the tumor accumulation of 5-fluorouracil (5-FU) delivered by RGD-PEG-liposomes was higher than that of nontargeted liposomes or free drug. RGD-PEG-liposomal 5-FU was effective at preventing lung metastasis and angiogenesis compared with the other two formulations tested above; 5 mice were metastasis free. RGD-PEG-liposomal 5-FU also demonstrated better antitumor activity and improved survival time compared with nontargeted liposomal 5-FU and free drug. | Dubey et al. (2004) |
| | Arg-Gly-Asp peptide (RGD peptide) | DOX-insensitive murine colon carcinoma (C26) | Liver > spleen > tumor ≈ blood > kidney > lung | In vitro, RGD-PEG-liposomes showed surface binding to human umbilical vein endothelial cells that was ~5-fold higher than nontargeted liposomes.<br>In vivo, RGD-PEG-liposomal DOX demonstrated antitumor efficacy in mice bearing DOX-insensitive C26 tumor. This formulation lowered the tumor volume by half compared with nontargeted liposomes, which showed no effect against DOX-insensitive tumors. | Schiffelers et al. (2003) |
| MT1-MMP (a member of matrix metalloproteinase) | Anti-MT1-MMP | Human fibrosarcoma (HT1080) | n/a | In vitro, anti-MT1-MMP-PEG-liposomes were taken up more effectively than nontargeted liposomes (5-fold higher) by HT1080 cells expressing MT1-MMP.<br>In vivo, anti-MT1-MMP-PEG-liposomal DOX showed a more efficacious antitumor activity and less side effects than nontargeted liposomal DOX, prolonging the survival time of all mice until the end of the study (5 weeks). The tumor accumulation of these two formulations was comparable, the improved efficacy of anti-MT1-MMP-PEG-liposomal DOX came from an increase in cellular internalization by targeting MT1-MMP. | Hatakeyama et al. (2007) |
| Aminopeptidase N (a member of matrix metalloproteinase) | Asn-Gly-Arg peptide (NGR peptide) | Human neuroblastoma (GI-ME-N, GI-LI-N, HTLA-230, IMR-32, and SH-SY5Y), and human Kaposi sarcoma (KS1767) | n/a | In vitro, NGR-liposomes bound to cancer cell lines that associated themselves with NGR peptide (e.g., KS1767 cells) and endothelial cells, but not to cancer cells that did not interact with NGR peptide (e.g., THP-1 leukemia cells).<br>In vivo, the tumor uptake of NGR-liposomal DOX was 10-fold higher than that of nontargeted liposomal DOX. Rapid tumor regression and metastases inhibition was observed in NGR-liposomal DOX-treated mice. In fact, 4 of 6 mice showed no sign of tumor, 1 had > 80% tumor mass reduction, and another demonstrated > 90% decrease in tumor vascular density. Metronomic administration of NGR-liposomal DOX into tumor-bearing mice resulted in complete tumor eradication. | Pastorino et al. (2003) |

A

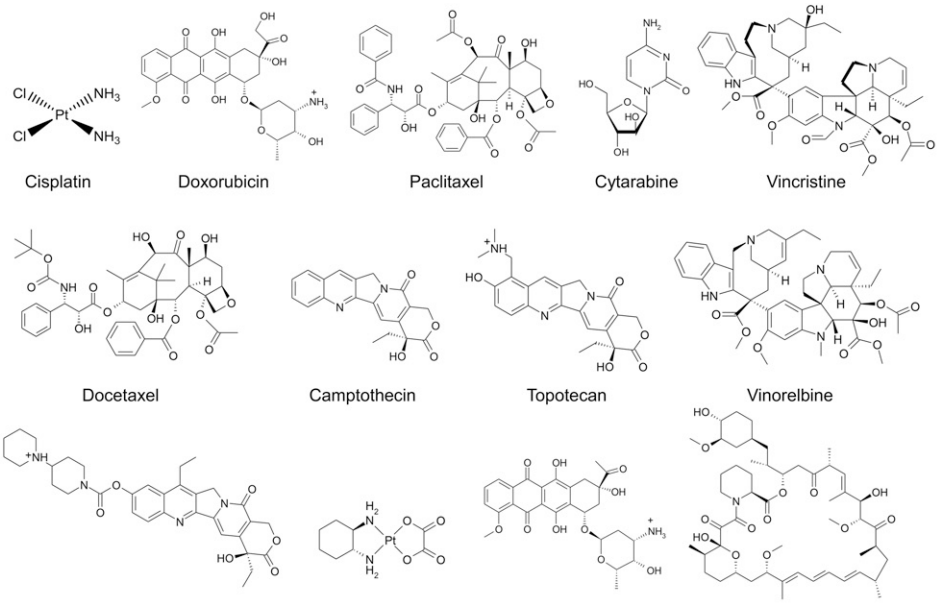


B

| Agent | Log *P* | Indications | Reference |
|---|---|---|---|
| Cisplatin | -2.21 | Testicular and ovarian cancer | Wilson and Lippard (2012); Kelland (2007) |
| Doxorubicin | 1.3 | Breast and ovarian cancer, sarcomas, pediatric solid tumors, Hodgkin's disease multiple myeloma and non-Hodgkin's lymphomas | Cai et al. (2010) |
| Paclitaxel | 3.96 | Ovarian and breast cancer, NSCLC, Kaposi's sarcoma | Surapaneni et al. (2012); Saari H et al. (2015) |
| Cytarabine | -1.25 | Leukemia, lymphoma | Bolwell et al. (1988); Kreder and Dmochowski (2007). |
| Vincristine | 1.16 | Acute lymphocytic leukemia, lymphomas and solid tumors | Lobert et al. (2000); Crom et al. (1994) |
| Docetaxel | 2.4 | Breast, NSCLC, ovarian and head and neck cancers | Ferrati et al. (2015); Clarke and Rivory (1999) |
| Camptothecin | 0.56 | Gastrointestinal cancer | Yadav et al. (2013); Wall and Wani (1995) |
| Topotecan | -2.88 | Ovarian and lung cancer | Yadav et al. (2013); Pommier (2006) |
| Vinorelbine | 1.32 | Breast cancer and NSCLS | Lobert et al. (2000) |
| Irinotecan | 4.37 | Colorectal cancer | Yang X-X et al. (2006); Pommier (2006) |
| Oxaliplatin | -1.65 | Testicular and ovarian cancer | Screnci et al. (2000) |
| Daunorubicin | 1.83 | Acute myeloid leukemia and acute lymphocytic leukemia | Hirschfeld et al. (2003); Nirmalanandhan (2015) |
| Rapamycin | 5.77 | Breast, colon, prostate, renal cell carcinomas | Forrest et al. (2006) |

**Fig. 1.** (A) Line drawings of the chemical structures of common chemotherapeutic agents and (B) their Log *P* values and indications, including Cisplatin, Doxorubicin, Paclitaxel, Cytarabine, Vincristine, Docetaxel, Camptothecin, Topotecan, Vinorelbine, Irinotecan, Oxaplatin, Daunorubicin, and Rapamycin (Bolwell et al., 1988; Crom et al., 1994; Wall and Wani, 1995; Clarke and Rivory, 1999; Lobert et al., 2000; Screnci et al., 2000; Hirschfeld et al., 2003; Forrest et al., 2006; Pommier, 2006; Yang et al., 2006; Kelland, 2007; Kreder and Dmochowski, 2007; Cai et al., 2010; Surapaneni et al., 2012; Wilson and Lippard, 2012; Yadav and Khan, 2013; Ferrati et al., 2015; Nirmalanandhan et al., 2015; Saari et al., 2015).

transferrin, macroglobulin, and high density lipoprotein (Kirby and Gregoriadis, 1980; Damen et al., 1981; Vemuri and Rhodes, 1995; Sharma and Sharma, 1997). These proteins tend to destabilize liposomes, and thus, decrease their capacity as a drug delivery system (Kirby and Gregoriadis, 1980; Damen et al., 1981). Although cholesterol has the ability to protect liposomes from being destabilized by blood proteins, the loss of liposomal phospholipids cannot be prevented completely (Kirby and Gregoriadis, 1980; Damen et al., 1981).

Apart from cholesterol, a small fraction of polymers containing hydrophilic groups, especially polyethylene glycol (PEG), are at times conjugated to the surface of liposomes. PEG is often used for its stealth functions in nanoparticle formulations because it is a hydrophilic

TABLE 2
Liposomal formulations of anticancer drugs in phase I clinical trials

| Product Name | Encapsulated Drugs | Type of Liposomes | Indications | Lipid Composition | Particle Size | Status | Reference |
|---|---|---|---|---|---|---|---|
| | | | | | *nm* | | |
| Alocrest | Vinorelbine | Optisomes | NSCLC and breast cancers, non-Hodgkin's lymphoma, Hodgkin's disease | Sphingomyelin and cholesterol | — | Phase I | NCT00364676[a] (accessed on 14/4/15); Semple et al. (2005); Cattaneo et al. (2010); |
| Aroplatin | Analog of cisplatin | MLVs | Advanced pancreatic and colorectal cancer, malignant pleural mesothelioma, advanced solid malignancies | DMPC and DMPG | — | Phase I/II | NCT00043199[a] (accessed on 14/4/15); Lu et al. (2005); Dragovich et al. (2006) |
| ATI-1123 | Docetaxel | Protein stabilized liposomes | NSCLC, gastric, pancreatic cancer, and soft tissue sarcoma | Phospholipids, cholesterol, human serum albumin, and sucrose | 60-80 | Phase I | Mahalingam et al. (2014) |
| Brakiva (TLI) | Topotecan | Optisomes | Small cell lung, ovarian cancers and advanced solid tumors | Sphingomyelin and cholesterol | 100 | Phase I | NCT00765973[a] (accessed on 14/4/15); Tardi et al. (2000) |
| NanoVNB | Vinorelbine | PEGylated liposomes | Advanced solid tumors | DSPC, DSPE-$PEG_{2000Da}$, cholesterol | 98 | Phase I | Yang et al. (2012b); Lin et al. (2013) |
| MCC-465 | Doxorubicin | Antibody conjugated PEGylated liposomes | Stomach cancer | DPPC, maleimidated DPPE, PEG, GAH | 143 | Phase I | Hamaguchi et al. (2004); Matsumura et al. (2004) |
| SGT-53 | p53 DNA plasmid | Anti-TfR conjugated cationic liposomes | Solid tumors | DOTAP and DOPE | 114 | Phase I | NCT00470614[a] (accessed on 15/4/15); Xu et al. (2001); Camp et al. (2013); Kim et al. (2015) |
| TKM-080301 (TKM-PLK1) | PLK1 siRNA | Cationic PEGylated liposomes | Gastrointestinal neuroendocrine tumors, adrenocortical carcinoma, hepatocellular carcinoma | DSPC, DLin-MC3-DMA, DMG-PEG, and cholesterol | 80-140 | Phase I/II | NCT01262235[a] (accessed on 15/4/15); Tam et al. (2013); Leung et al. (2014) |

[a]ClinicalTrials.gov identifier
DMPC, 1,2-dimyristoyl phosphatidylcholine; DMPG, 1,2-dimyristoyl phosphatidylglycerol; DPPE, 1,2-dipalmitoyl phosphatidylethanolamine; GAH, human monoclonal antibody; NSCLC, non-small cell lung cancer; DLin-MC3-DMA, heptatriaconta-6,9,28,31-tetraen-19-yl 4-(dimethylamino)butanoate; DMG-PEG, polyethylene glycol-dimyristolglycerol; TfR, transferrin receptor

and flexible polymer (Bergström et al., 1994). The conjugation of PEG to the surface of the liposomal phospholipid bilayer reduces the interaction of liposomes with plasma proteins through steric hindrance (Allen et al., 1985; Allen and Chonn, 1987; Gabizon and Papahadjopoulos, 1988; Allen et al., 1991b; Papahadjopoulos et al., 1991; Allen et al., 2002). As a result, this prevents plasma proteins, such as opsonin, from adsorbing to the surface of liposomes, which reduces opsonization and uptake of liposomes by the reticuloendothelial system (RES) (Allen et al., 1985, 1991b, 2002; Allen and Chonn, 1987; Gabizon and Papahadjopoulos, 1988; Papahadjopoulos et al., 1991). The conjugation of PEG or PEGylation allows liposomes to circulate within the body for a longer period of time, extending their circulation half-life and, consequently, increasing the accumulation of liposomes within tumors (Allen et al., 1991b; Woodle, 1995; Allen et al., 2002). The stealth function of PEG was supported by two research groups that demonstrated that PEGylated liposomes exhibited up to a 10-fold increase in their circulation half-life compared to non-PEGylated liposomes in a biologic environment (Klibanov et al., 1991; Lasic et al., 1991). Furthermore, Awasthi et al. (2003) demonstrated in a rabbit model that, although PEG is able to prolong the circulation half-life of liposomes, the amount observed within the circulation is dependent on their size. In fact, the levels of $^{99m}$TC-labeled liposomes remaining in the circulation after 24 hours decreased with increasing liposome size (Awasthi et al., 2003).

There are different ways in which PEG can be attached onto the surface of liposomes. The most common method is the inclusion of PEG-lipid conjugates into the lipid bilayer of the liposome formulation (Kostarelos and Miller, 2005). Consequently, when liposomes are hydrated, PEG polymers are exposed on the outside surface of liposomes (Kostarelos and Miller, 2005). Other methods involve the formation of liposomal platforms for the addition of PEG polymers. These include the postconjugation method, where PEG polymers are covalently attached to preformed liposomes (Wang and Thanou, 2010), and the postinsertion method, where preformed liposomes are incubated with PEG-lipid conjugates in an aqueous solution forming micellar structures (Hoarau et al., 2004).

Although PEGylation may help improve the half-life of liposomes by prolonging their circulation time and protecting them from RES, it is not so simple to prepare effective PEGylated liposomes for drug delivery purposes. There are several factors that must be taken into consideration for the preparation of effective PEGylated liposome nanocarriers. This is because each PEG polymer chain possesses a Flory dimension (Rf), which represents the volume occupied by a single polymer chain (Wang and Thanou, 2010). This value is influenced by both the polymer chain length and, more importantly, PEG density on the liposomal surface

TABLE 3
Liposomal formulations of anticancer drugs in phase II clinical trials

| Product Name | Encapsulated Drugs | Type of Liposomes | Indications | Lipid Composition | Particle Size | Status | Reference |
|---|---|---|---|---|---|---|---|
| | | | | | *nm* | | |
| CPX-1 | Irinotecan and floxuridine (1:1) | ULVs | Advanced solid tumors, including colorectal cancer | DSPC, DSPG, and cholesterol | 100 | Phase II | NCT00361842[a] (accessed on Apr 14, 2015); Batist et al. (2009) |
| EndoTAG-1 | Paclitaxel | Cationic liposomes | Solid tumors | DOTAP, DOPC | 180–200 | Phase II | Fasol et al. (2012); Lohr et al. (2012); Awada et al. (2014) |
| LEP-ETU | Paclitaxel | Anionic liposomes | Metastatic breast cancer | DMPC, DOPC, DSPC, cholesterol, and cardiolipin | 100–160 | Phase II | NCT01190982[a] (accessed on Apr 15, 2015); Zhang et al. (2005); Slingerland et al. (2013) |
| MBP-426 | Oxaliplatin | Tf-conjugated liposomes | Gastric, gastroesophageal, esophageal adenocarcinomas | DSPC, DSPE-PEG$_{2000Da}$, cholesterol and Tf -conjugated NGPE | 180 | Phase II | Suzuki et al. (2008); van der Meel et al. (2013) |
| OSI-211 | Lurtotecan | SUVs | NSCLC, breast, colorectal, ovarian, head and neck cancers | Soy PC and cholesterol | 100 | Phase II | Gamucci et al. (2000); Duffaud et al. (2004); Seiden et al. (2004) |

[a]ClinicalTrials.gov identifier
DSPG, 1,2-distearoyl-*sn*-glycerol-3-phospho-(1'-*rac*-glycerol); NGPE, *N*-glutaryl phosphatidylethanolamine; NSCLC, non-small cell lung cancer; Tf, transferrin

(Dos Santos et al., 2007; Wang and Thanou, 2010). The density of PEG on the liposomal surface also influences the distance between each individual PEG polymer (*D*). For example, an increase in the PEG-lipid concentration in the formulation increases surface PEG density and, ultimately, decreases *D* (De Gennes, 1987). When *D* is larger than Rf, PEG polymers will reorganize themselves and coil into a mushroom-like conformation (De Gennes, 1987). In contrast, when *D* is smaller than Rf, the lateral pressure between overcrowded PEG polymers forces each polymer chain to extend into a brush conformation (De Gennes, 1987). Notably, the mushroom conformation of liposomal surface PEG was observed when the PEG concentration was below 4 mol%, whereas the brush conformation was found at PEG concentrations above 4 mol% (De Gennes, 1987; Garbuzenko et al., 2005). It is the brush conformation of PEG that is believed to prolong the circulation time of liposomes by providing repulsive force against proteins and other liposomes (Jeon et al., 1991; Szleifer, 1997; Gbadamosi et al., 2002). Thus, PEG chain length and concentration plays an important role in determining: 1) an effective liposome preparation; 2) the PEG configuration; 3) liposome size; 4) encapsulation of drug; 5) membrane permeability; 6) liposomal stability; and 7) the effectiveness of PEG as a protective layer (Torchilin et al., 1994; Woodle, 1998; Vonarbourg et al., 2006; Wang and Thanou, 2010).

It has been reported that three different states exist in the liposomal phospholipid bilayer containing a mixture of PEG-dipalmityol phosphoethanolamine (DPPE) and PC: 1) a lamellar phase where all components exhibit some miscibility; 2) a lamellar phase where the components are phase separated; and 3) mixed micelles (Bedu-Addo et al., 1996a). For PEG of 1,000 and 3,000 Da, DPPE-PEG and PC in liposomal bilayers were uniformly mixed at a concentration of $<$ 5 mol% (Bedu-Addo et al., 1996a). However, phase separation in the form of micelle formation started to occur at concentrations beyond 7 mol%, and by 17 mol%, liposomal bilayers were completely solubilized to form micelles (Bedu-Addo et al., 1996a). A similar trend was observed with 5,000 Da PEG, although the three states were observed at different concentrations with the uniformly mixed bilayer showing phase separation beyond 8 mol%, whereas micelle formation occurred at 11 mol% (Bedu-Addo et al., 1996a). For long PEG chains of 12,000 Da, DPPE-PEG was not fully incorporated into the PC bilayer at any concentration (Bedu-Addo et al., 1996a). For instance, at 10 mol%, only 50% of DPPE-PEG was incorporated. Moreover, an increase in the concentration of DPPE-PEG resulted in the formation of micelles, which coexisted with liposomes and no liposomal bilayer solubilization was observed (Bedu-Addo et al., 1996a).

The molecular weight and concentration of PEG also affects the final size of the liposome, encapsulation, and

TABLE 4
Liposomal formulations of anti-cancer drugs in phase III clinical trials

| Product Name | Encapsulated Drugs | Type of Liposomes | Indications | Lipid Composition | Particle Size | Status | Reference |
|---|---|---|---|---|---|---|---|
| | | | | | *nm* | | |
| CPX-351 | Cytarabine and daunorubicin (5:1) | Bilamellar liposomes | Acute myeloid leukemia | DSPC, DSPG and cholesterol | 100 | Phase III | NCT01696084[a] (accessed on Apr 14, 2015); Feldman et al. (2011); Cortes et al. (2015) |
| Lipoplatin | Cisplatin | PEGylated liposomes | NSCLC, gastric, pancreatic, breast, head and neck cancers | PC, cholesterol, DPPG, DSPE-PEG$_{2000Da}$ | 110 | Phase III | Boulikas (2009); Stathopoulos et al. (2010) |
| MM-398 (PEP02) | Irinotecan | PEGylated liposomes | Metastatic pancreatic cancer | DSPC, DSPE-PEG$_{2000Da}$, cholesterol | 100-110 | Phase III | NCT01494506[a] (accessed on Apr 15, 2015); Drummond et al. (2006); Kang et al. (2015); Roy et al. (2013); Saif (2014) |
| Thermodox | Doxorubicin | Lyso-lipid temperature sensitive liposomes | Hepatocellular carcinoma and breast cancer | DPPC, MSPC, DSPE-PEG$_{2000Da}$ | 175 | Phase III | NCT00617981[a] (accessed on Apr 15, 2015); May and Li (2013) |

[a]ClinicalTrials.gov identifier
DPPC, 1,2-dipalmitoyl phosphatidylcholine; DPPG, 1,2-dipalmitoyl phosphatidylglycerol; MSPC, *mono*-stearoyl phosphatidylcholine; NSCLC, non-small cell lung cancer

liposomal membrane permeability (Nicholas et al., 2000). It was found that the size of multilamellar vesicles (MLVs) decreased as the concentration of DPPE-PEG$_{5000Da}$ conjugates increased, whereas the size of liposomes prepared via the vesicle extrusion technique was independent of DPPE-PEG$_{5000Da}$ concentration (Nicholas et al., 2000). Only when the temperature was increased to 50°C, did the size of these liposomes prepared by extrusion decrease at high DPPE-PEG$_{5000Da}$ (Nicholas et al., 2000). The decrease in size can be explained by the fact that the addition of PEG to the liposome surface strongly reduced the attractive van der Waals forces and increased repulsive forces (Kenworthy et al., 1995a). Increasing the phospholipid-PEG conjugate concentration caused the disintegration of liposome structures, resulting in a gradual reduction in size, and ultimately, the solubilization of liposomes to form micelles (Bedu-Addo et al., 1996a; Belsito et al., 2001).

Additionally, the encapsulation of D-glucose in liposomes and the permeability of the liposomal membrane to D-glucose were both reported to be dependent on the DPPE-PEG concentration (Nicholas et al., 2000). Indeed, the encapsulation of D-glucose was found to decrease as the concentration of DPPE-PEG increased (Nicholas et al., 2000). However, the decrease in D-glucose encapsulation was not as dramatic for DPPE-PEG$_{2000Da}$ relative to DPPE-PEG$_{5000Da}$. A significant decrease in encapsulation was only observed between 4 and 6 mol% for DPPE-PEG$_{2000Da}$, whereas it was observed at 0–2.5 mol% for DPPE-PEG$_{5000Da}$ (Nicholas et al., 2000). This was believed to be because PEG dramatically restricted the free volume inside the liposome to carry glucose (Nicholas et al., 2000). It was further suggested that the percentage encapsulation should be comparable for liposomes with either PEG mushroom or brush conformation (Nicholas et al., 2000). In contrast, the membrane permeability of liposomes to D-glucose was demonstrated to decrease as the concentration of DPPE-PEG increased (Nicholas et al., 2000). This may be due to the fact that there is an increase in membrane bilayer disorder because more DPPE-PEG conjugates are added to the membrane, creating more defects (Nicholas et al., 2000). In addition, the phase transition from mushroom to brush conformation can also contribute to the increase in defect formation (Kashchiev and Exerowa, 1983; Kenworthy et al., 1995b). The maximum liposomal membrane permeability was observed at 4 mol% of DPPE-PEG$_{2000Da}$ (Nikolova and Jones, 1996), whereas it was predicted to be 1.7 mol% for DPPE-PEG$_{5000Da}$ (Kenworthy et al., 1995a).

In terms of liposome stability and in vivo circulation, it was reported that 2–5 mol% of 1,2-distearoyl-*sn*-glycerol-3-phosphoethanolamine (DSPE)-PEG$_{2000Da}$ was able to separate each particle from aggregation (Dos Santos et al., 2007). The same study also

demonstrated that as little as 0.5% of DSPE-$PEG_{2000Da}$ was able to prolong the plasma circulation of cholesterol free liposomes in Balb/c mice (Dos Santos et al., 2007). A $PEG_{2000Da}$ concentration of 2 mol% was believed to result in the optimal plasma circulation time, because the circulation time observed for liposomes containing 2 mol% of $PEG_{2000Da}$ was comparable to those containing 5 mol% of $PEG_{2000Da}$ (Dos Santos et al., 2007). In addition, not much difference was observed in the amount of protein adsorption on liposomes between various PEG molecular weights or between $PEG_{2000Da}$ at 2 and 5 mol% concentration (Dos Santos et al., 2007). Similar results were also observed in a separate study in which the amount of protein adsorbed to the surface of the liposome in the presence of $PEG_{1000Da}$ was only 2 times more than when either $PEG_{2000Da}$ or $PEG_{5000Da}$ were present (Pozzi et al., 2014). Furthermore, it is believed that the presence of PEG on the surface of liposomes, regardless of the chain length, was able to neutralize the influence of charge on circulation time (Levchenko et al., 2002). Both 750 and 5000 Da PEG-PE conjugates at 6 mol% were able to improve the circulation time of cationic liposomes containing stearylamine and anionic liposomes containing phosphatidic acid in mice (Levchenko et al., 2002). However, only 5000 Da PEG-PE was able to improve the circulation time of anionic liposomes containing PS (Levchenko et al., 2002). Interestingly, in another investigation, it was demonstrated that $7 \pm 2$ mol% of DSPE-$PEG_{2000Da}$ would allow the greatest biologic stability of large unilamellar vesciles (LUVs) to be achieved (Garbuzenko et al., 2005). This is because at this concentration, the specific compressibility and additive packing parameter values for the mixture of matrix lipid, cholesterol, and DSPE-$PEG_{2000Da}$ for all liposome compositions reached their maximum (Garbuzenko et al., 2005). The greatest stability at $7 \pm 2$ mol% DSPE-$PEG_{2000Da}$ was demonstrated by the lack of liposome size and specific turbidity reduction as the temperature and PEG concentration increased (Garbuzenko et al., 2005).

Apart from PEG-phospholipid conjugates, the amphiphilic PEG-block-poly($\varepsilon$-caprolactone) copolymer has also been incorporated into liposomal formulations to produce stealth lipid nanoparticles (He et al., 2015). Similar to PEG-phospholipid conjugates, this alternative approach also allows PEG to be attached to the surface of liposomes. It was reported that the incorporation of PEG-block-poly($\varepsilon$-caprolactone) of 4000 and 10,000 Da resulted in liposomes that were as effective or more superior as stealth lipid nanoparticles compared with liposomes composed of PEG-phospholipid conjugates, depending on the copolymer molecular weight (He et al., 2015). PEG-block-poly($\varepsilon$-caprolactone) modified liposomes containing Paclitaxel (PTX; Fig. 1) were as stable as conventional PTX encapsulated PEGylated liposomes showing minimal particle size change and aggregation after a 48-hour incubation in 10% fetal bovine serum (He et al., 2015). However, the drug loading efficiency of PTX encapsulated PEGylated liposomes decreased much more rapidly than that found for PEG-block-poly($\varepsilon$-caprolactone) modified liposomes with copolymers of various molecular weight (He et al., 2015). Furthermore, modified liposomes containing PEG-block-poly($\varepsilon$-caprolactone) of 4000 Da showed a ~2-fold increase in internalization by 4T1 mouse mammary tumor cells relative to both PEGylated liposomes and liposomes containing PEG-block-poly($\varepsilon$-caprolactone) of 10,000 Da (He et al., 2015). In 4T1 mammary tumor xenografted mouse models, modified liposomes containing PEG-block-poly($\varepsilon$-caprolactone) of 4000 Da that encapsulated PTX were demonstrated to have the highest tumor growth inhibition rate (75.1%) compared with other PTX loaded liposomes, including PEGylated liposomes (56.3%) and modified liposomes containing PEG-block-poly($\varepsilon$-caprolactone) of 10,000 Da (49.5%) and free PTX (32.5%) (He et al., 2015). This may be due to the higher rate of internalization by cancer cells when liposomes were conjugated with PEG-block-poly($\varepsilon$-caprolactone) of smaller molecular weight (He et al., 2015).

Despite the fact that PEGylation helps improve circulation time and transport of liposomes to tumor sites efficiently (Wang and Thanou, 2010), the addition of PEG to the surface of liposomes may reduce the binding and the uptake of liposomes by cancer cells due to the steric hindrance provided by PEG. This was demonstrated by a decrease in the cellular binding of short-peptide-targeted liposomes to cancer cells in the presence of increasing concentrations of PEG (2000 Da) (Demirgoz et al., 2008; Garg et al., 2009). Therefore, the number of PEG molecules present on the surface of liposomes is thought to determine the uptake of liposomes by cancer cells (Wang and Thanou, 2010). Together, PEG chain length and PEG chain concentration influence the capacity of liposomes to act as drug carriers.

Of relevance, PEGylated liposomes have been reported to be recognized by anti-PEG antibodies (Wang et al., 2007a; Ishida et al., 2008; Tagami et al., 2009). This process occurs between 2 and 4 days after the first administration of PEGylated liposomes into the body, resulting in an accelerated blood clearance of PEGylated liposomes upon future administration (Ishida et al., 2006; Judge et al., 2006; Ishida and Kiwada, 2008). However, interestingly, increasing the concentration of the first injected dose of PEGylated liposomes (from 0.001 to 5 $\mu$mol/kg) was reported to decrease the blood clearance caused by anti-PEG antibodies during the second injection (Ishida et al., 2005). Furthermore, the concentration of PEG incorporated into liposomes was reported to influence the clearance rate of these particles (Ishida et al., 2005). This conclusion was reached in studies where 5 mol% PEG was incorporated

into the liposome and this was injected into rats for the second time after the initial dose of 0.001 $\mu$mol/kg. Indeed, a marked reduction in circulation time and increase in hepatic accumulation was observed (Ishida et al., 2005). However, increasing the PEG concentration to 10 and 15 mol% in the second dose improved both the circulation time and hepatic accumulation (Ishida et al., 2005). No improvement in circulation time and hepatic accumulation was observed when PEG chain length was increased from 2000 to 5000 Da (Ishida et al., 2005). These findings may be useful in identifying an appropriate strategy to minimize anti-PEG antibody induced PEGylated liposome clearance. In particular, using a higher dose during the initial injection may be a more appealing strategy than increasing the surface PEG concentration due to the destabilizing effect of PEG-phospholipid conjugates on the liposomal membrane at high mol% as mentioned above. Other steric stabilizers can also be used instead of PEG to improve the circulation time of liposomes. For more information on various synthetic polymers capable of extending the circulation time of nanoparticles, please see Torchilin and Trubetskoy (1995).

Alternatively, naturally derived polymers, such as chitosan, can be used to stabilize liposomes. Chitosan is a hydrophilic biodegradable polymer of low toxicity (Guo et al., 2003). Chitosan can be incorporated onto the surface of liposomes via an ionic interaction between positively charged chitosan and negatively charged phospholipids (Takeuchi et al., 1996). Chitosan has been reported to provide liposomes with high stability (Filipovic-Grcic et al., 2001). An incubation of chitosan-coated liposomes containing fluorescein isothiocyanate (FITC)-dextran in simulated gastric fluid demonstrated that these particles were relatively stable, retaining ~75–79% of their encapsulated contents after 30 minutes and ~25–37% after 2 hours (Filipovic-Grcic et al., 2001). In contrast, uncoated liposomes were able to retain only 11% of encapsulated FITC-dextran after 30 minutes and only 4% after 2 hours (Filipovic-Grcic et al., 2001). Although chitosan can provide steric stabilization to liposomes, some leakage of encapsulated FITC-dextran (Filipovic-Grcic et al., 2001) and leuprolide (Guo et al., 2003) was observed. This was thought to be due to the interaction between chitosan and the polar head groups of phospholipids on the liposomal membrane interfering with entrapment (Guo et al., 2003).

### *B. Types of Liposomes*

Liposomes can be classified by different factors. They can be classified by the method of their preparation, the number of bilayers present within the liposome vesicle, or the vesicle size (Vemuri and Rhodes, 1995). However, the most commonly known classes of liposomes are multilamellar vesicles (MLVs) and unilamellar vesicles (ULVs), which can be further classified into large unilamellar vesicles (LUVs) and small unilamellar vesicles (SUVs) as shown in Fig. 2. These liposome types are discussed in further detail below.

*1. Multilamellar Vesicles.* MLVs usually range in size between 0.05 and 10 $\mu$m and consist of multiple phospholipid bilayers (Fig. 2) (Sharma and Sharma, 1997). They can easily be prepared and are widely studied along with ULVs. The simplest and the most popular method for the preparation of MLVs is thin film hydration (Sharma and Sharma, 1997). In this method, MLVs can be formed spontaneously by adding an excess volume of aqueous buffer to a thin film of dry lipids at a temperature above the phase transition temperature (PTT) of lipids (Vemuri and Rhodes, 1995; Sharma and Sharma, 1997). For thin film hydration, the desired drug to be encapsulated within MLVs can either be included in the aqueous hydration buffer for hydrophilic drugs or in the lipid film for lipophilic drugs (Sharma and Sharma, 1997). Although it is easy to prepare MLVs using thin film hydration, such a method provides relatively poor drug encapsulation efficiency (5–15%). Therefore, the preparation procedure must be optimized and vesicles must be characterized carefully, as

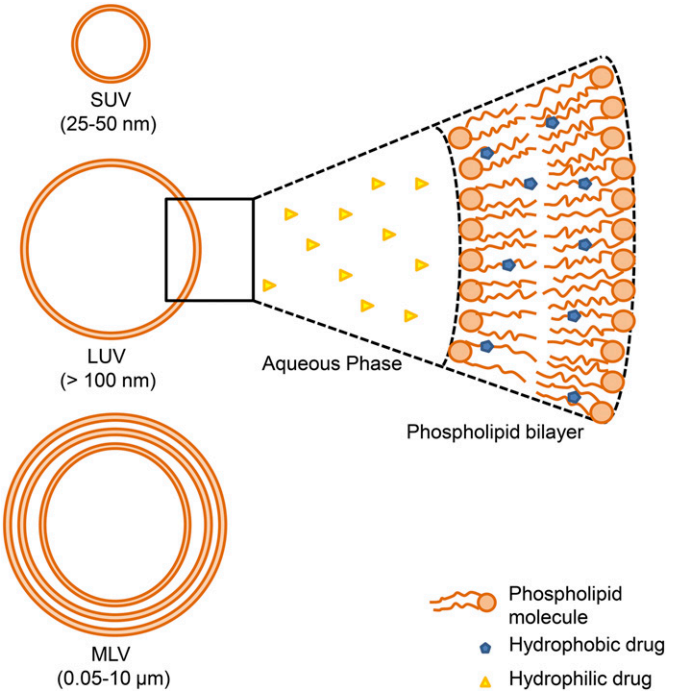


**Fig. 2.** Types of liposomes classified by size and lamellarity. Based on size and lamellarity, liposomes can be classified into 3 different types. Multilamellar vesicles (MLVs) typically range in the size between 0.05 and 10 $\mu$m and consist of multiple phospholipid bilayers. Large unilamellar vesicles (LUVs) are usually in the size >100 nm and consist of a single phospholipid bilayer. The size of LUVs is debatable, as vesicles of size 50–100 nm had been referred to as LUVs. Small unilamellar vesicles (SUVs) are usually in the size range of 25–50 nm and, like LUVs, consist of a single phospholipid bilayer. The SUVs are prepared from MLVs or LUVs by sonication or extrusion. In all types of liposomes, hydrophobic drugs are usually localized within the phospholipid bilayer, whereas hydrophilic drugs are usually encapsulated within the liposome cavity.

minor changes in the preparation can result in alternations to the liposomal characteristics and behavior (Vemuri and Rhodes, 1995).

In the preparation of MLVs using thin film hydration, a thin film of lipids is preferred because this enhances the encapsulation efficiency of drug (Bangham, 1982). This thin film of lipid can be prepared by removing an organic solvent from the lipid mixture under vacuum using a rotary evaporator (Bangham, 1982). The time allowed for the hydration of lipid film with aqueous or drug solution also influences the amount of drug trapped within liposomal vesicles (Olson et al., 1979). It was demonstrated by Olson et al. (1979) that lipid films with similar compositions could achieve greater drug entrapment by using a slower rate of hydration and gentle mixing. In addition, a small proportion (10–20 mol%) of negatively charged lipids, such as PS, PI, and PG, or positively charged lipids, such as stearylamine, can be added to a liposome formulation to increase the interlamellar distance between successive bilayers, and thus, increase the encapsulation capacity of MLV liposomes (Vemuri and Rhodes, 1995). These lipids with charged moieties can also reduce vesicular aggregation after MLV synthesis (Vemuri and Rhodes, 1995).

As thin film hydration provides low encapsulation efficiency, other methods of MLVs preparation with higher encapsulation efficiency have been proposed. One method involves the hydration of the lipid in the presence of an organic solvent using sonication or vortex mixing (Papahadjopoulos and Watkins, 1967; Gruner et al., 1985). In this method, MLVs are formed as the organic phase is removed by passing a stream of nitrogen through the system after sonication or vortex mixing (Papahadjopoulos and Watkins, 1967; Gruner et al., 1985). This technique has been reported to allow up to 40% encapsulation efficiency to be achieved (Gruner et al., 1985). However, large amounts of organic solvent are often left within the liposome formulation (Papahadjopoulos and Watkins, 1967; Gruner et al., 1985). Another method of preparation previously described involves the mixing of a preformed SUVs dispersion with an aqueous solution of the drug to be encapsulated, followed by lyophilization and rehydration of the mixture (Kirby and Gregoriadis, 1984; Ohsawa et al., 1984). This technique also allows for the formation of MLVs that achieve an encapsulation efficiency of up to 40% (Kirby and Gregoriadis, 1984; Ohsawa et al., 1984).

*2. Large Unilamellar Vesicles.* LUVs are liposomal vesicles consisting of a single phospholipid bilayer and are considered to be of a size greater than 100 nm (Fig. 2) (Sharma and Sharma, 1997). However, the size range of LUVs is debatable, because some investigators previously described unilamellar vesicles in a size range of 50–100 nm as LUVs (Vemuri and Rhodes, 1995). Unlike MLVs, LUVs have the ability to hold a larger volume of solution within their cavity. Therefore, LUVs have higher encapsulation efficiency than MLVs (Hauser, 1982; Vemuri and Rhodes, 1995). As LUVs exhibit a high encapsulation efficiency, they are more economical in terms of manufacturing as liposomal drug formulations, since a larger amount of drug can be encapsulated within a smaller quantity of lipids (mg of drug per mg of lipid) (Tyrrell et al., 1976; Vemuri and Rhodes, 1995). Other than high encapsulation efficiency, LUVs also provide a reproducible drug release rate, which is a crucial factor in a drug delivery system (Tyrrell et al., 1976). LUVs can be prepared by reverse-phase evaporation or detergent removal techniques, which are discussed below.

In the reverse-phase evaporation technique, a water-in-oil (w/o) emulsion is formed between water and phospholipids in an excess of organic solvent by mechanical means or by sonication (Szoka and Papahadjopoulos, 1978). When the organic solvent is removed from the mixture under vacuum, phospholipid droplets containing water are formed (Szoka and Papahadjopoulos, 1978). These droplets come together to form a gel-like matrix, which transforms into a smooth paste of LUV suspension once the organic solvent is completely removed (Szoka and Papahadjopoulos, 1978). The reverse-phase evaporation technique has been reported to allow a drug encapsulation efficiency of up to 60–65% to be achieved (Szoka and Papahadjopoulos, 1978). Although high encapsulation efficiency can be achieved using the reverse-phase evaporation technique, this method exposes drugs and biologically active molecules to organic solvents and mechanical forces (Vemuri and Rhodes, 1995). Thus, these molecules may undergo conformational changes, protein denaturation, or DNA strand breakage due to the harsh conditions used (Vemuri and Rhodes, 1995).

Alternatively, LUVs can also be prepared using a detergent removal technique. In this method, phospholipids and a detergent are allowed to mix together forming micelles. The detergent is then removed from the preparation, which results in micelles progressively becoming richer in phospholipids. Subsequently, these phospholipid-rich micelles come together to form single bilayer vesicles (Kagawa and Racker, 1971; Milsmann et al., 1978). It is important that detergents used for this technique are those with high critical micelle concentration (CMC) in the range of 10–20 mM, such as sodium cholate, sodium deoxycholate, and octylglucoside (Vemuri and Rhodes, 1995).

In the detergent removal technique, the detergent can be removed by different methods, such as dialysis, column chromatography, or adsorption using Bio-Beads (Bio-Rad Laboratories, Hercules, CA). The removal of the detergent by dialysis was first reported by Milsmann et al. (1978). In this technique, the detergent is allowed to flow through a dialysis cell from a phospholipid-detergent mixture, resulting in a homogeneous population

of single bilayer liposome vesicles ranging in size between 50 and 100 nm in diameter (Milsmann et al., 1978). The use of column chromatography to remove detergents was reported by Enoch and Strittmatter (1979). Using column chromatography, Enoch and Strittmatter separated deoxycholate from the phospholipid-deoxycholate mixture by passing the mixture through a Sephadex (GE Healthcare, Chicago, IL) G-25 column, which yielded single layer phospholipid vesicles with a diameter of 100 nm. Alternatively, adsorption using Bio-Beads can be implemented to remove detergents (Gerritsen et al., 1978). It was reported that Bio-Beads SM-2 were added directly into the phospholipid-detergent mixture (Gerritsen et al., 1978). This allowed the detergent to bind to Bio-Beads selectively and rapidly, separating phospholipid vesicles from the detergent (Gerritsen et al., 1978). However, a nonionic detergent must be used in this method (Gerritsen et al., 1978).

*3. Small Unilamellar Vesicles.* SUVs are usually found with diameters ranging between 25 and 50 nm (Fig. 2) (Huang, 1969). They can be prepared from MLVs or LUVs using sonication (Saunders et al., 1962; Huang, 1969) or extrusion under high pressure (Hamilton et al., 1980). In the preparation of SUVs using sonication, the MLVs or LUVs suspension is sonicated under nitrogen or argon gas to reduce the size of the vesicles to the SUV size range (Saunders et al., 1962; Huang, 1969). Both types of sonication, namely a bath or a probe sonicator, can be used to generate SUVs (Vemuri and Rhodes, 1995). However, bath sonication offers advantages over probe sonication, because the preparation of SUVs can be performed aseptically with sealed containers and the temperature can be controlled throughout the preparation (Vemuri and Rhodes, 1995). The characterization of SUVs generated by sonication has previously demonstrated that this method is able to synthesize liposomes with sizes ranging between 25 and 50 nm (Huang, 1969). Alternatively, MLVs or LUVs can be converted to SUVs by extrusion (Hamilton et al., 1980). In this method, MLVs or LUVs are forced multiple times through a narrow orifice under high pressure (20,000 psi) at 4°C, resulting in SUVs with sizes ranging between 15 and 30 nm (Hamilton et al., 1980). This technique allows for the reproducible production of SUVs (Hamilton et al., 1980). However, the temperature of the preparation cannot be accurately controlled using this technique, resulting in temperature fluxes during preparation that can affect phospholipid packing within the liposome (Hamilton et al., 1980).

In addition, SUVs can also be prepared directly by the solvent injection method using diethyl ether (Deamer and Bangham, 1976) or ethanol (Batzri and Korn, 1973). In general, using this method, lipids dissolved in an organic solvent are injected into an excess amount of aqueous solution or water by a syringe-type infusion pump, forming SUVs spontaneously (Batzri and Korn, 1973; Deamer and Bangham, 1976). The organic solvent is then removed from the preparation completely. This method has been reported to produce SUVs with sizes between 50 and 200 nm (Deamer and Bangham, 1976). Similar to other liposome preparations, it is almost impossible to completely remove organic solvents from the preparations when using this technique (Vemuri and Rhodes, 1995).

### *C. Lipid-core Micelles*

Another type of nanoparticle that can be generated from phospholipids are lipid-core micelles. Typically, micelles are prepared from amphiphilic copolymers, which contain both hydrophilic and hydrophobic ends (Kwon and Kataoka, 1995; Jones and Leroux, 1999; Torchilin, 2001). This characteristic of amphiphilic copolymers gives micelles the ability to solubilize poorly soluble drugs (Kwon and Kataoka, 1995; Jones and Leroux, 1999; Torchilin, 2001). The formation of lipid-core micelles was first observed when polyethylene glycol-phosphatidylethanolamine conjugate (PEG-PE) mixtures of certain compositions form micelles instead of PEGylated liposomes after their concentration exceeded a critical limit (Bedu-Addo et al., 1996b; Edwards et al., 1997). Soon after, the potential of PEG-PE micelles as a lipid-based nanoparticle drug delivery system was realized (Lukyanov and Torchilin, 2004). Not only does PEG-PE helps prolong the circulation time of micelles, the use of phospholipids as a hydrophobic block of copolymers for the preparation of lipid-core micelles also make these micelles highly stable (Lukyanov and Torchilin, 2004). This increase in stability is due to the hydrophobic interaction between double acyl chains of phospholipids and allows hydrophobic drugs to be solubilized (Lukyanov and Torchilin, 2004).

PEG-PE micelles can be generated spontaneously by shaking a dry PEG-PE film in the presence of an aqueous medium (Lukyanov and Torchilin, 2004). They can also be produced using a detergent or water miscible solvent removal method (Lukyanov and Torchilin, 2004). The process of micelle formation is driven by the decrease in free energy within the system, because hydrophobic blocks are removed from the aqueous surroundings, whereas hydrophilic blocks form hydrogen bonds with water (Jones and Leroux, 1999). The van der Waal interaction between hydrophobic blocks also contributes to the formation of a micelle core (Jones and Leroux, 1999). Generally, these particles are spherical in shape with a size in the nanometer range (Torchilin et al., 2003). The size of PEG-PE micelles ranges between 7 and 35 nm depending on the molecular weight of the PEG block, with higher molecular weights giving larger micelles (Lukyanov and Torchilin, 2004; Torchilin, 2007a).

Similar to polymeric micelles, the stability of lipid-core micelles is determined by their CMC; that is, the

concentration at which the copolymer chains start to associate themselves to form micelles (Jones and Leroux, 1999). It was found that many PEG-PE conjugates have CMCs in a range of $10^{-5}$ M, which is at least 100-fold lower than those of conventional detergents (Rosen and Kunjappu, 2012). The low CMC values mean that PEG-PE conjugates will be able to maintain their micellar structure under strong dilution (Lukyanov and Torchilin, 2004). Furthermore, it was reported that micelles prepared from DSPE-$PEG_{2000Da}$ and DSPE-$PEG_{5000Da}$ were able to maintain their size characteristics in blood plasma, even after a 48 hour incubation (Lukyanov et al., 2002). This observation suggested that the structure and integrity of DSPE-PEG micelles is not affected instantly by plasma components upon systemic administration (Lukyanov et al., 2002).

Drugs can be loaded into PEG-PE micelles by simply mixing PEG-PE conjugates and a drug of interest in a miscible volatile organic solvent and evaporating the solvent to form a dry PEG-PE film containing the appropriate drug (Lukyanov and Torchilin, 2004). The dry film is then hydrated with an aqueous buffer and shaken intensively to form micelles (Lukyanov and Torchilin, 2004). The drug loading efficiency of compounds within lipid-core micelles is believed to be correlated with the hydrophobicity of the compound (Lukyanov and Torchilin, 2004). The loading efficiency can be improved by the addition of another micelle-forming compound, such as egg PC (Gao et al., 2003; Krishnadas et al., 2003). For example, it was demonstrated that ~33 mg of PTX/g of micelle-forming material was encapsulated within PEG-PE-egg PC micelles (Gao et al., 2003) compared with only 15 mg/g in the case of PEG-PE micelles (Gao et al., 2002).

The effectiveness of PEG-PE micelles as a drug carrier has been investigated both in vitro and in vivo. For instance, PEG-PE-egg PC micelles containing PTX were reported to have comparable cytotoxicity as free PTX against a wide variety of different cancer cell types (Alkan-Onyuksel et al., 1994; Krishnadas et al., 2003). The administration of PEG-PE micelles containing radioactive indium-111 into mice with Lewis lung carcinoma (LLC) or EL4 T lymphoma (EL4) tumor xenografts further revealed that these lipid-core micelles had a circulation half-life of 1.2–2.0 hours. This was dependent on the molecular size of PEG, with the larger PEG block increasing the micelle circulation time (Lukyanov et al., 2002). However, the circulation time of PEG-PE micelles in the blood was reported to be shorter than PEGylated liposomes in the LLC tumor mouse model (Weissig et al., 1998). This finding was believed to be due to the faster rate of extravasation from the blood vessels due to their smaller size compared with liposomes (Weissig et al., 1998). The shorter circulation time was associated with higher accumulation of PEG-PE micelles than PEGylated liposomes in the LLC tumor, which has a small vasculature size cut-off (Weissig et al., 1998). Moreover, PEG-PE micelles were able to accumulate within LLC and EL4 tumors in mice more efficiently in comparison with normal muscle tissue, suggesting that PEG-PE micelles were more selective for tumors than normal tissues (Lukyanov et al., 2002; Lukyanov et al., 2003).

The efficiency of drug-loaded PEG-PE micelles can be improved by actively targeting cancer cells, which enhances the internalization of these micelles. As an appropriate example, the monoclonal antibody 2C5 has been conjugated to PEG-PE micelles to form 2C5-immunomicelles (Torchilin et al., 2003). These targeted micelles demonstrated higher binding capacity to LLC cells, EL4 cells, and human mammary adenocarcinoma cells (BT20) than nontargeted micelles (Torchilin et al., 2003). The accumulation of 2C5 PEG-PE immunomicelles containing PTX was also investigated in the LLC tumor mouse model (Torchilin et al., 2003). It was observed that the accumulation of these micelles within LLC tumors was ~30% higher than nontargeted micelles (Torchilin et al., 2003). Furthermore, the weight of the excised tumor was 2–3 times less in mice treated with 2C5 PEG-PE immunomicelles containing PTX compared with those treated with free PTX or nontargeted PTX encapsulated micelles (Torchilin et al., 2003). Alternatively, cationic lipids can be added to PEG-PE micelles to enhance intracellular drug release (Wang et al., 2005). It was demonstrated that the addition of cationic Lipofectin lipids to PEG-PE micelles could destabilize the endosomal membrane, releasing micelles containing PTX into the cytoplasm of BT20 cells (Wang et al., 2005). This observation was also associated with a higher cytotoxic effect of cationic PEG-PE micelles containing PTX compared with free PTX or normal PTX encapsulated micelles in both BT20 and human ovarian carcinoma (A2780) cells (Wang et al., 2005).

Other polymers can also be used to conjugate to PE to form lipid-core micelles. For more information on lipid core micelles, please see Lukyanov and Torchilin (2004) and Torchilin (2007a).

## III. Characteristics and Properties of Lipid-Based Nanoparticles

### *A. Morphology of Lipid-Based Nanoparticles*

Due to the most common modes of nanoparticle preparation technology available on the market, most nanoparticles are usually spherical (Wacker, 2013). However, this is not the case for lipid-based nanoparticles, such as liposomes. For these particles, the spherical shape is not induced by the preparative procedure but is a result of the electrostatic interaction between the polar or ionogenic phospholipid head group and the solvent medium and the nature of nonpolar lipid hydrocarbon moieties in the solvent (Bangham et al., 1965; Lasic, 1982). However, it has been shown

that it is possible to alter the shape of lipid-based nanoparticles by manipulating the inner compartment of these particles (Miyata and Hotani, 1992; Bunjes et al., 2001; Nickels and Palmer, 2003; Jores et al., 2004; Hasan et al., 2012). In liposomes encapsulating actin polymers, the polymerization of actin led to the deformation of spherical liposomes into dumbbell- and disk-shape particles (Miyata and Hotani, 1992; Nickels and Palmer, 2003). For other types of lipid-based nanoparticles, Particle Replication in Non-Wetting Template Technology has been used to produce polymeric core of lipid-polymer hybrid nanoparticles (LPNs) in a needle-like shape that is subsequently coated with phospholipids (Hasan et al., 2012). Furthermore, changes in the lipid type and composition of the lipid mixture during the preparation of solid lipid nanoparticles (SLNs) and nanostructured lipid carriers (NLCs) can lead to platelet-shaped particles (Bunjes et al., 2001; Jores et al., 2004) rather than spherical particles (Saupe et al., 2006; Luo et al., 2011). These alterations in components can further lead to a phase separation between liquid oil and solid lipid in the NLCs, resulting in platelet-shaped particles with an oil droplet on the surface (Bunjes et al., 2001; Jores et al., 2004).

In general, the shape of nanoparticles does have an effect on their cellular uptake and circulation time (Chithrani et al., 2006; Geng et al., 2007; Gratton et al., 2008; Wang et al., 2011). It is speculated that lipid-based nanoparticles would follow the same trend as other nanoparticles (Hasan et al., 2012). However, a direct comparison between different shapes of lipid-based nanoparticles has not been investigated. Although, in the case of SLNs and NLCs, changes in the shape of the particle can lead to a change in encapsulation efficiency (Jores et al., 2004, 2005). It has been suggested that platelet-shaped SLNs and NLCs exhibited no advantage in terms of drug incorporation rate compared with spherical particles because of a less than maximum volume available for drug encapsulation (Jores et al., 2004, 2005).

In addition, lamellarity also determines the stability, drug loading capacity, as well as drug release properties of liposomes (Maestrelli et al., 2006; Wacker, 2013; Pignatello et al., 2015). A higher degree of lamellarity often gives a more stable liposome vesicle compared with a vesicle with fewer layers (Tayebi et al., 2012). It was reported that vesicles with high lamellarity were able to resist deformation by osmotic stress and were more stable to changes in temperature (Tayebi et al., 2012).

Lamellarity can also affect the encapsulation efficiency of liposomes (Maestrelli et al., 2006; Pignatello et al., 2015). As MLVs contain multiple phospholipid bilayers, they are generally bigger than LUVs and SUVs (Vemuri and Rhodes, 1995). However, MLVs could only provide a comparable or slightly higher encapsulation efficiency than LUVs and SUVs, which are significantly smaller. For instance, MLVs of $3.71 \pm 0.1$ $\mu$m could entrap $75.1 \pm 0.7\%$ of the ketoprofen-cyclodextrin complex, whereas LUVs of $1.85 \pm 0.04$ $\mu$m were able to entrap $61.6 \pm 0.8\%$ of this complex (Maestrelli et al., 2006). In addition, SUVs that are only $0.26 \pm 0.01$ $\mu$m in size were able to encapsulate $54.8 \pm 1.1\%$ of the same complex (Maestrelli et al., 2006). A similar trend was also observed in liposomes encapsulating luteinizing hormone-releasing hormone (Pignatello et al., 2015). MLVs with a size larger than 2 $\mu$m were able to encapsulate 78.8—81.4% of luteinizing hormone-releasing hormone, whereas LUVs that were 241–269.5 nm in size could incorporate 66.7–77.9% of the same hormone (Pignatello et al., 2015).

Additionally, lamellarity may also have some influence over the release profile of drug encapsulated liposomes. It was reported by Maestrelli et al. (2006) that LUVs demonstrated a slower drug release profile for the ketoprofen-cyclodextrin complex than MLVs for all time points under investigation. The authors of this paper speculated that such results were due to the LUVs preparation method used, which allowed the generation of a liposomal dispersion of greater density and viscosity (Maestrelli et al., 2006), and thus, reflecting the higher phospholipid concentration per given volume of sample.

It is noteworthy that in terms of size and size distribution, the morphology of nanoparticles plays a role in the accuracy of their measurement (Wacker, 2013). The size and polydispersity of colloidal particles are usually measured by either dynamic light scattering or laser diffraction technology. These technologies require colloids with a spherical shape and a known refractive index for the medium and particles to achieve an adequate correlation between the signal and particle size (Ross Hallett, 1994). In fact, without prior knowledge of the particle shape, data obtained from dynamic light scattering is often interpreted with an assumption that particles are spherically shaped (Pencer and Hallett, 2003). This particular issue was observed in platelet-shaped SLNs and NLCs in which a relatively high polydispersity index was recorded for both types of lipid nanoparticles, indicating increased inaccuracy of size and size distribution measurement (Jores et al., 2004). Hence, particle morphology determines the accuracy of the size and size distribution of colloidal particles.

### *B. Size and Size Distribution*

Particle size is one of the most important parameters that governs the biodistribution and elimination of a colloidal drug delivery system (Wacker, 2013). Unlike microspheres, nanosized drug delivery systems are not filtered out by the capillary bed of the lungs after initial intravenous injection (Kreuter, 1994). However, rapid urinary excretion and renal elimination was observed

with particles exhibiting a hydrodynamic diameter below 5.5 nm (Choi et al., 2007). For larger particles that are not subjected to renal clearance, it is believed that these particles accumulate within the spleen and to a larger extent within the liver (Moghimi et al., 1993a; Moghimi et al., 1993b). Regardless of whether nanoparticles are coated with a stealth component or not, particles with a hydrodynamic diameter of more than 200 nm exhibit a faster rate of intravascular clearance via splenic filtration and hepatic sequestration than those with a hydrodynamic diameter of less than 200 nm (Moghimi et al., 1993b). There is also evidence that nanoparticles with a diameter between 150 and 250 nm are taken up by the bone marrow (Porter et al., 1992). However, bone marrow uptake was extremely low and contributed to only 0.05–1% of total nanoparticles in comparison with the liver (~60–90%) and spleen (~2–20%) (Kreuter, 1994).

In the spleen, uptake of lipid-based nanoparticles, such as liposomes, has been shown to be directly dependent on size (Litzinger et al., 1994; Awasthi et al., 2003). It was demonstrated by Litzinger et al. (1994) that an increase in liposome size (from 67.8 to 338 nm) resulted in higher liposome uptake in the spleen of C57BL/6 mice with colonic adenocarcinoma. A similar trend in splenic uptake of liposomes was also observed in a rabbit model when liposomal size was increased from 136.2 to 318 nm (Awasthi et al., 2003). In fact, a direct correlation between liposomal size and spleen uptake ($R^2$ = 0.98) could be observed in this rabbit model (Awasthi et al., 2003).

In the liver, the relationship between particle size and hepatic uptake is less obvious for lipid particles. For instance, it was reported that in a healthy human liver, the hepatic sinusoidal endothelial cells contain fenestrae with a pore size of 107 ± 1.5 nm in diameter (Wisse et al., 2008). This should allow particles with a diameter of no more than 100 nm to pass through and interact with parenchymal cells (Nagayasu et al., 1999). However, a study examining radioactive particles was unable to detect small liposomes (i.e., less 100 nm in diameter) within areas consisting of parenchymal cells (Litzinger et al., 1994). In fact, it is believed that most liposomes internalized by the liver are localized to Kupffer cells, regardless of their size (Litzinger et al., 1994). In contrast, liposomes prepared from phosphatidylserine with a size between 200 and 400 nm were found in both hepatic parenchymal cells and Kupffer cells in almost equal amounts, despite being larger than the endothelial fenestrae pore size (Daemen et al., 1997). Moreover, Awasthi et al. (2003) have reported that small and large liposomes (136.2 and 318.0 nm, respectively) were taken up more readily by the liver than liposomes that were 165.5–275.0 nm in size. In this study, larger liposomes were taken up by the liver to the greatest extent (Awasthi et al., 2003). It is notable that fenestrae size in the endothelium may vary between different species (Litzinger et al., 1994; Daemen et al., 1997; Awasthi et al., 2003), and this factor is also important to consider in terms of the differences in the sizes of the nanoparticles that have been reported to pass into the parenchyma of the liver.

The rapid clearance of nanoparticle drug delivery systems, including liposomes, from the circulation by the liver and spleen is due to the process known as opsonization, which leads to the recognition and subsequent uptake of nanoparticles by the reticuloendothelial system (RES), also known as the mononuclear phagocytic system (Owens and Peppas, 2006). Opsonization is the process by which opsonin proteins present in the blood adhere themselves to particles foreign to the body, making these particles recognizable by phagocytes of the RES (Owens and Peppas, 2006). Consequently, phagocytes sequester these particles and remove them from the circulation. However, if sequestered particles are nonbiodegradable, this may result in the accumulation of particles within RES organs, such as the liver or spleen, leading to toxic side effects (Owens and Peppas, 2006). Fortunately, opsonization can be reduced through surface modification using PEG, which decreases the nonspecific binding of plasma proteins, including opsonin proteins, to the surface of the nanoparticles (Owens and Peppas, 2006). It was shown that non-PEGylated liposomes that were 194 nm in diameter circulated in the blood for a shorter period of time and were taken up more rapidly by the liver than PEGylated liposomes of size 338 nm, despite being smaller (Litzinger et al., 1994).

The accumulation of nanoparticles in tumors is believed to be facilitated by highly permeable tumor blood vessels (Jain and Gerlowski, 1986; Dvorak et al., 1988). There are three possible pathways in which nanoparticles can travel across tumor blood vessels into the tumor interstitial space (Hashizume et al., 2000). These are intercellular openings between endothelial cells, transcellular holes, and endothelial cell fenestrae (Hashizume et al., 2000). However, the size of these pores varies in different types of tumors, tumor microenvironments, and species (Yuan et al., 1995; Hobbs et al., 1998). For instance, the functional pore size of the transvascular gap has been investigated based on the size at which particles, namely sterically stabilized liposomes and latex microspheres, can extravasate and the upper limit where there was no particle extravasation was defined (Yuan et al., 1995; Hobbs et al., 1998). It was found that the transvascular pore size cut-off for human colon adenocarcinoma (LS174T) xenografts was 400–600 nm in diameter (Yuan et al., 1995). In contrast, murine tumor xenografts, such as murine hepatoma (HCa-1) and murine mammary carcinoma (MCa IV), have a transvascular pore size cut-off of 380–550 nm and 1200–2000 nm, respectively (Hobbs et al., 1998). Moreover, the transvascular pore size cut-off was different when the xenograft was grown in a dorsal

chamber or a cranial window (Hobbs et al., 1998). For example, the pore size cut-off of a MCa IV tumor xenograft grown in a dorsal chamber was 1200–2000 nm, whereas the size cut-off was decreased dramatically to 380–550 nm when the same tumor was grown in cranial window (Hobbs et al., 1998). In general, it was suggested that the transvascular pore size cut-off for tumors grown subcutaneously is between ~200 and 1200 nm (Hobbs et al., 1998).

In conclusion, nanoparticle size is an important factor that needs to be considered carefully as it determines the biodistribution of the nanoparticle drug delivery system. Knowledge of the pore size for major sites of nanoparticle accumulation, such as liver and spleen, and for the transvascular opening assists in determining the optimal size of nanoparticles. However, other parameters, such as particle morphology and surface charges, must also be taken into account, which increases the difficultly of the preparation of the final nanoparticle formulation (Wacker, 2013). It should be noted that for liposomes, the deforming capacity of liposomes due to the flexible lipid membrane may also help in squeezing large particles through small intercellular pores (Nagayasu et al., 1999). In most cases, to achieve acceptable circulation time and tumor accumulation, an optimal colloidal size must be between 100 and 300 nm, depending upon surface charge and other parameters (Wacker, 2013).

### *C. Surface Charge*

As nanoparticles exhibit a high surface-to-volume ratio compared with larger particles, it is important that their surface characteristics be assessed and controlled precisely. One crucial marker used in the characterization of the nanoparticle surface charge is the zeta potential (Fig. 3).

When a colloidal particle develops a net charge on its surface, a change in the distribution of ions around the particle occurs, resulting in an increased concentration of oppositely charged ions close to the surface of the particle (Shaw and Costello, 1993). This new arrangement leads to the formation of an electrical double layer around the charged particle (Fig. 3) (Shaw and Costello, 1993). This layer consists of two parts: 1) an inner region called Stern layer, where counterions are strongly associated with the particle; and 2) an outer region called the diffuse layer, where counterions are less strongly associated (Fig. 3). A theoretical boundary exists inside the diffuse layer, where ions and the charged particle form a stable entity. As the particle moves, ions within this theoretical boundary move with it, whereas ions beyond this boundary stay with the bulk fluid (Shaw and Costello, 1993). The potential at this boundary is known as zeta potential, a potential difference between the bulk fluid and the layer of fluid containing oppositely charged ions that are associated with the particle (Fig. 3).

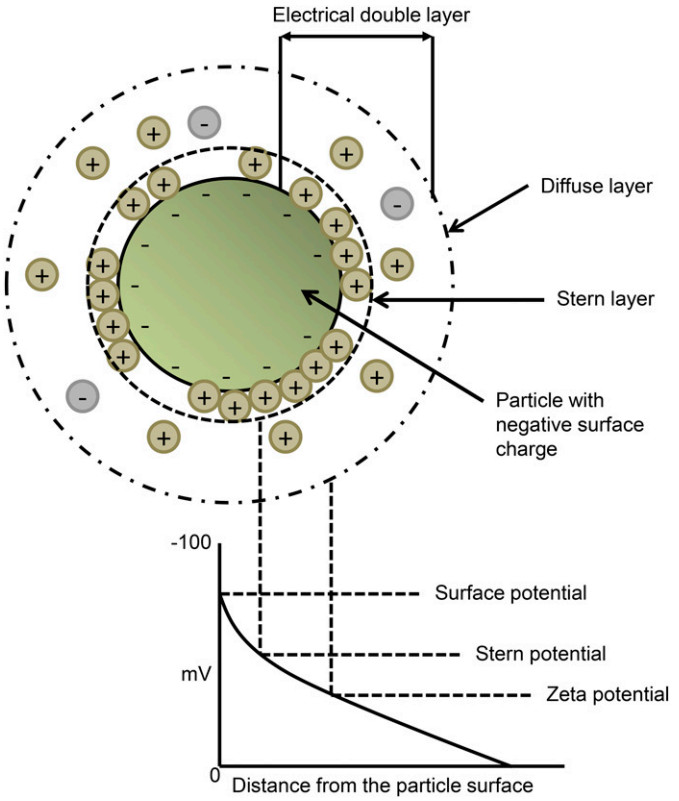


**Fig. 3.** Surface charge and zeta potential of colloidal particles. When a particle develops a net surface charge, oppositely charged ions accumulate around the charged particle surface. This arrangement forms an electrical double layer around the particle consisting of an inner layer called the Stern layer and an outer layer called the diffuse layer. Ions in the Stern layer are strongly bound to the particle, whereas ions in diffuse layer are less strongly associated. A theoretical boundary exists within the diffuse layer in which ions within this boundary form a stable entity with the particle, whereas ions beyond the boundary remain associated with the bulk fluid. Zeta potential is the potential difference between the bulk fluid and the layer of fluid containing oppositely charged ions that is associated with the particle.

When the surface charge of nanoparticles is close to neutral (known as the isoelectric point), the colloidal system is usually unstable and agglomeration takes place (Hunter, 1981; Shaw and Costello, 1993). This colloidal instability and agglomeration can be prevented by increasing the net surface charge of particles within the colloidal system (Hunter, 1981; Shaw and Costello, 1993). This in turn increases the intercolloidal repulsive forces between particles, preventing them from interacting with one another (Hunter, 1981; Shaw and Costello, 1993; Wacker, 2013).

Apart from influencing the stability of the colloidal system, the surface charge also influences the interaction between nanoparticles and their environment, which ultimately controls the biodistribution of nanoparticles within the body (Wacker, 2013). An increase in phagocytosis of poly(lactic-*co*-glycolic acid) (PLGA) microspheres with a positive zeta potential by human macrophages was observed previously (Brandhonneur et al., 2009). In addition, liposomes with an increasing zeta potential value, regardless of the type of charge,

were demonstrated to be removed from the system at a faster rate in mice (Levchenko et al., 2002). A similar trend was also observed in chitosan polymeric nanoparticles (He et al., 2010). He et al. (2010) showed that an increase in surface charge, either positive or negative, resulted in the escalated uptake of chitosan polymeric nanoparticles by murine macrophages. Interestingly, He et al. (2010) further demonstrated that when the absolute zeta potential values were identical, a higher percentage of positively charged nanoparticles were phagocytosed by macrophages compared with their negatively charged counterparts.

As lipid-based nanoparticles, like many other nanoparticles, are generally administered systematically, the interaction between cells and nanoparticles must be taken into consideration. It is believed that the inside surface of blood vessels, as well as the surface of endothelial cells, contain many negatively charged components (Davis et al., 2008). This is because vascular endothelial cells often express a sugar-rich protein coating called the glycocalyx (van Golen et al., 2012; Mitchell and King, 2014). Structurally, the glycocalyx is a network of mostly membrane-bound proteoglycans and some glycoproteins (Fuster and Esko, 2005; Reitsma et al., 2007). It is these proteoglycans that give the glycocalyx a negative charge, because they consist of a protein core covalently attached to various anionic sulfated glycosaminoglycans, namely heparin sulfate and chondroitin sulfate (Fuster and Esko, 2005; Reitsma et al., 2007). A different type of anionic glycosaminoglycan also exists in the glycocalyx called hyaluronic acid, which does not attach itself to core proteins but to the CD44 receptor (Fuster and Esko, 2005; Reitsma et al., 2007; van Golen et al., 2012). Together, the negative charge of glycosaminoglycans and the high molecular density of the glycocalyx help endothelial cells regulate vascular permeability and adhesive interactions between blood components, including nanoparticles, and the cell surface (Reitsma et al., 2007; van Golen et al., 2012). Similarly, cancer cells and tumor endothelial cells have also been associated with the overexpression of glycosaminoglycans, including heparin sulfate, chondroitin sulfate, and hyaluronic acid (Vijayagopal et al., 1998; Park et al., 2002; Davies et al., 2004; Abid et al., 2006; Fears et al., 2006). This may influence the distribution of nanoparticles and the uptake of nanoparticles by these cells (Campbell et al., 2002; Lee et al., 2002; Itano and Kimata, 2008; Mitchell and King, 2014).

Although it is quite certain that surface charge is involved in the nanoparticle-cell interaction, the type of charge beneficial to the delivery of nanoparticles to tumor site is not well understood as contradicting results have been reported. For instance, He et al. (2010) previously demonstrated that polymeric nanoparticles with a slight negative charge and a size of 150 nm in diameter were able to accumulate efficiently within H-22 mouse liver cancer tumors in vivo. In contrast, Lee et al. (2002) showed that the addition of cationic lipids to cisplatin (Fig. 1) encapsulated liposomes increased liposome uptake by human renal adenocarcinoma (ACHN) cells and murine osteosarcoma (LM8G5) cells in vitro and were more effective at reducing tumor growth in mice bearing LM8G5 tumors compared with neutral liposomes containing the same anticancer drug. Moreover, Campbell et al. (2002) reported that increasing the positive charge of liposomes resulted in an increase in liver liposome accumulation and a decrease in liposome blood circulation in mice bearing a human colon adenocarcinoma (LS174T) tumor, while having no effect on tumor uptake. As different studies have given contradicting results, it is difficult to conclude which type of charge is most beneficial for nanoparticle delivery. However, it has been suggested that the use of slightly negatively charged or slightly positively charged nanoparticles may give optimal results. This is because such nanoparticles would undergo minimal self to self and self to non-self-interactions (Davis et al., 2008).

### *D. Phase Transition Temperature*

In contrast to polymeric nanoparticles, which are relatively insensitive to temperature, liposomes undergo changes in viscosity, drug release properties, and interaction with RES upon changes in temperature (Sharma and Sharma, 1997; Wacker, 2013). This is an important factor in liposomal drug delivery, because the encapsulation of hydrophilic molecules occurs within the liposomal aqueous interior surrounded by the phospholipid bilayer, whereas lipophilic molecules are incorporated into the hydrophobic core of the phospholipid bilayer (Allen, 1997; 1998).

Different lipids have unique PTTs and exist in different physical states above or below this temperature (Sharma and Sharma, 1997). Below the PTT, lipids are usually in a more structured and well-ordered orientation (solid gel-like phase), whereas above this temperature, they are usually in a liquid-crystalline (fluid) phase (Sharma and Sharma, 1997). The PTT ultimately determines the fluidity of liposomes (Sharma and Sharma, 1997). By using phospholipids of different PTT, it is possible to alter the fluidity of liposomal bilayers (Sharma and Sharma, 1997; Anderson and Omri, 2004). In the presence of high PTT lipids (PTT $>$ 37°C), liposomal bilayers are usually less fluid and less leaky at physiologic temperature (Sharma and Sharma, 1997). On the other hand, in the presence of a high concentration of low PTT lipids (PTT $<$ 37°C), liposomal bilayers become more prone to leakage, because of their increased fluidity, allowing encapsulated hydrophilic drugs to escape from the liposome interior (Sharma and Sharma, 1997). However, hydrophobic drugs can still remain in the membrane. Furthermore, liposomes prepared from low PTT lipids

also interact more readily with macrophages in comparison with liposomes prepared from high PTT lipids, and thus, increasing their uptake by RES (Gabizon and Papahadjopoulos, 1988).

Apart from changing lipid compositions of liposomes, the addition of different concentrations of cholesterol can also reduce the effect of PTT of liposomes (Sharma and Sharma, 1997). By adding high concentrations of cholesterol, the liposomal bilayer becomes less fluid and less leaky at temperatures above their PTT, making liposomes more stable (Sharma and Sharma, 1997; Anderson and Omri, 2004).

### *E. Plasma Proteins Interactions-Particle Stability and Clearance*

Once nanoparticles are administered into the bloodstream, they can interact with plasma proteins, such as complement proteins (Roerdink et al., 1983; Funato et al., 1992; Wassef and Alving, 1993; Devine et al., 1994; Szebeni et al., 1994), lipoproteins (Pownall et al., 1978; Guo et al., 1980; Surewicz et al., 1986; Comiskey and Heath, 1990; Jian et al., 1997; Williams et al., 1998), immunoglobulins (Derksen et al., 1987; Cullis et al., 1998), and albumin (Guo et al., 1980; Sabin et al., 2009). This interaction is essential, because it determines the stability and clearance behavior of nanoparticles. In particular, lipid-based nanoparticles are more vulnerable to protein destabilization than other nanoparticles, as their interaction with certain proteins can lead to particle deformation and leakage of the encapsulated contents (Guo et al., 1980; Williams et al., 1998).

The interaction between lipid-based nanoparticles and complement proteins has been observed in a study using hemolysis assays (Szebeni et al., 1994). Notably, the injection of either liposomes containing hemoglobin or empty liposomes into rats resulted in a significant reduction in hemolytic complement activity, whereas free hemoglobin showed no effect (Szebeni et al., 1994). This finding suggested that liposomes interacted with complement proteins (Szebeni et al., 1994). The decrease in hemolytic complement activity observed was also closely associated with a rise in plasma thromboxane $B_2$ levels, indicating that the complement system was activated by liposomes (Szebeni et al., 1994). The interaction of lipid-based nanoparticles, such as liposomes, with complement proteins can lead to the uptake of these particles by macrophages of the RES through opsonization (Roerdink et al., 1983; Wassef and Alving, 1993). For instance, it was demonstrated in vitro that when galactosyl ceramide encapsulated liposomes opsonized with antigalactosyl ceramide antibodies were added to cultured mouse peritoneal macrophages in the presence of guinea pig complement, the uptake of these liposomes by macrophages increased 5- to 10-fold relative to nonopsonized liposomes (Roerdink et al., 1983). The uptake of liposomes opsonized with antibodies was reduced only when cultured macrophages were preincubated with metabolic inhibitors, suggesting that phagocytosis was inhibited (Roerdink et al., 1983). The interaction between liposomes and activated complement has also been shown to result in the destabilization of liposomes (Funato et al., 1992). It was reported that 25% of 5(6)-carboxyfluorescein was released from liposomes 15 minutes after being exposed to fresh rat plasma, whereas the same marker was not released from liposomes in phosphate-buffered saline for at least 60 minutes (Funato et al., 1992). The rapid release of 5(6)-carboxyfluorescein was completely inhibited when the plasma was preheated at 56°C for 30 minutes or pretreated with the chelating agent EDTA (Funato et al., 1992). These treatments are known to inactivate the complement system, because heat denatures proteins, whereas EDTA can chelate $Ca^{2+}$ and $Mg^{2+}$ ions, which are important for complement activation (Funato et al., 1992). Interestingly, three studies have shown that certain negatively charged phospholipids, such as phosphatidylserine and phosphatidylinositol, were able to suppress complement activation (Roerdink et al., 1983; Wassef and Alving, 1993; Devine et al., 1994).

Among plasma proteins, lipoproteins and their apolipoproteins, in particular, are a very important factor in liposome stability, because they are able to disrupt liposomes, resulting in the release of their encapsulated contents (Guo et al., 1980; Comiskey and Heath, 1990). It is primarily high density lipoprotein and its apolipoproteins that are responsible for this liposomal disruption (Pownall et al., 1978; Surewicz et al., 1986; Jian et al., 1997; Williams et al., 1998). The destabilization and solubilization of liposomes was observed when large multilamellar liposomes were incubated with human plasma apolipoprotein A-I isolated from high density lipoproteins at their PTT (Pownall et al., 1978; Surewicz et al., 1986). The incubation resulted in the disappearance of a turbid dispersion of liposomes and the formation of lipid-protein complexes, suggesting that these particles were solubilized by the apolipoproteins (Pownall et al., 1978; Surewicz et al., 1986). The rapid leakage of carboxyfluorescein (Guo et al., 1980) and methotrexate-γ-aspartate (Comiskey and Heath, 1990) from liposomes was also observed when exposed to lipoproteins and apolipoproteins. In the case of methotrexate-γ-aspartate encapsulated anionic liposomes, drug leakage was reduced significantly when lipoproteins were removed from the serum and the degree of leakage was suggested to be dependent on the phospholipid acyl chain length (Comiskey and Heath, 1990). The same study further suggested that the destabilization of liposomes by lipoproteins may be, in part, due to electrostatic interaction, because neutral liposomes demonstrated significantly lower leakage than negatively charged liposomes (Comiskey and Heath, 1990). The leakage of liposomal content was often associated with the formation of disc-like particles

(Guo et al., 1980). This is possible because apolipoproteins can insert their amphipathic helical domains into the liposomal bilayer, disturbing the phospholipid packing (Williams et al., 1998). This insertion, together with the phospholipid solubilizing capacity of apolipoproteins, breaks liposomes into disc-like particles, leading to leakage of liposomal content (Williams et al., 1998). The discoidal particles are then stabilized by the amphipathic helical domains, shielding the phospholipid acyl chains from contact with water (Williams et al., 1998).

Other plasma proteins, such as immunoglobulins and albumin, have been reported to have an effect on liposome clearance and stability (Guo et al., 1980; Derksen et al., 1987; Sabin et al., 2009). For instance, rabbit IgG antibodies covalently attached to liposomes have been reported to increase liposome uptake by rat Kupffer cells (Derksen et al., 1987). In addition, liposome destabilization was reported to occur upon incubation with bovine serum albumin (Guo et al., 1980). However, the destabilizing effect may have been caused by the small contamination of lipoproteins within commercial albumin preparations (Guo et al., 1980). Recently, both IgG and albumin were reported to penetrate the liposomal bilayer, but liposome disruption was not observed during the interaction (Sabin et al., 2009). For more information on liposome-protein interactions, please refer to Williams et al. (1998), Cullis et al. (1998), and Ishida et al. (2002).

## IV. Tumor Targeting of Lipid-Based Nanoparticles

As conventional chemotherapeutic agents exhibit only some tumor specificity and affect both normal and tumor cells to a certain degree, the effective dose required for the treatment of cancer is not optimal due to the toxicity that concurrently occurs. The tumor targeting ability of nanoparticle drug delivery systems, including lipid-based nanoparticles such as liposomes, represents an appealing strategy to increase anticancer drug selectivity toward tumor cells while reducing toxicity to their normal counterparts.

By specifically targeting tumor cells, nanoparticles are able to: 1) improve the drug's pharmacokinetics and pharmacodynamics profile; 2) control and sustain the release of drug; 3) increase the drug's specificity toward tumor cells; 4) enhance the internalization and intracellular delivery of drugs; and 5) reduce the drug's systemic toxicity (Danhier et al., 2010). Tumor targeting consists of two types of approach, passive targeting and active targeting, and these are described in detail below.

### *A. Passive Targeting*

Passive targeting makes use of the properties of the delivery system and the disease anatomy to specifically accumulate the drug at a targeted site and avoid nonspecific distribution (Fig. 4) (Ganta et al., 2008).

Tumor blood vessels are different from normal blood vessels in many ways. They are generally characterized by abnormalities, such as high proportions of proliferating endothelial cells, pericyte deficiency, and aberrant basement membrane formation (Danhier et al., 2010). As a result of these irregularities, most tumor blood vessels exhibit enhanced vascular permeability and are known to be leaky (Danhier et al., 2010). It is believed that particles in a size range between 10 and 500 nm can extravasate and accumulate inside the tumor interstitial space, because leaky blood vessels in most peripheral tumors are made up of porous endothelial lining with a pore size estimated to be between ~400 and 600 nm in diameter (Yuan et al., 1995; Torchilin, 2000; 2007b). Apart from enhanced vascular permeability, tumors also exhibit a nonfunctional lymphatic system, which contributes to ineffective drainage within tumor tissues (Matsumura and Maeda, 1986; Danhier et al., 2010). Consequently, any nanoparticles entering tumors are not efficiently removed by the lymphatic system, causing nanoparticle accumulation within the tumor (Maeda et al., 2001; Maeda et al., 2009). These two factors together form a passive phenomenon called the enhanced permeability and retention (EPR) effect, which was discovered by Matsumura and Maeda and plays a major role in the passive targeting of drugs and nanoparticles (Fig. 4) (Matsumura and Maeda, 1986; Maeda et al., 2001; Maeda et al., 2009). The characteristics of tumor and tumor blood vessels, such as: 1)

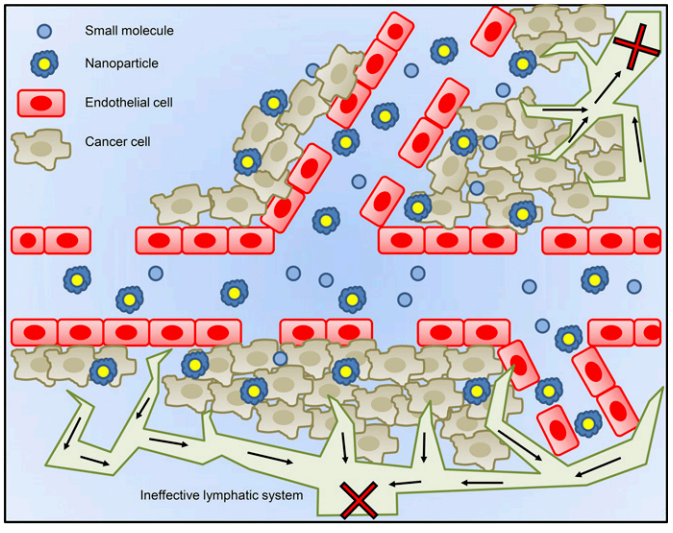


**Fig. 4.** Passive targeting of nanoparticles. Passive targeting uses the properties of the delivery system and the disease anatomy to specifically accumulate the encapsulated substance at a targeted site. Passive targeting of tumors by nanoparticles relies on a phenomenon called the enhanced permeability and retention (EPR) effect. The EPR effect is caused by the enhanced permeability of tumor blood vessels and an ineffective lymphatic system. Highly permeable tumor blood vessels allow nanoparticles ranging between 10 and 500 nm to extravasate and accumulate within the tumor interstitial space, whereas a dysfunctional lymphatic system prevents effective drainage within the tumor tissue. Thus, this further promotes the accumulation of nanoparticles within the tumor.

extensive angiogenesis; 2) hypervasculature; 3) inconsistent and turbulent blood flow; and 4) slow venous return that leads to particle accumulation within the tumor interstitium, also help contribute to the EPR effect in passive targeting (Danhier et al., 2010).

In 1987, Jain (1987) suggested that tumor interstitial fluid pressure must be high due to the tumor architecture. It is now well recognized that most solid tumors display an increased interstitial fluid pressure (Danhier et al., 2010). Although vascular abnormalities enhance nanoparticle transport across tumoral blood vessels into the tumor interstitial space, an increased tumor interstitial fluid pressure may impede efficient nanoparticles transcapillary movement into tumors (Jain, 1987). The interstitial fluid pressure is believed to be higher at the center of the tumor and is diminished toward the periphery (Boucher et al., 1990; DiResta et al., 1993; Heldin et al., 2004). This pressure gradient may result in the movement of fluid away from the central region of the tumor, reducing the ability of nanoparticles to reach the inner tumor mass (Danhier et al., 2010). However, nanoparticles of greater size (larger than 10 kDa) have been shown to be less affected by an increase in interstitial fluid pressure and are able to successfully overcome this barrier to accumulate within tumors (Heldin et al., 2004; Bouzin and Feron, 2007). This is a result of their size as well as the high magnitude of microvasculature pressure, which facilitates the extravasation of nanoparticles into tumors (Jain, 1987; Heldin et al., 2004; Bouzin and Feron, 2007).

The manipulation of nanoparticle size and surface charge, as well as the addition of PEG or poly(ethylene oxide), can further help to improve the effectiveness of passive targeting (Ganta et al., 2008). Nanoparticles less than 200 nm in diameter and those with a slight positive charge are known to preferentially accumulate within the tumor for a longer period of time than either neutral or negatively charged nanoparticles (van Vlerken et al., 2007; Ganta et al., 2008). In addition, the surface modification of nanoparticles with either PEG or poly(ethylene oxide) also allows for an increase in nanoparticle circulation time by reducing opsonin adhesion and opsonization, and thus, lowering nanoparticle recognition by RES (Ganta et al., 2008). This ultimately increases nanoparticle accumulation in solid tumors, as shown by stealth PEGylated doxorubicin-loaded liposomes (Doxil) (Noble et al., 2004) and poly(ethylene oxide)-modified poly($\varepsilon$-caprolactone) nanoparticles containing tamoxifen (Shenoy and Amiji, 2005).

Once passive targeting is completed, namely when the delivery system has accumulated passively within the tumor site, the active targeting process can then potentially occur (Bae, 2009).

### *B. Active Targeting*

Apart from passive targeting, nanoparticle drug delivery systems can be modified to be more selective toward cancer cells by means of active targeting. In active targeting, specific ligands (Table 1) recognized by cells at the disease site are coupled to the surface of nanoparticles (Figs. 5 and 6), and thus, allowing them to interact specifically with tumor cells.

The most common approach for active targeting is the use of a ternary structure composed of: a ligand or an antibody as a targeting moiety, polymers or lipids as a carrier, and an active pharmaceutical (Fig. 5) (Cho et al., 2008). When preparing ternary structures, some factors relating to the targeting moiety used must be considered to generate an effective delivery system. First, a cellular receptor and its ligand should exhibit properties that make them suitable as a tumor-specific target. For example, the receptor should be overexpressed on cancer cells and not expressed on normal

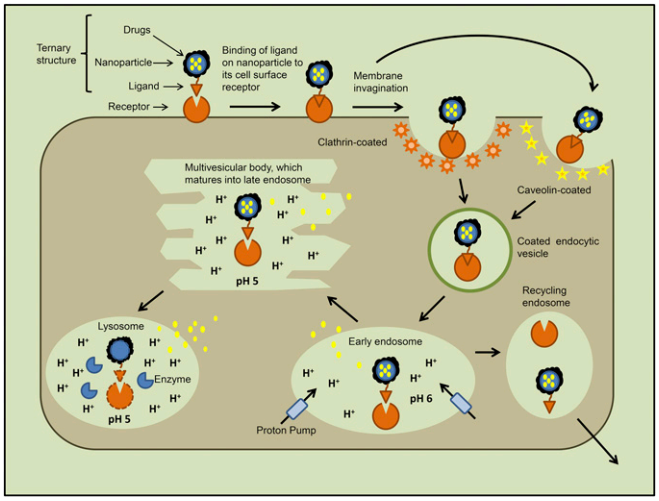


**Fig. 5.** Uptake of nanoparticles via receptor-mediated endocytosis. In the process of receptor-mediated endocytosis, one of the ligands on the surface of the nanoparticle binds to its cell surface receptor forming a ligand-receptor complex. Consequently, the plasma membrane forms an invagination surrounding the ligand-receptor complex preparing it for cellular internalization. This process is often assisted by clathrin or caveolin proteins, depending on the type of ligands and receptors, and results in the formation of an endocytic vesicle. The resulting vesicle is coated with either clathrin or caveolin. Once dissociated from the membrane, the coated endocytic vesicle travels through the cytoplasm to fuse with an early endosome, also known as a sorting endosome. As the early endosome matures, vacuolar ATPase pumps are recruited to pump $H^+$ ions into its lumen decreasing the pH to ~5–6. The decrease in pH facilitates the dissociation of the ligand from its receptor by causing conformational changes to the receptor. The reduced pH also facilitates the release of the encapsulated drug from the nanoparticle by partial degradation. At this point, the receptor and its ligand will either get recycled back to the plasma membrane or continue along the endolysosomal pathway for lysosomal degradation in a late endosome. However, this depends on the receptor and ligand under consideration. If the receptor and its ligand get recycled, they will be sorted to a recycling endosome, which travels to the plasma membrane. Such a receptor and ligand may be of limited use to drugs requiring intracellular accumulation for therapeutic action. If the receptor and its ligand continue along the endolysosomal pathway, it will enter into the multivesicular body, which matures into the late endosome. In the process of maturation from an early endosome into a late endosome, the pH decreases further to ~5, allowing more encapsulated drug to be released from the nanoparticle. Finally, the late endosome fuses with the lysosome where its content is degraded by the lysosomal enzymes in the acidic pH. This further allows more encapsulated drug to be released from the nanoparticle.

cells (Cho et al., 2008). Second, the chosen receptor should be expressed homogeneously on the surface of all targeted cancer cells (Cho et al., 2008; Danhier et al., 2010). Third, once the ligand binds to its receptor, the ligand-receptor complex should not be discharged into the blood circulation (Cho et al., 2008). Finally, the ligand-receptor complex must be internalized into the targeted cell after binding (Cho et al., 2008). These factors are important criteria for active targeting, because they determine the effectiveness of the receptor and its ligand as a candidate for such targeting.

The internalization of a ligand-receptor complex usually occurs via receptor-mediated endocytosis assisted by proteins, namely caveolin-1 or clathrin (Fig. 5). In the process of internalization, the plasma membrane forms an invagination enveloping the ligand-receptor complex forming an endocytic vesicle (Bareford and Swaan, 2007). The vesicle then enters into the cytoplasm, where it fuses with an early or sorting endosome (Bareford and Swaan, 2007). As the early endosome matures, vacuolar ATPase pumps are recruited to the endosome for the purpose of transporting $H^+$ ions into the endosome decreasing the endosomal pH to as low as ~5.0 (Clague et al., 1994; Lee et al., 1996; Nishi and Forgac, 2002).

The increased acidity within the early endosome can cause many receptors to change conformation, and thus, allows associated ligands to be released (Rudenko et al., 2002; Kamen and Smith, 2004). At this point, the receptor and its ligand will either get recycled back to the plasma membrane or continue along the endolysosomal pathway for lysosomal degradation in a late endosome depending on the receptor/ligand combination under consideration (Lakadamyali et al., 2006; Bareford and Swaan, 2007). For instance, the transferrin receptor together with its ligand, the low-density lipoprotein receptor, and the folate receptor are believed to be recycled back to the plasma membrane (Morgan, 1981; Anderson et al., 1982; Dautry-Varsat et al., 1983; Hopkins and Trowbridge, 1983; Paulos et al., 2004). In contrast, low-density lipoprotein, the epidermal growth factor receptor (EGFR) together with its ligand, and $\alpha$-2-macroglobulin are transported to multivesicular bodies, which mature into late endosomes for lysosomal degradation (Carpenter and Cohen, 1979; Van Leuven et al., 1980; Goldstein et al., 1985). It is important to note that the exact mechanism by which various types of endocytosis occur still remains unclear and requires further investigation.

For active targeting drug delivery, the final destination of the receptors and ligands may not be the main determinant of the efficacy of delivered drugs. Rather, their effectiveness depends more heavily on the chemical properties of the drugs, such as net ionic charge, log *P* value, and amphiphilicity (Weijer et al., 2015). For instance, the recycling of receptors and ligands to the plasma membrane may be of limited use to certain drugs, which require intracellular accumulation for therapeutic action (Bareford and Swaan, 2007). However, the same receptors and ligands may be beneficial for lipophilic drugs, namely lipophilic photosensitizers used for photodynamic therapy (PDT). These agents will likely remain within the lipid environment of the plasma membrane because of their lipophilicity and cause membrane disruption (Weijer et al., 2015).

Although the active targeting feature of nanoparticles is an attractive strategy in delivering drugs into tumor cells, their internalization pathway and final destination are still unclear and require more studies as contradicting results have been reported (Turek et al., 1993; Paulos et al., 2004; Chang et al., 2009). For instance, Turek et al. (1993) showed that transferrin-coated colloidal gold particles followed the same pathway as transferrin and transferrin receptor through clathrin-dependent, receptor-mediated endocytosis. In contrast, Chang et al. (2009) demonstrated that transferrin-coated PLGA nanoparticles were internalized via caveolin-assisted, receptor-mediated endocytosis within the blood-brain barrier. These investigators demonstrated that a caveolae inhibitor (filipin) was able to inhibit the uptake of transferrin-coated PLGA nanoparticles but not empty nanoparticles and albumin-coated nanoparticles (Chang et al., 2009). Turek et al. (1993) also showed that folate-protein-conjugated colloidal gold particles resided mainly in multivesicular bodies with some particles localized to secondary lysosomes and cytoplasm after 6 hours. However, Paulos et al. (2004) observed that only ~10–25% of $^{111}$In labeled folate-conjugated diethylene triamine pentaacetic acid-ethylenediamine-$\gamma$ was internalized by cancer cells, suggesting that the majority of folate conjugates either remained on the cell surface or were recycled through cell interior without unloading. This is possible because the intracellular folate content regulates the receptor-mediated accumulation of folate (Kamen and Capdevila, 1986).

In active targeting, there are two cellular targets in which nanoparticles can be directed to: 1) cancer cells, and 2) tumoral endothelium (Fig. 6) (Danhier et al., 2010).

*1. Cancer Cell Targeting.* The aim of cancer cell targeting is to improve the cellular uptake of nanoparticles into these cells (Fig. 6). In this strategy, it is the enhanced cellular internalization rather than the enhanced tumor accumulation that improves the efficacy of nanoparticles (Kirpotin et al., 2006). This cellular targeting will also cause a direct cell kill from the release of an encapsulated drug rather than starving cancer cells of nutrients and oxygen by blocking tumor vasculature (Pastorino et al., 2006). The following list of receptors and specific cell surface moieties (Table 1) are capable of being internalized and have been studied extensively with nanoparticles for active cancer cell targeting (Danhier et al., 2010), namely,

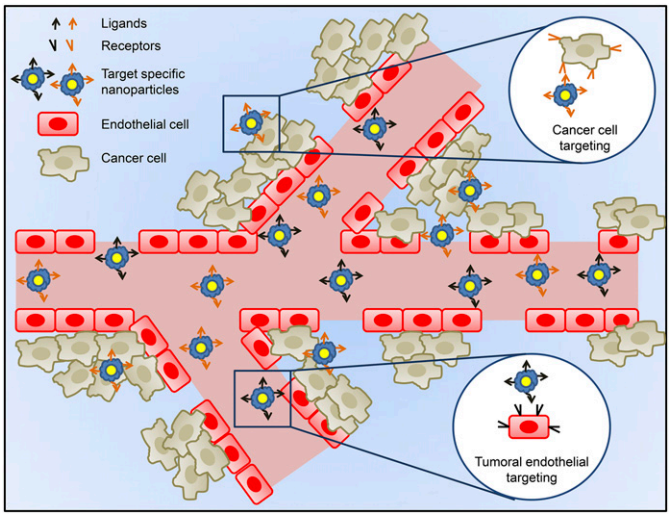


**Fig. 6.** Active targeting of nanoparticles to cancer tumors. In active targeting, specific ligands recognized only by cells at the disease site are coupled on to the surface of nanoparticles, allowing them to interact specifically with these cells. Active targeting can only occur once passive targeting is completed. This means it can only take place after nanoparticles have accumulated passively at the disease site. For the treatment of cancer, there are two cellular targets in which nanoparticles can be directed to via active targeting, namely, cancer cells and tumoral endothelium. The targeting of cancer cell aims at improving the uptake of nanoparticles by these cells. In contrast, the targeting of tumoral endothelium aims to kill cancer cells indirectly by starving them of oxygen and nutrients.

transferrin receptor, folate receptor, cell surface glycoproteins, epidermal growth factor receptor (EGFR), and ssDNA and RNA aptamers.

*a. Transferrin receptor.* Transferrin is a serum glycoprotein involved in the transport of iron throughout the body and into cells (Richardson and Ponka, 1997). To deliver iron to the cell, transferrin binds to the transferrin receptor, which subsequently internalizes transferrin into the cell via receptor-mediated endocytosis. As iron is vital to cellular proliferation, cancer cells exhibit a higher level of surface transferrin receptors than normal cells (Richardson and Baker, 1990; Richardson and Baker, 1992; Trinder et al., 1996; Kalinowski and Richardson, 2005). It is believed that there may be up to a 100-fold higher level of expression of transferrin receptor on the surface of cancer cells than on normal cells (Prost et al., 1998; Shinohara et al., 2000; Gomme et al., 2005; Daniels et al., 2006). Due to its surface accessibility, ability to internalize, and its significant role in human cancer pathology, the transferrin receptor makes an appealing target for cancer treatment. Thus, the conjugation of transferrin to nanoparticles as an active targeting strategy has been investigated (Chang et al., 2009; Ulbrich et al., 2009).

The effectiveness of transferrin receptor targeting of cancer cells has been investigated both in vitro and in vivo for its use in liposomal formulations (Table 1). In this case, Ishida et al. (2001a) demonstrated that transferrin conjugated to PEGylated liposomes became bound more readily to mouse colon carcinoma (colon 26) cells than nonconjugated PEGylated liposomes by almost ~14-fold (~1.4 versus ~0.1 $\mu$mol lipid/1 $\times$ $10^6$ cells). The increased binding was reduced almost completely in the presence of free transferrin, suggesting that this ligand competitively inhibited receptor-mediated endocytosis of transferrin conjugated liposomes (Ishida et al., 2001a). Liposomal doxorubicin (DOX; Fig. 1) conjugated to transferrin was also investigated in multidrug-resistant human small cell lung cancer SBC-3/ADM for its ability to target transferrin receptors (Kobayashi et al., 2007). In comparison with the free drug and nontargeted liposomal DOX, the transferrin conjugated formulation demonstrated a significantly higher cellular DOX accumulation over the course of a 90-minute incubation (Kobayashi et al., 2007). Furthermore, transferrin conjugated liposomal DOX was also 3.6-fold more cytotoxic than free DOX, suggesting that transferrin receptor targeting has the potential to overcome multidrug resistance in cancer cells (Kobayashi et al., 2007). The transferrin receptor also shows some potential as a targeting moiety in overcoming the blood-brain barrier (Soni et al., 2005). The intravenous administration of technetium $^{99m}$Tc-DTPA encapsulated liposomes conjugated with transferrin into normal albino rats demonstrated a 17-fold and 13-fold higher uptake from brain capillary endothelial cells compared with free $^{99m}$Tc-DTPA and nonconjugated $^{99m}$Tc-DTPA encapsulated liposomes, respectively (Soni et al., 2005).

*b. Folate receptor.* The folate receptor is a well-known tumor marker that binds strongly to its substrate, namely the vitamin folic acid, which is required for the synthesis of nucleotide bases. Apart from folic acid, the folate receptor also exhibits a high affinity for folate-drug conjugates and folate-grafted nanocarriers (Cho et al., 2008; Danhier et al., 2010). Like the transferrin receptor, the folate receptor internalizes folate via receptor-mediated endocytosis (Cho et al., 2008; Danhier et al., 2010).

In a study by Saba et al. (2009), it was demonstrated that the folate receptor was expressed in 45% of patients with primary squamous cell carcinoma of the head and neck and in 40% of patients with corresponding lymph node metastases, whereas 10 normal bone marrow samples from these patients did not show any sign of folate receptor expression. Furthermore, two isoforms of the folate receptor, namely the $\alpha$- and $\beta$-isoforms, are believed to be present on the surface of most cancer cells (Low and Kularatne, 2009). Approximately 40% of human cancers were found to overexpress the $\alpha$-isoform, whereas the $\beta$-isoform was identified on the surface of malignant cells of hematopoietic origin (Low and Kularatne, 2009). As the folate receptor was found to be expressed abundantly on the surface of cancer cells, this receptor represents another attractive target for nanoparticle drug delivery systems (Table 1). In fact, Yang et al. (2014b) reported that human oral cancer

KB cells incubated with folate receptor-targeted liposomes containing calcein exhibited a 31-fold higher fluorescence intensity in comparison to an incubation with nontargeted calcein containing liposomes. These results suggested that more folate receptor-targeted liposomes were taken up by cells than nontargeted liposomes (Yang et al., 2014b). Furthermore, Balb/c nude mice xenografted with KB tumors and treated with folate receptor-targeted liposomes containing the novel anticancer drug, ursolic acid, were reported to have the longest lifespan (56 days) relative to those treated with free drug (42 days) or the nontargeted formulation (47 days) (Yang et al., 2014b).

*c. Cell surface glycoproteins.* As mentioned previously, tumor cells have been associated with the overexpression of cell surface glycoproteins, such as chondroitin sulfate and hyaluronic acid (Lee et al., 2002; Itano and Kimata, 2008; Mitchell and King, 2014). Moreover, glycoproteins expressed on the surface of tumor cells usually contain carbohydrate moieties that are different from those found on normal cells (Bies et al., 2004). Lectins, which are proteins of nonimmunologic origin, can be used to specifically recognize and bind to carbohydrate moieties of these plasma membrane-bound glycoproteins (Bies et al., 2004; Minko, 2004; Danhier et al., 2010). This is because the specificity of lectins for sugar residues of glycoproteins can be as high as those of enzymes and substrates (Bies et al., 2004; Minko, 2004; Danhier et al., 2010). On the other hand, certain lectins are also expressed on the cell surface (Perillo et al., 1998). For instance, galectin-1 and galectin-3 were observed to be upregulated on the surface of colon cancer cells (Lotan et al., 1991; Ohannesian et al., 1994; Schoeppner et al., 1995; Kayser et al., 2001, 2002; Hittelet et al., 2003). This represents a potential use in colon cancer-specific drug delivery (Minko, 2004). There are two approaches in which lectins can be used to develop active-targeting nanoparticles: 1) direct lectin targeting—lectins are coupled on to the surface of nanoparticles as targeting moieties to direct the particles to cell-surface carbohydrates and 2) reverse lectin targeting—carbohydrate moieties are incorporated on to the surface of nanoparticles to target lectins (Bies et al., 2004; Minko, 2004; Cho et al., 2008; Danhier et al., 2010). The lectin, wheat germ agglutinin, was previously investigated as a targeting drug carrier protein for acid labile DOX against the solid cancer cell line human colon carcinoma (Caco-2) (Wirth et al., 1998). DOX conjugated to wheat germ agglutinin showed a binding capacity to colon carcinoma cells that was 4.5-fold higher than normal human colonocytes and lymphoblastic MOLT-4 cells (Wirth et al., 1998). The antiproliferative effect of DOX when conjugated to lectin was also higher in Caco-2 cells than in MOLT-4 cells (Wirth et al., 1998).

Alternatively, glycoproteins can also be used to target their receptors on the cell surface. For instance, the hyaluronic acid receptor has been reported to be overexpressed in several cancer cell types, including human breast epithelial cancer cells (Bourguignon et al., 2000), ovarian cancer cells (Catterall et al., 1999), colon cancer cells (Yamada et al., 1999), and lung cancer (Matsubara et al., 2000). By using this targeting strategy, *N*-(2-hydroxypropyl)methacrylamide linked to hyaluronic acid (which binds to the hyaluronic acid receptor) was conjugated with DOX to examine its specificity and cytotoxicity against various solid cancer-derived cell lines (Luo et al., 2002). By implementing hyaluronic acid conjugation, the cytotoxicity of DOX was higher against human breast cancer (HBL-100), ovarian cancer (SKOV-3), and colon cancer (HCT-116) cells compared with the nontargeted DOX formulation (Luo et al., 2002). This strategy of hyaluronic acid receptor targeting also demonstrated minimal toxicity against normal mouse NIH 3T3 fibroblast cells (Luo et al., 2002).

In addition, hyaluronic acid conjugated to DOX encapsulated liposomes was shown to be internalized by B16F10 murine melanoma cells overexpressing the CD44 receptor more avidly than normal CV-1 African green monkey kidney cells (Eliaz and Szoka, 2001). The $IC_{50}$ of DOX when encapsulated in hyaluronic acid conjugated liposomes (0.6 $\mu$M) was also found to be significantly lower than that of nontargeted liposomal DOX (>172 $\mu$M) and free DOX (6.4 $\mu$M) after 24 hours (Eliaz and Szoka, 2001). This improved specificity and anticancer activity was also reflected in tumor-bearing mice. Additionally, hyaluronic acid conjugated liposomes increased the tumor accumulation of DOX compared with nontargeted liposomes, PEGylated liposomes, and free DOX (Peer and Margalit, 2004b) (Table 1). Hyaluronic acid conjugation to liposomes further demonstrated enhanced antitumor efficacy, reducing tumor growth rate in mice and increased their lifespan significantly compared with other treatments (Peer and Margalit, 2004b). These improvements were observed across various tumors, namely mouse melanoma (B16F10.9), DOX-resistant murine leukemia (P388/ADR), mouse colon carcinoma (C-26), and human adenocarcinoma (PANC-1) (Peer and Margalit, 2004b). These results suggest that hyaluronic acid may be useful in drug delivery by active targeting.

*d. Epidermal growth factor receptor.* EGFR belongs to a family of tyrosine kinase receptors known as the ErbB family (Scaltriti and Baselga, 2006). Upon its activation, EGFR stimulates multiple processes important for tumor growth and progression, including proliferation, angiogenesis, invasion, and metastasis (Scaltriti and Baselga, 2006). EGFR is often overexpressed in different types of cancer, especially in breast cancer (Witton et al., 2003; Abd El-Rehim et al., 2004; Bossuyt et al., 2005). It was reported that EGFR was overexpressed in 15–20% of breast carcinomas (Witton et al., 2003; Abd El-Rehim et al., 2004), whereas human epidermal receptor-2 (HER-2) was found to be highly

expressed in 14–91% of breast cancer patients (Bossuyt et al., 2005). Other solid tumors that express or overexpress EGFR include colorectal cancer, non-small cell lung cancer, squamous cell carcinoma of head and neck, ovarian cancer, kidney cancer, pancreatic cancer, and prostate cancer (Danhier et al., 2010; Lurje and Lenz, 2009). In fact, the specificity of anti-HER-2 scFv antibody fragment conjugated to PEGylated liposomes containing DOX to HER-2 has been studied both in vitro and in vivo (Table 1) (Shmeeda et al., 2009). The in vitro binding of HER-2-targeted liposomes was 10- to 20-fold higher than nontargeted liposomes in two solid cancer-derived cell lines, HER-2 expressing breast cancer (SKBR-3) and human gastric carcinoma (N-87) (Shmeeda et al., 2009). The HER-2-targeted liposomal DOX formulation was also significantly more cytotoxic to cancer cells than the nontargeted formulation, both in vitro and also in vivo in the J6456 ascitic lymphoma mouse model (Shmeeda et al., 2009). The greater in vivo cytotoxicity of the HER-2-targeted formulation against this hematologic cancer model may be due to a high relative association of this formulation to HER-2 expressing tumor cells compared with the nontargeted formulation (Shmeeda et al., 2009).

*e. ssDNA and RNA aptamers.* Aptamers are ssDNA or RNA oligonucleotides that can be conjugated on to the surface of nanoparticles (Deshpande et al., 2013). Aptamers can interact with their target molecules with high affinity and specificity via electrostatic interactions, hydrogen bonding, and hydrophobic interactions (Deshpande et al., 2013). The use of aptamers for active targeting can be advantageous in that they are small and stable molecules, which can be easily synthesized and modified for conjugation as well as for improved target specificity (Kang et al., 2010; Deshpande et al., 2013).

Liposomes conjugated to sgc8 aptamers have been developed to target hematologic cancers, such as leukemia CCRF-CEM cells (Shangguan et al., 2007a; Shangguan et al., 2007b; Kang et al., 2010; Deshpande et al., 2013). It is believed that the sgc8 aptamer can bind to its target, protein tyrosine kinase 7, in these cells with high affinity (Table 1) (Kang et al., 2010; Deshpande et al., 2013). Through the use of flow cytometry, it was demonstrated that aptamer-conjugated liposomes could bind to target cells and subsequently release fluorescein-isothiocyanato-dextran within 30 minutes of incubation (Kang et al., 2010).

It is worth mentioning that the targeting of hematologic cancer cells may require the use of other targeting ligands apart from those described above. This is because blood cells possess their own specific markers that may not be present on other cell types. Some of the ligands capable of targeting hematologic cancers that have been investigated with lipid nanoparticles include CD19 and/or CD20 (Lopes de Menezes et al., 1998; Sapra and Allen, 2004; Laginha et al., 2005a; Cheng and Allen, 2008), CD74 (Lundberg et al., 2004; Mao et al., 2013), CD33 (Simard and Leroux, 2010), very late antigen-4 (Kiziltepe et al., 2012), and Apo2-ligand/TNF-related apoptosis-inducing ligand (De Miguel et al., 2013).

*2. Tumoral Endothelium Targeting.* In 1971, Judah Folkman (1971) suggested that the growth of tumors could be suppressed by preventing tumors from forming new blood vessels. This suggestion forms the basis of the design of nanomedicines that actively target tumor endothelial cells (Lammers et al., 2008). In contrast to directly targeting cancer cells, the targeting of tumoral endothelium aims to kill cancer cells by depriving cancer cells of oxygen and nutrients. In this strategy, ligand-targeted nanoparticles bind to and kill angiogenic blood vessels (Fig. 6), which in turn kills cancer cells that these blood vessels support in terms of providing nutrients. By inhibiting blood supply to tumors, the size and metastatic capabilities of tumors can be reduced (Danhier et al., 2010). The active targeting of the tumoral endothelium is also advantageous in that it can solve the issue of insufficient drug delivery to hypovascular tumors to some extent as: 1) the tumor vascular networks are more accessible to circulating nanoparticles than cancer cells localized in the tumoral interstitial matrix; 2) the extravasation of nanoparticles is not required to reach the targeted site; 3) the binding of ligands to their receptors is possible immediately after intravenous injection; 4) endothelial cells are genetically more stable than cancer cells and the risk of endothelial cells developing drug resistance is lower; 5) it has been estimated that the destruction of one endothelial cell could lead to the death of around 100 neoplastic cells, whereas the targeting of cancer cells requires the direct eradication of both accessible and inaccessible tumor cells to be considered effective; 6) the targeting of tumor vascular endothelium can achieve therapeutic efficacy without having to penetrate deep into the tumor, therefore, it is not heavily affected by tumor interstitial hypertension and does not require highly perfused or vascularized blood vessels; and 7) most endothelial cell markers are expressed across a wide range of tumor-types, and thus, broad application is possible (Denekamp and Hobson, 1982; Denekamp, 1984; Danhier et al., 2010).

The following proteins are the main candidates for tumoral endothelium targeting, namely, vascular endothelial growth factor (VEGF) and its receptors, VEGFR-1 and VEGFR-2; $\alpha_v\beta_3$ integrin; vascular cell adhesion molecule-1 (VCAM-1); and matrix metalloproteinases (MMPs) (Table 1). Alternatively, cationic liposomes can be used to target the negatively charged surface of tumor endothelial cells via an electrostatic interaction (Campbell et al., 2009; Weijer et al., 2015).

*a. Vascular endothelial growth factor and its receptors, vascular endothelial growth factor receptor-1 and vascular endothelial growth factor receptor-2.* VEGF and

its receptors are essential to tumor angiogenesis and neovascularization (Carmeliet, 2005). The upregulation of VEGF is influenced by tumor hypoxia and oncogenes (Carmeliet, 2005). This subsequently increases the expression of VEGF receptors on tumor endothelial cells.

There are two main approaches for the targeting of angiogenesis via the VEGF pathway that have been investigated. The first approach involves the targeting of VEGFR-2, which will reduce VEGF-binding through induction of endocytosis of VEGFR-2. In contrast, the second approach involves the targeting of VEGF, which will inhibit ligand-binding to the VEGFR-2 receptor (Shadidi and Sioud, 2003; Carmeliet, 2005; Byrne et al., 2008).

It was demonstrated in mice bearing Hep3B tumor xenografts that the administration of liposomes containing *VEGF* siRNA was able to reduce both tumor hemorrhage and microvascular density to the same extent as the anti-VEGF antibody, bevacizumab (Tabernero et al., 2013). Furthermore, liposomes containing both *VEGF* and *kinesin spindle protein* (*KSP*) siRNA were able to suppress the expression of these two genes by 50% within 24 hours (Table 1) (Tabernero et al., 2013). This response improved the mean animal survival time by 50% compared with control liposomes (Tabernero et al., 2013). The antitumor efficacy of *VEGF* and *KSP* siRNA liposomes was also observed in a clinical study in which 1 patient attained a complete response for over 26 months and 3 patients achieved stable disease at all anatomic sites for ~8–12 months (Tabernero et al., 2013).

*b. The* $\alpha_v\beta_3$ *integrin.* This protein is an endothelial cell receptor for extracellular matrix proteins, including fibrinogen (fibrin), vibronectin, thrombospondin, osteopontin, and fibronectin (Desgrosellier and Cheresh, 2010). The $\alpha_v\beta_3$ integrin protein is highly expressed in tumor cells and angiogenic endothelial cells but not in resting endothelial cells in most normal organs (Byrne et al., 2008). This distribution of expression is because $\alpha_v\beta_3$ integrin is important for the calcium-dependent pathway involved in endothelial cell migration (Nisato et al., 2003; Byrne et al., 2008). Cyclic or linear derivatives of the Arg-Gly-Asp (RGD) oligopeptide have been studied extensively to bind to endothelial $\alpha_v\beta_3$ integrin, which may be exploited for tumoral endothelium targeting (Hood et al., 2002; Desgrosellier and Cheresh, 2010).

The conjugation of the RGD oligopeptide to PEGylated liposomes resulted in a ~5-fold greater binding to human umbilical vein endothelial cells relative to nontargeted liposomes (Table 1) (Schiffelers et al., 2003). The inclusion of DOX into this liposomal formulation was also able to improve its therapeutic efficacy against the DOX-insensitive C26 tumor mouse model compared to nontargeted liposomes (Schiffelers et al., 2003). Despite the fact that RGD conjugated liposomal DOX demonstrated a comparable tumor accumulation as nontargeted formulations and exhibited an even higher liver accumulation, it was able to reduce the tumor volume by half, whereas the nontargeted formulations did not show any effects against DOX-insensitive tumors at all (Schiffelers et al., 2003).

*c. Vascular cell adhesion molecule-1.* VCAM-1 is an immunoglobulin-like trans-membrane glycoprotein that is expressed on the surface of tumor endothelial cells (Danhier et al., 2010). VCAM-1 is vital to the angiogenesis process, because it promotes cell-to-cell adhesion (Danhier et al., 2010). It was reported previously that the overexpression of VCAM-1 was observed in various solid cancers, including lung and breast cancer, melanoma, renal cell carcinoma, gastric cancer, and nephroblastoma (Dienst et al., 2005).

In vitro, PEGylated immunoliposomes targeting VCAM-1 were reported to bind to TNF-$\alpha$ activated murine endothelial cells overexpressing VCAM-1 with high specificity under both static and simulated blood flow conditions compared with nontargeted liposomes (Table 1) (Gosk et al., 2008). In mice bearing human multiple myeloma (Colo677) tumor xenografts, the tumor accumulation of radiolabeled anti-VCAM-1 PEGylated immunoliposomes was only slightly higher than that of nontargeted liposomes (Gosk et al., 2008). However, there was a difference in terms of the intratumoral localization between the two formulations (Gosk et al., 2008). Although nontargeted liposomes accumulated within tumor tissue by passive diffusion, the anti-VCAM-1 PEGylated immunoliposomes were localized to tumor blood vessels via VCAM-1 targeting (Gosk et al., 2008).

*d. Matrix metalloproteinases.* MMPs are a family of zinc-dependent endopeptidases that mediate the degradation of the extracellular matrix (Vihinen et al., 2005). MMPs are important in angiogenesis and metastasis because they are involved in endothelial cell invasion and migration, the formation of capillary tubes, and in the recruitment of accessory cells (Genis et al., 2006). Membrane type 1 matrix metalloproteinase (MT1-MMP) has been found on endothelial cells of various solid tumors, including malignant lung, gastric, colon, and cervical carcinoma, as well as in gliomas and melanomas (Genis et al., 2006). Another well-known member of the MMP family is aminopeptidase N\CD13, a metalloproteinase that removes amino acids from the unblocked *N*-terminal segments of peptides or proteins (Saiki et al., 1993). Aminopeptidase N\CD13 also acts as an endothelial cell surface receptor that facilitates cancer cell invasion and degradation of extracellular matrix during metastasis both in vitro and in vivo (Saiki et al., 1993). It was reported that Asn-Gly-Arg (NGR) oligopeptide exhibits the ability to bind to aminopeptidase (Pasqualini et al., 2000), and this represents a strategy for targeting MMPs.

In fact, it was reported that liposomes conjugated to NGR peptides were only able to bind to human Kaposi sarcoma cells (KS1767) or endothelial cells that could specifically associate with the NGR peptide (Table 1) (Pastorino et al., 2003). In contrast, liposomes conjugated to NGR peptides were unable to bind to THP-1 cells, which did not interact with the NGR peptide (Pastorino et al., 2003). The study of NGR peptide conjugated liposomal DOX has also been investigated in mice bearing neuroblastoma tumor xenografts (Pastorino et al., 2003). In these animal models, NGR conjugated liposomal DOX demonstrated a 10-fold higher accumulation of DOX in the tumor than the nontargeted formulation (Pastorino et al., 2003). Furthermore, treatment with NGR conjugated liposomal DOX also resulted in rapid tumor regression and metastases inhibition in tumor-bearing mice compared with nontargeted liposomal DOX (Pastorino et al., 2003). It was reported that 4 of 6 mice treated with NGR conjugated liposomal DOX showed no signs of tumor (Pastorino et al., 2003). The remaining two mice were reported to have >80% reduction in tumor mass or >90% decrease in tumor vascular density (Pastorino et al., 2003). Interestingly, metronomic administration of NGR conjugated liposomal DOX into tumor-bearing mice further improved the efficacy of the liposomal formulation and resulted in complete tumor eradication (Pastorino et al., 2003).

*e. Cationic liposome targeting of tumor endothelium.* Upon intravenous administration, nanoparticles will first interact with the glycocalyx on the surface of endothelial cells before reaching the interstitial space. As mentioned in section III.C, this layer is made up of negatively charged proteoglycans and glycosaminoglycans and regulates the vascular permeability and adhesive interactions between macromolecules and the cell surface. The exact composition and expression of each component of the glycocalyx varies greatly depending on the tissue type and the pathology present (Campbell et al., 2009). For instance, a member of the dermatan sulfate proteoglycan class, namely endocan, was demonstrated to be preferentially expressed in the endothelial lining of human non-small cell lung cancer (NCI-H1437), rat glioma (C6), and human renal cell carcinoma (786-0) tumor xenografts in athymic nude mice (Abid et al., 2006). In contrast, only a low level of expression of *endocan* mRNA was observed in normal mouse FVB embryos (Abid et al., 2006). The differential expression of syndecans and glypican, which are members of the heparin sulfate proteoglycan family, have also been investigated (Davies et al., 2004). In this case, it was demonstrated that syndecan-1 was expressed on the surface of epithelial and stromal cells of benign and borderline tumors, as well as in ovarian adenocarcinomas, but not in normal ovarian cells (Davies et al., 2004). In contrast, syndecan-2, 3, 4, and glypican-1 expression were detected in normal, benign, and malignant ovarian tumors (Davies et al., 2004). Furthermore, syndecan-2 was found highly expressed in mouse solid cancer gliomas (GL261) cells and may be involved in cell motility and formation of capillary tube-like structures during angiogenesis of MvEC mouse brain microvascular endothelial cells (Fears et al., 2006). The overall expression and the expression of different types of proteoglycans have also been observed to vary between normal and cancerous tissues (Vijayagopal et al., 1998). The total proteoglycan content of breast adenocarcinoma tissue was demonstrated to be significantly higher than normal breast tissue (Vijayagopal et al., 1998). The levels of chondroitin sulfate in cancerous tissue were found to be 32.2% higher than in normal tissue, whereas the expression of dermatan sulfate and heparin sulfate were detected to be 18.5 and 29.6% lower in cancerous tissue than in normal tissue, respectively (Vijayagopal et al., 1998).

It is believed that cationic liposomes can associate with the negatively charged glycocalyx of angiogenic endothelial cells by electrostatic interaction (Weijer et al., 2015). This is supported by the evidence that cationic liposomes have the tendency to accumulate more extensively with tumor vessels (~25–28% of the administered dose) than with normal vessels (~4% of the administered dose) (Campbell et al., 2002). Similarly, angiogenic endothelial cells of the RIP-Tag2 tumor mouse model demonstrated up to a 33-fold increase in the uptake of cationic liposomes composed of dioleoyl-trimethylammonium propane (DOTAP) and cholesterol (at a ratio of 55:45 mol%) compared with normal endothelial cells (Thurston et al., 1998). The association of cationic liposomes with a negatively charged surface may also be facilitated by the overexpression of anionic glycoproteins, such as sialic acid-rich glycoproteins, in the tumor endothelium (Diaz et al., 2009; Weijer et al., 2015).

The antitumor efficacy of chemotherapeutic-loaded cationic liposomes has been shown to be quite promising (Strieth et al., 2004; Eichhorn et al., 2007). Cationic liposomes encapsulating PTX (called MBT-0206) have demonstrated efficacy at reducing tumor perfusion and vascular diameter, as well as slowing the growth of A-Mel-3 melanoma in mouse models (Strieth et al., 2004). This formulation is composed of DOTAP, 1,2-dioleoyl-*sn*-glycero-3-phosphocholine (DOPC) and PTX at a concentration of 0.1, 0.094, and 0.006 mmol, respectively (Strieth et al., 2004). Furthermore, a cationic liposomal formulation of camptothecin (EndoTAG-2) composed entirely of DOTAP was also able to greatly reduce the microvessel density and tumor perfusion in mouse models of LLC-1 by up to 50% (Eichhorn et al., 2007).

### *C. Stimuli-sensitive Drug Release Strategy*

To enhance the effectiveness of passive and active targeting in delivering anticancer agents to a tumor

site, a specific stimuli-sensitive drug release strategy can be incorporated into nanoparticles. This strategy allows encapsulated drugs to be released from nanoparticles in the presence of their stimuli (Ganta et al., 2008). The acidic environment usually observed in tumors, as well as in lysosomes and endosomes, represents one of the most attractive strategies for stimuli-sensitive drug release.

*1. pH-sensitive Liposomes.* Due to defects in their mitochondrial respiratory chain and hypoxic nature, tumors generally exhibit a lower extracellular pH than normal tissue (Feron, 2009). This is due to their metabolism heavily relying on glycolysis to produce energy and is known as the Warburg effect (Warburg, 1956a,b). In the tumor microenvironment where glycolysis is highly active, lactate is constantly being produced as a byproduct of pyruvate to generate nicotinamide adenine ($NAD^+$) required by various glycolytic enzymes. Consequently, lactate is transported out of tumor cells via monocarboxylate transporters to avoid lactate cytotoxicity and maintain a high metabolic activity (Dimmer et al., 2000; Feron, 2009). The process of lactate elimination progressively increases the acidity of the tumor extracellular space as the monocarboxylate transporter also simultaneously exports one proton out of tumor cells with each lactate molecule (Dimmer et al., 2000; Cardone et al., 2005). It has been shown that the extracellular pH of tumor tissues is between 6.0 and 7.0, whereas the extracellular pH of normal tissues and the blood is approximately 7.4 (van Sluis et al., 1999; Cardone et al., 2005).

By using pH-sensitive lipids and polymers, nanoparticles that release encapsulated drugs in the presence of low pH within tumors, as well as in endosomes and lysosomes, can be prepared (Shenoy et al., 2005a,b). As liposomes are versatile drug delivery systems, pH-sensitive liposomes have been investigated.

Originally, PE and its derivatives were often used in the preparation of pH-sensitive liposomes together with amphiphilic compounds containing an acidic group that acts as a stabilizer at neutral pH (Ellens et al., 1985; Liu and Huang, 1989; Duzgunes et al., 2001; Torchilin, 2005; Karanth and Murthy, 2007). Unlike other phospholipids, PE consists of a small head group that is weakly hydrated and which occupies a low molecular volume relative to its acyl chain (Cullis and de Kruijff, 1979; Seddon et al., 1983). This characteristic gives PE a cone shape instead of a cylinder shape observed in bilayer stabilizing phospholipids and impedes the formation of a lamellar phase (Cullis and de Kruijff, 1979; Seddon et al., 1983). In contrast, the cone shape of PE molecules favor the formation of a strong intermolecular interaction between the amine and phosphate groups of the phospholipid polar heads (Karanth and Murthy, 2007). As a result, PE molecules have a strong tendency to possess an inverted hexagonal phase above its PTT (Karanth and Murthy, 2007).

The incorporation of amphiphilic molecules containing an acidic group, which can be protonated, in between PE molecules can promote electrostatic repulsion allowing a bilayer structure to be formed, and ultimately, the generation of liposomes under physiologic pH and temperature (Duzgunes et al., 1985; Lai et al., 1985). Although stable liposomes containing PE can be prepared under physiologic pH, destabilization of liposomes can occur when the negatively charged acidic groups of amphiphilic molecules are protonated at low pH (Duzgunes et al., 1985; Lai et al., 1985; Torchilin et al., 1993; Karanth and Murthy, 2007). This is because under this latter condition, amphiphiles lose their bilayer stabilizing capacity, allowing PE molecules to acquire their inverted hexagonal phase (Duzgunes et al., 1985; Lai et al., 1985; Torchilin et al., 1993; Karanth and Murthy, 2007). It is the tendency of PE to form an inverted hexagonal phase in the absence of sufficient bilayer stabilizing agents at low pH that gives liposomes containing PE their pH-sensitive property (Torchilin et al., 1993).

Various other pH-sensitive polymers and strategies have been used to exploit the acidic microenvironment of tumors. For example, succinylated poly(glycidol), PEG derivatives containing carboxyl groups, were reported previously to promote the fusion of liposomes under acidic conditions (Kono et al., 1994; Kono et al., 1997). The incorporation of these PEG derivatives into liposomes composed of egg yolk-PC demonstrated enhanced calcein leakage from liposomes, liposomal aggregation and fusion as the pH decreased (Kono et al., 1994). Moreover, these liposomes containing succinylated poly(glycidol) were relatively stable under normal physiologic conditions at pH 7.4 (Kono et al., 1994). A lipid mixing assay further revealed that egg yolk-PC liposomes bearing succinylated poly(glycidol) fused with endosomal and/or lysosomal membranes (Kono et al., 1997). These studies suggested that these liposomes delivered their contents into the cytoplasm by fusing with the endosomal membrane once they were internalized by cells via endocytosis (Kono et al., 1997). Additionally, an examination of egg yolk-PC liposomes bearing succinylated poly(glycidol) in normal CV-1 renal cells also demonstrated that once internalized, these liposomes were able to deliver calcein into the cytoplasm more efficiently than liposomes made up of egg yolk-PC only (Kono et al., 1997).

The use of pH-sensitive liposomes has shown some promising results for their future application in cancer therapy. For instance, pH-sensitive octylamine grafted polyaspartic acid was incorporated into cytarabine encapsulated liposomes (Wang et al., 2014). This new liposomal formulation was compared with conventional non-pH-sensitive cytarabine encapsulated liposomes and standard cytarabine (Fig. 1) for its antitumor effect and cytotoxicity in both human HepG2 hepatoma cells and normal human liver L02 cells (Wang et al., 2014).

The new formulation was found to be more effective at killing cancer cells than both the non-pH-sensitive liposomal formulation and standard cytarabine at all concentrations tested after 48 hours (Wang et al., 2014). In contrast, the non-pH-sensitive liposomal formulation of cytarabine and standard cytarabine were more cytotoxic to normal liver cells than the pH-sensitive liposomal formulation of cytarabine, with the latter formulation showing 100% cell viability at all concentration tested after 48 hours (Wang et al., 2014). Similar results were observed when PEG-poly(monomethyl itaconate)-CholC6 copolymer was incorporated into rapamycin encapsulated liposomes (Ghanbarzadeh et al., 2014). This formulation was able to deliver rapamycin (Fig. 1) to HT-29 colon cancer cells more efficiently than conventional liposomes, while showing less cytotoxicity to human umbilical vein endothelial cells than the latter formulation (Ghanbarzadeh et al., 2014). In addition, the incorporation of either oleyl alcohol or dimethyldioctadecylammonium bromide into liposomes composed of egg-PC, 3$\beta$-hydroxy-5-cholestene 3-hemisuccinate (CHEMS) and Tween-80 was also reported to demonstrate pH sensitivity under an acidic environment (Shi et al., 2002; Sudimack et al., 2002). Both formulations were able to efficiently retain encapsulated calcein within liposomes at pH = 7.4, while undergoing rapid calcein release and liposome destabilization upon acidification (Shi et al., 2002; Sudimack et al., 2002). Furthermore, both types of liposomes (i.e., those containing either oleyl alcohol or dimethyldioctadecylammonium bromide) showed better retention of their pH sensitivity in 10% serum compared with pH-sensitive liposomes composed of 1,2-dioleoyl-*sn*-glycero-3-phosphoethanolamine (DOPE) (Shi et al., 2002; Sudimack et al., 2002). The conjugation of folate to these two formulations for the targeting of the folate receptor in human oral cancer-derived KB cells also demonstrated improved cytoplasmic delivery of cytosine-$\beta$-D-arabinofuranoside in comparison with folate receptor-targeted non-pH-sensitive liposomes (Shi et al., 2002; Sudimack et al., 2002). This was reflected in a 17-and 11-fold increase in cytotoxicity of cytosine-$\beta$-D-arabinofuranoside when encapsulated in folate receptor-targeted liposomes containing either oleyl alcohol or dimethyldioctadecylammonium bromide, respectively, compared with folate receptor-targeted non-pH-sensitive liposomes (Shi et al., 2002; Sudimack et al., 2002).

Other strategies reported previously that can be employed to target the acidic tumor environment include the incorporation of fusogenic peptide together with encapsulated substances and zinc oxide-liposome nanocomplexes. It was reported that the coencapsulation of both pH-dependent fusogenic peptide (diNF-7) and diphtheria toxin A chain into non-pH-sensitive immunoliposomes targeting the EGFR could induce fusion and leakage of encapsulated contents at low pH (Mastrobattista et al., 2002). Consequently, the destabilization of liposomes observed led to an increase in cytosolic delivery of liposomal contents (Mastrobattista et al., 2002). Furthermore, the coencapsulation of diNF-7 and diphtheria toxin A chain resulted in increased cytotoxicity of EGFR-targeted immunoliposomes against ovarian carcinoma OVCAR-3 cells compared with immunoliposomes without the diNF-7 peptide (Mastrobattista et al., 2002). More recently, zinc oxide nanoparticles were incorporated into the liposomal bilayer, resulting in the formation of zinc oxide-liposome nanocomplexes (Tripathy et al., 2015). This complexation gave liposomes a pH-sensitive property, as zinc oxide nanoparticles are dissociated under the acidic condition of lysosomes, and thus, releasing the encapsulated content from the liposomes (Tripathy et al., 2015). These nanocomplexes encapsulating daunorubicin were found to be significantly more cytotoxic to alveolar adenocarcinoma A549 cells than conventional daunorubicin (Fig. 1) encapsulated liposomes and also than the unencapsulated drug, because they rapidly released their contents upon lysosomal localization (Tripathy et al., 2015).

*2. Temperature-sensitive Liposomes.* The concept of temperature-sensitive liposomes was first introduced in 1978 by Yatvin et al. (1978) who reported that the release of the encapsulated content from liposomes could be achieved by applying heat to the target site to create a mild local hyperthermia. These liposomes were observed to be stable under normal physiologic temperature, while becoming leaky at higher temperature (Yatvin et al., 1978). In cancer treatment, the use of temperature-sensitive liposomes would involve local heating of the tumor site to trigger liposomal drug release (Deshpande et al., 2013). Furthermore, the hyperthermic condition would also enhance the liposomal drug delivery to tumors by increasing vascular perfusion and extravasation of liposomes across tumoral blood vessels (Ponce et al., 2006). These enhancements were observed in tumor-bearing mice, where the uptake of non-temperature-sensitive liposomes increased by ~2- to 4-fold in heated tumors in comparison with nonheated tumors (Kong et al., 2000; 2001). A 2- to 16-fold increase in liposome delivery to heated tumors was also observed in cats with soft tissue sarcomas relative to nonheated tumors (Matteucci et al., 2000).

As phospholipid bilayers can undergo phase transition, such as gel-to-liquid crystalline and lamellar-to-hexagonal transition, it is possible for them to become highly permeable to water soluble molecules (Ganta et al., 2008). This allows certain phospholipids to be used in the generation of temperature-sensitive liposomes. Often, 1,2-dipalmitoyl phosphatidylcholine (DPPC) is used as the main component of temperature-sensitive liposomes, as this phospholipid undergoes gel-to-liquid crystalline phase transition at 41°C and causes the leakage of encapsulated substances (Yatvin et al., 1978; Jeong et al., 2009).

Initially, temperature-sensitive liposomes prepared by Yatvin et al. (1978) included DPPC together with 1,2-distearoyl-*sn*-glycerol-3-phosphocholine (DSPC) at a ratio of 7:1 (Yatvin et al., 1978). Consequently, the inclusion of DSPC increased the PTT of the liposomal membrane from 41°C to 43–45°C, where the maximum content release from liposomes was observed (Yatvin et al., 1978; Yatvin et al., 1981; Mills and Needham, 2005; Marsh, 2013). The content release of this formulation was reported to be slightly improved over non-temperature-sensitive liposomes (Mills and Needham, 2005). However, the release was still too slow to be used for therapeutic purposes (Mills and Needham, 2005). Moreover, the temperature required to trigger release was marginally higher than that achievable clinically (Kong and Dewhirst, 1999). As a result, micelle-forming lysolipids, such as 1-palmitoyl-2-hydroxy-*sn*-glycero-3-phosphocholine (MPPC) and 1-steroyl-2-hydroxy-*sn*-glycero-3-phosphocholine (MSPC), have been incorporated into temperature-sensitive liposome formulations to increase the permeability of the liposomal membrane to their encapsulated contents (Needham et al., 2000; Needham et al., 2013).

Liposomal DOX composed of DPPC, MPPC, and DSPE-$PEG_{2000Da}$, at a molar ratio of 90:10:4, was found to release ~45% of the encapsulated drug within 20 seconds of being exposed to a temperature of 42°C (Needham et al., 2000). In contrast, liposomes composed of pure DPPC released 20% of their encapsulated DOX over 1 hour at 42°C, whereas non-temperature-sensitive liposomes demonstrated no release at the same temperature (Needham et al., 2000). Liposomes containing MPPC were also more superior than the traditional temperature-sensitive liposomes composed of DPPC, hydrogenated soy-PC, cholesterol, and DSPE-$PEG_{2000Da}$ (molar ratio 100:50:30:6), which released 40% of their contents after 30 minutes at 42°C (Needham et al., 2000). Furthermore, the trigger temperature for the release of DOX from temperature-sensitive liposomes containing MPPC was found to be as low as 39–40°C (Needham et al., 2000).

In mice bearing human squamous cell carcinoma (FaDu) xenografts, temperature-sensitive MPPC liposomal DOX demonstrated essentially no antitumor activity at 34°C (Needham et al., 2000). However, at a tumor temperature of 42°C, this liposomal DOX formulation showed dramatic anticancer activity, with all 11 mice in this group achieving a complete response and none showed any cancer regrowth. Animals in this group also remained tumor-free for up to 60 days (Needham et al., 2000). In comparison, non-temperature-sensitive liposomes also showed some antitumor activity at 42°C (Needham et al., 2000). However, the efficacy of this formulation was not as great in extending the tumor growth inhibition time of these animals relative to the temperature-sensitive liposomes (Needham et al., 2000). Similarly, the inclusion of MSPC into the liposomal formulation led to a rapid release of liposomal contents under mild hyperthermic conditions (Needham et al., 2013). In fact, incorporation of MSPC into the liposomal formulation at 5.0, 7.4, 8.5, and 9.3 mol% accelerated the initial DOX release rate, with the 8.5 and 9.3 mol% formulations releasing 80% of their content within 4 and 3 minutes, respectively (Needham et al., 2013).

The rapid release of encapsulated content from temperature-sensitive liposomes containing lysolipids can be explained by the fact that these single chain lipids can increase the fluidity of the liposomal membrane and reduce the PTT slightly by ~1°C (Needham et al., 2013). More importantly, lysolipids can form porous defects that are stabilized by DSPE-$PEG_{2000Da}$ within the liposomal bilayer along the grain boundary between solid and liquid lipid at the PTT (Needham et al., 1997; Zhelev, 1998; Mills and Needham, 2005; Needham et al., 2013).

The use of MSPC in the preparation of temperature-sensitive liposomes has demonstrated to be quite effective at inducing rapid liposomal drug release under mild hyperthermic conditions. This led to the development of ThermoDox, a temperature-sensitive liposomal DOX formulation. ThermoDox (Celsion Corporation, Lawrenceville, NJ) is composed of DPPC:MSPC: DSPE-$PEG_{2000Da}$ at 86.5:9.7:3.8 mol% (Needham et al., 2013). In rabbits bearing the Vx2 tumor, the use of ThermoDox resulted in a 3- to 4-fold increase in DOX levels within heated tumors compared to nonheated tumors and an 8-fold increase in comparison to free DOX (Ranjan et al., 2012). Similarly, mice bearing fibrosarcoma FSA-1 tumor xenografts were found to have a 10-fold higher DOX level when administered as ThermoDox to hyperthermic tumors compared with control tumors at 37°C (Ponce et al., 2007). The higher DOX concentration also resulted in enhanced antitumor activity in mice treated with ThermoDox and hyperthermia (Ponce et al., 2007). Currently, ThermoDox is being investigated in phase II clinical trials for breast cancer and colorectal liver metastases and also in phase III trials for the treatment of hepatocellular carcinoma (May and Li, 2013). For more information on ThermoDox, please refer to Grull and Langereis (2012) and May and Li (2013).

There are many ways in which mild tumor hyperthermia (~39–42°C) can be generated to trigger drug release from temperature-sensitive liposomes. This includes implementing: 1) radio frequency heating via an array of antennas (van der Zee et al., 2000) or a catheter (Wood et al., 2012); 2) focused microwaves (Hauck et al., 2006); 3) infrared laser (Salomir et al., 2005); and 4) ultrasound (Deckers et al., 2008; Frenkel, 2008). More recently, high-intensity focused ultrasound (HIFU) has emerged as a promising technology for noninvasively applying heat to deep-seated tumors by focusing multiple ultrasound waves at the focal point

(Grull and Langereis, 2012). This results in the deposition of high acoustic intensity and subsequent local heating of the tumor (Grull and Langereis, 2012). The induction of hyperthermia by ultrasound is associated with the absorption of acoustic energy by the fluids and tissues and occurs as a result of a rise in power density when HIFU is focused on the target tissue (Ahmed et al., 2015). For more information, please refer to Lu et al. (1996), Huber et al. (2001), and Leighton (2007).

HIFU has been used in combination with magnetic resonance imaging for magnetic resonance guided HIFU (MR-HIFU) treatment (Grull and Langereis, 2012). For temperature-sensitive liposomal drug delivery, this strategy would allow the heating of a predefined volume of tumor to be more controlled and precise (Grull and Langereis, 2012). This is because magnetic resonance imaging can map in detail the treatment field and monitor near-real time temperature changes (Grull and Langereis, 2012). The benefits and problems of this technology were apparent in animal studies using ThermoDox, where DOX levels within the heated tissue were significantly higher compared with nonheated tissue and free DOX (Ponce et al., 2007; Ranjan et al., 2012; Staruch et al., 2012). However, partial thermal ablation was also observed in the heated tissue, which is believed to be due to imperfect temperature control (Ranjan et al., 2012). It is worth noting that MR-HIFU will be used in phase II clinical trials investigating the use of ThermoDox for the treatment of prostate cancer metastases to bone (May and Li, 2013). For more information on HIFU, please refer to Grull and Langereis (2012) and May and Li (2013).

Apart from the incorporation of lysolipids to generate temperature-sensitive liposomes, polymers with a low critical solution temperature (LCST) have also been investigated as an alternative composition for preparing this type of stimuli-sensitive liposomes (Ganta et al., 2008). When polymers with a LCST are incorporated into liposomes, they remain hydrated below the LCST and stabilize the liposomes (Ganta et al., 2008). However, above the LCST, these polymers become dehydrated and destabilize the liposomal membrane, causing the release of their encapsulated contents (Ganta et al., 2008).

By using polymers with a LCST that is slightly above normal physiologic temperature, liposomes with thermosensitive properties can be prepared (Sawant and Torchilin, 2010). Polymers that have been investigated for their use in temperature-sensitive liposome preparations include poly(*N*-isopropylacrylamide) (Kono et al., 2002), poly(*N*-iso isopropylacrylamide-*co*-acrylamide) (Han et al., 2006) and Pluronic F127 (Chandaroy et al., 2001). However, poly(*N*-isopropylacrylamide) is not biodegradable, and therefore, can result in unwanted side effects associated with polymer accumulation (Sawant and Torchilin, 2010). Please see a review by Kono (2001) for detailed information on temperature-sensitive polymer modified liposomes.

The use of pH-sensitive and temperature-sensitive drug release is considered to be an effective stimuli-responsive strategy, which shows promising results for clinical use in cancer therapy. However, other stimuli-sensitive liposomes also exist and are further discussed in section VIII.

## V. The Cellular Uptake of Liposomal Drug Delivery Systems

The delivery of liposomal-encapsulated drugs into cells is influenced by various parameters. The contents of liposomes are transported into cells by different mechanisms depending on liposome phase state, lipid compositions, cell-type, surface properties and stability (Fig. 7).

By varying lipid composition, liposomes of different charges and other properties can be synthesized (Vemuri and Rhodes, 1995). For instance, neutral liposomes can be prepared from neutral phospholipids, such as PC and PE, whereas anionic liposomes can be prepared from phospholipids, such as PS, PG, phosphatidic acid, and PI, which are negatively charged (Miller et al., 1998; Wu et al., 2003). Additionally, positively charged lipids, such as stearylamine, can be added to liposomal formulations and will give rise to cationic liposomes (Senior et al., 1991; Miller et al., 1998). For more information on cationic lipids, please refer to Campbell et al. (2009). It is also worth considering that *3β*-[*N*-(*N'*,*N'*-dimethylaminoethane)-carbomoyl] cholesterol (DC-cholesterol) can also be used in the preparation of positively charged liposomes (Broekgaarden et al., 2014, 2015). The use of DC-cholesterol can be quite beneficial because this modified cholesterol is generally less toxic in comparison with other cationic lipids (Choi et al., 2004). Moreover, liposomes containing DC-cholesterol were shown to be internalized readily by both cancer cells (Broekgaarden et al., 2014, 2015) and tumor endothelial cells (Thurston et al., 1998), even when liposomes were PEGylated. Furthermore, the addition of PEG or stimuli-sensitive components (e.g., pH-sensitive) can also make the liposomal membrane more hydrophilic, resulting in steric stability and stealth properties or make them more vulnerable to various stimuli for triggered drug release as discussed in sections II.A, IV.C, and VIII. Together, these modifications can influence the properties of liposomes and the mechanism by which different types of liposomes are taken up by cells (Gabizon and Martin, 1997; Sharma and Sharma, 1997; Allen, 1998; Gabizon et al., 2003b).

As surface modifications for active targeting have already been discussed above in terms of the cellular uptake mechanism (section IV.B), the following section will focus on the internalization of liposomes with other surface properties, including negatively charged

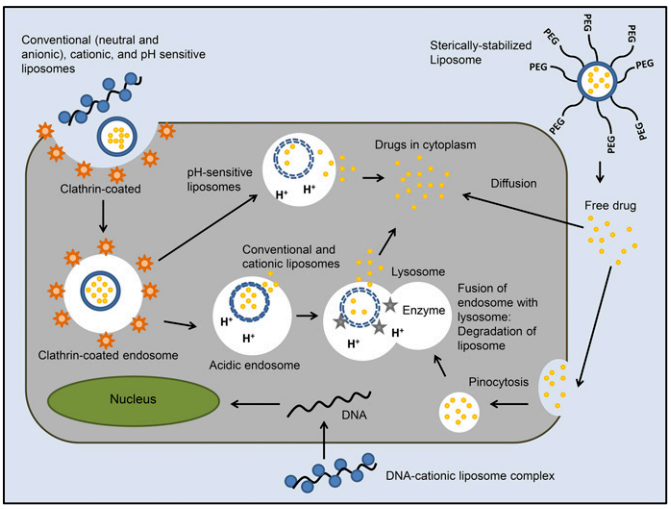


**Fig. 7.** Cellular uptake of different types of liposomes. Conventional liposomes (negatively charged and neutral) are taken up by cells via the process of clathrin-coated pit endocytosis. This process generates a clathrin-coated endosome, which undergoes acidification and fusion with lysosomes. In the presence of lysosomal enzymes and low pH, liposomes within the clathrin-coated endosome become destabilized and eventually get degraded by lysosomal enzymes (represented by dashed lines), releasing their contents into the cytoplasm. Additionally, pH-sensitive liposomes follow the same uptake pathway as conventional liposomes. However, these liposomes became destabilized (represented by dashed lines) and degraded once the endosome is acidified releasing their content into the cytoplasm. Positively charged or cationic liposomes can enter cells by two pathways. That is, via either clathrin-coated pit endocytosis or via membrane fusion. However, the primary route of entry for cationic liposomes is via clathrin-coated pit endocytosis similar to conventional liposomes. Although they are able to extravasate through the endothelium layer of small blood vessels, including those of tumors, sterically stabilized liposomes are generally not readily taken up by cells because of steric hindrance and the decreased hydrophobic interaction between the particle and the cell surface. Instead, these liposomes slowly release their contents into the interstitial fluid, which then enter cells via diffusion or pinocytosis.

liposomes, neutral liposomes, pH-sensitive liposomes, cationic liposomes, and sterically stabilized liposomes.

### *A. Conventional Liposomes—Negatively Charged and Neutral Liposomes*

It is believed that negatively charged or anionic liposomes enter cells by the process of clathrin-coated pit endocytosis, where the subsequent release of liposomal contents occurs via the acidification of endosomes upon fusion with the lysosome (Fig. 7). This concept was supported by several studies (Poste and Papahadjopoulos, 1976; Straubinger et al., 1983; Dijkstra et al., 1984).

When endocytosis was inhibited by cytochalasin B or a combination of azide and deoxyglucose, Poste and Papahadjopoulos (1976) found that the uptake of negatively charged liposomes made up of PS, DSPC, and 1,2-dipalmitoyl-*sn*-glycero-3-phosphocholine in a ratio of 1:4.5:4.5 by noncancerous 3T3 fibroblast cells was reduced by 80–90%, suggesting that these liposomes entered cells primarily via endocytosis. This finding was further supported by Straubinger et al. (1983), who reported the observation of a punctate fluorescence pattern in cultured normal CV-1 renal cells upon their incubation with negatively charged liposomes composed of PS:cholesterol (2:1) containing the fluorescent dye, calcein, and colloidal gold. This observation suggested that negatively charged liposomes could be endocytosed into cells (Straubinger et al., 1983). Consequently, thin section electron micrographs of colloidal gold-containing liposomes showed that such liposomes were bound to coated pits or localized to intracellular coated vesicles, suggesting that anionic liposomes are endocytosed via the coated pit pathway (Straubinger et al., 1983).

A similar result was also reported by Dijkstra et al. (1984) in which the uptake of negatively charged liposomes prepared from PC:cholesterol:PS (4:5:1) was examined using normal rat Kupffer cells. In this study, it was discovered that anionic liposomes containing the fluorescently tagged markers, FITC-dextran or -horseradish peroxidase, were internalized by rat Kupffer cells through endocytosis (Dijkstra et al., 1984). Moreover, upon inhibition by metabolic inhibitors, the uptake of these liposomes by Kupffer cells was reduced dramatically (Dijkstra et al., 1984). In addition to proving that anionic liposomes were endocytosed by cells, both Straubinger et al. (1983) and Dijkstra et al. (1984) also demonstrated that following endocytosis, liposomes were localized to lysosomes. This was shown by thin section electron microscopy (Straubinger et al., 1983) and by the intracellular degradation of liposomal-encapsulated albumin in lysosomes after their uptake (Dijkstra et al., 1984). These studies provided further evidence that negatively charged liposomes are endocytosed by cells as their localization to lysosomes can only occur after endocytosis (Straubinger et al., 1983; Dijkstra et al., 1984).

The uptake of negatively charged liposomes into cancer cells was expected to follow the same route as observed in normal cells. The endocytosis of anionic liposomes was demonstrated using liposomes composed of 1,2-dioleolyl-*sn*-glycero-3-PC and negatively charged 1,2-dioleolyl-*sn*-glycero-3-PS (11:1 and 4:1 ratio) in HeLa cells derived from a human ovarian carcinoma (Miller et al., 1998). These liposomes contained the pH-dependent fluorescent dye 1-hydroxypyrene-3,6,8-trisulfonic acid that was able to differentiate liposomes at normal pH (bound to cell surface) and at low pH (within endosomes and lysosomes) (Miller et al., 1998). These studies demonstrated that upon incubation of these cells with anionic liposomes, a change in fluorescence was observed between extracellular liposomes and those within endosomes and lysosomes (Miller et al., 1998).

Apart from negatively charged liposomes, neutral liposomes have also been suggested to enter cells via endocytosis (Fig. 7). It was found that the uptake of neutral PC liposomes by normal 3T3 cells was inhibited by 80–90% when the cells were treated with the endocytosis inhibitor, cytochalasin B, or a combination

of azide and deoxyglucose (Poste and Papahadjopoulos, 1976). Similarly, Jansons et al. (1978) demonstrated that preincubation of mouse leukemia L1210 cells with the metabolic inhibitor, azide, significantly reduced the uptake of neutral liposomes composed of PC:cholesterol (4:3) by these cells. This observation suggested that cells internalized neutral liposomes primarily via endocytosis. The endocytosis of neutral liposomes was further confirmed by Pires et al. (1999) in an attempt to study the fusion activity of liposomes of different surface charges to monocytic THP-1 cells. Pires et al. (1999) demonstrated that liposomes made up of PC:PE displayed low cell-binding ability and extremely limited cell fusion, which suggested that neutral liposomes are internalized mainly by an endocytic mechanism. Although the exact endocytosis mechanism responsible for the uptake of neutral liposomes is still unclear, it has been speculated that such a mechanism may involve the binding of liposomes to a trypsin-sensitive site (Pagano and Takeichi, 1977). In fact, it was demonstrated that the interaction of neutral PC liposomes to Chinese hamster V79 fibroblasts could only be dissociated in the presence of trypsin (Pagano and Takeichi, 1977).

*B. pH-sensitive Liposomes*

It is believed that pH-sensitive liposomes are internalized more effectively than non-pH-sensitive liposomes (Schroit et al., 1986; Chu et al., 1990). This is due to the fact that liposomes containing PE are prone to aggregation as a result of poor hydration of PE head groups, which results in liposomes with high ability to adhere to cells (Chu and Szoka, 1994; Collins, 1995). Once pH-sensitive liposomes bind to cells, they are internalized via endocytosis and are kept within early endosomes, which mature into late endosomes (Collins, 1995; Karanth and Murthy, 2007). At this point, the acidic environment within the endosomes can destabilize pH-sensitive liposomes, causing these particles to release their contents (Collins, 1995; Yoshimura et al., 1995; Karanth and Murthy, 2007). It was demonstrated that liposomes composed of DOPE, CHEMS, and DSPE-$PEG_{2000Da}$ at a ratio of 6:4:0.3 were unable to enter into monocytic human THP-1 cells derived from acute monocytic leukemia when treated with a mixture of metabolic inhibitors, such as antimycin, sodium fluoride, and sodium azide (Simoes et al., 2001). This observation suggested that these pH-sensitive liposomes were internalized mainly by endocytosis (Simoes et al., 2001). Furthermore, incubation of THP-1 cells with either chloroquine, bafilomycin $A_1$, or ammonium chloride that inhibit the acidification of endosomes was able to prevent the intracellular release of the encapsulated contents from liposomes composed of DOPE: CHEMS:DSPE-$PEG_{2000Da}$ (Slepushkin et al., 1997; Simoes et al., 2001). These studies further indicated that acidic conditions are involved in the destabilization of pH-sensitive liposomes that leads to the intracellular release of liposomal contents (Slepushkin et al., 1997; Simoes et al., 2001).

Three mechanisms have been proposed for the intracellular delivery of encapsulated content from pH-sensitive liposomes (Collins, 1995; Ropert et al., 1996; Karanth and Murthy, 2007): 1) the destabilization of pH-sensitive liposomes, resulting in the perturbation of the endosomal membrane via pore formation and the release of the encapsulated content into the cytoplasm; 2) the diffusion of encapsulated contents across the endosomal membrane into the cytoplasm following destabilization of liposomes; and 3) the fusion of liposomes with the endosomal membrane, leading to the release of liposomal contents into the cytoplasm. However, it has been suggested that the first and second hypotheses are the most widely accepted mechanisms of intracellular delivery of pH-sensitive liposomes (Karanth and Murthy, 2007). This was demonstrated by the differential destabilization of liposomes under various conditions when composed from different types of PE, namely DOPE, egg-PE, and phosphatidylethanolamine prepared by transesterification of egg-PC (Ellens et al., 1985; Ellens et al., 1986). It was shown that below their PTT, these liposomes formed aggregates and induced leakage at pH = 4.5 or at pH = 9.5 in the presence of calcium ions, whereas no aggregation and leakage at pH = 9.5 was observed in the absence of calcium ions (Ellens et al., 1986). It was also reported that this destabilization of liposomes might be due partly to liposome/liposome contact (Ellens et al., 1986). On the other hand, only a small extent of fusion (lipid mixing and mixing of liposomal contents) was observed at pH = 4.5, which increased slightly at pH = 9.5 in the presence of calcium ions (Ellens et al., 1986). These results suggested that membrane destabilization and liposomal leakage could occur under an acidic environment, whereas additional factors, such as alkalinity (pH = 9.5) and calcium ions, may be required to initiate liposomal fusion (Ellens et al., 1986). It is worth noting that both liposomal leakage and lipid fusion were found to be temperature dependent, increasing as the temperature rose toward the PTT (Ellens et al., 1986). However, no fusion was observed above the PTT, which was believed to be due to the formation of the inverted hexagonal phase of PE (Ellens et al., 1986).

In addition to the physicochemical characteristics of PE that facilitate the destabilization of pH-sensitive liposomes and their intracellular delivery of encapsulated contents, proteins may also be involved in these processes. By using lipid mixing assays to monitor the fusion of endosomes with liposomes composed of DOPC and DOPE at a molar ratio of 6:4, it was reported that the treatment of endosomes with trypsin inhibited the interaction of endosomal vesicles with liposomes (Vidal and Hoekstra, 1995). This suggested that endosomal-associated proteins may be involved in the destabilization of pH-sensitive

liposomes, as well as their fusion with endosomes (Vidal and Hoekstra, 1995).

### C. Positively Charged Liposomes

Positively charged or cationic liposomes are believed to enter cells via two mechanisms, endocytosis or membrane fusion (Fig. 7). However, endocytosis is believed to be the primary route of entry for these liposomes. In a study by Jansons et al. (1978), it was shown that the uptake of PC:cholesterol:stearylamine (4:3:1) cationic liposomes by L1210 cells was about 20-fold higher than either neutral or anionic liposomes. Furthermore, their uptake was dramatically reduced when the cells were pretreated with 5 mM sodium azide and, to a greater extent, when the cells were pretreated with both 5 mM sodium azide and 20 mM 2-deoxyglucose (Jansons et al., 1978). The reduction in the uptake of cationic liposomes after inhibition of energy metabolism, provided evidence that positively charged liposomes entered cells to a major extent by an endocytic mechanism. Friend et al. (1996) also demonstrated in different cell types that the majority of cationic liposomes entered cells via endocytosis using transmission electron microscopy. It was observed that complexes of gold particles and liposomes prepared from synthetic cationic dioleyloxypropyl-trimethylammonium chloride and dioleoyl-PE were associated with the cell surface, clathrin-coat assembly, plasma membrane invagination, and maturing endocytic vesicles, indicating clathrin-coated pit-mediated endocytosis (Friend et al., 1996).

Despite the fact that the majority of positively charged liposomes enter cells by endocytosis, the membrane fusion pathway of these liposomes remains an attractive route of entry, especially for DNA delivery, into cells. The use of cationic liposomes for cellular delivery of DNA was first described by Felgner et al. (1987). Felgner and colleagues demonstrated that liposomes prepared from cationic dioleyloxypropyl-trimethylammonium chloride and dioleoyl-PE were able to form complexes with DNA strands exhibiting 100% encapsulation (Felgner et al., 1987) compared with 12% achieved by conventional liposomes (Cudd and Nicolau, 1985). By using fluorescent lipids, Felgner et al. (1987) also observed a spontaneous fusion of DNA-liposome complexes with the plasma membrane, leading to both the uptake and the expression of the DNA. Furthermore, the fluorescence intensity was found to increase over time, with fluorescent lipid diffusing throughout intracellular membrane compartments (Felgner et al., 1987). Interestingly, when dioleoyl-PE was replaced with dioleoyl-PC during liposome preparation, only punctate fluorescence was observed, suggesting that liposomes were either adsorbed to the cell surface or endocytosed rather than undergoing fusion (Felgner et al., 1987). These contrasting results could be explained by the fact that PE is capable of destabilizing the bilayer membrane because of its tendency to form an inverted hexagonal phase, as discussed in section IV.C above. In contrast, PC tends to form a lamellar phase that is able to maintain the bilayer membrane structure (Cullis and de Kruijff, 1979; Duzgunes et al., 1981; Duzgunes et al., 1985; Karanth and Murthy, 2007).

This initial work by Felgner et al. (1987) was further investigated by Pires et al. (1999), who studied the interaction of cationic liposomes with monocytic THP-1 leukemia cells. It was demonstrated in Pires's study that after the binding of cationic DOTAP:dioleoyl-PE (1:1) liposomes to THP-1 cells, there was extensive fusion of the liposomes with the plasma membrane as measured by the fluorescence lipid mixing assay. In contrast, membrane fusion could not be observed when DOTAP:dioleoyl-PC (1:1) liposomes were examined, although they were observed to bind to the cell surface to the same extent as the former formulation (Pires et al., 1999). Moreover, Pires et al. (1999) also showed that when DNA-liposome complexes were formed, their transfection activity was dependent upon the net charge exhibited by the complexes. When DNA-liposome complexes exhibited a net positive or neutral charge, an increase in transfection activity was observed (Pires et al., 1999). However, when these complexes exhibited a net negative charge, a decrease in transfection activity was observed (Pires et al., 1999). Although extensive membrane fusion of cationic liposomes was visible in Pires et al. (1999), there was a significant decrease in DNA transfection when cells were treated with endocytosis inhibitors, suggesting that endocytosis was the primary route of DNA delivery.

In addition, it was previously suggested that the process of membrane fusion by cationic liposomes might be a sequential event, where fusion only occurred after liposomes were internalized by cells (Noguchi et al., 1998). This concept was first explored by Wrobel and Collins (1995), where they proposed that cationic liposomes fused with the endosomal membrane after crossing the plasma membrane via endocytosis and only then was their contents released into the cytoplasm. By using the fluorescence lipid mixing assay, Wrobel and Collins (1995) demonstrated that the binding of cationic DOTAP:dioleoyl-PE liposomes to HepG2 and CHO D cells was insufficient for the liposomes to undergo membrane fusion. However, changes in the fluorescence of the lipids were observed when endosomes were formed and had entered the cytoplasm, suggesting that lipid mixing had occurred between liposomes and the endosomal membrane, leading to membrane fusion (Wrobel and Collins, 1995).

Confocal laser scanning microscopy studies investigating the transfection of NIH3T3, COS-7, and HeLa cells with cationic cholesteryl-3$\beta$-carboxyamidoethylenedimethylamine:dioleoyl-PE liposomes and fluorescein-conjugated antisense oligonucleotide complexes further supported the idea of a multiple-step process (Noguchi et al., 1998). In all cell types, the transfection using these

complexes was completely blocked by nigericin, which acts to dissipate the pH gradient across the endosomal membrane, although these complexes were present inside the endosomes (Noguchi et al., 1998). It can be speculated that acidification may have neutralized the net negative charge on the DNA-liposome complex to enable fusion with the endosomal membrane (Noguchi et al., 1998). Furthermore, liposome complexes were shown to be absent in all cell types when the endocytosis inhibitor wortmannin was added to the cells (Noguchi et al., 1998). These results suggested that membrane fusion may occur after endosome formation via endocytosis. Thus, there may be more than one step involved in DNA transfection by cationic liposomes (Noguchi et al., 1998).

Studies examining the targeting of tumor endothelial cells by cationic liposomes also showed that they are taken up by these cells via endocytosis (Thurston et al., 1998). Electron microscopic analysis of the association between gold-labeled cationic liposomes and tumor endothelial cells revealed that ~53% of these liposomes were internalized into endosomes and multivesicular bodies after 20 minutes (Thurston et al., 1998). Interestingly, it is believed that there are some vascular domains lacking negatively charged surface proteoglycans and glycoprotein potentially involved in endocytosis and transcytosis (Vincent et al., 1988; Campbell et al., 2009). These areas of low negative charge can be observed on the luminal surface of capillary endothelium, particularly on the surface of plasmalemmal vesicles, which facilitate the internalization of circulating molecules, including liposomes (Simionescu et al., 1981; Ghinea and Simionescu, 1985; Simionescu et al., 1985; Campbell et al., 2009).

### *D. Sterically Stabilized Liposomes*

The interaction between sterically stabilized liposomes and cells has also received extensive investigation. Sterically stabilized liposomes composed of either monosialoganglioside ($G_{m1}$) or PEG modified polymers have been shown to be able to extravasate through the endothelium of small blood vessels, including those of tumors (Huang et al., 1992) and Kaposi sarcoma-like lesions in mice (Huang et al., 1993). However, it was observed by electron microscopy that $G_{m1}$-modified liposomes containing gold particles were not taken up by C-26 mouse colon carcinoma cells, because no gold particles were visible in the cytoplasm of these cells (Huang et al., 1992).

It is believed that the addition of $G_{m1}$ or PEG can reduce the uptake of liposomes by cells in general, because these polymers bind to cells and induce a decrease in cell surface hydrophobicity (Vertut-Doi et al., 1996). This was evident by: 1) a 45% inhibition in the uptake of the fluid-phase endocytosis marker, sulforhodamine B, in J774 cells in the presence of PEG-cholesterol-containing liposomes or free PEG-cholesterol (Vertut-Doi et al., 1996); 2) a reduction in the uptake of $G_{m1}$ and PEG-PE containing liposomes by cultured bone marrow macrophages (Allen et al., 1991a); 3) a reduction in the uptake of liposomes containing PEG-PE by HeLa cells (Miller et al., 1998); and 4) a reduction in cellular binding of short peptide-targeted liposomes to CT26. WT, HCT116, and RKO colon cancer cells and LNCaP prostate cancer cells in the presence of increasing concentrations of PEG on the liposome surface (Demirgoz et al., 2008; Garg et al., 2009). These observations suggest that sterically stabilized liposomes deliver pharmaceutics into cells by slowly releasing their contents extracellularly instead of entering cells by the endocytosis pathway (Fig. 7). However, the extent by which sterically stabilized liposomes are taken up by cancer cells can be influenced by the size of the liposome (Broekgaarden et al., 2014). In fact, more efficient uptake of PEGylated liposomes containing zinc phthalocyanine for PDT by human extrahepatic cholangiocarcinoma-derived Sk-Cha1 cells was observed when liposomes of smaller diameter were used. This increased uptake resulted in enhanced cell death post-PDT treatment (Broekgaarden et al., 2014).

### *E. Liposome-cell Fusion*

Some early studies on liposomes suggested that it is possible for these particles to fuse with the cell membrane under appropriate conditions and this represents an alternative cellular internalization pathway (Papahadjopoulos et al., 1973; Pagano et al., 1974; Poste and Papahadjopoulos, 1976). Upon metabolic inhibition by cytochalasin B or a combination of sodium azide and deoxyglucose, it was reported that the uptake of liposomes composed of PS and PC was reduced by only 30–40% (Poste and Papahadjopoulos, 1976). This suggested that liposomes were able to interact with the cell membrane by another mechanism apart from endocytosis, possibly by liposomal fusion (Poste and Papahadjopoulos, 1976). Furthermore, using electron microscopy and radioactive markers, it was demonstrated that liposomes could associate themselves with the cell membrane. Additionally, some of the radiolabeled liposomal phospholipids were also found incorporated within the cell membrane (Poste and Papahadjopoulos, 1976).

It is possible that the fusion of liposomes with the plasma membrane may occur via bilayer fusion intermediates, namely by hemifusion structures and fusion pores (Lentz et al., 2000; Chernomordik and Kozlov, 2003; 2008). Hemifusion structures occur as a result of the connection between the outer leaflets of adjacent membrane bilayers, whereas the inner leaflets remain separated (Chernomordik and Kozlov, 2008). Hemifusion has been demonstrated experimentally to allow lipid mixing without content mixing or the mixing of outer leaflets but not the inner leaflets (Chernomordik et al., 1987; Chanturiya et al., 1997; Chernomordik and Kozlov, 2008). It was reported that hemifusion is a

transient event, which may result in either the dissociation of connecting membranes into two separate entities or the formation of fusion pores (Chanturiya et al., 1997; Lentz et al., 2000; Chernomordik and Kozlov, 2008).

In contrast to hemifusion, fusion pores represent a connection between merging membranes involving both the outer and the inner leaflets (Chernomordik and Kozlov, 2008). The formation of fusion pores allows the aqueous compartments initially separated by adjacent membrane bilayers to come in contact and undergo mixing (Chanturiya et al., 1997; Chernomordik and Kozlov, 2008). This process has been studied by electrophysiological approaches and monitoring the mixing of aqueous contents and/or lipids of the inner leaflets (Chanturiya et al., 1997). These investigations also reported that it is possible for fusion pores to close and that the edges of these pores consist of the polar head groups of phospholipids (Chernomordik et al., 1987). The formation of the fusion pore after the interaction of two liposomes has been shown to result in the mixing of the encapsulated contents (Papahadjopoulos et al., 1973). Considering this observation, it can be speculated that the interaction of the liposome with the plasma membrane and the subsequent formation of the fusion pore may result in the release of the liposomal contents into the cytoplasm.

It has been suggested that the tendency of liposomes to undergo fusion with cellular membranes may be dependent on lipid compositions, the molecular shapes of lipids making up the liposomes, and the degree of inter-bilayer contact (Chernomordik and Kozlov, 2008). Studies by Papahadjopoulos et al. (1973), as well as Poste and Papahadjopoulos (1976), demonstrated that liposomes composed purely of PS, or PS in a 1:9 mixture with PC, could induce cell-cell fusion of 3T3, L929, and BHK21 cells, whereas pure PC liposomes were unable to cause such fusion (Papahadjopoulos et al., 1973). Furthermore, PG:DPPC (1:9 ratio) liposomes were able to induce cell-cell fusion to a greater extent than PG: DSPC (1:9 ratio) liposomes (Papahadjopoulos et al., 1973). In this study, it was suggested that the cell-cell fusion may have taken place because of the fusion of liposomes to the plasma membrane of two adjacent cells forming a bridge between these cells (Papahadjopoulos et al., 1973).

Moreover, liposomes possessing membranes in the fluid-phase state may be taken up by cells via membrane fusion, whereas liposomes with membranes in the gel-phase state are likely to enter cells via endocytosis (Poste and Papahadjopoulos, 1976). The molecular shape of phospholipids could also play a role in facilitating membrane fusion. For instance, it is believed that PE with an inverted cone shape can induce hemifusion, while inhibiting fusion pore formation (Chernomordik and Kozlov, 2008). In contrast, lyso-PC with a cone shape can promote fusion pore formation but not hemifusion (Chernomordik and Kozlov, 2008). Finally, another factor that can induce membrane fusion is the distance between the two adjacent membranes. These membranes must have sufficiently close inter-bilayer contact for fusion to occur (Chernomordik and Kozlov, 2008). This condition can be promoted by a direct dehydration of the membrane, which could drive the membranes that do not merge spontaneously into close proximity with one another (Yang and Huang, 2003). For more information on membrane fusion, please refer to reviews by Wilschut and Hoekstra (1986), Lentz et al. (2000), Chernomordik and Kozlov (2003), and Chernomordik and Kozlov (2008).

## VI. Pharmacological Characteristics and Toxicity of Lipid-based Nanoparticles

### *A. Pharmacokinetics and Pharmacodynamics of Lipid-Based Nanoparticles*

Regardless of the types of liposomes, the tissues and organs responsible for the uptake of these lipid particles are relatively similar. In cancer therapy, the sites of liposome accumulation, apart from the tumor, include the liver, spleen, kidney, lung, skin, and muscles.

The organ distribution and tumor uptake of MLVs containing annamycin (size $\sim$1.88 $\mu$m) compared with free annamycin and DOX has been investigated in the B16 melanoma tumor mouse model (Zou et al., 1993). The majority of these liposomes were found in liver $>$ spleen $\approx$ kidney $>$ lung $>$ tumor $>$ heart $>$ brain $\approx$ plasma (Zou et al., 1993). Compared with free annamycin, the MLV formulation of annamycin resulted in 2-fold higher levels of the drug in the liver, plasma, and tumor (Zou et al., 1993). However, its distribution within the brain was 2-fold lower than that of free annamycin (Zou et al., 1993). In all organs, the distribution of the MLV formulation of annamycin was significantly higher than that of free DOX (Zou et al., 1993). For instance, the spleen and tumor uptake of MLVs containing annamycin was 9- and 10-fold higher than that of free DOX (Zou et al., 1993). This variation in drug distribution might have been the result of the difference in physicochemical properties between these two drugs (e.g., the higher lipophilicity of annamycin relative to DOX) and the use of the liposomal drug delivery system in the case of annamycin (Zou et al., 1993).

In a clinical study investigating the pharmacology of negatively charged MLVs composed of dimyristoylphosphatidylcholine and dimyristoylphosphatidylcholine (7:3 molar ratio), these liposomes were labeled with $^{99m}$Tc and administered intravenously into 7 patients with various cancers (Lopez-Berestein et al., 1984). It was reported that $^{99m}$Tc labeled MLVs exhibited a biphasic half-life ($\alpha$ = $\sim$5.53 minutes and $\beta$ = $\sim$289 minutes) (Lopez-Berestein et al., 1984). Similar to the in vivo study mentioned above, the majority of these radiolabeled

liposomes accumulated within highly vascularized organs rich in RES cells, such as the liver (~44.5%), spleen (~25.5%), and lung (~14.5%) after 24 hours (Lopez-Berestein et al., 1984). Cumulative urinary excretion was found to be 13.4% after 24 hours, and no adverse side effects were observed in patients upon MLV administration (Lopez-Berestein et al., 1984). Although MLVs are able to improve the therapeutic efficacy of anticancer drugs, they may be of limited overall use in the clinics. This is suggested because significant, but manageable, toxicity is still present in an MLV formulation of the cisplatin analog, *cis-bis*-neodecanoato-*trans-R,R*-1,2-diaminocyclohexane platinum(II) (Perez-Soler et al., 1990; Lu et al., 2005). Another disadvantage of MLVs is that after administration, they have limited access to the systemic circulation, as demonstrated by the 17- to 49-fold higher exposure of MLVs containing *cis-bis*-neodecanoato-*trans-R,R*-1,2-diaminocyclohexane platinum(II) in the peritoneal relative to the plasma compartment (Verschraegen et al., 2003). In addition, MLVs generally exhibit a short circulation half-life due to the rapid clearance by a complement-mediated process (Szebeni et al., 1999; Szebeni et al., 2000).

As SUVs and LUVs are both unilamellar vesicles, the difference between the two liposomes is essentially their size. PEGylated unilamellar vesicles labeled with $^{99m}$Tc were found to be distributed in the liver > spleen > muscle > skin > kidney of the rabbit (Awasthi et al., 2003). As mentioned above, the accumulation of unilamellar vesicles within various organs is influenced by their size as well as charge (see section III.B and III.C). In fact, it is believed that larger liposomes above ~210 nm have higher accumulation within the liver and spleen compared with smaller particles (Awasthi et al., 2003). The half-life of PEGylated LUVs of 318 nm in size was also found to be significantly shorter than that of PEGylated SUVs of size 136 nm (8.9 versus 21.7 hours, respectively) (Awasthi et al., 2003). This was confirmed by an in vivo pharmacological study on various liposomal DOX formulations, including Doxil, administered to monkeys (Mamidi et al., 2010). Compared with SUVs like Doxil (size = ~102 nm) at an equivalent dose, the LUV formulation of DOX (size = 336 nm) demonstrated a significantly shorter half-life (78.1 versus 45.1 hours, respectively) and a lower area under the curve (AUC; by almost 4-fold), while showing a 4-fold higher clearance rate than Doxil (Mamidi et al., 2010). Greater toxicity of DOX was also associated with the LUV formulation of DOX when prepared at 196 and 336 nm in diameter (Mamidi et al., 2010).

Furthermore, it was observed in mice bearing Yoshida sarcoma tumors that the uptake of unilamellar vesicles by RES was size dependent. An increase in the size of liposomes from SUVs (39–43 nm) to LUVs (317–394 nm) resulted in an increase in liposome uptake by the RES from 35.9 to 73.7% (Uchiyama et al., 1995). The rapid clearance of LUVs may be due to the high extent of complement activation by larger particles (Bradley et al., 1998; Szebeni and Alving, 1999). In addition, it is believed that the half-life of unilamellar vesicles also follows a biphasic model similar to MLVs as observed with Doxil and the liposomal formulation of docetaxel (DTX; Fig. 1) (Gabizon et al., 1994; Immordino et al., 2003). Interestingly, the pharmacological characteristics of SUVs and long-circulating monosialoganglioside ($G_{m1}$) grafted SUV formulations of annamycin have been compared with MLV formulations of this drug (Zou et al., 1995). Although all formulations demonstrated a biphasic half-life in the B16 melanoma mouse model, the distribution and terminal half-life of SUVs (1.73 and 64.3 hours, respectively) and $G_{m1}$ grafted SUVs (7.33 hour and 128 hour, respectively) were significantly higher than that of MLVs (1.2 and 30.5 hours, respectively) (Zou et al., 1995). The plasma AUC of SUV and $G_{m1}$ grafted SUV formulations of annamycin were also higher than the MLV formulation by 2-fold and 3-fold, respectively (Zou et al., 1995). In tumors, the annamycin concentration and the AUC was much greater when delivered as either SUVs or $G_{m1}$ grafted SUVs in comparison with MLVs (Zou et al., 1995). Only within the liver and kidney was the annamycin concentration significantly higher when delivered as MLVs relative to SUVs, and $G_{m1}$ grafted SUVs, which suggested rapid elimination (Zou et al., 1995).

Another type of lipid-based nanoparticle, lipid micelles, are made solely of polymer-phospholipid conjugates. These nanoparticles are believed to exhibit similar long-circulating properties as PEGylated liposomes due to the presence of amphiphilic polymers on the outer shell of the particles (Lukyanov and Torchilin, 2004). In fact, lipid micelles prepared from PEG-PE have a circulation half-life that ranges from 1.2 to 2 hours, depending on the molecular weight of PEG polymer (Lukyanov et al., 2002). Furthermore, these lipid micelles also demonstrated higher accumulation in LLC and EL4 T-lyphoma tumors in mouse models than in muscle tissue (Lukyanov et al., 2002). However, in comparison with PEGylated liposomes, the circulation time of PEG-PE micelles in mice bearing LLC tumors was significantly shorter after the first 4 hour postinjection (Weissig et al., 1998). This may be explained by the more rapid vascular extravasation of micelles than PEGylated liposomes because of their smaller size compared with liposomes (~5–50 versus ~100 nm) (Weissig et al., 1998). Moreover, PEG-PE micelles demonstrated significantly higher levels of accumulation within LLC tumors 23 hours postinjection compared with PEGylated liposomes, suggesting that the small sized PEG-PE micelles were able to travel across blood vessels into the tumor more efficiently (Weissig et al., 1998). Interestingly, the accumulation of lipid

micelles and PEGylated liposomes within the liver and spleen after 23 hours was comparable (Weissig et al., 1998). It is worth mentioning that LLC tumors are characterized by a small vasculature cutoff size, which represents a challenge for liposomes (Hobbs et al., 1998; Weissig et al., 1998). Thus, lipid micelles may represent an alternative drug delivery system that has a potential to overcome this problem (Lukyanov and Torchilin, 2004).

Upon examination of those liposomal formulations that are commercially available or that have successfully entered into clinical trials for the treatment of cancer (see section VII and Tables 2–4), it is evident that unilamellar vesicles of size ~60–200 nm are the most effective lipid-based drug delivery systems for cancer therapy. This is because they demonstrate high tumor accumulation, while being taken up by organs of RES and normal tissues to a lesser extent compared with other types of liposomes as mentioned above. This results in lower levels of toxicity mediated by the drug delivery system (Bradley et al., 1998). However, in tumors with small vasculature cutoff size, where liposomes have limited excess, lipid micelles may represent a useful alternative drug delivery system.

### *B. Toxicity of Lipid-Based Nanoparticles.*

It is widely argued that basic phospholipid bilayers do not constitute any proteins, and therefore, they are not immunogenic (Szebeni et al., 2011). However, this is not the case against innate immunity that provides a nonspecific, first-line of defense against foreign objects entering the body (Szebeni et al., 2011). This is because lipid-based nanoparticles, particularly liposomes and lipid micelles, resemble the size and shape of pathogenic microorganisms, which the innate immune system targets (Szebeni et al., 2011). It has been known for many years that lipid-based nanoparticles, including liposomes and lipid micelles, can activate the complement system through both classic and alternative pathways (Szebeni, 1998, 2001; Szebeni et al., 1998, 2001, 2003). The activation of the complement system by these particles is often associated with complement activation-related pseudoallergy, an acute hypersensitivity or infusion reaction (Szebeni et al., 1999, 2011; Szebeni, 2005). It is believed that all types of liposomes can activate the complement system. However, SUVs composed of neutral lipids are the least immunogenic (Szebeni et al., 2011). The following factors have been observed to enhance complement activation in vitro (Szebeni et al., 1999, 2000): 1) positive or negative charge; 2) an increase in size from 70 to 300 nm; 3) heterogeneity in size and composition of liposomes; 4) liposomal aggregation; 5) presence of high cholesterol concentrations in liposomes (>71 mol%); and 6) the incorporation of anionic PEG-PE, but not neutral PEG-propandiol distearoyl ester (Szebeni et al., 1999, 2000).

In the clinical setting, the most common symptoms of complement activation-related pseudoallergy include flushing, rash, shortness of breath, dyspnea, chest pain, back pain, and distress (Szebeni et al., 2011). These symptoms often occur during the first treatment and can be delayed to a certain extent by premedication (Szebeni et al., 2011). However, it is also possible that these hypersensitivity symptoms may occur during subsequent treatments (Szebeni et al., 2011). Although no specific method of prevention of these adverse reactions has been studied, a "kitchen sink" approach can be used to reduce or prevent these pseudoallergic reactions. This involves using a variety of premedications, including antihistamines and corticosteroids, and/or a reduction in the administration rate of the liposomal drug (Gabizon and Muggia, 1998; Lenz, 2007). If the reaction is severe, discontinuation of drug administration with or without supportive therapy (e.g., fluids and bronchodilators) may be required (Lenz, 2007). For example, premedication with dexamethasone, slowing the administration rate and the dilution of liposomes with a larger infusion volume were sufficient to reduce the pseudoallergic reactions observed upon Doxil administration (Gabizon and Muggia, 1998). For more information, please refer to excellent reviews by Szebeni (2001) and Szebeni et al. (2002, 2011).

## VII. Liposomal Formulations in the Treatment of Cancer

### *A. Doxil*

*1. Doxorubicin.* DOX (Fig. 1) is an anticancer drug of the anthracycline family (Blum and Carter, 1974). Like other members within this family, it is produced by *Streptomyces* bacteria (*Streptomyces peucetius* var. *caesius*) (Blum and Carter, 1974). DOX interacts with nucleic acids of dividing cells by two mechanisms (Yang et al., 2014a). First, it inhibits the synthesis of DNA and RNA by intercalating between base pairs of the nucleic acid strand with high affinity, and thus, preventing rapidly dividing cancer cells from undergoing replication and transcription (Yang et al., 2014a). Second, it inhibits the topoisomerase II$\alpha$ enzyme, impeding the ability of supercoiled DNA from unfolding, and thus, further blocking DNA replication and transcription (Gewirtz, 1999). Apart from interacting with nucleic acids, DOX can also form iron complexes to generate redox-active free radicals that are detrimental to nucleic acids, proteins, and membrane lipids (Keizer et al., 1990).

The redox activity of DOX may contribute partially to the drug's high cumulative dose-dependent cardiotoxicity, because cardiac muscle is enriched with mitochondria, which contain a high level of anionic diphosphatidylglycerol (cardiolipin) that interacts strongly with DOX (Goormaghtigh et al., 1980). This can lead to lipid peroxidation within cardiac tissue (Keizer et al., 1990).

Similarly, as hepatocytes also contain high levels of mitochondria, it is possible that the redox activity of DOX may cause lipid peroxidation within the liver, leading to hepatotoxicity (Keizer et al., 1990; Bagchi et al., 1995; Damodar et al., 2014). The redox activity of DOX within the liver was supported by an increase in malondialdehyde, as well as hepatic enzymes involved in free radical metabolism, such as superoxide dismutase, glutathione peroxidase, and catalase (Kalender et al., 2005). However, the severity of DOX-induced hepatotoxicity may not be as severe as the cardiotoxicity. This may be because of the fact that semiquinone radicals of DOX tend to react with oxygen to form less harmful superoxide radicals in the liver, whereas they react preferentially with hydrogen peroxide to form highly reactive hydroxyl radicals in cardiac tissue (Nohl and Jordan, 1983). In addition, the lower level of NADPH cytochrome P-450 reductase in sarcosomes of the cardiac tissue compared to liver microsomes can lead to an inefficient reduction of DOX to its semiquinone form, which may contribute to the preferential reaction of DOX with hydrogen peroxide in the heart (Nohl and Jordan, 1983).

Typically, the standard treatment of cancers using conventional DOX is performed by an intravenous infusion at a dose between 10 and 60 mg/m$^2$, with an upper accumulative dose of 550 mg/m$^2$ to reduce its side effects and toxicities (Skeel and Khleif, 2011; Easson and Pointon, 1985). Other side effects of DOX, apart from cardiotoxicity, include myelosuppression, nausea and vomiting, stomatitis, alopecia, local tissue damage, and hyperpigmentation of skin (Peng et al., 2005; Takimoto and Calvo, 2008; Skeel and Khleif, 2011).

Although DOX exhibits a high level of toxicity, it was still selected as a candidate for liposomal drug delivery systems because of its effectiveness against cancers (Barenholz, 2012b). DOX is considered to be one of the most effective anticancer drugs ever discovered with activity against a broad range of cancer types, including both hematologic cancers (leukemia and lymphoma) and solid cancers (breast, uterine, ovarian, and lung cancers) (Weiss, 1992). Until today, it remains one of the most effective first line treatments for cancer (Weiss, 1992). Other practical reasons that lead to the selection of DOX for a liposomal drug delivery system are its distinct absorbance and fluorescence properties (Barenholz, 2012b). With a fluorescence excitation wavelength of 480 nm and a fluorescence emission wavelength of 550 nm, the easy and accurate quantification of DOX concentration, its chemical degradation, its state of aggregation, and changes in its local environment due to the difference in its fluorescence excitation and emission spectra, can be examined (Karukstis et al., 1998). The fluorescence properties of DOX also enable the drug's DNA-binding activity to be detected through the fast quenching of the fluorescent DOX (Barenholz, 2012b). Altogether, the molecular characteristics of DOX allow its pharmacokinetic and biodistribution to be studied over a long period of time (Gabizon et al., 1991; Amselem et al., 1993a).

*2. The Early Days of Liposomal Doxorubicin Formulation.* The first generation of liposomal DOX that led to the later development of Doxil was initially prepared in the 1980s by Alberto Gabizon and Yechezkel Barenholz (Barenholz, 2012a). This negatively charged, medium-size multilamellar liposomal DOX formulation prepared from low $T_m$ egg-derived PC, negatively charged egg-derived PG, and cholesterol (OLV-DOX) was able to enter into the "first in man" clinical trial in 1989 (Gabizon et al., 1989). Notably, OLV-DOX reduced DOX toxicity by lowering the peak level of the free drug and changing the drug's biodistribution, leading to a higher maximum tolerated dose (MTD) compared with conventional DOX (Gabizon et al., 1989). Despite these pharmacological improvements, OLV-DOX was not granted a further clinical trial as a result of its inferior therapeutic efficacy (Gabizon et al., 1989).

Through studies focusing on the pharmacokinetics and biodistribution of OLV-DOX, it was concluded that the ineffectiveness of OLV-DOX was a result of two separate issues with the formulation: 1) the rapid clearance of OLV-DOX by hepatic and splenic RES, while the accumulation of OLV-DOX in the tumor was avoided; and 2) the plasma clearance of fast released free DOX from liposomes (Gabizon et al., 1991; Amselem et al., 1993a). It was believed that the high clearance level of OLV-DOX was contributed to by its inferior physicochemical characteristics. These characteristics included: 1) the drug localization within the liposome membrane bilayer instead of being encapsulated inside the liposome interior, leading to rapid release upon a large dilution, such as during an intravenous infusion to humans (Amselem et al., 1993a,b; Barenholz and Cohen, 1995; Barenholz, 2003); 2) the high level of negative charge on the liposome due to the incorporation of a high concentration of PG into liposome bilayer, which may increase uptake by RES and induce complement activation (Gabizon and Papahadjopoulos, 1988; Szebeni et al., 2007; Szebeni et al., 2011); and 3) the large size of OLV-DOX (200–500 nm) inhibited the extravasation of liposomes into tumoral tissue, and thus, decreased the EPR effect (Hwang, 1987).

Although the development of OLV-DOX for human use was a failure, the inferior characteristics of OLV-DOX did shed some light on the improvements that could be made for the development of a new generation of liposomal DOX, namely Doxil. Doxil was a product developed by Liposome Technology Inc., which changed its name to Sequus and was eventually owned by Johnson & Johnson (Barenholz, 2012b). For a more effective delivery system, Doxil was designed to be in the nano-scale (~100 nm) range to take advantage of the EPR effect and the permeable tumoral blood vessles. However, this approach posed some challenges, because

nanosized liposomes exhibit an extremely small volume, whereas DOX required a relatively high dosage to achieve therapeutic efficacy (10–50 mg/m$^2$). Moreover, the low solubility of DOX also limited the use of conventional drug loading methods. It was rationalized that an appropriate nanosized liposome must be able to extend the plasma circulation time compared with OLV-DOX to improve its efficacy. As a result, a remote loading technique and sterically stabilized liposomes were developed by Liposome Technology Inc. for the manufacture of Doxil (Barenholz, 2012b).

*3. The Development of Doxil.*

*a. Remote loading.* In remote loading (also known as active loading), a transmembrane gradient of ammonium sulfate, $[(NH_4)_2SO_4]_{liposome} >> [(NH_4)_2SO_4]_{medium}$, is used as a driving force for the efficient and stable loading of amphipathic weak base drugs, such as doxorubicin-$NH_2$ (DOX-$NH_2$), into preformed nanoliposomes (Fig. 8) (Haran et al., 1993; Bolotin et al., 1994; Lasic et al., 1995). This strategy involves preparing nanosized liposomes that exhibit a transmembrane concentration gradient consisting of a high intraliposomal concentration of $(NH_4)_2SO_4$ and a low extraliposomal concentration of $(NH_4)_2SO_4$ (Haran et al., 1993). Depending on the pH, intraliposomal $(NH_4)_2SO_4$ can exist in the ionized form and the ionized species ($NH_4^+$ and $SO_4^{2-}$) usually exhibit very low permeability coefficients. Therefore, these ions either do not, or very slowly, permeate through the liposomal lipid bilayer (Haran et al., 1993). Only upon base exchange between $NH_4^+$ and DOX-$NH_2$ during drug loading will the unionized ammonia molecules ($NH_3$) be formed, which can then traverse across the liposomal lipid bilayer. The counterion, $SO_4^{2-}$, also plays an important role in the drug loading process. This anion regulates the state of aggregation and precipitation/crystallization of DOX inside the liposome by forming a $(DOX\text{-}NH_3)_2SO_4$ salt, which can be observed as long and fiber-like crystals within liposomes (Fig. 9). In doing so, $SO_4^{2-}$ controls the efficiency and stability of both remote loading and drug release (for more information on remote loading see: Barenholz, 2007; Barenholz and Haran, 1994; Bolotin et al., 1994; Haran et al., 1993; Lasic et al., 1995).

By using remote loading, it is possible to encapsulate more than 90% of DOX within liposomes. However, the efficiency of this loading technique and the stability of liposomal DOX, such as Doxil, depend on the following factors (Barenholz, 2012b):

- The large difference in permeability coefficient of the uncharged $NH_3$ ($10^{-1}$ cm/s) and the anionic $SO_4^{2-}$ ($>10^{-12}$ cm/s).
- The initial pH gradient having a higher concentration of intraliposomal $H^+$ than extraliposomal $H^+$.
- The low solubility of the $(DOX\text{-}NH_3)_2SO_4$ salt, which dramatically reduces the intraliposomal osmotic pressure and, therefore, helps prevent liposomes from collapsing (Fig. 9).
- The asymmetry of the DOX partition coefficient ($K_p$) with higher extraliposomal $K_p$ than intraliposomal $K_p$.

Not only was Doxil designed as a nanoscale particle, it was also engineered to be sterically stabilized in order to extend its circulation time within human plasma. To improve the short plasma half-life of OLV-DOX, DSPE-$PEG_{2000Da}$ was incorporated into the lipid bilayer of Doxil. According to Barenholz (2012b), who played a key role in the design and development of Doxil, this idea came from the work of Frank Davis, Abraham Abuchowski, and colleagues (Abuchowski et al., 1977). These investigators conjugated PEG to proteins (Abuchowski et al., 1977) and later demonstrated that PEGylation helped reduce the immunogenicity of therapeutics as well as improve their safety and

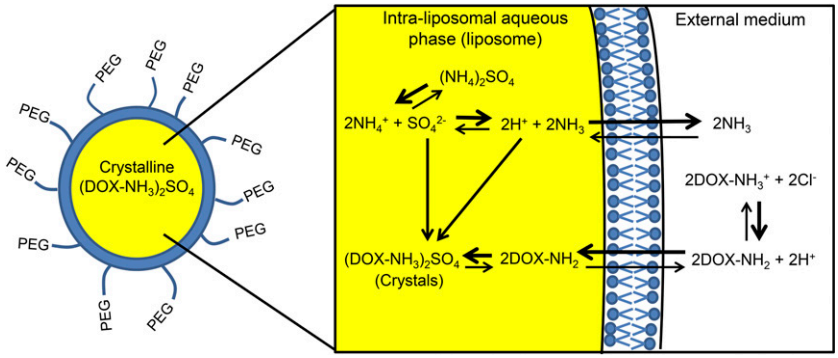


**Fig. 8.** Remote loading of DOX into Doxil liposomes using $(NH_4)_2SO_4$ gradient. The remote loading of DOX into a Doxil liposome uses a transmembrane concentration gradient consisting of a high intraliposomal concentration of $(NH_4)_2SO_4$ and a low extraliposomal concentration of $(NH_4)_2SO_4$ as a driving force for DOX loading. In this process, the ammonium salt of DOX (DOX-$NH_3^+$) donates $H^+$ to form an amphipathic weak base DOX-$NH_2$, which can diffuse across the phospholipid bilayer of the liposome. Within the liposome, $(NH_4)_2SO_4$ dissociates to form $NH_4^+$ and $SO_4^{2-}$. Then $NH_4^+$ undergoes a base exchange with DOX-$NH_2$ to form $NH_3$ and DOX-$NH_3^+$ within the liposome. Two molecules of DOX-$NH_3^+$ quickly precipitate or crystallize with $SO_4^{2-}$ to form the $(DOX\text{-}NH_3)_2SO_4$ salt inside the liposome cavity, whereas $NH_3$ diffuses across liposome membrane into the external medium.

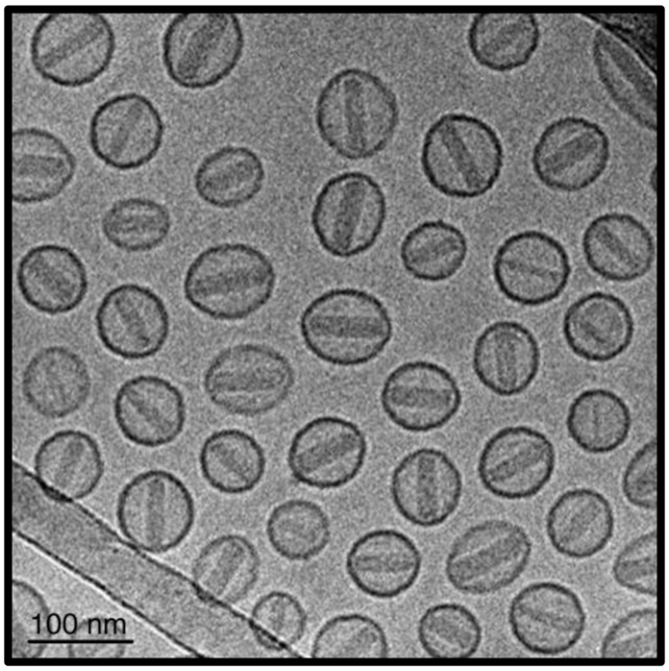


**Fig. 9.** Cryotransmission electron microscopy (cryo-TEM) of commercial Doxil liposomes. In a commercial Doxil formulation, remote loading produces doxorubicin sulfate [$(DOX\text{-}NH_3)_2SO_4$] crystals within PEGylated nanoliposomes. These crystals are clearly shown by cryo-TEM as long and fiber-like structures within liposomes. In addition, it can also be seen from cryo-TEM that $(DOX\text{-}NH_3)_2SO_4$ rods come into contact with the liposome membrane, slightly changing the shape of spherical liposomes. Reprinted with permission from Elsevier from Barenholz (2012b).

efficacy (Veronese, 2001; Veronese and Pasut, 2005). Through experimentation with PEG polymers of different sizes (350–15000 Da) and some consideration regarding the metabolism of PEGylated lipids and their kidney excretion rate, a 2000 Da PEG residue was the polymer of choice for the development of Doxil (Barenholz, 2012b). The addition of PEG polymers to Doxil was believed to reduce nonspecific protein-binding and cell interaction, allowing liposomes to stay in the circulation for an extended period of time (Barenholz, 2012b). The current formulation of Doxil is composed of hydrogenated soy-PC:cholesterol:DSPE-$PEG_{2000Da}$ at a ratio of 56.4: 38.3:5.3 (Mamidi et al., 2010).

*4. Preclinical Studies of Doxil.* Through a number of animal studies, it is believed that Doxil liposomes can escape highly permeable tumor blood vessels and subsequently accumulate within the tumor as intact liposomes (Huang et al., 1992; Working et al., 1994; Yuan et al., 1994; Vaage et al., 1997). Within the tumor tissue, Doxil liposomes travel and distribute themselves across the tumor mass by diffusion in a similar manner as macromolecules (Gabizon et al., 2003b). In contrast, free DOX is distributed throughout the body, but its movement toward the tumor is restricted by the tumor interstitial hypertension, which decreases the free drug's ability to enter tumor tissue (Jain, 1987; Jain et al., 2007). Unfortunately, Doxil's mechanism of drug release and its internalization are still unclear. However, two mechanisms have been proposed to be responsible for DOX release and the internalization of Doxil (Barenholz, 2012b): 1) intact Doxil liposomes are taken up by cells followed by intracellular drug release; and/or 2) DOX is released extracellularly into the tumor interstitial fluid, which is then taken up by cells as the free drug. Factors that may cause the release of DOX from Doxil include the collapse of the $(NH_4)_2SO_4$ gradient and the liposomal destabilization of Doxil by phospholipases that hydrolyze phospholipids (Huang et al., 1992; Working et al., 1994; Mouritsen and Jorgensen, 1998). However, the latter factor may only be partially involved, because the presence of cholesterol in the liposome bilayer can dramatically decrease phospholipase activity (Mouritsen and Jorgensen, 1998). Interestingly, it was recently suggested that ammonia produced at the tumor site by glutaminolysis may enhance the release of DOX from Doxil (Silverman and Barenholz, 2015). This may also represent a new strategy for stimuli-responsive drug release, as the level of ammonia observed in the tumor was much higher than in the plasma. For more details, please see Silverman and Barenholz (2015).

Doxil treatment has been shown to be more superior than free DOX in terms of its pharmacokinetic and pharmacodynamic properties in vivo (Lu et al., 2004; Laginha et al., 2005b; Anders et al., 2013). In mice bearing murine hepatocarcinoma ($H_{22}$) solid tumor xenografts, a single dose of 5 mg/kg Doxil was able to prolong the elimination half-life of DOX, extending the duration from ~24 hours (observed with a single dose of 5 mg/kg free DOX) to ~46 hours (Lu et al., 2004). Furthermore, the AUC upon Doxil treatment was shown to be 6.8-fold higher than free DOX after a single 5 mg/kg dose of each treatment (Lu et al., 2004). At either a 5 or 10 mg/kg dose administered intravenously, Doxil was demonstrated to be more effective than free DOX, showing a significantly higher tumor inhibition rate in $H_{22}$ hepatocarcinoma-bearing mice after 2 and 7 days (Lu et al., 2004). Another pharmacokinetic study comparing Doxil to free DOX has also been reported using murine mammary carcinoma (4T1)-bearing mice (Laginha et al., 2005b). This study measured the amount of DOX released from Doxil (at an equivalent DOX dose of 9 mg/kg) in comparison with free DOX (at a single dose of 9 mg/kg) (Laginha et al., 2005b). It was reported that although ~49% of DOX was bioavailable from Doxil compared with ~95% of free DOX, the AUC of DOX in the tumor available from a single dose of Doxil (measured 7 days after administration) was 87-fold higher than that of a single dose of free DOX (measured 24 hours after administration) (Laginha et al., 2005b). Hence, these studies demonstrated the far greater half-life and distribution of Doxil compared to free DOX within the animal. In fact, Doxil was demonstrated to increase the half-life of DOX from 25 hours observed for "free DOX" to 151 hours and reduce the clearance rate

from 89 g/h/kg for free DOX to 1.5 g/h/kg for Doxil (Laginha et al., 2005b).

For the purpose of studying breast cancer brain metastases, athymic mice were inoculated intracerebrally with invasive human breast adenocarcinoma MDA-MB-231-BR-luciferase-expressing cells and then treated with either Doxil or free DOX (Anders et al., 2013). It was reported that Doxil improved the serum and intracranial tumor AUC of DOX in these mice in comparison to free DOX by 1500- and 20-fold, respectively (Anders et al., 2013). Doxil also improved the median survival time of these intracranial tumor-bearing mice compared with free DOX, in this case, by 32 versus 23.5 days (Anders et al., 2013). Additionally, the toxicity of Doxil in vivo was shown to be less than free DOX. In fact, intravenous administration of a single dose of Doxil (10 mg/kg) to $H_{22}$ hepatocarcinoma-bearing mice led to no significant toxicity to the gastric mucosa, intestinal mucosa, and heart muscle (Lu et al., 2004). However, severe damage was observed when free DOX of an equivalent dose was used, most likely because of the higher level of this drug in these tissues (Lu et al., 2004).

*5. Clinical Studies of Doxil.* The "first in human" clinical trial for Doxil aimed to study the plasma pharmacokinetics and the accumulation of DOX administered as Doxil compared with free DOX (Gabizon et al., 1994). This study clearly demonstrated that a significantly higher level of DOX was present in both tumor cells and tumor interstitial fluid after administration of Doxil compared with free DOX (Gabizon et al., 1994). Moreover, using cationic ion exchangers, it was shown that more than 98% of the plasma DOX remained associated with liposomes after the intravenous administration of Doxil (Gabizon et al., 1994), indicating the improved stability of Doxil over the former OLV-DOX formulation. It was also demonstrated that the elimination time of Doxil followed a biexponential curve having a half-life of 2 and 45 hours, with most of the drug being eliminated after the second half-life (Gabizon et al., 1994). In addition, the clearance rate of DOX derived from Doxil was shown to be much slower than that of free DOX (0.1 l/h for Doxil compared with 45 l/h for free DOX) as well as its volume of distribution, which was lower for Doxil (4 liters) compared with free DOX (254 liters) (Gabizon et al., 1994). As expected, DOX metabolites derived from the urine of patients treated with Doxil were identical to those from patients treated with free DOX. However, the total amount of metabolites from daily urinary excretion was significantly lower in patients treated with Doxil (Gabizon et al., 1994).

The improvement of Doxil over conventional DOX was also indicated by the levels of the drug in malignant effusions, which was 4–16 times higher than that of free DOX (Gabizon et al., 1994). Furthermore, the tumoral DOX levels peaked between 3 and 7 days after the administration of Doxil, suggesting the exposure of tumor cells to the drug was much higher and for a longer period (Gabizon et al., 1994, 2003b; Solomon and Gabizon, 2008). Overall, Doxil with PEG modification and remote loading exhibited more superior characteristics than free DOX in a number of clinical trials (see section VII.A.7 below). For more information on Doxil's performance, see the review by Gabizon et al. (2003b).

*6. Side Effects and Safety of Doxil.* Although the development of Doxil significantly reduced the cardiotoxicity of DOX, allowing a higher accumulated dose and extended treatment duration to be achieved, two side effects typically not observed with free DOX are apparent after Doxil treatment. The first and more dominant side effect is grade 2 or 3 desquamating dermatitis, also known as palmar plantar erythrodysthesia (PPE) or "foot and hand syndrome," which appears as redness, tenderness, and peeling of the skin (Solomon and Gabizon, 2008). The severity of PPE increases with dosage and is more pronounced after treatment intervals of 3 weeks rather than 4 weeks. Thus, the latter interval time is used to lessen PPE symptoms, because there is no solution to counteract this side effect (Solomon and Gabizon, 2008). The second side effect is an infusion-related reaction, which is a common side effect of nano-scale drug delivery systems and appears as flushing and shortness of breath. This Doxil-induced infusion reaction is a complement activation-related pseudoallergy, an acute hypersensitivity, which can be reduced by slowing the infusion rate and by appropriate premedication (Solomon and Gabizon, 2008; Barenholz, 2012b). Although Doxil shows minimal hepatotoxicity during clinical trials (Northfelt et al., 1998; Gordon et al., 2001; O'Brien et al., 2004; Orlowski et al., 2007), interestingly, changes in size (from 102 to 196 and 336 nm) and composition (from hydrogenated soy-PC:cholesterol: DSPE-$PEG_{2000Da}$ 56.4:38.3:5.3 to 52.7:38.3:9) of the Doxil formulation have resulted in significantly elevated liver enzymes in the blood of mice, indicating liver damage (Mamidi et al., 2010).

*7. Indications of Doxil.* Due to the improved therapeutic index profiles reported during phase III clinical trials, Doxil was approved by the FDA and/or EMA for the following cancer types:

*a. AIDS-related kaposi sarcoma.* Doxil was approved for the treatment of AIDS-related Kaposi sarcoma in 1995 after showing some improvements in both selectivity and activity at lower doses compared with free DOX (Northfelt et al., 1996). Doxil was able to be deposited in the skin lesions of Kaposi sarcoma at levels between 5.2- to 11.4-fold higher than that of normal skin owing to the EPR effect, and thus, Doxil showed high specificity for tumor tissue (Northfelt et al., 1996). There were equivalent or higher response rates and less toxic side effects observed in AIDS-related Kaposi sarcoma patients treated with Doxil compared with

patients receiving combination therapy with conventional chemotherapeutic agents (DOX, bleomycin, and vincristine) (Krown et al., 2004). The objective response rate for Doxil treatment was also found to be nearly double when compared with combination therapy (Krown et al., 2004). A subtoxic Doxil dose of 20 mg/m$^2$ was recommended to be safe and effective for the treatment AIDS-related Kaposi sarcoma (Solomon and Gabizon, 2008).

*b. Recurrent ovarian cancer.* The use of Doxil for the treatment of recurrent ovarian cancer was approved in 1998. A superior efficacy and safety profile were observed when Doxil was compared with a standard treatment (topotecan; Fig. 1) during a phase III clinical trial (Gordon et al., 2001). It was demonstrated that the overall response rate for Doxil was 19.7% compared with 17.0% for topotecan. The overall survival time for Doxil-treated patients was also significantly increased to 108 weeks from 71.1 weeks observed in topotecan-treated patients (Gordon et al., 2004). Furthermore, an improvement was also demonstrated in patients classified as platinum sensitive, whose tumors reappeared more than 6 months after chemotherapy completion. In this group, a survival time of 9 months was achieved, an improvement of 54% in overall survival relative to topotecan (Thigpen et al., 2005).

Additionally, combination therapy using platinum-based drugs and Doxil has been reported to be beneficial for recurrent ovarian cancer patients. In fact, a combination of carboplatin and Doxil was shown to improve the response rate and increase the duration of response (du Bois et al., 2006). As there were no overlapping toxicities, the combination therapy between Doxil and platinum drugs was well tolerated and might even decrease the incidence of PPE (Lyass et al., 2001).

*c. Metastatic breast cancer.* The use of Doxil in the treatment of metastatic breast cancer was approved in 2003 after showing a significant result during a multicenter phase III trial (O'Brien et al., 2004). In this trial, the effectiveness of Doxil (50 mg/m$^2$ every 4 weeks) was compared with free DOX treatment (60 mg/m$^2$ every 3 weeks). Despite the lower dose intensity (Doxil dose intensity: 12.5 mg/m$^2$ per week versus free DOX: 20 mg/m$^2$ per week), response rates, including both complete and partial response, median duration of response, and median overall survival were relatively similar between Doxil and free DOX (i.e., 33 versus 38%, 7.3 versus 7.1 months, and 21 versus 22 months, respectively). A more positive result was observed in Doxil's safety profile, where a significantly lower risk of cardiac events and congestive heart failure was observed with Doxil treatment (O'Brien et al., 2004). Furthermore, a reduction in myelosuppression, alopecia, and nausea was also found in Doxil-treated patients (O'Brien et al., 2004).

*d. Multiple myeloma.* Approved in 2007, Doxil in combination with vincristine and dexamethasone demonstrated equivalent efficacy and improved safety profile, showing less cardiotoxicity compared with the standard DOX combination for this disease (i.e., DOX, vincristine, and dexamethasone) (Rifkin et al., 2006). The former combination also required less hospitalization, no central venous catheter, and reduced toxic side effects (alopecia and severe leucopenia) (Rifkin et al., 2006).

*8. The Shortage of Doxil and the Lack of Generic Doxil.* In 2011, Ben Venue Laboratories, the sole supplier of Doxil, made the decision to shut down its Bedford site in Ohio temporarily because of the lack of Good Manufacturing Practices cited by the FDA (Barenholz, 2012b). However, the shutdown was made permanent in 2013 because of legal and financial reasons. As a result, the supply of Doxil has been scarce since 2011, with thousands of people still waiting for Doxil treatment. Fortunately, in 2013 the FDA took action to temporarily approve a generic version of Doxil called Lipodox, supplied by Sun Pharmaceutical Industries Ltd (Mumbai, India) (Gaspani and Milani, 2013).

Recently, one study demonstrated that Lipodox did not show equivalent efficacy as Doxil in patients for the treatment of ovarian cancer (Smith et al., 2015). In this study, data from ovarian cancer patients receiving Lipodox (from 21st February 2012–1st March 2013) was compared with data from ovarian cancer patients receiving Doxil (from 1st January 1996–30th June 2006). For every three patients receiving Doxil ($n$ = 120), their data were compared with the results from one patient treated with Lipodox ($n$ = 40) by matching their age, stage of cancer, dose of liposomal DOX, platinum sensitivity, and number of prior treatments. It was found that the overall response rate of ovarian cancer patients treated with Lipodox was 4.3% compared with 18% for those treated with Doxil, whereas the mean time to progression was 4.1 $\pm$ 2.8 months for the Lipodox-treated group and 6.2 $\pm$ 7.2 months for the Doxil-treated group (Smith et al., 2015).

An indirect comparison between two separate clinical trials examining the efficacy of Lipodox and Doxil also demonstrated the lower anticancer activity of Lipodox (Gordon et al., 2001; Chou et al., 2006). In a study by Chou et al. (2006), 29 recurrent platinum-resistant/refractory ovarian cancer patients were treated with Lipodox at a dose of 45 mg/m$^2$ for an average of 4.6 cycles. This study reported a median progression free survival of 5.4 months. On the other hand, a study by Gordon et al. (2001) reported a progression free survival of 7.2 months for recurrent epithelial ovarian carcinoma patients treated with Doxil. In this investigation, 239 patients were given Doxil at a dose of 50 mg/m$^2$ for six cycles (Gordon et al., 2001).

The inferior efficacy of Lipodox relative to Doxil may be due to the lower uptake of Lipodox in tumor tissue compared with Doxil (Smith et al., 2016). This

explanation was suggested by a preclinical study of human ovarian cancer ($SKOV_3$-GFP-LUC) tumor-bearing mice treated with either Lipodox or Doxil at a dose of 5 and 10 mg/kg for three cycles (Smith et al., 2016). It was found that the intratumoral concentration of Lipodox was lower than that of Doxil at both the 5 mg/kg (1.0–25.5 ng/ml versus 2.7–42.2 ng/ml) and 10 mg/kg (2.9–35.6 ng/ml versus 2.0–76 ng/ml) doses (Smith et al., 2016). Furthermore, compared with Doxil, there was a 15.7% and 21.3% decrease in the efficacy of Lipodox at both 5 and 10 mg/kg, respectively (Smith et al., 2016). This suggested that the lower efficacy of Lipodox observed might have been the result of lower tumor accumulation (Smith et al., 2016). It is worth noting that although both the preclinical and data comparison studies have suggested the lower anticancer activity of Lipodox compared to Doxil, a direct comparative clinical study between Lipodox and Doxil must be performed to ensure a more accurate assessment.

Despite the fact that the patent protection of Doxil in the United States ended in early March 2010 (Barenholz, 2012b), there is still a surprising lack of generic PEGylated liposomal DOX formulations approved by the FDA and EMA. The reason for the lack of generic Doxil may be because of the complexity of the approvals required by the authorities. In fact, generic Doxil does not only need to meet the requirements for the approval of generic low molecular weight drugs and biologicals, but it must also meet the physical and physiochemical requirements for liposomal products (Barenholz, 2012b).

### *B. Myocet*

Considering the success of liposome technology, Sopherion Therapeutics developed a non-PEGylated liposomal DOX formulation, named Myocet. This agent has been approved by the EMA and Health Canada for the treatment of metastatic breast cancer in combination with cyclophosphamide (Batist et al., 2001; Chan et al., 2004).

*1. The Development of Myocet.* The current formulation of Myocet is composed of egg PC and cholesterol in the ratio of 55:45 mol% (Swenson et al., 2001). Similar to Doxil, the encapsulation of DOX in Myocet is carried out by remote loading. However, the preparation of Myocet uses a pH gradient rather than the $(NH_4)_2SO_4$ gradient as a driving force for DOX remote loading (Fig. 10) (Swenson et al., 2001). In this approach, sodium carbonate is added to an aqueous suspension of proton-rich liposomes containing citrate buffer, and thus, an acidic environment inside the liposomes (pH = 4) is created with a neutral pH environment outside the liposomes (pH = 7.8) (Swenson et al., 2001). Once added to the suspension, DOX is forced to accumulate within the liposomes by the lower intraliposomal pH. This condition allows more DOX to be loaded into the liposomes that is well beyond its solubility limit (Swenson et al., 2001). The accumulation of DOX within the liposomes is further facilitated by the unique complexation of DOX with citrate anions, which forms bundle-like structures within the liposomes (Fig. 11). This complexation also reduces the rate at which DOX diffuses from the acidic liposomes (Li et al., 2000).

The exact interaction between citrate anions and DOX inside Myocet remains unclear. However, it is certain that the multivalency of the citrate anion is crucial for DOX complexation, because similar DOX bundle formations were observed in di-anionic sulfate containing liposomes (Lasic et al., 1992) but not in liposomes containing mono-anionic species (Li et al., 1998). By using pH gradient remote loading, it is possible to encapsulate more than 95% of DOX inside liposomes of size ~150 nm with a final DOX/lipid molar ratio of 0.27 (Swenson et al., 2001). Upon physical characterization of Myocet, DOX appears as bundles of fibers inside the liposomes, where DOX monomers stack to form each fiber (Fig. 11A). These fibers are believed to be flexible, because cryoelectron microscopy revealed them to be in different geometries, such as straight, curved, and circulars (Fig. 11, B and C) (Li et al., 1998).

*2. Preclinical Studies of Myocet.* The higher efficacy of Myocet over conventional DOX is thought to be due to an increase in its circulation time and tumor accumulation, as well as a reduction in DOX toxicity. In fact, an injection of $^{14}$C-labeled DOX into male beagle dogs as either Myocet or the free drug demonstrated that Myocet localized less readily to normal tissue and was eliminated in the bile much slower than free DOX (Potchoiba et al., 1996). The radioactivity of $^{14}$C-labeled DOX also revealed that the AUC of Myocet in

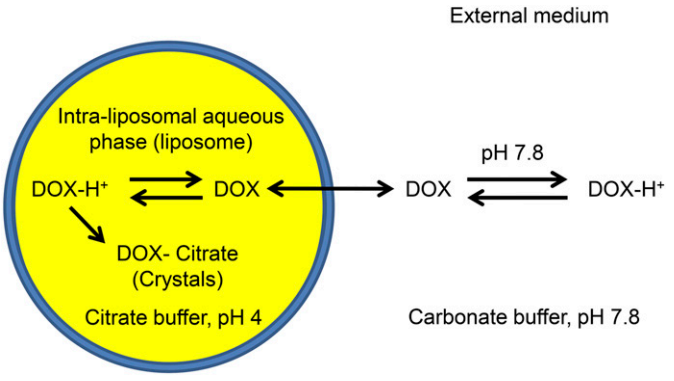


**Fig. 10.** Remote loading of DOX into Myocet liposomes using a pH gradient. In contrast to Doxil, Myocet uses a pH gradient as a driving force to actively load DOX into liposomes. In this approach, sodium carbonate buffer creates a neutral pH environment (pH = 7.8) outside the liposome, whereas citrate buffer creates an acidic environment (pH = 4) inside the liposome. Outside the liposome, DOX-$H^+$ is deprotonated to DOX, which can diffuse through liposomal membrane into the liposome cavity. Within the liposome, the acidic pH protonates DOX back to DOX-$H^+$, which interacts with citrate anions to form the DOX-citrate salt that precipitates into a crystal.

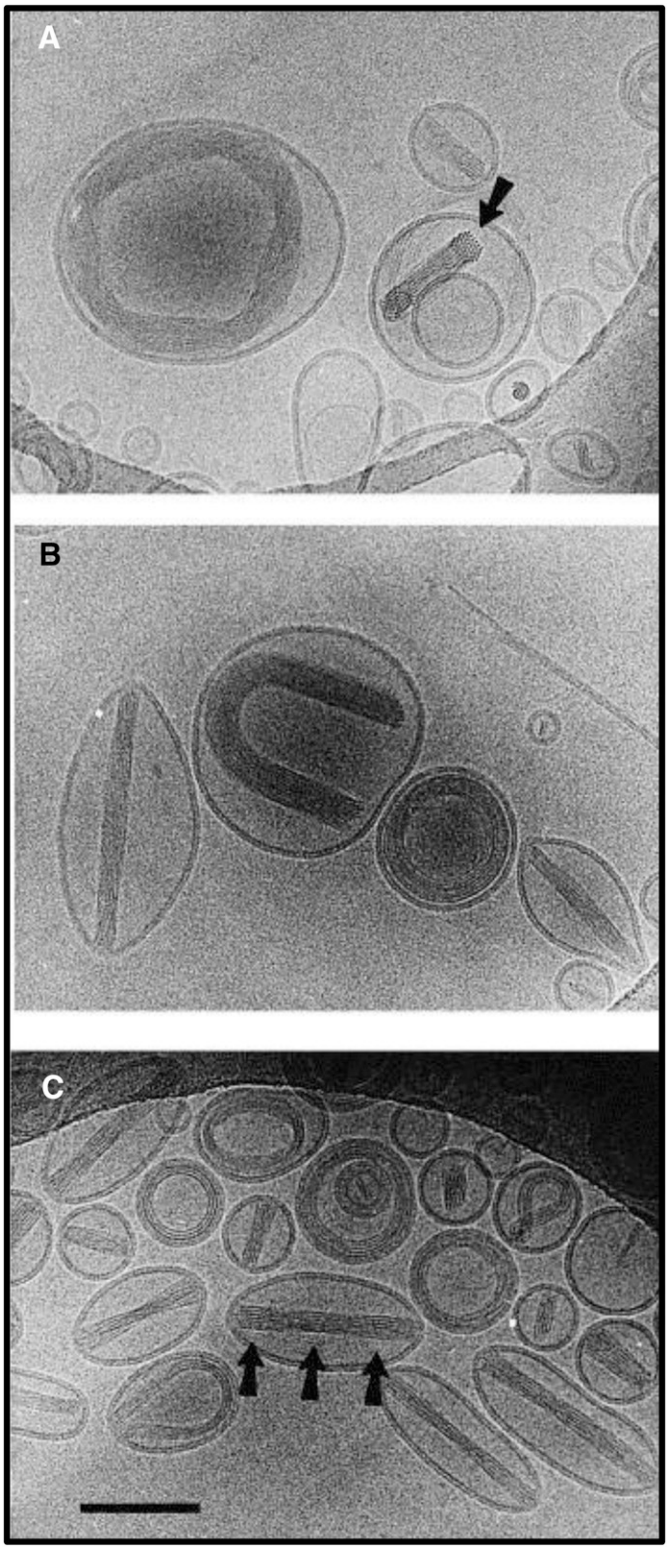


**Fig. 11.** Cryotransmission electron microscopy (cryo-TEM) of Myocet liposomes. The unique complexation of DOX with citrate anions during the remote loading of DOX into Myocet liposomes results in the formation of bundles of DOX fibers within the liposome. (A) The arrow shows the end of a DOX fibrous bundle with each fiber within the bundle being ~3–3.5 nm apart. (B) The flexibility of these DOX fibers is demonstrated by their ability to exist as fibrous bundles in different geometries, including U-shape, circle, and straight. (C) The arrow shows striated regions in DOX fibrous bundles that repeat approximately every 50 nm. Reprinted with permission from Elsevier from Li et al. (1998).

myocardial tissues of beagle dogs to be ~67% of that found for conventional DOX-treated animals, suggesting that Myocet would potentially cause less cardiotoxicity (Potchoiba et al., 1996).

The reduction in cardiotoxicity after Myocet treatment was demonstrated in another study in which beagle dogs were administered intravenously with either Myocet or free DOX at a dose of 1.5 mg/kg every 3 weeks for a total of 8 cycles (Kanter et al., 1993). It was shown that all dogs treated with free DOX exhibited histologic evidence of anthracycline-induced cardiotoxicity by the end of the treatment (157–164 days) (Kanter et al., 1993). In contrast, none of the dogs in the Myocet-treated group showed any signs of microscopic or macroscopic damage to the heart by the end of the treatment (Kanter et al., 1993). Furthermore, dogs treated with free DOX were found to be five times more likely to experience vomiting and diarrhea compared with those treated with Myocet (Kanter et al., 1993). Alopecia and gastrointestinal bleeding were also present in the free drug-treated group, whereas none was observed in the Myocet-treated group (Kanter et al., 1993). This improved safety may be due to the lower accumulation of DOX in normal tissue when administered as Myocet, because normal tissues do not possess permeable blood vessels from which the liposomes can escape (Kanter et al., 1993).

The improved anticancer activity of Myocet in comparison with free DOX was observed in mice bearing the SC115 Shionogi mouse mammary tumor (Mayer et al., 1990a). In this comparative study, tumor-bearing mice were administered with either Myocet or free DOX at 6.5 mg/kg (the MTD for free DOX) weekly for 3 weeks. At this dose, DOX levels within the tumor after Myocet treatment increased from 2.6 $\mu$g/g of tissue after 1 hour to 5.5 $\mu$g/g of tissue after 24 hours (Mayer et al., 1990a). In contrast, the DOX levels within the tumor for the conventional free drug was 2.0 $\mu$g/g of tissue after 1 hour and remained constant over 24 hours (Mayer et al., 1990a). In addition, there was an increase in tumor growth inhibition observed in mice treated with Myocet compared with free DOX (Mayer et al., 1990a).

A further increase in the administration dose of Myocet to 13 mg/kg (the MTD for Myocet) weekly for 3 weeks resulted in greater tumor accumulation of DOX and tumor growth inhibition. It was found that at this dose, the DOX tumor concentration was 5.7 $\mu$g/g of tissue after 1 hour and 10.2 $\mu$g/g of tissue after 24 hours (Mayer et al., 1990a). Moreover, this treatment led to a significant reduction in tumor weight, from 5 to 0.5 g (Mayer et al., 1990a). Complete tumor regression was also observed in 25% of mice treated with 13 mg/kg of Myocet, which lasted over the 50-day study period (Mayer et al., 1990a).

*3. Clinical Studies of Myocet.* The advantage of Myocet over conventional DOX has been demonstrated previously for the treatment of metastatic breast

cancer. The plasma level of total DOX was shown to be substantially higher for Myocet than for conventional DOX, whereas peak plasma levels of free DOX were shown to be lower for Myocet than for conventional DOX (Swenson et al., 2001). Three pivotal phase III clinical trials evaluating Myocet for the treatment of metastatic breast cancer reported the improved safety of DOX when administered as Myocet with patients showing a lower incidence of cardiotoxicity, whereas the therapeutic efficacy of Myocet remained comparable to that of conventional DOX (Batist et al., 2001; Harris et al., 2002; Chan et al., 2004).

In a study by Batist et al. (2001), metastatic breast cancer patients were given either a combination of cyclophosphamide (600 mg/m$^2$) and Myocet (60 mg/m$^2$) or conventional DOX (60 mg/m$^2$) for a median of 6 cycles/patient. Both groups showed comparable antitumor activity with a response rate of 43%. Additionally, the combination of cyclophosphamide with Myocet or conventional DOX resulted in a median time to progression of 5.1 versus 5.5 months, a median time to treatment failure of 4.6 versus 4.4 months, and a median survival time of 19 versus 16 months, respectively (Batist et al., 2001). Although the therapeutic efficacy of Myocet and conventional DOX was similar, there were fewer patients in the Myocet-treated group that developed cardiotoxicity compared with the group receiving conventional DOX treatment (6 versus 21%, respectively) (Batist et al., 2001). None of the patients treated with Myocet suffered congestive heart failure, although five cases were found in the conventional DOX-treated patients (Batist et al., 2001). The estimated median cumulative lifetime dose of DOX at which cardiotoxicity first appears was reported to be $>$2220 mg/m$^2$ for Myocet compared with 480 mg/m$^2$ for conventional DOX (Batist et al., 2001). Finally, patients receiving Myocet also showed fewer incidence of grade 4 neutropenia compared with conventional DOX-treated patients (61 versus 75%, respectively) (Batist et al., 2001).

A study on Myocet as a monotherapy for the treatment of metastatic breast cancer was also investigated (Harris et al., 2002). In this study, 75 mg/m$^2$ of Myocet ($n$ = 108) was compared with a dose of 75 mg/m$^2$ of conventional DOX ($n$ = 116) for a median of four cycles. Both treatment groups demonstrated an overall response rate of 26% and a similar time to disease progression of 3.8 months for the Myocet-treated group versus 4.3 months for the conventional DOX-treated group (Harris et al., 2002). The survival time was reported to be 16 months for patients receiving Myocet and 20 months for patients receiving conventional DOX (Harris et al., 2002). Furthermore, it was shown in the study that cardiac events sufficient to remove patients from the trial were more than twice as likely in patients receiving conventional DOX than in those receiving Myocet (29 versus 13%, respectively). Nine cases of congestive heart failure were found in the conventional DOX-treated group, whereas only two were found in the Myocet-treated group (Harris et al., 2002). In addition to lower cardiotoxicity, Myocet-treated patients also showed fewer incidences of grade 3 or 4 infections and grade 3 or 4 nausea/vomiting (Harris et al., 2002). Similar to the previous mentioned clinical trial by Batist et al. (2001), the estimated median cumulative lifetime dose of DOX at which cardiotoxicity first appeared was higher for Myocet than for conventional DOX (785 versus 533 mg/m$^2$, respectively) (Harris et al., 2002).

As patients with high risk factors for cardiotoxicity have a greater possibility of suffering cardiac damage when treated with conventional DOX, it is important that they are considered for Myocet treatment. In light of this, a subset analysis of high risk patients (namely those with previous DOX exposure or history of cardiac disease) was performed in individuals treated with Myocet (Batist et al., 2006). This analysis included 68 patients who had been previously treated with adjuvant conventional DOX. Although these patients received a higher cumulative dose of DOX in the Myocet-treated group (308 mg/m$^2$) compared to the conventional DOX-treated group (225 mg/m$^2$), the incidence of cardiac events was still significantly lower in the Myocet-treated group relative to conventional DOX (22 versus 39%, respectively). The median cumulative lifetime dose at which cardiotoxicity first appeared was 780 mg/m$^2$ for Myocet versus 580 mg/m$^2$ for convention DOX (Batist et al., 2006). Furthermore, antitumor efficacy was shown to be significantly higher in the Myocet-treated group with a response rate of 31 versus 11% in conventional DOX-treated group (Batist et al., 2006). The median time to treatment failure was also higher in Myocet-treated group than the conventional DOX-treated group (4.2 versus 2.1 months, respectively). However, there was no difference in the survival time between both treatment groups (Batist et al., 2006).

In another phase III clinical trial evaluating Myocet for the treatment of metastatic breast cancer, patients were randomized to receive either Myocet (75 mg/m$^2$) or epirubicin (75 mg/m$^2$), a stereoisomer of DOX known to be less cardiotoxic (Chan et al., 2004). Both groups were treated in combination with cyclophosphamide (600 mg/m$^2$) for a maximum of 8 cycles. Myocet was reported to be more effective than epirubicin in this study, showing a significantly longer time to progression (7.7 versus 4.4 months, respectively) and time to treatment failure (5.7 versus 4.4 months, respectively). There were no significant differences observed between the Myocet or epirubicin groups regarding the overall response rate (46 versus 39%, respectively) or overall survival time (18.3 versus 16 months, respectively) (Chan et al., 2004). Both the Myocet and epirubicin treatment groups also showed a lower incidence of cardiotoxicity with only 11.8 versus 10.2%, respectively, showing asymptomatic impairment in the left ventricular ejection fraction (Chan et al., 2004). No clinical

congestive heart failure was observed in both groups. However, Myocet in combination with cyclophosphamide did exhibit increased hematologic toxicity compared with epirubicin showing a significantly higher incidence of grade 4 neutropenia (87 versus 67%, respectively), although the frequency of prolonged or febrile grade 4 neutropenia was similar in both groups (Chan et al., 2004). This may be because of the difficulty in finding a comparable equivalent dose between the two drugs.

*4. Myocet versus Doxil.* No direct comparative studies between Myocet, Doxil, and conventional DOX have been conducted in humans to date. This may be because each of these formulations exhibits strikingly different DOX pharmacokinetics (Swenson et al., 2001; Leonard et al., 2009), and thus, making it difficult to determine a comparable effective dose for each formulation. However, Myocet (~46.7 l/h) is believed to have a slower clearance rate than conventional DOX (~5.1 l/h), but is not as slow as Doxil (Leonard et al., 2009). Due to its long circulation time and low clearance rate, Doxil is able to penetrate into skin tissues readily, making it more effective for the treatment of AIDS-related Kaposi sarcoma (Gordon et al., 1995; Swenson et al., 2001). However, as previously mentioned, Doxil has been observed to result in PPE as a side effect (Gordon et al., 1995). This problem is rarely observed in Myocet-treated metastatic breast cancer patients (<0.5%), which may be due to the fact that non-PEGylated liposomes are phagocytosed by mononuclear phagocytes more frequently than PEGylated liposomes (Sparano and Winer, 2001).

### C. DaunoXome

*1. The Development of DaunoXome.*

*a. Identification of lipid compositions for liposomal formulation and the selection of daunorubicin.* DaunoXome is a liposomal formulation of daunorubicin (Fig. 1) (Forssen, 1997), a member of anthracycline family that is similar to DOX (Forssen, 1997). Like DOX, the anticancer activity of daunorubicin is due to: 1) its ability to inhibit DNA synthesis by DNA intercalation and/or inhibition of DNA polymerase activity; 2) interference with topoisomerase to induce DNA damage; and 3) generation of free radicals by redox reactions that can cause molecular damage, such as lipid peroxidation. Interestingly, it was reported that daunorubicin is more effective at inhibiting DNA than RNA synthesis compared with DOX (Bremerskov and Linnemann, 1969). Apart from nucleic acid and oxidative damage that contributes to daunorubicin's anticancer activity, it was demonstrated that daunorubicin can also induce cancer cell apoptosis by initiating sphingomyelin hydrolysis, which subsequently produces ceramide (Jaffrezou et al., 1996). Currently, conventional daunorubicin is primarily used for the treatment of acute myeloid leukemia in contrast to DOX, which is implemented for the treatment of various solid tumors (Gewirtz, 1999).

The reason that daunorubicin was selected over other anthracyclines for the DaunoXome liposomal formulation was due to its enhanced stability in aqueous solution (Bosanquet, 1986) and its significant activity against various solid tumors (Hortobagyi, 1997) with therapeutic efficacy comparable to that of DOX (Michieli et al., 1993; Iwasaki et al., 1995; Nagasawa et al., 1996). Furthermore, daunorubicin is less cardiotoxic than DOX on a cumulative basis after prolonged administration (Forssen, 1997). DaunoXome was approved by the FDA and EMA in 1996 for the treatment of AIDS-related Kaposi sarcoma (Gill et al., 1996). It was also approved by the FDA for the treatment of acute myeloid leukemia in 2008 (Latagliata et al., 2008).

The development of DaunoXome began with the identification of suitable liposome compositions and physical characteristics that would allow for the maximum uptake of the encapsulated therapeutic by tumors (Forssen, 1997). This identification step was conducted by an in vivo screening approach developed by Mauk and colleagues (Hwang and Mauk, 1977; Mauk and Gamble, 1979b; Mauk et al., 1980). In this approach, a radioactive gamma emitter, indium-111 ($^{111}$In), was actively loaded into liposomes (Fig. 12), enabling the investigators to assess the stability and release of the encapsulated content from liposomes as a function of the formulation (Mauk and Gamble, 1979a). The radioactive indium was actively loaded into a preformed liposome by incorporating ionophores (A23187) into the liposomal membrane bilayer, allowing $^{111}In^{3+}$ ions to pass through the membrane (Fig. 12).

Once inside the liposome, $^{111}In^{3+}$ ions were trapped within the liposomal cavity upon complexation with the weak chelating agent, nitrilotriacetic acid (NTA) (Mauk and Gamble, 1979a). Although NTA could trap $^{111}In^{3+}$ within the liposome, only weak binding between $^{111}In^{3+}$ and NTA occurred, and thus, allowing the high affinity association of $^{111}In^{3+}$ with biologic macromolecules to occur (Mauk and Gamble, 1979a). By using active loading, >90% of $^{111}In^{3+}$ could be encapsulated within liposomes. As $^{111}In^{3+}$ binds strongly to tissues and is known to have minimal redistribution (Hwang et al., 1982), the total $^{111}In^{3+}$ released from liposomes into the targeted tissue can be estimated with accuracy.

From extensive in vivo screening of different liposomal formulations, liposomes composed of DSPC and cholesterol in a 2:1 molar ratio and with a diameter between 40 and 80 nm were the most effective formulation for the delivery of encapsulated $^{111}$In to tumor tissues in vivo (Proffitt et al., 1983b; Turner et al., 1988; Williams et al., 1988). These DSPC:cholesterol liposomes were able to deliver encapsulated $^{111}$In to tumor cells selectively in a number of murine tumor models, including the mammary adenocarcinomas, EMT-6 and 16C, B16 melanoma, Lewis lung carcinoma, P1798

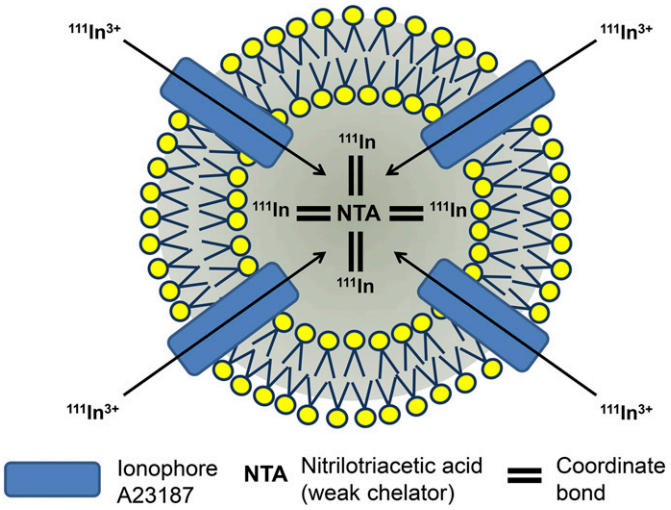


**Fig. 12.** Remote loading of $^{111}In$ into liposomes. The ionophore A23187 is inserted into the lipid bilayer of liposomes. The incorporation of ionophores into liposomal membrane allows $^{111}In^{3+}$ ions to cross the membrane into the liposome cavity. The weak chelator, nitrilotriacetic acid, inside the liposome then traps $^{111}In$ by forming a weak complex with $^{111}In^{3+}$ ions.

lymphosarcoma, sarcoma 180, and colon carcinoma 51 (Proffitt et al., 1983a,b; Patel et al., 1985). This liposomal formulation was subsequently developed into an $^{111}In$-based tumor imaging agent (VesCan), which could image a wide range of solid neoplasms (Presant et al., 1988, 1990). In particular, Kaposi sarcoma demonstrated the highest level of $^{111}In$ uptake of all tumors investigated (Presant et al., 1990). It was suggested that the high uptake of $^{111}In$ in Kaposi sarcoma lesions might be due to their highly vascularized nature, which allowed small particles, such as liposomes, to extravasate readily (Wu et al., 1993; Brown et al., 1996). As a result of the high accumulation of liposomal $^{111}In$ within Kaposi sarcoma lesions, the development of DaunoXome using DSPC:cholesterol (2:1 molar ratio) began.

Apart from delivering liposomal contents efficiently, liposomes prepared from a DSPC:cholesterol (2:1 molar ratio) formulation also posed other advantages (Forssen, 1997). First, liposomal membranes composed of these lipid compositions exhibit a high PTT (Forssen, 1997). This means that, under physiologic or ambient conditions, DSPC:cholesterol liposomes remain stable and are more resistant to the leakage of their entrapped contents. Second, having only two key components in a liposomal formulation simplifies the manufacturing conditions and formulation parameters suitable for both the active ingredients and the carrier (Forssen, 1997). Third, as the in vivo delivery mechanism of these liposomes depends mostly upon the physiologic properties of tumors and their highly vascularized nature, these liposomes can target a wide range of solid tumors and are less affected by targeting problems, such as antigenic drift (Forssen, 1997). Although antigenic drift usually occurs in viruses where the virus undergoes mutations in the antigenic epitopes (antibody binding site) to escape recognition by antibodies and cytotoxic T-lymphocytes, tumors have also been reported to use a similar process as one of the mechanisms to avoid the immune system (Bai et al., 2003). For more detail, please see Bai et al. (2003).

*b. Incorporation of daunorubicin into liposomes.* Initially, two approaches were investigated for the preparation of liposomal daunorubicin (Forssen, 1997). The first approach involved incorporating daunorubicin into the membrane bilayer of liposomes as an associated complex between the drug and negatively charged 1,2-distearoyl-*sn*-glycero-3-phospho-(1′-*rac*-glycerol). On the other hand, the second approach involved encapsulating daunorubicin within the liposome interior in the form of a citrate salt similar to that used with Myocet (Forssen, 1997; Swenson et al., 2001). Although both approaches demonstrated some improvements over the free drug, the encapsulation of daunorubicin within the liposome cavity was shown to be more effective in terms of biodistribution and antitumor activity during animal studies than the former membrane-associated approach (Forssen et al., 1992).

The poorer activity of membrane-bound daunorubicin liposomes could be explained by the lower serum stability of this formulation compared with the liposomal encapsulated daunorubicin, which was most likely due to the high exposure of the drug to serum proteins and its leakage from the membrane bilayer (Forssen et al., 1992). In contrast, when the drug was encapsulated within the liposome interior, it became less accessible to the liposomal membrane, making it less likely to leak or interact with serum proteins (Forssen et al., 1992).

The difference in serum stability between the two formulations was investigated in fetal calf serum at 37°C. Liposomal encapsulated daunorubicin demonstrated a significantly higher retention time over membrane-bound daunorubicin liposomes (Forssen et al., 1992). It was shown in this study that membrane-bound daunorubicin liposomes released more than one-third of the drug after 3 hours of incubation, whereas the release of only 2% of liposomal encapsulated daunorubicin was observed after 50 hours (Forssen et al., 1992). Furthermore, the encapsulation of daunorubicin within the liposome interior meant that no anionic phospholipid was required, and thus, resulted in enhanced tumor uptake, because less negatively charged liposomes were shown to be more effective at delivering drugs to tumors (Juliano and Stamp, 1975; Gregoriadis, 1988; Krasnici et al., 2003; Jung et al., 2009).

*2. Preclinical Studies of DaunoXome.* Once it was established that the formulation in which liposome encapsulated daunorubicin within its interior was the most effective delivery approach, preclinical studies

were investigated to evaluate the efficacy, toxicity, and pharmacokinetic profile of this formulation.

The examination of the in vitro cytotoxicity of DaunoXome and conventional daunorubicin against P1798 tumor cells demonstrated that the relative potency of these two forms of daunorubicin varied widely depending on the incubation time (Forssen et al., 1996). For incubation periods under 8 hours, DaunoXome was observed to be less cytotoxic than free daunorubicin. This could be explained by the high membrane permeability of the conventional drug, allowing it to become fully available immediately after it was added to the culture medium. However, after a longer incubation period, DaunoXome was more cytotoxic than conventional daunorubicin (Forssen et al., 1996). A similar result was observed by confocal microscopy imaging of P1798 cells incubated with either free daunorubicin or DaunoXome (Forssen et al., 1996).

It was suggested that DaunoXome is internalized by cells via endocytosis (Forssen, 1997) and subsequently enters the lysosomal compartment, like other nanoparticles (Harding et al., 1991; Turek et al., 1993; Naito et al., 1996; Nam et al., 2009). The study of DaunoXome's mechanism of uptake was examined by Forssen (1997). In these studies, the indigo dye precursors, 5-bromo-4-chloro-3-indolyl-$\beta$-D-galactopyranoside or 5-bromo-4-chloro-3-indolyl-$\beta$-D-phosphate, were encapsulated within DSPC:cholesterol liposomes and used to investigate the mechanism of uptake of these liposomes into cells. These precursors, when not encapsulated within liposomes, were poorly taken up by cells both in vitro and in vivo. Furthermore, when activated by the lysosomal enzymes $\beta$-galactosidase (for 5-bromo-4-chloro-3-indolyl-$\beta$-D-galactopyranoside) or alkaline phosphatase (for 5-bromo-4-chloro-3-indolyl-$\beta$-D-phosphate), these agents form an insoluble blue-violet dye (Tsou et al., 1972). When liposomes containing these precursors were examined in tissue culture, a compartmentalized blue-violet dye was observed within the cytoplasm (Forssen, 1997). In contrast, this dye formation was absent when the same compounds in their free forms were used to treat these cells (Forssen, 1997). Thus, these observations were consistent with liposome endocytosis followed by lysosomal fusion.

Two murine models bearing P1798 lymphosarcoma and mammary adenocarcinoma MA16C xenografts were used in the preclinical animal studies of DaunoXome (Forssen et al., 1992). In the fast growing P1798 lymphosarcoma animal model, the single-dose efficacy of DaunoXome and conventional daunorubicin were compared. At equivalent daunorubicin doses, DaunoXome generated a significantly higher median survival time than the conventional drug at all doses investigated (Forssen et al., 1992). The maximum median survival time of tumor-bearing mice achieved for the conventional drug-treated group was 18.5 days at 30 mg/kg, whereas a dose of 40 mg/kg became too toxic, reducing the median survival time to 12.5 days (Forssen et al., 1992). There were no long-term survivors observed in the conventional drug-treated group. In comparison, the maximum median survival time for the DaunoXome-treated mice at 30 mg/kg was 21.5 days. Moreover, there were three long-term survivors observed (>60 days) in this group (Forssen et al., 1992).

In the slow growing mammary adenocarcinoma MA16C model, tumor-free long-term survivors were observed in mice treated with conventional daunorubicin at a dose of 10 and 20 mg/kg, with one and four survivors observed, respectively (Forssen et al., 1992). The remaining mice in this group either developed detectable tumors or died of drug toxicity at higher doses (Forssen et al., 1992). In the DaunoXome-treated group, the occurrence of tumor-free long-term survivors was much more frequent. Forty-nine mice in this group were treated with DaunoXome at doses ranging from 2 to 35 mg/kg, with only three mice having small residual tumors after treatment (two mice at 2 mg/kg and one at 20 mg/kg). In contrast, the other remaining 46 mice were observed to be tumor free (Forssen et al., 1992). Additionally, an apparent complete cure was observed in DaunoXome-treated mice at 25 mg/kg, with all mice becoming tumor free at this dose (Forssen et al., 1992).

The direct cytotoxic effect of DaunoXome against tumors in vivo was also demonstrated by a significant reduction in tumor volume of DaunoXome-treated mice in comparison with conventional drug-treated mice (Forssen et al., 1992). In the conventional drug-treated group, regardless of the dose level, each established tumor eventually grew to a size of >500 mg (Forssen et al., 1992). In contrast, of the 40 mice treated with DaunoXome at doses between 15 and 30 mg/kg, 14 of them were observed to have tumors that regressed and disappeared completely. Based on these data, it was suggested that the tumor growth suppression of DaunoXome at 2 mg/kg was approximately equivalent to the effect observed with conventional daunorubicin at 15 mg/kg (Forssen et al., 1992).

The effectiveness of DaunoXome over conventional daunorubicin can be explained in terms of altered pharmacokinetics. Significant differences in the pharmacokinetics of these two formulations were observed in plasma and also using P1798 solid tumor xenografts (Forssen et al., 1992). The plasma level of daunorubicin-eq (daunorubicin fluorescent equivalent; parent drug plus fluorescent metabolites) produced by DaunoXome after 1 hour was 268 $\mu$g/ml, a 185-fold increase over the level produced by the conventional drug (i.e., 1.4 $\mu$g/ml). Additionally, the plasma AUC value of DaunoXome was 227-fold higher than the conventional drug (Forssen et al., 1992). The daunorubicin-eq levels in tumors 1 hour postinjection of the conventional drug was 9.6 $\mu$g/g. On the other hand, DaunoXome produced an accumulation of daunorubicin-eq within the tumor that

continued to increase 8 hour postinjection, peaking at 100 $\mu$g/g (Forssen et al., 1992).

The tissue daunorubicin AUC ratios for DaunoXome and the conventional drug were also compared (Forssen et al., 1992). The comparison demonstrated a 10-fold increase in the AUC ratio produced by DaunoXome in tumor tissue relative to conventional daunorubicin (Forssen et al., 1992). In contrast, the AUC ratios of DaunoXome for hepatic, splenic, and brain tissue increased slightly, with no significance difference being found relative to conventional daunorubicin (Forssen et al., 1992). In addition, a slight decrease in the AUC ratio was observed in both the heart and lungs relative to daunorubicin. Hence, as shown by these results, DaunoXome was able to accumulate daunorubicin within tumor tissues at a higher level than other tissue types compared with conventional daunorubicin (Forssen et al., 1992). From preclinical data, it was concluded that DaunoXome operated through targeted delivery, as shown by a 10-fold increase in the tumor AUC value in comparison with a 0.4- to 1.6-fold change observed in normal tissues (Forssen et al., 1992). This finding demonstrated the improved tumor selectivity of DaunoXome over free daunorubicin.

*3. Clinical Studies of DaunoXome.*

*a. Clinical trials for AIDS-related kaposi sarcoma.* The therapeutic efficacy and safety of DaunoXome has also been investigated in human trials. The effectiveness of DaunoXome in humans was observed to be similar to the results found in preclinical studies and was well tolerated (Money-Kyrle et al., 1993; Presant et al., 1993). In phase I/II dose escalation clinical studies involving 22 patients with AIDS-related Kaposi sarcoma, an overall response rate (including both partial and complete responses) of 55% was noted at the dose levels of 50 and 60 mg/m$^2$ every fortnight (Gill et al., 1995). In another human study, Presant et al. (1993) investigated the efficacy and toxicity of DaunoXome by treating HIV-associated Kaposi sarcoma of poor prognosis patients ($n$ = 25) with DaunoXome at 40 mg/m$^2$ every 2 weeks. At this dosage, 2 patients demonstrated complete remission (8.3%), whereas 13 patients had a partial remission (54.2%), including 5 of 11 patients diagnosed with DOX-resistant Kaposi sarcoma (Presant et al., 1993). The side effects of DaunoXome were well tolerated, with myelosuppression being the most common adverse event. Vomiting, stomatitis, and alopecia were rare and mild, whereas no serious cardiotoxicity was observed in any patients (Presant et al., 1993).

A similar result was also achieved in phase II clinical studies investigating the efficacy and toxicity of DaunoXome (Money-Kyrle et al., 1993). In this study, 11 advanced AIDS-related Kaposi sarcoma patients with a life expectancy of at least 8 weeks were given DaunoXome at 40 mg/m$^2$ every 2 weeks. By the end of the study, 1 patient died before receiving any treatment, whereas 4 of 10 patients had a partial response (Money-Kyrle et al., 1993). However, 2 of these 4 patients with a partial response were subsequently observed to have a relapse. The remaining 6 patients had stabilized disease, which lasted until the end of the trial (Money-Kyrle et al., 1993). This study also demonstrated that liposomal daunorubicin, DaunoXome, was generally well tolerated with no sign of cardiotoxicity. However, nausea, vomiting, stomatitis, alopecia, and neutropenia were evident (Money-Kyrle et al., 1993). In addition, there was no evidence of serious complications, such as hepatotoxicity.

A more comprehensive, randomized phase III clinical trial was conducted by Gill et al. (1996). The aim of this trial was to compare the therapeutic efficacy of DaunoXome to the standard regimen of DOX, bleomycin, and vincristine (ABV) for the treatment of AIDS-related Kaposi sarcoma. This involved treating 232 AIDS-related Kaposi sarcoma patients with either DaunoXome (40 mg/m$^2$) or a combination of DOX (10 mg/m$^2$), bleomycin (15 U), and vincristine (1 mg; ABV). Patients were given the treatment every 2 weeks until: 1) a complete response was achieved; 2) unacceptable toxicity was observed; or 3) the disease continued to progress. Interestingly, the results were comparable between DaunoXome and the ABV combination. The overall response rate was 25% (3 complete responses and 26 partial responses of 116 patients) for the DaunoXome-treated group and 28% (1 complete response and 30 partial responses of 111 patients) for the ABV-treated group (Gill et al., 1996). In general, there was no significant difference between the two treatments in terms of their response rate, survival time, and median time to disease progression. However, toxicities induced by the two treatments were significantly different (Gill et al., 1996). The ABV-treated group had a higher incidence of alopecia and neuropathy, whereas the DaunoXome-treated group exhibited a higher incidence of grade 4 neutropenia (Gill et al., 1996). In addition, the cardiac functions of all patients were normal, with neither treatment group showing any signs of anthracycline-associated cardiotoxicity (Gill et al., 1996).

*b. Clinical trials for acute myeloid leukemia.* DaunoXome was approved for the treatment of acute myeloid leukemia by the FDA in 2008. Latagliata et al. (2008) conducted a randomized phase III clinical trial in 301 patients aged over 60 years diagnosed with acute myeloid leukemia to compare the efficacy of DaunoXome versus daunorubicin. Patients received either DaunoXome (45 mg/m$^2$, days 1–3) plus cytarabine (100 mg/m$^2$, days 1–7 by continuous infusion) or daunorubicin (80 mg/m$^2$, days 1–3) plus cytarabine (100 mg/m$^2$, days 1–7 by continuous infusion). Patients with a complete response received a further course of the assigned treatment, followed by a randomized treatment of cytarabine plus *trans* retinoic acid or no treatment. Of 148 patients receiving DaunoXome, 73 (49.3%) achieved a complete response, 47 (31.8%) were resistant to the treatment and 28 (18.9%) died during the study

(Latagliata et al., 2008). On the other hand, of 153 patients receiving daunorubicin, 78 (51.0%) achieved a complete response, 55 (35.9%) were resistant to the treatment, and 20 (13.1%) died during the study. In patients demonstrating a complete response, those receiving DaunoXome showed a higher rate of early deaths relative to those receiving conventional daunorubicin (12.5 versus 2.6% at 6 months, respectively), but a lower incidence of relapse beyond 6 months (59 versus 78% at 24 months, respectively). In conclusion, although DaunoXome performance may be inferior to daunorubicin in term of its short-term efficacy, its long-term anticancer activity was slightly greater than daunorubicin, because it improved both overall survival and disease free survival time (Latagliata et al., 2008).

*3. Side Effects and Safety of DaunoXome.* Overall, DaunoXome provides an effective and safe alternative to conventional drugs for the treatment of AIDS-related Kaposi sarcoma and acute myeloid leukemia. It has demonstrated a significant rate of tumor regression even in patients who have failed prior chemotherapy (Gill et al., 1996). Side effects of DaunoXome have been shown to be milder than free daunorubicin, with no evidence of anthracycline-related cardiotoxicity. Furthermore, because of the minimal myelosuppression observed with DaunoXome, anti-HIV therapies, such as azidothymidine, can be used together with DaunoXome, further improving patient treatment (Forssen and Ross, 1994; Forssen, 1997).

### *D. Marqibo*

Marqibo is a liposomal formulation of vincristine sulfate. It was approved by the FDA in 2012 under the accelerated program for the treatment of adult patients with Philadelphia chromosome-negative acute lymphoblastic leukemia after a second or further relapse, or whose disease progressed after two or more antileukemia therapies (Silverman and Deitcher, 2013). The composition of Marqibo liposomes consisted of sphingomyelin and cholesterol, which were designed to: 1) enhance the loading and retention of vincristine; 2) improve the circulation time of encapsulated vincristine; 3) increase the extravasation of vincristine into tumors; and 4) sustain vincristine release into the tumor interstitium (Zhigaltsev et al., 2005; Johnston et al., 2006).

*1. Vincristine.* Vincristine (Fig. 1) is a cell-cycle dependent anticancer drug that has been commercially available on the market since 1963 (Silverman and Deitcher, 2013). It directly binds to tubulin, causing microtubule depolymerization, M-phase arrest, and apoptosis in cells undergoing mitosis (Silverman and Deitcher, 2013). The most effective treatment strategy for vincristine occurs when cancer cells are exposed to a high concentration of vincristine over a long period of time. Unfortunately, this is unachievable because vincristine also induces autonomic and peripheral sensorymotor polyneuropathy, which is due to a blockage in axon transport and axon degradation caused by nonfunctional microtubules (Moore and Pinkerton, 2009). As a result of its dose-limiting toxic side effects, vincristine dosage is usually restricted to 2 mg/m$^2$ (Moore and Pinkerton, 2009). Hence, vincristine sulfate liposomal injection (i.e., Marqibo) was developed to improve the pharmacokinetic and pharmacodynamic profiles of vincristine.

*2. The Development of Marqibo.* Early studies investigating the liposomal formulation of vincristine examined the encapsulation of the drug within egg PC/cholesterol or DSPC/cholesterol liposomes, both at a lipid composition ratio of 55:45 (Mayer et al., 1990b; Boman et al., 1995; Waterhouse et al., 2005). The loading of vincristine into these liposomes was conducted by remote loading using a pH gradient, where the intra- and extraliposomal pH were 4.0 and 7.5, respectively (Mayer et al., 1990b). Although remote loading was able to encapsulate a high concentration of vincristine with an encapsulation efficiency of 98% in both liposome formulations, the release of vincristine from these liposomes was not as prolonged and sustained as expected (Mayer et al., 1990b). In fact, the egg PC/cholesterol liposomal formulation of vincristine showed a release of 96% of the entrapped content into whole blood after just 24 hours at 37°C (Mayer et al., 1993). Only a small improvement was observed when egg PC was replaced by DSPC, with ~80% of vincristine being released after 24 hours at 37°C (Mayer et al., 1993). A similar result was observed in vivo, where encapsulated vincristine escaped the liposomes rapidly into the plasma after an intravenous injection into mice inoculated with L1210 leukemia (Mayer et al., 1993).

However, a significant improvement in terms of prolonged vincristine release was observed when DSPC was substituted with sphingomyelin. Such substitution led to a reduction in both the liposomal vincristine leakage rate and hydrolysis rate by 1.42-fold and 100-fold in vitro, respectively (Webb et al., 1995) and a ~75% retention of encapsulated vincristine within liposomes 24 hours after an intravenous injection into mice (Boman et al., 1994, 1995; Webb et al., 1995; Johnstone et al., 2001; Krishna et al., 2001). Furthermore, the mean particle size of ~100 nm helped prolong the circulation time of liposomal vincristine (Peixoto Júnior et al., 2009; Thomas et al., 2009; Silverman and Deitcher, 2013). A negligible level of bovine and human plasma protein binding was also observed on the surface of liposomal vincristine during in vitro studies, which was probably due to the neutral charge of the sphingomyelin/cholesterol composition and a tight lipid arrangement (Webb et al., 1995; Oja et al., 1996). This minimal protein binding may have further extended the circulation time of sphingomyelin/cholesterol liposomes (Webb et al., 1995). As such, the sphingomyelin/cholesterol (55:45)

liposomal formulation was used to encapsulate vincristine in the production of Marqibo.

*3. Preclinical Studies of Marqibo.* Preclinical studies demonstrated Marqibo to be more effective than free vincristine without imposing additional toxicities by means of prolonged plasma circulation time, increased drug penetration, and increased plasma drug concentration (Kanter et al., 1994; Webb et al., 1998). A significantly higher AUC and a lower total vincristine clearance and volume of distribution compared with standard vincristine were observed across mice, rats, and dog models treated with Marqibo, suggesting that the encapsulated drug remained within the body for a longer period of time (Kanter et al., 1994). This was supported by the delay in vincristine excretion in rats injected with Marqibo. In fact, a radiolabeled mass-balance study in rats demonstrated that 90% of Marqibo administered was detected in the urine and feces more than 72 hours after the initial administration (Kanter et al., 1994), a delay of 12–48 hours compared with standard vincristine (Castle et al., 1976).

In addition, Webb et al. (1998) demonstrated that vincristine concentration in the blood and plasma were at least 2-fold higher in mice treated with Marqibo (2 mg/kg of encapsulated vincristine) than in those given unencapsulated vincristine at an identical dose. There was also at least a 10-fold higher drug concentration accumulated within lymph nodes, heart, kidney, liver, skin, small intestine, and spleen in mice treated with liposomal vincristine than in those treated with free drug 1 day after administration (Webb et al., 1998). The study further showed that the increased drug exposure as a result of liposomal encapsulation was not associated with increased drug toxicity. It was reported that mice bearing a P388 ascitic tumor given Marqibo (2, 3, or 4 mg/kg) had a survival rate of at least 50% in all treatment groups, with a 4 mg/kg dose being the most effective (8–9 of 10 mice survived past 60 days depending on drug:lipid ratio). In contrast, mice treated with free vincristine at an identical dose displayed only a 33–38% survival rate (Webb et al., 1998).

By using the liposomal formulation, vincristine was proven to be more efficacious and tolerable than its standard formulation (Shan et al., 2006; Silverman and Deitcher, 2013). In these studies, mice bearing Namwala tumor xenografts were injected intravenously with 1.0, 1.5 and 2.5 mg/kg of Marqibo and compared with those injected with 0.5, 1.0, and 1.5 mg/kg of standard vincristine (Silverman and Deitcher, 2013). The mice injected with Marqibo demonstrated greater tumor suppression than those given standard vincristine, with the Marqibo dose of 2.5 mg/kg showing the highest activity. The MTD for Marqibo was 2.5 mg/kg, a dose unachievable by standard vincristine treatment, where a MTD of 1.5 mg/kg was observed (Silverman and Deitcher, 2013). A similar result was reported using the LX-1 human small-cell lung carcinoma xenograft mouse model, in which Marqibo was shown to have greater antitumor activity than its free drug formulation at the equivalent dose of 1.0 mg/kg (Shan et al., 2006). This study also investigated the extravasation kinetics and accumulation of liposomal encapsulated vincristine using intravital microscopy imaging. Notably, significantly faster extravasation of liposomes was observed in tumor blood vessels than in normal tissues after a single dose of fluorescently labeled liposomal encapsulated vincristine (Shan et al., 2006). Furthermore, the accumulation of liposomal vincristine within the interstitium was ~70-fold higher in tumor tissue than in normal tissues at 1 hour and remained greater even after 48 hours (Shan et al., 2006).

Silverman and Deitcher (2013) summarized the effect of Marqibo over standard vincristine in 18 animal tumor models representing 11 different cancer types to show the superior anticancer activity of Marqibo. In all cases, Marqibo showed equivalent or higher anticancer activity than standard vincristine for the same dose level. The dose-dependent antitumor activity of Marqibo was observed in 13 of 18 models. Three models were not sensitive to either Marqibo or standard free drug, whereas one was highly sensitive to both treatments (Silverman and Deitcher, 2013).

*4. Clinical Studies of Marqibo.* As observed in animal models, Marqibo administered to humans demonstrated a similar improvement over standard vincristine (Thomas et al., 2009; Yan et al., 2012; O'Brien et al., 2013). Indeed, higher doses of Marqibo were able to be administered to patients compared with standard vincristine (Hagemeister et al., 2013; O'Brien et al., 2013). As vincristine in excess of 2 mg has been associated with severe neuropathy, a standard vincristine dose of 1.5 mg/m$^2$ has a dose cap of 2.0 mg per single administration, regardless of the total body surface area (Haim et al., 1994). This helps limit the amount of vincristine exposed to patients with a total body surface area >1.33 m$^2$ (Raj et al., 2013). In contrast, this dose cap was not assigned to the liposomal encapsulated vincristine formulation Marqibo during two clinical studies (Hagemeister et al., 2013; O'Brien et al., 2013). It was also identified in two phase I clinical studies that the dose-limiting toxicities and MTD of Marqibo monotherapy were 2.8 and 2.4 mg/m$^2$, respectively, whereas the dose-limiting toxicities and MTD of Marqibo in combination with dexamethasone were 2.4 and 2.25 mg/m$^2$, respectively (Gelmon et al., 1999; Thomas et al., 2009).

Liposomal encapsulation of vincristine was also recently reported to improve the pharmacokinetics of this drug. A single dose injection of 2.0 mg/m$^2$ Marqibo into patients with solid tumors demonstrated an increase in the plasma AUC and a reduction in the clearance rate of encapsulated vincristine compared with patients treated with a single 2.0 mg/m$^2$ dose of standard vincristine (Yan et al., 2012). However, the concentration-dependent

efficacy of Marqibo was not significantly different in this study when the Marqibo dose was changed to 1.5 or 2.3 mg/m$^2$.

Further positive results with Marqibo treatment in humans were reported in clinical trials conducted for its approval (Thomas et al., 2006; O'Brien et al., 2013). In a phase II clinical trial for Marqibo monotherapy (Thomas et al., 2006), 16 adult patients with recurrent or refractory acute lymphocytic leukemia were given liposomal encapsulated vincristine/sodium phosphate mixture (concentration of 0.16 mg/ml) via an intravenous infusion over 60 minutes at a dose of 2 mg/m$^2$. The administration was repeated every 2 weeks provided that there was no sign of rapid disease progression or dose-limiting toxicities observed in each patient. Of 14 patients eligible for evaluation, 2 patients (14%) met the overall objective response criteria. This result consisted of one complete response after three doses of liposomal encapsulated vincristine and one partial response after two doses (Thomas et al., 2006).

In the landmark phase I trial of Marqibo that led to its approval by the FDA, some positive responses were observed in adult patients with advanced relapsed or refractory Philadelphia chromosome-negative–acute lymphoblastic leukemia (O'Brien et al., 2013). Sixty-five patients were treated with Marqibo on a weekly basis at a dose of 2.25 mg/m$^2$ with no dose capping via intravenous infusion over 60 minutes (O'Brien et al., 2013). The primary efficacy end point was defined as the proportion of patients who achieved a complete response or a complete response with incomplete recovery of peripheral blood neutrophil counts or platelet counts. The overall response rate obtained was 35%, with 20% achieving either a complete response or a complete response with incomplete recovery (O'Brien et al., 2013). Complete response/complete response with incomplete recovery was observed in 25% of patients with an untreated relapse and 14% of patients with a relapse previously refractory to single- or multi-agent antileukemic therapy (O'Brien et al., 2013). Median complete response/complete response with incomplete recovery duration was 23 weeks, with 12 patients proceeding to hematopoietic cell transplantation after Marqibo treatment, whereas 5 patients were long-term survivors (O'Brien et al., 2013).

Apart from being studied as a monotherapy, Marqibo had been investigated in combination with various anticancer drugs. For example, a phase I multi-center study assessed Marqibo in combination with dexamethasone for the treatment of relapsed or refractory acute lymphoblastic leukemia (Thomas et al., 2009). In this investigation, 36 patients were administered with Marqibo (i.v.) weekly at 1.5, 1.825, 2.0, 2.25, or 2.4 mg/m$^2$, whereas dexamethasone (40 mg) was given on days 1 through 4 and on days 11 through 14 of each 4-week cycle (Thomas et al., 2009). This study reported the complete response rate of 29% for the 14 patients who underwent therapy as their first salvage attempt (Thomas et al., 2009).

Furthermore, a phase II clinical trial examining the long-term effects of Marqibo in multidrug therapy where conventional vincristine was replaced with Marqibo also demonstrated positive results in patients with hematologic cancer (Hagemeister et al., 2013). This study included 72 patients with untreated aggressive non-Hodgkin lymphoma, 60 of whom had diffuse large B-cell lymphoma. Patients received a combination of cyclophosphamide, DOX, Marqibo (2.0 mg/m$^2$ without dose cap), and prednisone with or without rituximab via intravenous infusion for six cycles. Furthermore, patients with disease regression were prescribed up to eight cycles, whereas patients with no enlargement of lymph node larger than 5 cm were subjected to three cycles followed by local radiotherapy (Hagemeister et al., 2013). The overall response rate was 96% (69/72), including 65 (90%) complete responses, 2 (3%) with unconfirmed complete responses, and 2 (3%) with partial responses. The median progression free survival and overall survival were not reached at median follow up of 8 and 10.2 years, respectively. In addition, the 5 and 10 year progression free survival and overall survival were 75 and 63, 87 and 77%, respectively (Hagemeister et al., 2013). Apart from this study, Marqibo is also currently being investigated as a multidrug therapy (prednisone with or without rituximab) in a phase III clinical trial for elderly patients with untreated diffuse large B-cell lymphoma (Hagemeister et al., 2013).

*5. Side Effects and Safety of Marqibo.* Despite higher vincristine exposure in Marqibo compared with standard vincristine, Marqibo treatment was well tolerated in most patients (Thomas et al., 2006, 2009; Hagemeister et al., 2013; O'Brien et al., 2013). Thomas et al. (2006) reported two patients with grade 1 peripheral neuropathy after 2 and 4 doses of Marqibo. However, both patients had a history of vincristine-related peripheral neuropathy. They also reported one patient with grade 2 orthostasis and intermittent headaches (Thomas et al., 2006). O'Brien et al. (2013) reported that of 65 patients, 86% had neuropathy-associated adverse events, with 23% reported to be grade 3 peripheral neuropathy-related events. In addition, one grade 4 peripheral neuropathy-related adverse event was also observed in this study. The high incidence of adverse side effects could be explained by the fact that 77% of these patients had reported neuropathy-related symptoms before the study (O'Brien et al., 2013). Apart from neuropathy-related side effects, grade 1–2 constipation, nausea, and vomiting were observed in 34, 22, and 11% of patients, respectively (O'Brien et al., 2013).

In combination therapy studies, patients treated with Marqibo and dexamethasone were reported to exhibit constipation (67%), fatigue (61%), peripheral neuropathy (55%), anemia (50%), and pyrexia (50%), most of

which were of grade 1–2 (Thomas et al., 2009). Furthermore, clinically relevant toxicities of grade 3–4 were only observed when the MTD of 2.25 mg/m$^2$ was reached (Thomas et al., 2009). Similarly, combination therapy of Marqibo with multiple anticancer agents was also reported to be well tolerated, despite the exposure of up to 35 mg of liposomal encapsulated vincristine (Hagemeister et al., 2013). All nervous system-related adverse events in this latter study were of grade 1–2 magnitude, except for grade 3 peripheral neuropathy that was reported in 2 of 72 patients. No patients reported grade 4 neuropathy-related adverse events (Hagemeister et al., 2013). Constipation of any grade was reported in 15% of patients with no patient reporting grade 3–4 constipation (Hagemeister et al., 2013).

### *E. DepoCyt*

DepoCyt (also known as DTC 101) is the liposomal formulation of the anticancer drug cytarabine (Fig. 1) (Murry and Blaney, 2000; Angst and Drover, 2006). It was approved by the FDA in 2000 for the intrathecal injection treatment of lymphomatous meningitis (Dagher et al., 2004). To understand why the development of DepoCyt was necessary, it is important to understand the pathology of neoplastic meningitis (NM) and its current form of treatment.

*1. Conventional Cytarabine Treatment and Neoplastic Meningitis.* NM, also known as leptomeningeal metastases, is characterized by the infiltration of leptomeninges by cancerous cells (Little et al., 1974; Olson et al., 1974; Theodore and Gendelman, 1981). Once inside the leptomeninges, cancerous cells use cerebrospinal fluid (CSF) as a mean to metastasize throughout the neuraxis (Chamberlain and Corey-Bloom, 1991). NM most often occurs in patients with primary hematologic malignancies, solid tumors of the breast and lungs, and melanoma (Kaplan et al., 1990). The main obstacle for the treatment of NM has always been the poor penetration of chemotherapeutic agents administered systemically across the blood-brain barrier into the CSF (Angst and Drover, 2006). As a result, the treatment of NM may involve radiation therapy and intrathecal chemotherapy (Shapiro et al., 1977). Although radiation therapy is effective in the treatment of leukemic meningitis, its long-term efficacy in other types of NM is uncertain (Murry and Blaney, 2000). Furthermore, craniospinal radiation has been shown to cause acute toxicity, such as myelosuppression, as well as long-term neurologic and neuroendocrine complications (Murry and Blaney, 2000). Consequently, intrathecal administration of the antimetabolites cytarabine and methotrexate has been chosen as a preferred standard treatment of NM (Murry and Blaney, 2000; Angst and Drover, 2006).

The cytotoxic effects of both cytarabine and methotrexate are cell-cycle specific and only occur during the synthesis of DNA (Graham and Whitmore, 1970). The optimal therapeutic efficacy of these cell-cycle-specific agents requires cancer cells to be exposed to low or moderate concentrations of these compounds for a prolonged period of time (Graham and Whitmore, 1970). However, such treatment is limited by the short half-life of these chemotherapeutic agents in the CSF (Bleyer et al., 1978; Zimm et al., 1984). Typically, to achieve the effective drug concentration and to solve the problem of their short half-life, cytarabine and methotrexate are administered by frequent intrathecal injections or a continuous infusion, both of which pose the risk of infections and are inconvenient as well as time consuming for patients (Angst and Drover, 2006). Thus, a sustained release delivery system generating a minimum cytotoxic drug concentration over an extended period of time after an initial intrathecal injection may solve the problems presented in the current standard treatment of NM (Angst and Drover, 2006).

*2. The Development of DepoCyt.* DepoCyt is essentially cytarabine encapsulated in multivesicular liposomes (MVLs) generated by DepoFoam technology derived from a water-in-oil-in-water (w/o/w) double emulsification process (Mantripragada, 2002). DepoFoam MVLs containing cytarabine are microscopic spherical particles usually ranging between 3 and 30 $\mu$m in size (Murry and Blaney, 2000; Angst and Drover, 2006). Each particle is composed of numerous nonconcentric polyhedral aqueous compartments separated by a lipid bilayer membrane made of lipids, such as dioleoyl PC, dipalmitoyl PG, cholesterol, and triolein (Fig. 13) (Murry and Blaney, 2000; Angst and Drover, 2006). It is possible to imagine MVLs as architecturally analogous to aggregated soap bubbles (Angst and Drover, 2006). As MVLs are much larger than typical unilamellar or multilamellar liposomes, they provide a much greater drug loading capacity. Typical DepoFoam MVLs are composed of ~4% lipid and 96% water, which are suitable for encapsulating hydrophilic drugs, such as cytarabine (Murry and Blaney, 2000). Although the cytarabine encapsulated MVLs (i.e., DepoCyt) are not considered nanoparticles, they are worth discussing, because they represent a different type of liposome that is capable of encapsulating hydrophilic drugs as well as sensitive molecules, such as proteins, and provide an alternative mean for sustained release.

*3. Preclinical Studies of DepoCyt.* The evidence for DepoCyt providing sustained drug release was first demonstrated in animal studies (Kim and Howell, 1987a,b; Kim et al., 1987b). Studies in mice demonstrated that when DepoCyt was injected subcutaneously or intraperitoneally, the serum half-life of cytarabine was significantly longer than that found with conventional cytarabine (Kim and Howell, 1987a,b; Kim et al., 1987b). For example, after a single subcutaneous injection of DepoCyt into BDF1 mice inoculated with L1210 leukemia cells, the half-life of cytarabine was 4 days (96 hours) compared with

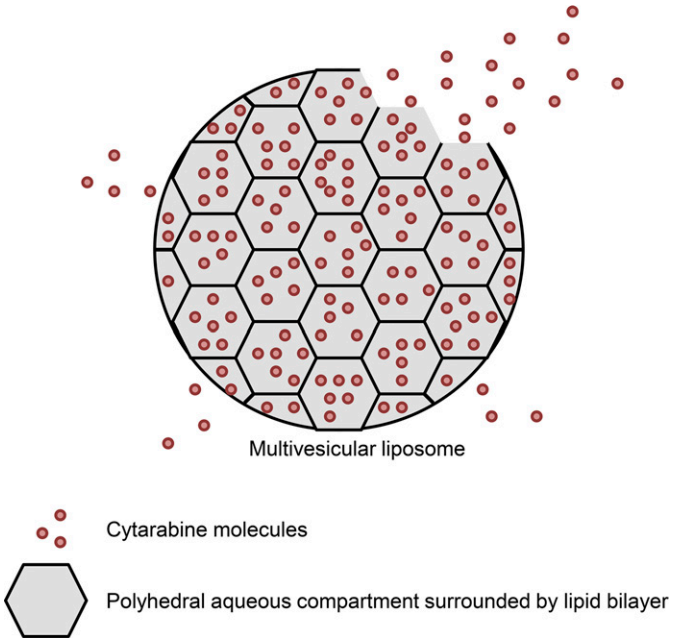


**Fig. 13.** Morphology of DepoCyt liposomes prepared using DepoFoam Technology. The production of DepoCyt uses DepoFoam technology, which generates multivesicular liposomes (MVLs). Each DepoCyt MLV is composed of numerous non-concentric polyhedral aqueous compartments separated by a lipid bilayer membrane. The arrangement of the MVL gives the whole DepoCyt particle a resemblance of aggregated soap bubbles. DepoCyt MLVs are microscopic spherical particles that usually range in size between 3 and 30 $\mu$m.

10 minutes when unencapsulated cytarabine was administered (Kim and Howell, 1987b). Furthermore, a single dose of DepoCyt was demonstrated to be curative to systemic leukemia in these mice (Kim and Howell, 1987b). A similar result was observed in mice administered with DepoCyt via the intraperitoneal route, showing a terminal half-life of 21 hours versus 16 minutes for the unencapsulated cytarabine (Kim and Howell, 1987a).

The lateral ventricular intrathecal administration of DepoCyt into Sprague-Dawley rats demonstrated an increase in the CSF terminal half-life of cytarabine by a factor of 55 (from 2.7 to 148 hours) and resulted in the maintenance of cytarabine levels above the minimal cytotoxic CSF level of 0.1 $\mu$g/ml for at least 14 days (Kim et al., 1987a). Rhesus monkeys (*Macaca mulatta*) have also been used to study the pharmacokinetics of DepoCyt (Kim et al., 1993b). In this study, six rhesus monkeys of similar weight (9–12 kg) were injected with a single dose of DepoCyt (2 mg/monkey) via an intralumbar route, and one, also of similar weight, was injected with a single dose of conventional unencapsulated cytarabine (2 mg/monkey). Both DepoCyt and unencapsulated cytarabine displayed a biexponential elimination pattern (Kim et al., 1993b). The cytarabine terminal half-life of 156 hours was observed after the intrathecal administration of DepoCyt, whereas a terminal half-life of only 0.74 hour was observed for unencapsulated cytarabine (Kim et al., 1993b). In addition, the cytarabine concentration was maintained above the minimal cytotoxic concentration of 0.1 $\mu$g/ml for a longer period of time after DepoCyt administration compared with unencapsulated cytarabine administration (Kim et al., 1993b).

*4. Clinical Studies of DepoCyt.* Due to the positive results observed in animal studies, clinical trials focusing on the antitumor activity, pharmacokinetics, and safety of these multivesicular liposomes encapsulating cytarabine were investigated further in patients with NM secondary to various hematologic and nonhematologic malignancies. In a phase I clinical trial, nine patients with leptomeningeal metastasis were given 1–7 cycles of DepoCyt (cytarabine 10 mg/ml) into the lateral ventricle using an Ommaya reservoir (Chamberlain et al., 1993). DepoCyt was administered such that the final quantity of cytarabine ranged from 25 to 125 mg/dose. It was reported in this study that the ventricular concentration of free cytarabine released from DepoCyt into CSF exhibited a biexponential half-life with an initial half-life of 7.2 $\pm$ 1.7 hours and a terminal half-life of 140 $\pm$ 49 hours. Five of six patients who were eligible for CSF cytologic evaluation responded well to the treatment, with the CSF being cleared of malignant cells within 3 weeks after initial treatment (Chamberlain et al., 1993). The duration of the response was found to be between 2 to greater than 14 weeks (median of 11 weeks), whereas the dose limiting toxicities and MTD were identified to be at a DepoCyt dose of 125 and 75 mg, respectively (Chamberlain et al., 1993).

The second clinical study conducted by the same group of investigators further demonstrated the improved pharmacokinetics of cytarabine in the form of a DepoCyt injection (Kim et al., 1993a). In this second investigation, 12 patients received an increasing dose of DepoCyt by mean of a single intraventricular injection or lumbar intrathecal injection every 2–3 weeks for 15–27 cycles. Therapeutic ventricular CSF concentration of cytarabine was maintained for 9 $\pm$ 2 days after the intraventricular injection (Kim et al., 1993a). On the other hand, therapeutic intralumbar concentration of cytarabine was maintained for up to 14 days after the intralumbar injection, with 7 of 9 patients receiving DepoCyt via this route exhibiting some cytologic responses (Kim et al., 1993a). This response was defined as two consecutive negative CSF cytology examinations at least 1 week apart. Although both routes were able to maintain cytarabine concentrations above the minimal cytotoxic level for about 14 days, intralumbar administration was shown to result in higher cytarabine CSF concentrations (Kim et al., 1993a).

A pivotal randomized trial of 28 patients with lymphomatous meningitis was conducted to examine the efficacy and safety of DepoCyt in comparison with conventional cytarabine (Glantz et al., 1999b). From this trial, it was demonstrated that DepoCyt injection

(50 mg) every 2 weeks was more effective than a conventional 50 mg injection of cytarabine every 2 weeks. The elimination of malignant cells from CSF was significantly better in DepoCyt-treated patients relative to conventional cytarabine (71 versus 15%, respectively) and the time to neurologic progression of disease (79 versus 42 days, respectively) as well as survival time (100 days versus 63 days, respectively) were observed to be longer (Glantz et al., 1999b). Additionally, patients receiving DepoCyt were observed to be more functional during their daily activities with no sign of cumulative toxicity present. However, DepoCyt treatment was frequently associated with transient symptoms of arachnoiditis, such as headache (27 versus 2%) and nausea/vomiting (9 versus 2%) relative to cytarabine.

Two other studies involving larger numbers of participants were also investigated previously (Jaeckle et al., 2001, 2002). In the first study examining 51 patients diagnosed with NM due to breast cancer, patients were given a 50 mg intrathecal injection of DepoCyt for 1 month followed by an additional 3 months of therapy if patients responded to the initial treatment (Jaeckle et al., 2001). Of 43 patients cytologically evaluated, 28% showed no sign of malignant cells in the CSF, whereas the median time to neurologic progression was 49 days and median survival time was 88 days. In the second study, 110 patients diagnosed with NM were given the same treatment as the first study above (Jaeckle et al., 2002). Similarly, 19 of 70 patients cytologically evaluated (27%) showed some responses, whereas the median time to neurologic progression and median survival time were 55 days and 95 days, respectively (Jaeckle et al., 2002). Only mild headache (4–11%) and arachnoiditis (6–19%) were observed throughout both studies (Jaeckle et al., 2001, 2002).

Apart from being investigated in comparison with conventional cytarabine, DepoCyt was also previously compared with an alternative drug, methotrexate, in patients with NM secondary to solid tumors (Glantz et al., 1999a). On an intent-to-treat basis, 8 of 31 patients (26%) receiving DepoCyt compared with 6 of 30 (20%) patients receiving methotrexate, demonstrated some responses. The median time to disease progression was 58 days for DepoCyt-treated patients compared with 30 days for those treated with methotrexate. Median survival time was also found to be higher for patients receiving DepoCyt compared with those receiving methotrexate (105 versus 78 days), although the improvement was not significant (Glantz et al., 1999a).

*5. Side Effects and Safety of DepoCyt.* The toxic side effects associated with DepoCyt are similar to those of conventional cytarabine. In the phase I clinical study, the predominant toxic side effects of DepoCyt observed at the MTD of 75 mg were symptoms associated with drug-induced chemical arachnoiditis (Chamberlain et al., 1993). These symptoms included grade 1–2 fever (50%), grade 1–2 headache (38%), grade 1–2 back and/or neck pain (38%), and grade 1–2 nausea or vomiting (25%). Less than 15% of patients had grade 3–4 nausea or vomiting. The observed side effects of DepoCyt were transient, occurring typically on day 2 to day 4 and were not apparent on day 1 and days 5 to 7. These toxicities were confirmed in two larger studies (Jaeckle et al., 2001, 2002). Both studies (51 and 110 patients) reported symptoms of headache, nausea, vomiting, and arachnoiditis, predominately at a grade 1–2 magnitude (Jaeckle et al., 2001, 2002). All side effects were also generally transient, resolving after the end of the treatment cycle they occurred in. In all studies, the toxic side effects could be ameliorated by a concomitant systemic administration of dexamethasone 2–4 mg twice daily for 5 days, beginning on the day of initial DepoCyt administration (Chamberlain et al., 1993; Jaeckle et al., 2001, 2002).

DepoCyt is currently formulated as a sterile suspension in NaCl 0.9% weight/volume solution for intrathecal injection. It is available in a ready-to-use, single-use vial, with each vial containing 50 mg cytarabine in 5 mL of NaCl solution (Murry and Blaney, 2000). A single dose of DepoCyt administered intrathecally at 50 and 75 mg was shown to elevate the levels of cytarabine above its minimum cytotoxic concentration ($>0.1\ \mu g/mL$) for 2 weeks (Murry and Blaney, 2000). Thus, the recommended DepoCyt dosage for adults is 50 mg every fortnight. In addition, as DepoFoam particles are generally denser than the suspending medium, DepoCyt must be resuspended by gently shaking the vial immediately before injection (Murry and Blaney, 2000).

## VIII. Advances in Liposome Technology for Cancer Therapy

As liposomal drug delivery systems have proven to be quite effective at enhancing the efficacy and safety of chemotherapeutic agents for cancer treatment, many novel liposomal formulations are currently being investigated, some of which have already entered late stage clinical trials (Slingerland et al., 2012; May and Li, 2013; Oberoi et al., 2013; Wicki et al., 2015). The most recent example is ThermoDox, a temperature-sensitive liposomal formulation of DOX, which is currently being investigated in a phase III clinical trial for hepatocellular carcinoma and a phase II clinical trial for breast cancer and colorectal liver metastases (May and Li, 2013).

Other examples include liposomal formulations of platinum drugs (Oberoi et al., 2013), such as: 1) Lipoplatin (Regulon Inc., Mountain View, CA), a liposomal cisplatin formulation, that has received orphan drug status from the EMA for the treatment of pancreatic adenocarcinoma and is also being investigated in phase II/III clinical trials for different cancer-types (Boulikas,

2009); 2) Lipoxal (Regulon Inc., Mountain View, CA), a liposomal formulation of oxaliplatin (Fig. 1), that has been under investigation for advanced gastrointestinal cancer in a phase I clinical trial (Stathopoulos et al., 2006); and 3) MBP-426 (Mebiopharm Co. Ltd, Tokyo, Japan), a transferrin conjugated liposomal formulation of oxaliplatin, currently undergoing a phase II clinical trial for solid tumors (for more information on liposomal formulation of platinum drugs see Oberoi et al., 2013). Tables 2–4 provide information regarding liposomal drug formulation, in terms of product name, drug, liposome-type, indications, lipid compositions, particle size, and status in phase I (Table 2), phase II (Table 3), and phase III (Table 4) clinical trials.

Additionally, new generations of liposomes have also been developed over the last 40 years. Investigations focusing on the development of newer liposomal technologies, including redox-sensitive liposomes, ultrasound-responsive liposomes, magnetic liposomes, enzyme-sensitive liposomes, liposomes for photodynamic therapy (PDT) and multifunctional "SMART" liposomes are discussed below.

*A. Redox-sensitive Liposomes.* A high redox potential difference exists between the intracellular compartment and extracellular space due to the abundant amount of reducing agents, such as glutathione, within cells compared with extracellular fluid (Schafer and Buettner, 2001). The distinction in redox potential between the two compartments may be exploited by redox-sensitive liposomes. Disulfide bonds can be used as a linker to conjugate specific ligands onto the surface of liposomes or it can be used as a disulfide bridge to prepare thiolated lipid, which can be incorporated into liposomes (Ganta et al., 2008). Upon arrival into intracellular compartment, ligands conjugated by disulfide bond or thiolated liposomes can be destabilized by the reduction of the disulfide bond by glutathione, resulting in the release of the encapsulated contents (Ganta et al., 2008).

Disulfide-mediated redox-sensitive liposomes are generally prepared by using a mixture of standard phospholipids and a small amount of lipids containing disulfide bonds linking their hydrophobic and hydrophilic regions together (Ganta et al., 2008). The coupling of $PEG_{2000Da}$ to DSPE via 3,3′dithiopropionate resulted in a DSPE-$PEG_{2000Da}$ derivative containing a disulfide bond, known as PEG-$\alpha$-aminocarbonylethyl-dithiopropionyl-DSPE, or PEG-DTP-DSPE (Kirpotin et al., 1996). When PEG-DTP-DSPE was incorporated into DOPE liposomes, liposomal fusion and the rapid and complete release of encapsulated contents was observed after thiolytic cleavage of PEG from liposomes (Kirpotin et al., 1996). Similarly, anti-CD19-targeted liposomes composed of DOPE, CHEMS and PEG-DTP-DSPE exhibiting both pH and redox sensitivity also demonstrated improved DOX delivery and anticancer activity against B-lymphoma cells compared with non-pH-sensitive liposomes (Ishida et al., 2001b). The in vivo study of these liposomes in mice bearing B-cell lymphoma also showed their improved antitumor activity over non-pH-sensitive anti-CD19-targeted liposomes, despite having a faster rate of drug release and higher clearance (Ishida et al., 2001b). Another DSPE-$PEG_{2000Da}$ derivative containing the disulfide bond linkage was prepared using dithiobenzylurethane (Zalipsky et al., 1999). This derivative is believed to be more effective than PEG-DTP-DSPE because it does not require potent thiolytic agents for its cleavage (Zalipsky et al., 1999). The cleavage of the dithiobenzylurethane linkage by cysteine, a mild thiolytic agent, was reported to be relatively efficient, resulting in a release of dye from DOPE liposomes within 60 minutes (Zalipsky et al., 1999). For more information, please refer to Sawant and Torchilin (2010), Ganta et al. (2008), and Saito et al.(2003).

Although enhanced drug delivery by redox-sensitive liposomes may be promising, the cleavage of these liposomes requires high concentration of reducing agents, which may not be present in some pathologic tissues (Sawant and Torchilin, 2010). In addition, the reduction of redox-sensitive liposomes may not be optimal, because many liposomes enter cells via endosomes, whereas the reduction process takes place within the cytosol (Sawant and Torchilin, 2010). Therefore, redox-sensitive liposomes must escape from the endosome first before destabilization (Sawant and Torchilin, 2010).

*B. Ultrasound-responsive Liposomes.* Ultrasound can be classified into low frequency and high frequency ultrasound (Ahmed et al., 2015). High frequency ultrasound is often associated with thermal effects and can be used to trigger drug release from temperature-sensitive liposomes as described above in section IV.C.2 (Ahmed et al., 2015). In contrast, low frequency ultrasound (LFUS) is associated with mechanical effects, such as oscillation and cavitation (Nyborg, 2001). Acoustic cavitation occurs as a result of the interaction between acoustic waves and gas bubbles (Leighton, 2007). When ultrasound excites gas bubbles, they oscillate in response to acoustic pressure (Ahmed et al., 2015). When acoustic pressure is increased further, the oscillation becomes nonlinear (Ahmed et al., 2015). This can lead to the increase in size of the gas bubble and their eventual collapse (Ahmed et al., 2015). It was shown that LFUS can be used to trigger the release of liposomal contents mechanically.

A study on the release of DOX from Doxil after exposure to LFUS (20 kHz) for 30 minutes reported that 85% of DOX was released from Doxil in saline solution, and 61% was released in human plasma (Schroeder et al., 2009b; Ahmed et al., 2015). In contrast, exposure to 30 minutes of higher frequency ultrasound (1 MHz) resulted in the release of 58% of DOX from Doxil in saline and 5% release in human plasma.

A further reduction in DOX release was observed when 3 MHz ultrasound was used (Schroeder et al., 2009b; Ahmed et al., 2015). In mice bearing J6456 murine lymphoma tumors, exposure to LFUS for 2 minutes resulted in the release of nearly 70% of cisplatin from PEGylated liposomes (hydrogenated soybean PC:cholesterol:DSPE-$PEG_{2000Da}$ 51:44:5 mol%) compared with the release of <3% of cisplatin from PEGylated liposomes without LFUS (Schroeder et al., 2009a). Furthermore, when these liposomes were injected intravenously into mice bearing C26 colon adenocarcinoma tumors followed by LFUS 24 hours postadministration, they demonstrated more efficacious antitumor activity than free cisplatin and PEGylated liposomal cisplatin without LFUS (Schroeder et al., 2009a). For more information on ultrasound-responsive liposomes, please refer to reviews by Ahmed et al. (2015) and Schroeder et al. (2009b).

As liposomes contain no gas, they are only partially sensitive to ultrasound (Ahmed et al., 2015). Recently, liposomes with echogenic properties were developed that contain a gas phase or an emulsion that is vaporizable, making them more responsive to ultrasound (Ahmed et al., 2015). For instance, liposomes containing a liquid emulsion of perfluorocarbons, called eLiposomes, have been investigated (Javadi et al., 2012; Lattin et al., 2012; Javadi et al., 2013). These liposomes can be ruptured by reducing the local pressure below the vapor pressure of the perfluorocarbon emulsion, allowing it to vaporize and making the liposome sensitive to ultrasound (Ahmed et al., 2015). However, more studies on these eLiposomes are needed because their design still requires optimization. For more information on these liposomes, please refer to Javadi et al. (2012, 2013) and Lattin et al. (2012).

Alternatively, liposomal DOX containing perfluorobutane microbubbles has been investigated in comparison with normal liposomal DOX formulations (Lentacker et al., 2010). This microbubble-liposome system was demonstrated to increase BLM melanoma cell death in vitro by 2-fold when exposed to ultrasound (1 MHz) compared with standard liposomal DOX (Lentacker et al., 2010). This was suggested to be due to the sonoporation of the cell membrane by the implosion of microbubbles upon ultrasound exposure, causing an increase in the cellular uptake of DOX (Lentacker et al., 2010).

*C. Magnetic Liposomes.* The use of magnetic liposomes is a relatively recent approach in targeted drug delivery using a magnet as a means of targeting (Nobuto et al., 2004). In this strategy, liposomes are loaded with a drug and a ferromagnetic material and are infused into the subject intravenously. The subject's tissue affected by cancer is subsequently placed between two poles of a magnet to direct nanoparticles to the targeted site. Generally, iron oxide nanoparticles of size less than 10 nm, namely, magnemite and magnetite, are incorporated into liposomes to achieve the magnetic property (Sawant and Torchilin, 2010; Deshpande et al., 2013). In one study, hamsters bearing a limb osteosarcoma were intravenously administered with magnetic liposomes encapsulating DOX, and the limb was subsequently placed between two poles of a 0.4 Tesla magnet (Nobuto et al., 2004). After 60 minutes, a 4-fold increase in the tumor drug concentration was observed (Nobuto et al., 2004). Alternatively, the magnet can be implanted within the tumor. Using the same osteosarcoma-bearing hamster model, this strategy demonstrated enhanced accumulation of DOX encapsulated magnetic liposomes in the tumor vasculature and improved inhibition of tumor growth (Kubo et al., 2001). This strategy also demonstrated a 25-fold increase in the accumulation of $^{99m}$Tc-albumin loaded magnetite-containing liposomes within the kidney implanted with a magnet (Babincova et al., 2000). However, because iron oxide nanoparticles must be incorporated into magnetic liposomes together with the encapsulated drug, it is important that the incorporation of these particles does not affect the efficacy of the entrapped drug (Sawant and Torchilin, 2010). It was reported that the drug loading efficiency of magnetic liposomes was affected at high magnetite concentrations, and thus, the incorporation of these iron oxide nanoparticles decreased drug encapsulation (Dandamudi and Campbell, 2007).

It is also possible to modify magnetic liposomes to give them temperature-sensitive and active targeting properties. For example, magnetic nanoparticles and DOX have been incorporated into temperature-sensitive liposomes composed of DPPC, cholesterol, DSPE-$PEG_{2000Da}$, and DSPE-$PEG_{2000Da}$-folate at a molar ratio of 80:20:4.5:0.5 (Pradhan et al., 2010). When these liposomes were targeted to KB and HeLa cell cultures by a magnetic field, the cellular uptake of DOX was increased substantially compared with Doxil, nonmagnetic folate receptor-targeted liposomal DOX, and free DOX (Pradhan et al., 2010). Furthermore, the application of hyperthermia (at 42.5 and 43.5°C) and a magnetic field synergistically increased the antitumor activity of these folate receptor-targeted temperature-sensitive magnetic liposomes containing DOX (Pradhan et al., 2010).

*D. Enzyme-sensitive Liposomes.* Stimuli-sensitive liposomes can be generated to exploit the expression of various enzymes within the tumor (Deshpande et al., 2013). Enzymes that have been found to be overexpressed within tumor tissue include MMPs, phospholipase $A_2$, alkaline phosphatase, transglutaminase, and PI-specific phospholipase (Arias, 2011). In the presence of these catalytic proteins, enzyme-sensitive liposomes can be engineered to destabilize and release their encapsulated contents at the tumor site (Arias, 2011). A linker that is cleavable by enzymes that are overexpressed in tumors can be used to modify the liposomes (Danhier et al., 2010; Zhu et al., 2012).

For instance, a matrix metalloproteinase 2 (MMP-2)-cleavable octapeptide linker composed of Gly-Pro-Leu-Gly-Ile-Ala-Gly-Gln has been used to conjugate $PEG_{2000Da}$ with DSPE and incorporated into liposomal formulations (Zhu et al., 2012). It was reported that these MMP-2-sensitive DSPE-$PEG_{2000Da}$ conjugates were incorporated into liposomes modified with cell-penetrating peptide, namely transactivator of transcription peptide (TATp), and antinucleosome antibody 2C5 (Zhu et al., 2012). Consequently, MMP-2-sensitive DSPE-$PEG_{2000Da}$ acts as a steric shield for these liposomes, which become detached in the presence of high concentrations of MMP-2 enzymes, leading to the exposure of other surface functionalities (Zhu et al., 2012). During in vitro studies, Gly-Pro-Leu-Gly-Ile-Ala-Gly-Gln octapeptides were cleaved in the presence of MMP-2, removing the PEG shield from liposomes and exposing other active-targeting moieties (Zhu et al., 2012). Subsequently, the enhanced cellular internalization of these liposomes by mouse breast cancer cells (4T1) was observed (Zhu et al., 2012).

Additionally, a lipopeptide generated by the conjugation of matrix metalloproteinase-9 (MMP-9) substrate peptide to a fatty acid chain, has been incorporated into liposomes (Banerjee et al., 2009; Deshpande et al., 2013). These liposomes were reported to rapidly release a significant amount of encapsulated contents in breast cancer cells (MCF-7) expressing high levels of MMP-9, while slowly releasing their contents in colorectal adenocarcinoma cells (HT-29) with low levels of MMP-9 (Banerjee et al., 2009).

### *E. Photodynamic Therapy Using Liposomes.*

Another use for liposomes is in PDT for the treatment of superficial tumors. In this treatment, light-sensitive photosensitizers are exposed to light of appropriate wavelength, which then mediates the generation of reactive oxygen species that compromise and kill cancer cells (Weijer et al., 2015). Liposomes can be used to encapsulate these photosensitizers, acting as both the drug carrier and the enhancer, which results in many advantages (Weijer et al., 2015), including: 1) the prevention of these molecules from aggregating within aqueous solution, including biologic fluids (Dhami and Phillips, 1996; Damoiseau et al., 2001; Garcia et al., 2011); 2) the use of a lower dose of photosensitizers encapsulated within liposomes due to the higher payload of liposomes relative to the unencapsulated formulation; 3) the minimization of photosensitizer accumulation within the skin, and thus, reducing phototoxicity and increasing photosensitizer bioavailability within the tumor (Jori, 1990; Derycke and de Witte, 2004); 4) the coencapsulation of a chemotherapeutic agent together with the photosensitizer within a single liposomal drug delivery system, further enhancing antitumor efficacy; and 5) the modification of photosensitizer encapsulated liposomes to improve target specificity similar to other liposomal formulations.

Cetyl-polyethyleneimine-modified liposomes containing a benzoporphyrin derivative have been examined in antiangiogenic PDT (Takeuchi et al., 2004). These liposomes were found to be effectively internalized by human umbilical vein endothelial cells, where they became localized to the intranuclear region or mitochondria (Takeuchi et al., 2004). In animal models, photofrin encapsulated liposomes demonstrated better efficacy against human gastric cancer than unencapsulated photofrin during PDT (Igarashi et al., 2003). Moreover, improved PDT results were observed in nude mice bearing human adenocarcinoma tumors due to the enhanced accumulation of dimyristoyl-PC liposomes containing SIM01 porphyrin derivatives (Bourre et al., 2003). Finally, a commercial liposomal formulation of the benzoporphyrin derivative monoacid ring A was found to be active against sarcomas in mice (Ichikawa et al., 2004). For further reading on the use of liposomes in PDT, please refer to reviews by Weijer et al. (2015) and Campbell et al. (2009).

### *F. Multifunctional "SMART" Liposomes.*

The stimuli-sensitive properties of PEG polymer coatings can be used to prepare a multifunctional nanoparticle drug delivery system (Sawant and Torchilin, 2010). In this concept, the ideal multifunctional "SMART" nanoparticles must be able to accumulate precisely within the desired tissue or organ and then penetrate the target cells specifically to unload their contents (Sawant and Torchilin, 2010). The accumulation of multifunctional nanoparticles within target tissue/organ can be achieved by passive targeting (e.g., the EPR effect) or by active targeting using specific antibodies (Kale and Torchilin, 2007; Sawant and Torchilin, 2010). On the other hand, their intracellular delivery can be achieved by using certain internalizable ligands, such as folate, transferrin, or peptides (Kale and Torchilin, 2007; Sawant and Torchilin, 2010). In liposomes, this system consists of multiple functional moieties attached to the liposomal surface that are shielded by the PEG coating under normal conditions but become exposed in the presence of certain stimuli that remove the PEG coating (Sawant and Torchilin, 2010). Furthermore, each functional moiety attached must be able to perform its task once it is exposed to a specific stimulus after the PEG coating is detached (Sawant and Torchilin, 2010).

For example, PEGylated immunoliposomes capable of penetrating cells were prepared previously (Sawant et al., 2006). These liposomes consisted of cell-penetrating peptide, TATp, pH-sensitive PEG-PE conjugates, and PEG-PE conjugated to monoclonal antibodies specific to myosin and cancer cells, namely, the antimyosin antibody 2G4 and the antinucleosome antibody 2C5, respectively (Sawant et al., 2006). It is

believed that under normal pH, the nonselective cell-penetrating property of TATp would be shielded by the protective layer of pH-sensitive PEG, and thus, allowing these liposomes to travel in circulation without interacting and penetrating nontargeted cells (Sawant et al., 2006; Kale and Torchilin, 2007). Moreover, the incorporation of PEG-PE-antibody conjugates into these multifunctional liposomes further allows for the specific binding of these liposomes to the target site (Sawant et al., 2006). In the presence of an acidic environment (e.g., within tumor), the pH-sensitive PEG-PE conjugates are hydrolyzed, exposing the TATp functional moieties to targeted cells to enhance the cellular internalization of these multifunctional liposomes (Sawant et al., 2006). It was reported in an in vitro study that at pH = 7.5–8.0, such liposomes demonstrated an enhanced specific binding with antibody substrates, but showed minimal internalization by cells (Sawant et al., 2006). However, at lower pH (pH = 5.0–6.0), liposomes lost their protective PEG shell upon hydrolysis of hydrazone bond and were subsequently taken up by cells effectively (Sawant et al., 2006). Such a multifunctional approach represents an important chemotherapeutic delivery strategy that deserved further attention.

## IX. New Generation of Lipid Nanoparticles

### *A. Solid Lipid Nanoparticles*

In the early 1990s, a new class of lipid particle drug carrier was developed called solid lipid nanoparticles (SLNs), which are also known as lipospheres or solid lipid nanospheres (Muller et al., 2000b; Wong et al., 2007). They are submicron particles ranging in size between 50 and 100 nm prepared from lipids that remain in the solid state at room and body temperature (Fig. 14) (Wong et al., 2007). In this case, the solid lipid is used as a matrix material for drug encapsulation and can be selected from a variety of lipids, including mono-, di-, or triglycerides; glyceride mixtures; and lipid acids. The lipid matrix is then stabilized by biocompatible surfactants (Wong et al., 2007). SLNs can be produced by a number of techniques, including high-pressure homogenization, microemulsion, and precipitation of lipid particles by solvent evaporation. The preparation of SLNs is discussed briefly below. For more information on the preparation of SLNs, please refer to reviews by Muller et al. (2000a,b) and Mehnert and Mader (2001).

Apart from offering the advantages of physical stability, protection of labile drug degeneration, controlled release, and easy preparation (Wissing et al., 2004), SLNs can also be produced through economical large-scale production and exhibit fewer drug storage and leakage problems compared with other nanoparticles, such as liposomes (Heath, 1988; Muller et al., 2000a,b; Wong et al., 2007). Moreover, toxicity and acidity issues associated with biodegradable polymers (Smith, 1986; Muller et al., 1996) are not observed in SLNs, because the lipids used to prepare SLNs are more biocompatible and biodegradable than polymeric materials (Muller et al., 2000b).

*1. Preparation of Solid Lipid Nanoparticles.*

*a. Preparation of solid lipid nanoparticles by high-pressure homogenization.* The preparation of SLNs by homogenization can be divided into two basic production methods, namely the hot and cold homogenization technique (Schwarz et al., 1994; Muller et al., 2000b). In both techniques, the drug is dissolved in a lipid that has been heated to a temperature 5–10°C above its melting point. However, in the hot homogenization technique, the mixture of the molten lipid and drug is dispersed in an aqueous surfactant solution of the same temperature to form a pre-emulsion (Muller et al., 2000b). The pre-emulsion is then homogenized using a piston-gap homogenizer. The homogenization process produces a hot oil-in-water (o/w) nanoemulsion as a result, which is allowed to cool to room temperature to recrystallize the lipid and leads to SLN formation (Muller et al., 2000b). In the hot homogenization technique, it is important that lipid recrystallization occurs once the molten lipid has cooled down to room temperature (Muller et al., 2000b). The hot homogenization technique can be used for the preparation of SLNs containing moderately temperature-sensitive drugs, because the exposure to high temperature is relatively short. However, for highly temperature-sensitive agents, the cold homogenization technique must be used (Muller et al., 2000b).

In the cold homogenization technique, the mixture of molten lipid and the drug is cooled down to form the solid lipid, which is ground further to form microparticles of a

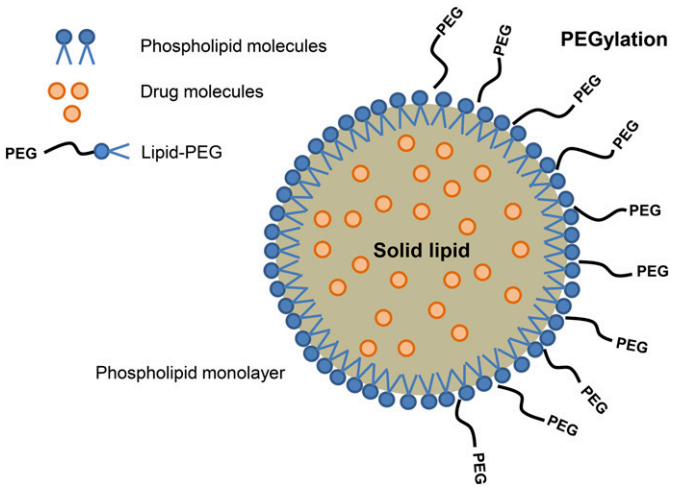


**Fig. 14.** Structure of solid lipid nanoparticles (SLNs). SLNs are submicron particles that range between 50 and 100 nm in size, which are prepared from lipids that remain solid at room temperature and body temperature. The solid lipid is used as a matrix material in which hydrophobic drugs can be stored. The lipid matrix is then stabilized by biocompatible surfactants, which in this case, are phospholipid and/or lipid-PEG.

size between 50 and 100 $\mu$m (Mehnert and Mader, 2001). Lipid microparticles are then dispersed in a cold surfactant solution to form a presuspension. Subsequently, this presuspension is homogenized at room temperature or lower (Mehnert and Mader, 2001). The cavitation forces produced by the high-pressure homogenizer are sufficient to break the lipid microparticles directly into SLNs (Mehnert and Mader, 2001). For the cold homogenization technique, it is important that the difference between the melting point of the lipid and the homogenization temperature is large enough to prevent the lipid melting within the homogenizer (Muller et al., 2000b).

*b. Preparation of solid lipid nanoparticles by the microemulsion technique.* To produce SLNs by the microemulsion technique, the lipid used must be solid at room temperature and the microemulsion process must be performed at temperatures higher than the melting point of the lipid (Gasco, 1993; Muller et al., 2000b). In this process, the lipid is melted to a temperature above its melting point, and a mixture of water, cosurfactants, and surfactants at the same temperature is added to the molten lipid under mild stirring (Gasco, 1993; Muller et al., 2000b). The ratio of surfactant to lipid for microemulsion formulation must be correct to form a transparent, thermodynamically stable system (Mehnert and Mader, 2001). The microemulsion formed is then dispersed in cold water (2–3°C) with mild stirring to ensure that small particles are formed upon precipitation (Boltri et al., 1993; Gasco, 1997).

By using the microemulsion technique, it is possible to scale-up the production of SLNs for commercial use (Muller et al., 2000b). The scale-up requires preparing a microemulsion in a large, temperature-controlled tank, which is then pumped into a cold water tank in the precipitation step (Muller et al., 2000b). However, parameters such as the temperature of the microemulsion and the water, as well as the mixing conditions must be maintained constantly to achieve SLNs of identical characteristics.

*c. Preparation of solid lipid nanoparticles by precipitation using solvent-evaporation technique.* Similar to polymeric nanoparticles, SLNs can also be prepared by the precipitation method using the solvent-evaporation technique (Sjostrom and Bergenstahl, 1992; Sjostrom et al., 1993). This method requires the use of an organic solvent to dissolve the lipid. The organic phase is then emulsified in an aqueous phase, and the organic solvent is subsequently allowed to evaporate (Siekmann and Westesen, 1996). The evaporation of the organic solvent results in the precipitation of the lipid to form nanoparticles (Siekmann and Westesen, 1996). However, the disadvantages of this method involve difficulties in removing organic solvent, which can be toxic, and scale-up problems associated with the production of SLNs using the precipitation method (Mehnert and Mader, 2001).

*2. Drug Incorporation and Drug Loading Capacity.* The drug loading capacity of SLNs is determined by the following parameters: 1) the solubility of the drug in the molten lipid; 2) the miscibility of the melted drug and molten lipid; 3) the chemical and physical structures of solid lipid matrix; and 4) the polymorphic state of the lipid material (Muller et al., 2000b).

To achieve adequate drug loading in SLNs, the encapsulated drug must be sufficiently soluble in the molten lipid. As solubility decreases with decreasing temperature, it is also necessary for the drug to have sufficiently high solubility to avoid separation from the molten or solid lipid (Mehnert and Mader, 2001). Solubilizers can be added to improve drug solubility in the molten lipid (Muller et al., 2000b). Additionally, the presence of mono- and diglycerides in the lipid mixture used to prepare the SLN matrix can further improve drug solubilization (Muller et al., 2000b).

The nature of lipid, including its chemical and physical structure, also plays an important role in drug loading capacity. Lipids that form particles with a perfect crystalline lattice matrix will cause the expulsion of the drug (Westesen et al., 1997). In contrast, a complex lipid mixture consisting of different types of lipids and fatty acid chain lengths produces imperfect crystalline lattices within the SLN matrix, and thus, will accommodate more drugs within the matrix as a result of lattice imperfections (Muller et al., 2000b).

As the degree of crystallization of the lipid matrix determines the drug loading capacity of SLNs, lipid crystal polymorphism may also play a crucial role in the drug loading efficiency of SLNs (Muller et al., 2000b). The crystallization of the lipids in nanoparticles is different from that of the bulk material (Westesen et al., 1993). Although the lipids in nanoparticles recrystallize partially into a less stable $\alpha$-crystalline form, the bulk lipid usually recrystallizes preferentially and rapidly into the more stable $\beta$-crystalline form via $\beta$-modification (Westesen et al., 1993). With increasing levels of the stable $\beta$-crystalline form within SLNs, the crystalline lipid lattice becomes more perfect and the number of imperfections decreases (Westesen et al., 1993, 1997). Thus, fewer drug molecules can be accommodated within SLN matrices with higher levels of the $\beta$-crystalline form, which promotes drug expulsion and the lowering of the drug loading capacity (Bunjes et al., 1996; Westesen et al., 1997). On the other hand, an increase in the $\alpha$-crystalline form within SLNs improves the drug loading capacity of these particles (Westesen et al., 1997).

*3. Studies of Solid Lipid Nanoparticles in Cancer Therapy.* A number of anticancer drug classes have been encapsulated within SLNs and examined both in vitro and in vivo since the early 1990s, including anthracyclines, taxanes, camptothecins, etoposide, flurodeoxyuridine, and retinoic acid (Cavalli et al., 1993; Yang et al., 1999; Wang et al., 2002; Lim et al.,

2004; Serpe et al., 2004; Harivardhan Reddy et al., 2005).

Animal studies have shown that SLNs can increase the AUC of encapsulated drugs by 3- to 20-fold, as well as significantly extending the half-life of the encapsulated agent compared with the corresponding free drug (Yang et al., 1999; Zara et al., 1999; Fundaro et al., 2000; Wang et al., 2002; Zara et al., 2002). Moreover, the stealth form of SLNs that are generated by PEGylation further improves the AUC and the half-life of encapsulated drugs to a greater extent than non-stealth SLNs (Fundaro et al., 2000; Zara et al., 2002). The cytotoxicity of cholesteryl butyrate, DOX, and PTX encapsulated SLNs were previously investigated in the human colorectal HT-28 cancer cell line (Serpe et al., 2004). SLNs containing cholesteryl butyrate and DOX demonstrated higher cytotoxicity than their conventional drug formulations, showing lower $IC_{50}$ values (Serpe et al., 2004). Similarly, PTX encapsulated SLNs exhibited higher cytotoxicity than an equivalent amount of the conventional PTX formulation (Serpe et al., 2004).

To overcome resistance to anticancer agents, P-glycoprotein inhibiting chemosensitizers have been incorporated into SLNs (Fischer et al., 1998; Krishna and Mayer, 2000; Ugazio et al., 2002; Planting et al., 2005). The incorporation of chemosensitizers into SLNs could potentially improve the potency, safety, and specificity of these compounds (Krishna and Mayer, 2000). Additionally, their incorporation may reduce the interaction between chemosensitizers and cytotoxic drugs observed in conventional formulations when administered simultaneously (Fischer et al., 1998; Planting et al., 2005). Previously, the chemosensitizer cyclosporin-A was successfully encapsulated within SLNs (Ugazio et al., 2002). Such a delivery system was shown to release cyclosporin-A slowly over a long period of time with less than 4% of the chemosensitizer released after 120 minutes (Ugazio et al., 2002).

The enhanced specificity by active targeting has been investigated in a number of nanoparticles for many years (Chang et al., 2009; Low and Kularatne, 2009; Ulbrich et al., 2009). Recently, this strategy was assessed on SLNs encapsulating anticancer drugs (Stevens et al., 2004). Folate receptor-targeting SLNs containing the PTX-prodrug were shown to improve both the uptake and cytotoxicity of this agent in cells expressing the folate receptor compared with nontargeted SLNs (Stevens et al., 2004). This improvement was also observed in vivo, where folate receptor-targeted SLNs containing the PTX-prodrug significantly increased tumor growth inhibition and animal survival time relative to nontargeted SLNs and PTX in Cremophor EL (BASF SE, Lugwigshafen, Germany) (Stevens et al., 2004).

Similar to liposomes, SLNs have been investigated for their potential use in gene delivery (Tabatt et al., 2004a,b), because it is believed that these particles should be at least as effective as liposomes in delivering genetic material (Wong et al., 2007). Both SLNs and liposomes incorporating the same cationic lipid were demonstrated to have similar transfection efficiency in vitro in Cos-1 monkey kidney fibroblast-like cells (Tabatt et al., 2004a). Furthermore, alterations in the lipid composition between the two delivery systems were able to influence the transfection efficiency (Tabatt et al., 2004a). In addition, low toxicity and high transfection efficiency could be achieved by selecting combinations of two-tailed cationic lipids and matrix lipids (Tabatt et al., 2004b). Hence, there is a great possibility that SLN delivery system may be used in gene therapy for cancer management (Wong et al., 2007).

*4. Disadvantages of Solid Lipid Nanoparticles.* Although SLNs provide many advantages over existing nanoparticle drug delivery systems, they do possess some drawbacks, particularly low encapsulation of hydrophilic drugs and nonuniform drug release (Wong et al., 2007). SLNs exhibit poor encapsulation of hydrophilic drugs as the drug to be encapsulated must be adequately dissolved within the melted lipid droplets to achieve high drug loading during SLN preparation (Mehnert and Mader, 2001). The addition of organic counterions during SLN preparation to form ionic pairs with charged drug molecules has been proposed to solve this problem (Cavalli et al., 1993, 2000). Another strategy involves the formation of polymer-lipid hybrid nanoparticles (PLNs), in which ionic drugs are electrostatically neutralized by polymer counterions and the drug-polymer complexes are subsequently incorporated into lipids for nanoparticle preparation (Fig. 15) (Wong et al., 2004, 2006; Li et al., 2006; Wong et al., 2006). Such a strategy has been shown to improve the encapsulation efficiency of ionic drugs, such as DOX-HCl and verapamil HCl from 20 to >80% (Wong et al., 2004, 2006). PLNs are not to be confused with lipid-polymer hybrid nanoparticles discussed below (see section IX.C).

The issue of nonuniform drug release by SLNs is related to the burst release or burst effect, which is the fast initial release of a large dose of the encapsulated drug followed by slow incomplete release (zur Muhlen et al., 1998). Burst release can create serious complications because of the cytotoxicity of anticancer drugs (Wong et al., 2007). Such behavior is attributed to the uneven distribution of the drug within SLNs due to the perfect lipid crystal structure that forms the SLN matrix (Westesen et al., 1993; Siekmann and Westesen, 1994; Bunjes et al., 1996), which lacks free space to accommodate large quantities of drug molecules. Thus, the majority of the drug is concentrated at or near the surface of the particles, which can then diffuse away rapidly into the surrounding medium, resulting in the burst release effect (zur Muhlen et al., 1998). This problem can be avoided by: 1) reducing the surfactant concentration; 2) cooling the lipid emulsion quickly to allow nanoparticles to be made up mainly of solid drug;

and/or 3) by selecting lipid compositions that do not form perfect crystal lattices, such as mono-, di-, or triglycerides of different chain lengths (Wissing et al., 2004).

### *B. Nanostructured Lipid Carriers*

Nanostructured lipid carriers (NLCs) are the second generation of lipid nanoparticles with SLNs being the first generation. NLCs were developed in 1999/2000 by Muller et al. (2002) to improve the burst release problem observed with SLNs. NLCs are lipid nanoparticles composed of a solid lipid matrix incorporated with liquid lipid or oil (Fig. 16) (Iqbal et al., 2012). The solid lipid matrix immobilizes the drug and prevents the particles from coalescing with one another, whereas the liquid oil droplet within the solid matrix increases the drug loading capacity of the particles (Fig. 16) (Iqbal et al., 2012). As a result, the mixture of lipids enables poorly structured lipid crystals to be formed within the particles, allowing more drugs to be encapsulated evenly and preventing rapid drug diffusion from the surface of the particles (Fig. 16).

*1. Preparation of Nanostructured Lipid Carriers.* NLCs can be produced by several methods, most of which are adopted from polymeric nanoparticle preparations. These methods include high-pressure homogenization (Stecova et al., 2007; Huang et al., 2008; Ruktanonchai et al., 2009); microemulsion (Doktorovova et al., 2010; Souza et al., 2011); phase inversion (Souto et al., 2007); emulsification by sonication (Das and Chaudhury, 2011); emulsification-solvent-evaporation (ESE) (Lin et al., 2010); solvent diffusion and solvent injection/solvent displacement (Schubert and Muller-Goymann, 2003); and the membrane contactor method (Charcosset et al., 2005). However, the most preferred method of NLC preparation is high-pressure homogenization (Iqbal et al., 2012).

*2. Studies of Nanostructured Lipid Carriers in Cancer Therapy.* As NLCs are a relatively new development, not many studies have been focused on their use with anticancer drugs. Docetaxel encapsulated NLCs (DTX-NLCs) were developed for in vitro assessment against three human cancer cell lines (HepG2, SKOV3, and A549) and one murine B16 malignant melanoma cell line (Liu et al., 2011). In comparison with Duopafei (Qilu Pharmaceutical Co. Ltd, Jinan, China; the standard formulation of Docetaxel), DTX-NLCs were demonstrated to have a significantly lower $IC_{50}$ value than Duopafei in all cell lines and were more cytotoxic against A549 cells by inducing a higher level of apoptosis and $G_2$/M arrest (Liu et al., 2011). This study further investigated the in vivo anticancer activity of DTX-NLCs against Duopafei in Kunming mice bearing murine B16 malignant melanoma xenografts (Liu et al., 2011). Consequently, DTX-NLCs were reported to be more effective than Duopafei in vivo, and showed a higher inhibition rate at doses of 10 and 20 mg/kg (62.69 and 90.36% compared to the control, respectively) relative to Duopafei at 10 mg/kg, which exhibited an inhibition rate of 42.7% of the control (Liu et al., 2011).

PTX- and DOX-loaded NLCs, as well as NLCs that have been surface modified with folic acid and stearic acid have also been investigated against cancer cells, including multi-drug resistant (MDR) cells (Zhang et al., 2008b). Indeed, PTX-NLCs demonstrated a high level of cytotoxicity in MCF-7 and MCF-7/ADR cells, whereas DOX-NLCs only showed a high level of cytotoxicity against MCF-7/ADR cells (Zhang et al., 2008b). The ability of PTX-NLCs and DOX-NLCs to reverse MDR was 34.3- and 6.4-fold greater than the free drugs, respectively (Zhang et al., 2008b). A similar trend in cytotoxicity was also observed using SKOV3 and SKOV3-TR30 cells, where DOX-NLCs and PTX-NLCs were 2.2- and 31.0-fold more effective at reversing drug resistance, respectively, than the free drugs (Zhang et al., 2008b). In addition, the surface

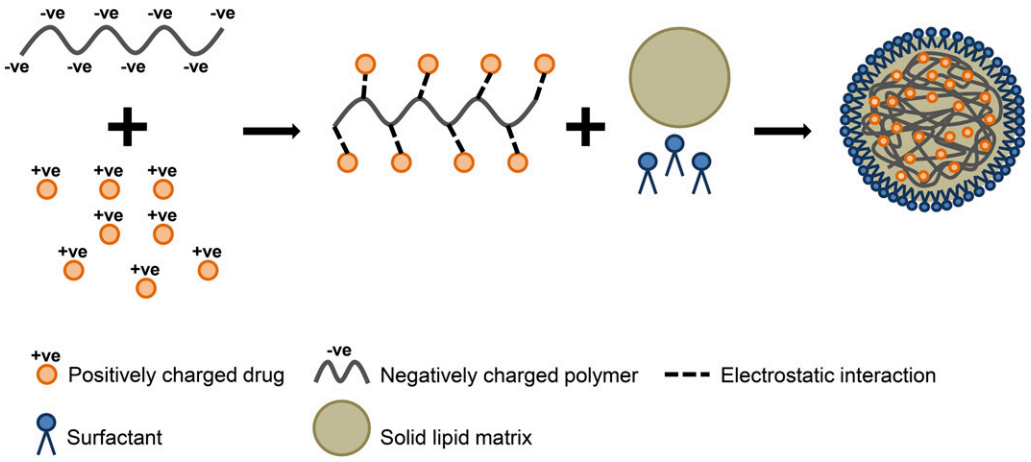


**Fig. 15.** Incorporation of hydrophilic drugs into SLNs using polymers. One of the strategies for incorporating hydrophilic drugs into SLNs is to use charged polymers. In this procedure, the ionic form of the hydrophilic drug is electrostatically neutralized by counterions on the polymer. The drug-polymer complexes are subsequently incorporated into lipids for SLN preparation. This strategy gives rise to polymer-lipid hybrid nanoparticles (PLNs), which are not to be confused with lipid-polymer hybrid nanoparticles (LPNs).

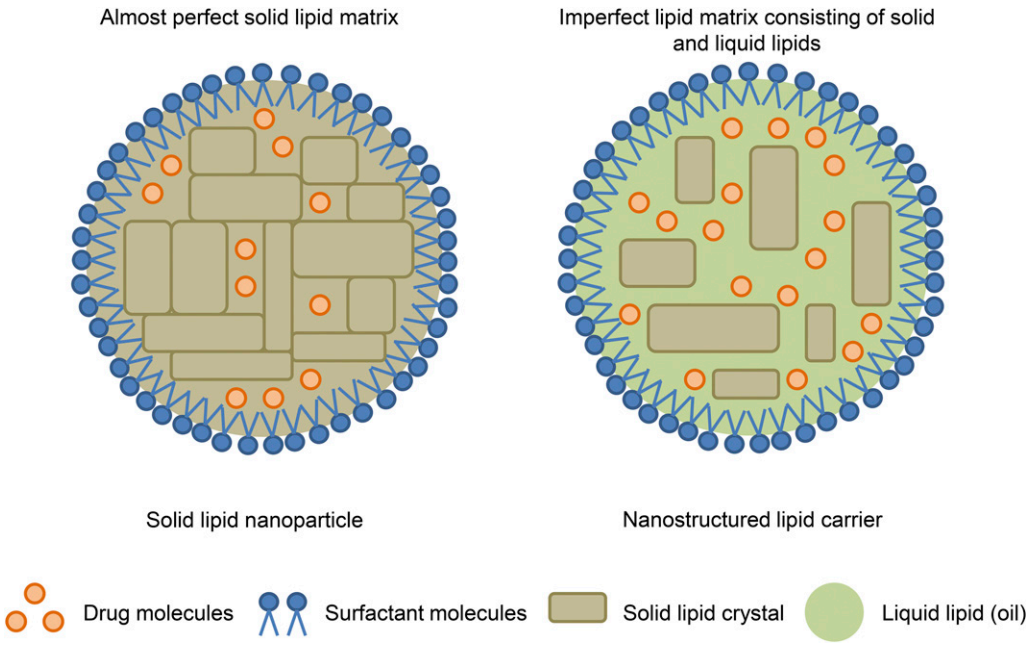


**Fig. 16.** Morphology of nanostructured lipid carriers (NLCs) and their improvements over SLNs. NLCs are lipid nanoparticles composed of solid lipid matrix immersed in liquid lipid (oil) droplets. The solid lipid is used as a matrix to immobilize the drug and prevent particles from coalescing with one another, whereas the liquid lipid increases the drug loading capacity. The mixture of lipids of different phases also allows an imperfect lipid crystal lattice to be formed within NLCs, in contrast to SLNs, where a solid lipid matrix is almost perfect, forcing encapsulated drugs to the surface of the particle. As a result, more drugs can be encapsulated within NLCs, preventing rapid drug release from the surface of the particles, which is observed with SLNs.

modification of NLCs with folic and stearic acid further enhanced the cytotoxicity of PTX and DOX against cancer cells, including MDR cells (Zhang et al., 2008b).

Additionally, PTX has been incorporated into hyaluronic acid-coated NLCs (HA-NLCs) to improve nanoparticle specificity (Yang et al., 2013). It was demonstrated that PTX was released slowly from PTX-loaded HA-NLCs and these nanoparticles were more cytotoxic than standard PTX in three cancer cell lines (i.e., the B16, CT26, and HCT116 cell lines) (Yang et al., 2013). In vivo studies further showed that PTX-loaded HA-NLCs exhibited a higher anticancer efficacy and were better tolerated by B16-bearing Kumming mice compared to conventional PTX. This could be due to the prolonged circulation time of PTX-loaded HA-NLCs and the increased accumulation of these nanoparticles in the tumor (Yang et al., 2013).

PEG-NLCs have also been prepared to encapsulate 10-hydroxycamptothecin (HCPT) and compared with free HCPT and HCPT encapsulated NLCs (HCPT-NLCs) (Zhang et al., 2008c). During in vitro studies, such PEGylated particles were able to accumulate within human lung adenocarcinoma epithelial A549 cells and, during in vivo studies, had longer circulation times and decreased uptake by the RES compared with free HCPT and unmodified HCPT-NLCs (Zhang et al., 2008c). Moreover, PEGylated HCPT-NLCs demonstrated superior antitumor efficacy against A549 lung cancer xenografts in vivo compared to free HCPT and unmodified HCPT-NLCs (Zhang et al., 2008c).

### *C. Lipid-polymer Hybrid Nanoparticles*

Finally, the most recent development in the field of lipid nanoparticles is lipid-polymer hybrid nanoparticles (LPNs). LPNs combine the characteristics of both polymeric nanoparticles and liposomes. They consist of three components (Fig. 17) (Hadinoto et al., 2013): 1) a polymeric core in which pharmaceuticals are encapsulated; 2) a lipid layer surrounding the polymeric core, which prevents the encapsulated content from leakage and slows down polymer degradation by limiting inward water diffusion; and 3) an outer lipid-PEG stealth layer, which helps prolong the in vivo circulation of nanoparticles by reducing opsonization and providing steric stabilization. When lipid-PEG is added, its hydrophobic tail usually extends into the inner lipid layer, whereas its hydrophilic PEG head group projects out into the aqueous environment (Zhang et al., 2008a). Due to its hybrid architecture, LPNs show high structural integrity, stability, and controlled release owing to their polymeric core, whereas its lipid/lipid-PEG layer provides biocompatibility and bioavailability (Chan et al., 2009).

LPNs can be prepared by the original two-step method or a more recently developed one-step procedure. These two methods and the parameters governing each are discussed below (for more details see Hadinoto et al., 2013).

*1. Preparation of Lipid-polymer Hybrid Nanoparticles: The Two-step Preparation Method.*

*a. The conventional two-step method.* The conventional two-step method of LPNs preparation generally involves the mixing of preformed polymeric nanoparticles with preformed lipid vesicles, which leads to the adsorption of lipid vesicles to polymeric nanoparticles due to an electrostatic interaction (Hadinoto et al., 2013). The polymeric nanoparticles used for preparing LPNs can be generated by nanoprecipitation (Thevenot et al., 2007), ESE (Mieszawska et al., 2012), or high-pressure homogenization (Fenart et al., 1999). The preformed polymeric nanoparticles are then added to either a dried thin lipid film prepared by dissolving the lipid in an organic solvent and evaporating the solvent (Thevenot et al., 2007) or to preformed lipid vesicles prepared by hydrating a thin lipid film (Messerschmidt et al., 2009). Subsequently, the LPNs are generated by vortexing or ultrasonicating the mixture of polymer/lipid suspension at a temperature higher than the gel-to-liquid transition temperature of the lipid (Hadinoto et al., 2013). Once LPNs are generated, the suspension is subjected to ultracentrifugation to separate LPNs from the unused lipid (Hadinoto et al., 2013). In terms of their size distribution, a monodispersed population of LPNs can be prepared by extruding an LPN suspension through a porous membrane (Barichello et al., 1999; Sengupta et al., 2005; Messerschmidt et al., 2009) or by using a high-pressure homogenizer (Fenart et al., 1999; De Miguel et al., 2000).

*b. The nonconventional two-step method.* The nonconventional two-step method of preparing LPNs has been developed by various groups (Hitzman et al., 2006; Li et al., 2010b; Hasan et al., 2012). For example, Hitzman et al. (2006) dispersed polymeric nanoparticles (400–500 nm in size) in a dichloromethane solution containing lipid, which was then subjected to spray drying to form lipid-coated polymeric nanoparticles. Another strategy involved the use of Particle Replication in Non-Wetting Templates technology to prepare polymeric nanoparticles, which were stabilized by a poly(vinyl alcohol) coating (Hasan et al., 2012). This poly(vinyl alcohol) coating was subsequently replaced with a lipid-coating to form LPNs (Hasan et al., 2012).

*c. Parameters governing the two-step method.* In the two-step method, the parameters governing the physical characteristics of LPNs are: 1) size homogeneity of the preformed lipid vesicles; 2) charge on the lipid formulation; 3) ionic strength of the continuous phase in which the lipid vesicles and polymeric nanoparticles are dispersed; 4) the lipid vesicle-to-polymeric nanoparticle ratio ($A_v/A_p$); and 5) the presence of lipid-PEG (Hadinoto et al., 2013).

Lipid vesicles of a small and uniform size allow small monodispersed LPNs to be formed (Hadinoto et al., 2013). This can be achieved by extruding lipid vesicles through a membrane before the addition of lipid vesicles to a preformed polymeric nanoparticles suspension (Troutier et al., 2005). LPN monodispersity can also be influenced by the net charge of the lipid formulation. The use of lipids with opposite charge produces LPNs that are

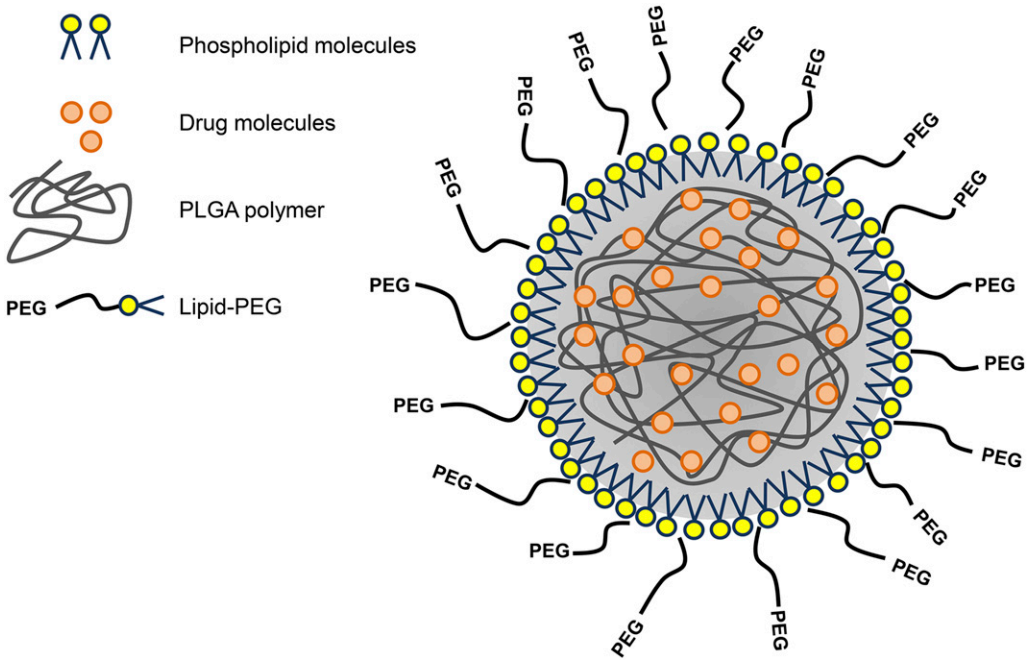


**Fig. 17.** Morphology of lipid-polymer hybrid nanoparticles (LPNs). LPNs exhibit characteristics of both polymeric nanoparticles and liposomes. They consist of three components: 1) a polymeric core made of polymers, such as PLGA or PLA, in which drugs are encapsulated; 2) a phospholipid layer surrounding the polymeric core, which prevents the encapsulated content from leakage and slows down polymer degradation by limiting inward water diffusion; and 3) an outer lipid-PEG stealth layer, which helps prolong the in vivo circulation time of LPNs and sterically stabilizes the particles.

prone to aggregation due to electrostatic interactions. However, minimal LPN aggregation can be achieved by using lipids of the same charge (Troutier et al., 2005). Other than the charge on lipid formulations that governs the aggregation of LPNs, the $A_v/A_p$ ratio significantly affects the stability and the aggregation of LPNs (Troutier et al., 2005). At a high $A_v/A_p$ ratio, lipid vesicles can act as a stabilizer to prevent LPNs from aggregating. However, at a low $A_v/A_p$ ratio, an incomplete lipid coating of preformed polymeric nanoparticles occurs, exposing parts of the LPN polymeric interior to the surroundings (Troutier et al., 2005). Aggregation can then take place as a consequence of the charge on the polymeric core being opposite to the charge on the lipid coating (Troutier et al., 2005).

The presence of lipid-PEG also plays a role in the colloidal stability of LPNs. However, this is dependent on the chain length of the PEG moiety (Thevenot et al., 2007). It was demonstrated that despite having a lower PEG-PE concentration and zeta potential, LPNs with a longer PEG chain exhibited a higher colloidal stability in NaCl solution than LPNs with a shorter PEG chain and a higher zeta potential (Thevenot et al., 2007).

*2. Preparation of Lipid-polymer Hybrid Nanoparticles: The One-step Preparation Method.* In contrast to the two-step method, the more recently developed one-step method involves mixing polymer with a lipid solution, which leads to self-assembly of lipid molecules around the polymer core by either nanoprecipitation or ESE forming the LPNs (Hadinoto et al., 2013). The one-step method is thought to be more efficient than the two-step method because it does not require preformed polymeric nanoparticles and lipid vesicles. Therefore, the one-step method requires less time and energy than the two-step method (Hadinoto et al., 2013). In the one-step method, lipid is used as a stabilizer to produce LPNs rather than as an ionic/nonionic surfactant used in the preparation of polymeric nanoparticles by nanoprecipitation or ESE (Hadinoto et al., 2013).

*a. The conventional one-step method by nanoprecipitation.* According to Hadinoto et al. (2013), conventional nanoprecipitation involves dissolving the polymer and the substance to be encapsulated in a water-miscible organic solvent (e.g., acetone) and adding it dropwise into lipid and/or a lipid-PEG aqueous dispersion under continuous stirring. Such an addition causes the polymer to precipitate forming nanoparticles. Simultaneously, lipid molecules within the water will self-assemble around the polymeric nanoparticles because of the hydrophobic interaction in which the hydrophobic tails of lipid molecules interact with the polymer core, whereas the hydrophilic heads face the aqueous surroundings (Hadinoto et al., 2013). As a result, LPNs are formed and stabilized by the lipid. This process can be made more efficient by heating the lipid and/or the lipid-PEG solution to ~65–70°C during lipid dispersion in order to form a homogeneous lipid mixture (Hadinoto et al., 2013). The resultant LPNs can be recovered by centrifugation at high speed after the solvent has been evaporated.

*b. Advances and modifications in lipid-polymer hybrid nanoparticle preparation by nanoprecipitation.* The rapid nanoprecipitation process was recently developed by Fang et al. (2010). This process involves supplying a high and uniform energy input via bath sonication to enable rapid LPN assembly. This development was able to increase the productivity of nanoprecipitation by 20-fold compared with the conventional method (Fang et al., 2010). This method also reduced the time required for solvent evaporation, because it used a smaller amount of organic solvent, which evaporated quickly during the self-assembly process. The size monodispersity of LPNs was optimized by changing the concentration ratio between different components leading to a low LPN polydispersity index (PDI) of ~0.08 (Fang et al., 2010).

The use of a microchannel during nanoprecipitation can also improve the size homogeneity of LPNs, as demonstrated recently by Valencia et al. (2010). This approach allowed the mixing of lipids and polymers to be precisely controlled at a microscale, leading to homogeneous polymer nucleation, which in turn produced LPNs of uniform size (Valencia et al., 2010). Additionally, the precise microscale mixing also enabled a uniform lipid coating of the polymer core (Valencia et al., 2010). The mixing of the aqueous and organic phase was further improved by using a micromixing structure, called the Tesla mixer, in conjunction with the microchannel (Valencia et al., 2010). This would enable a complete displacement of the organic phase to occur at a shorter time scale than the time required to form the polymer core, resulting in the formation of homogeneous polymeric nanoparticles (Valencia et al., 2010). Furthermore, the mixer allowed the two processes, that is, minimum lipid coating to stabilize the polymer core and polymer core formation, to take place within the same time scale as one another (Valencia et al., 2010). These processes would occur provided that the lipid-to-polymer mass ratio (L/P ratio) was optimized, which would lead to stable monodispersed LPNs (Valencia et al., 2010; Hadinoto et al., 2013).

In a study by Kim et al. (2012), the microchannel apparatus used for preparing LPNs (Valencia et al., 2010) was improved upon by using a three-inlet setup. This consisted of the organic phase going through the central inlet, while the aqueous phase was injected through two inlets on either side (Kim et al., 2012). This setup enabled a three-dimensional flow to generate a symmetrical microvortex, which led to the dispersion of large aggregates into smaller particles, resulting in a 200-fold improvement in LPN throughput compared with the original method (Valencia et al., 2010; Kim et al., 2012). A larger-scale microfluidic

nanoprecipitation process using a multi-inlet vortex reactor with four radially symmetrical inlets was also developed recently by Fang et al. (2012). This latter setup represents an appropriate method for commercial production of LPNs.

*c. Parameters governing nanoprecipitation.* The L/P ratio is a property unique to LPNs and influences their overall characteristics, including stability, encapsulation efficiency, release kinetics, etc. (Zhang et al., 2008a; Chan et al., 2009). Higher L/P ratios than the optimal value were reported to result in lipid concentrations being higher than the critical micelle concentration (Zhang et al., 2008a). Consequently, liposomes were formed in addition to LPNs (Zhang et al., 2008a). On the other hand, lower L/P ratios than the optimal value were reported to result in LPN aggregation because of an insufficient coating of lipid (Chan et al., 2009).

The L/P ratio was also suggested to influence the encapsulation efficiency, loading, and release kinetics of the encapsulated pharmaceutic indirectly via a lipid coating of the polymer core (Zhang et al., 2008a). Lipid coating serves as a barrier keeping the encapsulated substance inside the polymer core during the self-assembly process (Hadinoto et al., 2013). Consequently, it promotes a higher encapsulation efficiency and loading. It also serves to reduce the drug release from LPNs by keeping dissolution fluid medium away from the core (Hadinoto et al., 2013). This was observed in the study by Zhang et al. (2008a) who demonstrated that at the optimal L/P ratio, LPNs exhibited a higher encapsulation efficiency of docetaxel (DTX) ($\sim 59 \pm 4\%$) than nonhybrid PLGA ($37 \pm 4\%$) and PEGylated-PLGA ($19 \pm 3\%$) nanoparticles. Notably, LPNs with an optimal L/P ratio also showed prolonged drug release with 50% of the drug effluxed in 20 hours, relative to 50% released in 7 and 10 hours for PLGA and PEGylated-PLGA nanoparticles, respectively (Zhang et al., 2008a).

As observed in the two-step method described above (see section IX.C.1.c), the lipid-PEG fraction in a lipid formulation also influences colloidal stability in nanoprecipitation. It was observed that in the absence of the lipid-PEG component, lecithin-coated PLGA nanoparticles were unstable and formed aggregates (size $\sim 2\ \mu$m) in phosphate buffer saline. Only when DSPE-$PEG_{2000Da}$ was added to the lipid formulation were LPNs more stable (Chan et al., 2009). This could be explained by the capacity of PEG to provide steric stability to LPNs.

Although nanoprecipitation is highly effective and can be scaled up readily for a larger production, this method is still limited by the fact that substances to be encapsulated must be soluble in water-miscible organic solvents (Cheow and Hadinoto, 2011). Moreover, only a low encapsulation efficiency of water-soluble substances can be achieved because of the leakage of these substances into the aqueous phase (Su et al., 2011). To improve the range of substances to be encapsulated, ESE must be used.

*d. One-step method by emulsification-solvent-evaporation.* ESE can be divided into a single and double emulsification. A single ESE is suitable for substances that are soluble in a water-immiscible solvent (oil phase). In this method, polymer and pharmaceutical to be encapsulated are dissolved in the oil phase, whereas the lipid is dispersed in the aqueous phase (Bershteyn et al., 2008). Consequently, the oil phase is added to the aqueous phase under constant stirring or ultrasonication to form an o/w emulsion (Bershteyn et al., 2008). The polymer core is formed when the oil phase is evaporated and simultaneously lipid molecules self-assemble around the polymer core to form LPNs (Bershteyn et al., 2008). The dissolution of lipid in the oil phase together with the polymer and agent to be encapsulated before emulsification has also been reported (Cheow and Hadinoto, 2011). It should be noted that as stable emulsions must first be formed during the emulsification step, ESE usually generates larger LPNs compared with nanoprecipitation (Hadinoto et al., 2013).

A double ESE (w/o/w) is used when the substance to be encapsulated is insoluble in organic solvent and, therefore, cannot be added together with the polymer. This substance must be dissolved in the aqueous phase and emulsified in the oil phase containing the polymer and lipid, forming a water-in-oil (w/o) emulsion (Cheow and Hadinoto, 2011). The resultant w/o emulsion is then emulsified for the second time in an aqueous phase containing lipid-PEG to produce a w/o/w emulsion (Cheow and Hadinoto, 2011). Consequently, the oil phase is evaporated from the w/o/w emulsion forming LPNs (Cheow and Hadinoto, 2011). By using the double ESE method, the LPNs generated usually contain an inner lipid layer surrounding an aqueous core, a middle layer containing a polymer, and an outer lipid-PEG layer.

*e. Parameters governing emulsification-solvent-evaporation.* Similar to nanoprecipitation, the most important parameter controlling ESE is the L/P ratio (Cheow and Hadinoto, 2011). At low L/P ratios, the LPN size was observed to be relatively large ($\sim$800–1000 nm) because of aggregation. Conversely, increasing the L/P ratio was found to reduce the LPN size to $\sim$260–400 nm (Cheow and Hadinoto, 2011).

Apart from stability and size regulation, it was suggested that the L/P ratio also influences the spatial configuration of the self-assembled lipid (Bershteyn et al., 2008). Bershteyn et al. (2008) discovered that high L/P ratios caused either the formation of multilamellar lipid coating or the formation of free liposomes by excess lipid. The lipid coating configuration was further found to be dependent on the lipid type, because the use of zwitterionic 1,2-dioleoyl-*sn*-glycero-3 phosphocholine resulted in the formation of onion-like,

multilamellar stacks of lipid coating. In contrast, the mixture of zwitterionic and cationic lipids led to a typical core-shell LPN structure with a single lipid layer (Bershteyn et al., 2008).

As the L/P ratio controls the LPN size and lipid coating, it indirectly influences the encapsulation efficiency in a similar manner observed in the nanoprecipitation method (Liu et al., 2010b). Typically, high L/P ratios give rise to smaller LPNs, leading to a lower ability to encapsulate drugs (Liu et al., 2010b). At the same time, the presence of a high level of lipid on the surface of the polymer core due to high L/P ratios can increase the surface pressure and, consequently, reduces drug leakage (Liu et al., 2010b). Therefore, LPNs with high encapsulation efficiency can be obtained by optimizing the L/P ratio.

As observed in the two-step method and also nanoprecipitation, the lipid-PEG fraction in a lipid formulation also influences the colloidal stability of the resulting LPNs in ESE (Chu et al., 2011). A lower mass ratio of lipid-PEG to polymer was demonstrated to cause aggregation, reducing the fraction of LPNs in the sub-50 nm size (Chu et al., 2011). In contrast, a higher mass ratio increased the LPN fraction in the sub-50 nm size from less than 20% to as high as 85% (Chu et al., 2011).

Finally, another factor governing the ESE process is the ionic interaction between the drug and the lipid (Cheow and Hadinoto, 2011). This parameter is unique to ESE. It was discovered by Cheow and Hadinoto (2011) that an unsuccessful emulsification process occurred, causing the LPN formation to fail when oppositely charged lipid and drug components were used. However, this problem could be solved by adding counterionic surfactants to the emulsion prior to LPN formation. In addition, the drug loading and release kinetics were shown to be dependent on drug lipophilicity (Cheow and Hadinoto, 2011). A higher drug loading and a slower drug release were observed with highly lipophilic drugs as a result of strong hydrophobic interactions between the drug and the lipid layer (Cheow and Hadinoto, 2011).

It is worth mentioning that generally the ESE method results in a higher encapsulation efficiency than nanoprecipitation, which is due to the larger size of LPNs produced by the ESE method (Hadinoto et al., 2013). By using nanoprecipitation, the encapsulation efficiency of DTX in 50–60 nm LPNs was 20% (Chan et al., 2009), whereas 200–300 nm LPNs prepared using the ESE method were able to encapsulate up to ~60% of PTX (Liu et al., 2010b).

*3. Studies of Lipid-polymer Hybrid Nanoparticles in Cancer Therapy.* A single-drug delivery system using LPNs has been studied against various cancer cell-types in vitro, such as breast, prostate, lung, liver, and cervical cancer (Hitzman et al., 2006; Zhang et al., 2008a; Chan et al., 2009; Liu et al., 2010b; Chu et al., 2011). For instance, Liu et al. (2010b) encapsulated PTX within LPNs, which led to a sustained release of the drug and a 6- to 7-fold greater in vitro cytotoxicity against MCF-7 breast cancer cells after a 24 and 72-hour incubation, respectively, compared with standard taxol. In addition, LPNs exhibited cellular uptake after a 4-hour incubation that was ~70% higher than nonhybrid polymeric nanoparticles (Liu et al., 2010b). These LPNs released 100% of PTX within 7 days compared with 30% released by polymeric nanoparticles over the same period (Liu et al., 2010b).

More attention has been given to the capacity and potential of LPNs as a combinatorial drug delivery system (Sengupta et al., 2005; Aryal et al., 2010, 2011, 2012; Wang et al., 2010a,b; Kong et al., 2013). By using various strategies, it is possible to incorporate multiple drugs within LPNs (Fig. 18). For instance, different drugs can be conjugated to polymers or lipids separately before LPN preparation (Fig. 18, A and B) or encapsulated within preformed polymeric nanoparticles and lipid vesicles in the case of the two-step method (Fig. 18C). Alternatively, a second drug can be conjugated to the surface of LPNs postpreparation (Fig. 18D). The use of LPNs as a combinatorial drug delivery system would improve multidrug therapy by overcoming difficulties in obtaining a precise level of therapeutic exposure caused by variations in the pharmacokinetic and biodistribution of different drugs (Hadinoto et al., 2013).

Sengupta et al. (2005) incorporated the anticancer drug DOX and antiangiogenesis drug combretastatin into LPNs via a two-step method. Combretastatin was incorporated into the lipid layer of LPNs, whereas DOX was loaded into the polymeric core. This arrangement allowed an instant release of combretastatin to collapse the tumoral vasculature, trapping DOX-encapsulated polymeric nanoparticles within the tumor (Sengupta et al., 2005). Such LPNs were taken up rapidly by tumor vasculature within 5 hours after initial exposure and were retained within the tumor for at least 24 hours (Sengupta et al., 2005). In vivo studies using these LPNs also demonstrated greater tumor growth inhibition and a longer lifespan of mice bearing B16/F10 melanoma or Lewis lung carcinoma compared with DOX and combretastatin-loaded liposomes (Sengupta et al., 2005).

By using the nanoprecipitation technique, DOX and the radiotherapeutic agents Indium-111 or Yttrium-90 have also been successfully incorporated into LPNs (Wang et al., 2010a). The resulting LPNs, called Chemo-Rad, were taken up rapidly by LNCaP prostate cancer cells within 45 minutes and exhibited a higher in vitro cytotoxicity than LPNs containing only one of the agents (Wang et al., 2010a). No interference to the encapsulation or the sustained release of DOX by the radiotherapeutics was observed using these LPNs, with 100% of DOX being released within 7 days (Wang et al., 2010a). Furthermore, stimuli-responsive combinatorial LPNs were developed by Kong et al. (2013), who

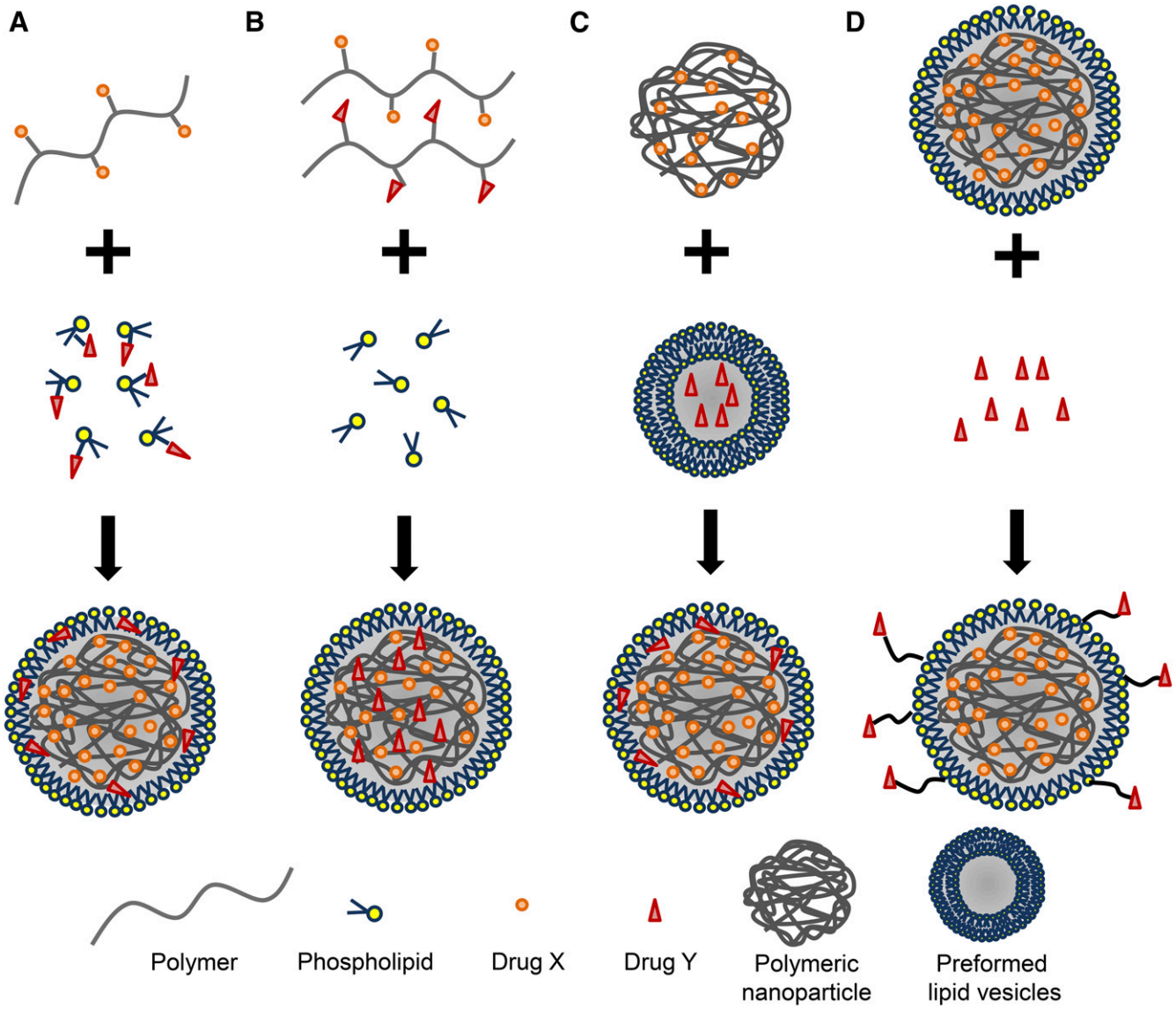


**Fig. 18.** Various strategies for combinatorial drug delivery using LPNs. (A) Separate covalent conjugation of different drugs (drug X and Y) to the polymer and phospholipid precursors before LPN preparation. For instance, drug X can be attached to the polymer, whereas drug Y can be attached to phospholipid molecules or vice versa. (B) Separate covalent conjugation of different drugs to polymer precursors prior to preparation. (C) Fusion of preformed polymeric nanoparticles and lipid vesicles via a two-step method of preparation. Different drugs are encapsulated within polymeric nanoparticles and liposomes separately before particle fusion. (D) Conjugation of the second drug (drug Y) to the surface of LPNs postpreparation. The first drug (drug X) is encapsulated within the polymeric core during LPN preparation.

generated camptothecin-loaded LPNs containing magnetic $Fe_3O_4$ nanoparticles. Upon the application of a remote radio frequency magnetic field, more than 90% of the encapsulated drug was released within 46 hours, and a greater growth inhibition of MT2 cancer cells was observed compared with nonhybrid magnetic nanoparticles (Kong et al., 2013).

Active targeting strategies have also been examined using LPNs. The conjugation of folic acid onto the surface of LPNs containing DTX was shown to increase their uptake by ~54% compared with unmodified LPNs after only 2 hours of incubation with MCF-7 breast cancer cells (Liu et al., 2010a). This increased uptake led to enhanced in vitro cytotoxicity by ~51% compared with the unmodified counterpart (Liu et al., 2010a). Similar results were observed in HeLa cells, both in vitro and in vivo, when folic acid-conjugated LPNs containing PTX were tested in comparison with their unmodified counterparts (Zhao et al., 2012). Other targeting ligands that have been examined include aptamers (Zhang et al., 2008a), antibody (Hu et al., 2010), transferrin (Zheng et al., 2010), and peptides (Chan et al., 2010, 2011).

Apart from the incorporation of cytotoxic chemotherapeutic agents into LPNs as a single or combinatorial drug transport system with/without active targeting, LPNs have been used for the delivery of genes (Li et al., 2010a; Zhong et al., 2010), siRNA (Shi et al., 2011; Hasan et al., 2012; Yang et al., 2012a), and diagnostic imaging agents (Kandel et al., 2011; Mieszawska et al., 2012).

## X. Conclusion

The development of nanoparticle drug delivery systems, such as lipid-based nanoparticles, and particularly liposomes, has emerged as a promising strategy for the treatment of cancer. Since their discovery in the 1960s, liposome technology has advanced rapidly from being used as an apparatus for cell membrane research to becoming a versatile drug carrier. Similar to other types of nanosized drug delivery systems, liposomes can improve the specificity and efficacy of chemotherapeutics, while reducing their toxic side effects by means of passive and active targeting. However, lipid-based nanoparticles are more advantageous over other nanoparticles because of the more biocompatible and biodegradable nature of their constituents relative to synthetic polymers found in other types of nanoparticles. Moreover, the amphiphilic properties of phospholipids that make up liposomes allow these nanoparticles to encapsulate both hydrophobic and hydrophilic anti-cancer agents.

Presently, a variety of liposomal encapsulated anticancer drugs are clinically approved and commercially available, while many more formulations are being investigated in different stages of clinical trials or are awaiting approval. Moreover, the development of various liposome technologies, such as different types of stimuli-sensitive liposomes and multifunctional "SMART" liposomes, has also demonstrated the promising potential of liposomes as effective anticancer agent delivery systems. Furthermore, advances in liposomal design have seen the emergence of the next generation of lipid-based nanoparticles, including lipid micelles, solid lipid nanoparticles, nanostructured lipid carriers, and lipid-polymer hybrid nanoparticles. Such innovations are believed to be capable of overcoming current drawbacks observed in liposome technology. However, more studies are still required to optimize their capacity as drug delivery systems. Together with other forms of targeted drug delivery systems, liposomes and lipid-based nanoparticles will help improve the efficacy and safety profile of anticancer agents and, more importantly, the fate of cancer patients.

#### Acknowledgments

Phatsapong Yingchoncharoen would like to dedicate this review to Mrs. Sujira Yingchoncharoen, "my loving mother, my first teacher, and my best friend", who died from lung cancer with leptomeningeal metastases on the 30th of April 2014. Phatsapong Yingchoncharoen also thanks the Yingchoncharoen family, Thaveesakvilai family, Leehacharoenkul family, Uthayaratana family, Thongkongtoon family, and Ms. Kulvarong Kijtanasopa for their support through this hardship.

#### Authorship Contributions

*Wrote or contributed to the writing of the manuscript:* Yingchoncharoen, Kalinowski, and Richardson.

#### References

Abd El-Rehim DM, Pinder SE, Paish CE, Bell JA, Rampaul RS, Blamey RW, Robertson JF, Nicholson RI, and Ellis IO (2004) Expression and co-expression of the members of the epidermal growth factor receptor (EGFR) family in invasive breast carcinoma. *Br J Cancer* **91**:1532–1542.

Abid MR, Yi X, Yano K, Shih S-C, and Aird WC (2006) Vascular endocan is preferentially expressed in tumor endothelium. *Microvasc Res* **72**:136–145.

Abuchowski A, McCoy JR, Palczuk NC, van Es T, and Davis FF (1977) Effect of covalent attachment of polyethylene glycol on immunogenicity and circulating life of bovine liver catalase. *J Biol Chem* **252**:3582–3586.

Ahmed SE, Martins AM, and Husseini GA (2015) The use of ultrasound to release chemotherapeutic drugs from micelles and liposomes. *J Drug Target* **23**:16–42.

Alkan-Onyuksel H, Ramakrishnan S, Chai H-B, and Pezzuto JM (1994) A mixed micellar formulation suitable for the parenteral administration of taxol. *Pharm Res* **11**:206–212.

Allen C, Dos Santos N, Gallagher R, Chiu GN, Shu Y, Li WM, Johnstone SA, Janoff AS, Mayer LD, and Webb MS, et al. (2002) Controlling the physical behavior and biological performance of liposome formulations through use of surface grafted poly(ethylene glycol). *Biosci Rep* **22**:225–250.

Allen TM, Austin GA, Chonn A, Lin L, and Lee KC (1991a) Uptake of liposomes by cultured mouse bone marrow macrophages: influence of liposome composition and size. *Biochim Biophys Acta* **1061**:56–64.

Allen TM and Chonn A (1987) Large unilamellar liposomes with low uptake into the reticuloendothelial system. *FEBS Lett* **223**:42–46.

Allen TM, Hansen C, Martin F, Redemann C, and Yau-Young A (1991b) Liposomes containing synthetic lipid derivatives of poly(ethylene glycol) show prolonged circulation half-lives in vivo. *Biochim Biophys Acta* **1066**:29–36.

Allen TM (1997) Liposomes. Opportunities in drug delivery. *Drugs* **54** (Suppl 4):8–14.

Allen TM (1998) Liposomal drug formulations. Rationale for development and what we can expect for the future. *Drugs* **56**:747–756.

Allen TM, Ryan JL, and Papahadjopoulos D (1985) Gangliosides reduce leakage of aqueous-space markers from liposomes in the presence of human plasma. *Biochim Biophys Acta* **818**:205–210.

Amselem S, Cohen R, and Barenholz Y (1993a) In vitro tests to predict in vivo performance of liposomal dosage forms. *Chem Phys Lipids* **64**:219–237.

Amselem S, Gabizon A, and Barenholz Y (1993b) A large-scale method for the preparation of sterile and non-pyrogenic liposomal formulations of defined size distributions for clinical use, in *Liposome Technology: Liposome Preparation and Related Techniques* (Gregoriadis G ed) pp 501–525, CRC Press, Boca Raton.

Anders CK, Adamo B, Karginova O, Deal AM, Rawal S, Darr D, Schorzman A, Santos C, Bash R, and Kafri T, et al. (2013) Pharmacokinetics and efficacy of PEGylated liposomal doxorubicin in an intracranial model of breast cancer. *PLoS One* **8**: e61359.

Anderson RG, Brown MS, Beisiegel U, and Goldstein JL (1982) Surface distribution and recycling of the low density lipoprotein receptor as visualized with antireceptor antibodies. *J Cell Biol* **93**:523–531.

Anderson M and Omri A (2004) The effect of different lipid components on the in vitro stability and release kinetics of liposome formulations. *Drug Deliv* **11**:33–39.

Angst MS and Drover DR (2006) Pharmacology of drugs formulated with DepoFoam: a sustained release drug delivery system for parenteral administration using multivesicular liposome technology. *Clin Pharmacokinet* **45**:1153–1176.

Arias JL (2011) Drug targeting strategies in cancer treatment: an overview. *Mini Rev Med Chem* **11**:1–17.

Aryal S, Hu C-MJ, Fu V, and Zhang L (2012) Nanoparticle drug delivery enhances the cytotoxicity of hydrophobic-hydrophilic drug conjugates. *J Mater Chem* **22**: 994–999.

Aryal S, Hu C-MJ, and Zhang L (2010) Combinatorial drug conjugation enables nanoparticle dual-drug delivery. *Small* **6**:1442–1448.

Aryal S, Hu C-MJ, and Zhang L (2011) Polymeric nanoparticles with precise ratiometric control over drug loading for combination therapy. *Mol Pharm* **8**:1401–1407.

Awada A, Bondarenko IN, Bonneterre J, Nowara E, Ferrero JM, Bakshi AV, Wilke C, and Piccart M; CT4002 study group (2014) A randomized controlled phase II trial of a novel composition of paclitaxel embedded into neutral and cationic lipids targeting tumor endothelial cells in advanced triple-negative breast cancer (TNBC). *Ann Oncol* **25**:824–831.

Awasthi VD, Garcia D, Goins BA, and Phillips WT (2003) Circulation and biodistribution profiles of long-circulating PEG-liposomes of various sizes in rabbits. *Int J Pharm* **253**:121–132.

Azarmi S, Tao X, Chen H, Wang Z, Finlay WH, Löbenberg R, and Roa WH (2006) Formulation and cytotoxicity of doxorubicin nanoparticles carried by dry powder aerosol particles. *Int J Pharm* **319**:155–161.

Babincová M, Altanerová V, Lampert M, Altaner C, Machová E, Srámka M, and Babinec P (2000) Site-specific in vivo targeting of magnetoliposomes using externally applied magnetic field. *Z Naturforsch C* **55**:278–281.

Bae YH (2009) Drug targeting and tumor heterogeneity. *J Control Release* **133**:2–3.

Bagchi D, Bagchi M, Hassoun EA, Kelly J, and Stohs SJ (1995) Adriamycin-induced hepatic and myocardial lipid peroxidation and DNA damage, and enhanced excretion of urinary lipid metabolites in rats. *Toxicology* **95**:1–9.

Bai X-F, Liu J, Li O, Zheng P, and Liu Y (2003) Antigenic drift as a mechanism for tumor evasion of destruction by cytolytic T lymphocytes. *J Clin Invest* **111**: 1487–1496.

Banerjee J, Hanson AJ, Gadam B, Elegbede AI, Tobwala S, Ganguly B, Wagh AV, Muhonen WW, Law B, and Shabb JB, et al. (2009) Release of liposomal contents by cell-secreted matrix metalloproteinase-9. *Bioconjug Chem* **20**:1332–1339.

Bangham AD (1982) Preparation of liposomes and methods for measuring their permeabilities, in *Technique in Life Science - Technique in Lipid and Membrane Biochemistry Part II* (Hesketh TR, Kornberg HL, Metcalfe JC, Northcote DH, Pogson CI, and Tipton KF eds) pp 1–25, Elsevier/North-Holland, Amsterdam.

Bangham AD, Hill MW, and Miller NGA (1974) Preparation and use of liposomes as models of biological membranes, in *Methods in Membrane Biology*, **Vol. 1** (Korn ED ed) pp 1–68, Springer US, Boston.

Bangham AD, Standish MM, and Watkins JC (1965) Diffusion of univalent ions across the lamellae of swollen phospholipids. *J Mol Biol* **13**:238–252.

Bareford LM and Swaan PW (2007) Endocytic mechanisms for targeted drug delivery. *Adv Drug Deliv Rev* **59**:748–758.
Barenholz Y (2003) Relevancy of drug loading to liposomal formulation therapeutic efficacy. *J Liposome Res* **13**:1–8.
Barenholz Y (2007) Amphipathic weak base loading into preformed liposomes having a transmembrane ammonium ion gradient: From the bench to approved DOXIL, in *Liposome Technology: Entrapment of drugs and other materials into liposomes* (Gregoriadis G ed) pp 1-25, CRC Press, Boca Raton, FL.
Barenholz Y (2012a) Doxil® - the first FDA-approved nano-drug: from an idea to a product, in *Handbook of Harnessing Biomaterials in Nanomedicine: Preparation, Toxicity, and Applications* (Peer D ed) pp 335–398, Pan Stanford Publishing, Singapore.
Barenholz Y (2012b) Doxil®–the first FDA-approved nano-drug: lessons learned. *J Control Release* **160**:117–134.
Barenholz Y and Cohen R (1995) Rational design of amphiphile-based drug carriers and sterically stabilized carriers. *J Liposome Res* **5**:905–932.
Barenholz Y and Haran G (1994) inventors, Yissum Research Development Company of the Hebrew University of Jerusalem, assignee. Methods of amphipathic drug loading in liposomes by ammonium ion gradient. U.S. patent US5316771. 1992 Dec 18.
Barichello JM, Morishita M, Takayama K, and Nagai T (1999) Encapsulation of hydrophilic and lipophilic drugs in PLGA nanoparticles by the nanoprecipitation method. *Drug Dev Ind Pharm* **25**:471–476.
Batist G, Gelmon KA, Chi KN, Miller WH Jr, Chia SK, Mayer LD, Swenson CE, Janoff AS, and Louie AC (2009) Safety, pharmacokinetics, and efficacy of CPX-1 liposome injection in patients with advanced solid tumors. *Clin Cancer Res* **15**: 692–700.
Batist G, Harris L, Azarnia N, Lee LW, and Daza-Ramirez P (2006) Improved antitumor response rate with decreased cardiotoxicity of non-pegylated liposomal doxorubicin compared with conventional doxorubicin in first-line treatment of metastatic breast cancer in patients who had received prior adjuvant doxorubicin: results of a retrospective analysis. *Anticancer Drugs* **17**:587–595.
Batist G, Ramakrishnan G, Rao CS, Chandrasekharan A, Gutheil J, Guthrie T, Shah P, Khojasteh A, Nair MK, and Hoelzer K, et al. (2001) Reduced cardiotoxicity and preserved antitumor efficacy of liposome-encapsulated doxorubicin and cyclophosphamide compared with conventional doxorubicin and cyclophosphamide in a randomized, multicenter trial of metastatic breast cancer. *J Clin Oncol* **19**: 1444–1454.
Batzri S and Korn ED (1973) Single bilayer liposomes prepared without sonication. *Biochim Biophys Acta* **298**:1015–1019.
Bedu-Addo FK, Tang P, Xu Y, and Huang L (1996a) Effects of polyethyleneglycol chain length and phospholipid acyl chain composition on the interaction of polyethyleneglycol-phospholipid conjugates with phospholipid: implications in liposomal drug delivery. *Pharm Res* **13**:710–717.
Bedu-Addo FK, Tang P, Xu Y, and Huang L (1996b) Interaction of polyethyleneglycol-phospholipid conjugates with cholesterol-phosphatidylcholine mixtures: sterically stabilized liposome formulations. *Pharm Res* **13**:718–724.
Belsito S, Bartucci R, and Sportelli L (2001) Lipid chain length effect on the phase behaviour of PCs/PEG:2000-PEs mixtures. A spin label electron spin resonance and spectrophotometric study. *Biophys Chem* **93**:11–22.
Bergström K, Osterberg E, Holmberg K, Hoffman AS, Schuman TP, Kozlowski A, and Harris JH (1994) Effects of branching and molecular weight of surface-bound poly(ethylene oxide) on protein rejection. *J Biomater Sci Polym Ed* **6**: 123–132.
Bershteyn A, Chaparro J, Yau R, Kim M, Reinherz E, Ferreira-Moita L, and Irvine DJ (2008) Polymer-supported lipid shells, onions, and flowers. *Soft Matter* **4**: 1787–1791.
Bies C, Lehr C-M, and Woodley JF (2004) Lectin-mediated drug targeting: history and applications. *Adv Drug Deliv Rev* **56**:425–435.
Bleyer WA, Pizzo PA, Spence AM, Platt WD, Benjamin DR, Kolins CJ, and Poplack DG (1978) The Ommaya reservoir: newly recognized complications and recommendations for insertion and use. *Cancer* **41**:2431–2437.
Blum RH and Carter SK (1974) Adriamycin. A new anticancer drug with significant clinical activity. *Ann Intern Med* **80**:249–259.
Bolotin EM, Cohen R, Bar LK, Emanuel N, Ninio S, Barenholz Y, and Lasic DD (1994) Ammonium sulfate gradients for efficient and stable remote loading of amphipathic weak bases into liposomes and ligandoliposomes. *J Liposome Res* **4**: 455–479.
Boltri L, Canal T, Esposito PA, and Carli F (1993) Lipid nanoparticles: evaluation of some critical formulation parameters. *Proc Int Symp Control Release Bioact Mater* **20**:346–347.
Bolwell BJ, Cassileth PA, and Gale RP (1988) High dose cytarabine: a review. *Leukemia* **2**:253–260.
Boman NL, Bally MB, Cullis PR, Mayer LD, and Webb MS (1995) Encapsulation of vincristine in liposomes reduces its toxicity and improves its anti-tumor efficacy. *J Liposome Res* **5**:523–541.
Boman NL, Masin D, Mayer LD, Cullis PR, and Bally MB (1994) Liposomal vincristine which exhibits increased drug retention and increased circulation longevity cures mice bearing P388 tumors. *Cancer Res* **54**:2830–2833.
Bosanquet AG (1986) Stability of solutions of antineoplastic agents during preparation and storage for in vitro assays. II. Assay methods, adriamycin and the other antitumour antibiotics. *Cancer Chemother Pharmacol* **17**:1–10.
Bossuyt V, Fadare O, Martel M, Ocal IT, Burtness B, Moinfar F, Leibl S, and Tavassoli FA (2005) Remarkably high frequency of EGFR expression in breast carcinomas with squamous differentiation. *Int J Surg Pathol* **13**:319–327.
Boucher Y, Baxter LT, and Jain RK (1990) Interstitial pressure gradients in tissue-isolated and subcutaneous tumors: implications for therapy. *Cancer Res* **50**: 4478–4484.
Boulikas T (2009) Clinical overview on Lipoplatin: a successful liposomal formulation of cisplatin. *Expert Opin Investig Drugs* **18**:1197–1218.
Bourguignon LY, Zhu H, Shao L, and Chen YW (2000) CD44 interaction with tiam1 promotes Rac1 signaling and hyaluronic acid-mediated breast tumor cell migration. *J Biol Chem* **275**:1829–1838.
Bourré L, Thibaut S, Fimiani M, Ferrand Y, Simonneaux G, and Patrice T (2003) In vivo photosensitizing efficiency of a diphenylchlorin sensitizer: interest of a DMPC liposome formulation. *Pharmacol Res* **47**:253–261.
Bouzin C and Feron O (2007) Targeting tumor stroma and exploiting mature tumor vasculature to improve anti-cancer drug delivery. *Drug Resist Updat* **10**:109–120.
Bradley AJ, Devine DV, Ansell SM, Janzen J, and Brooks DE (1998) Inhibition of liposome-induced complement activation by incorporated poly(ethylene glycol)-lipids. *Arch Biochem Biophys* **357**:185–194.
Brandhonneur N, Chevanne F, Vié V, Frisch B, Primault R, Le Potier M-F, and Le Corre P (2009) Specific and non-specific phagocytosis of ligand-grafted PLGA microspheres by macrophages. *Eur J Pharm Sci* **36**:474–485.
Bremerskov V and Linnemann R (1969) Some effects of daunomycin on the nucleic acid synthesis in synchronized L-cells. *Eur J Cancer* **5**:317–330.
Broekgaarden M, de Kroon AI, Gulik TM, and Heger M (2014) Development and in vitro proof-of-concept of interstitially targeted zinc- phthalocyanine liposomes for photodynamic therapy. *Curr Med Chem* **21**:377–391.
Broekgaarden M, Kos M, Jurg FA, van Beek AA, van Gulik TM, and Heger M (2015) Inhibition of NF-κB in tumor cells exacerbates immune cell activation following photodynamic therapy. *Int J Mol Sci* **16**:19960–19977.
Brown LF, Tognazzi K, Dvorak HF, and Harrist TJ (1996) Strong expression of kinase insert domain-containing receptor, a vascular permeability factor/vascular endothelial growth factor receptor in AIDS-associated Kaposi's sarcoma and cutaneous angiosarcoma. *Am J Pathol* **148**:1065–1074.
Bunjes H, Drechsler M, Koch MH, and Westesen K (2001) Incorporation of the model drug ubidecarenone into solid lipid nanoparticles. *Pharm Res* **18**:287–293.
Bunjes H, Westesen K, and Koch MH (1996) Crystallization tendency and polymorphic transitions in triglyceride nanoparticles. *Int J Pharm* **129**:159–173.
Byrne JD, Betancourt T, and Brannon-Peppas L (2008) Active targeting schemes for nanoparticle systems in cancer therapeutics. *Adv Drug Deliv Rev* **60**: 1615–1626.
Cai S, Thati S, Bagby TR, Diab H-M, Davies NM, Cohen MS, and Forrest ML (2010) Localized doxorubicin chemotherapy with a biopolymeric nanocarrier improves survival and reduces toxicity in xenografts of human breast cancer. *J Control Release* **146**:212–218.
Camp ER, Wang C, Little EC, Watson PM, Pirollo KF, Rait A, Cole DJ, Chang EH, and Watson DK (2013) Transferrin receptor targeting nanomedicine delivering wild-type p53 gene sensitizes pancreatic cancer to gemcitabine therapy. *Cancer Gene Ther* **20**:222–228.
Campbell RB, Fukumura D, Brown EB, Mazzola LM, Izumi Y, Jain RK, Torchilin VP, and Munn LL (2002) Cationic charge determines the distribution of liposomes between the vascular and extravascular compartments of tumors. *Cancer Res* **62**: 6831–6836.
Campbell RB, Ying B, Kuesters GM, and Hemphill R (2009) Fighting cancer: from the bench to bedside using second generation cationic liposomal therapeutics. *J Pharm Sci* **98**:411–429.
Cardone RA, Casavola V, and Reshkin SJ (2005) The role of disturbed pH dynamics and the $Na^+/H^+$ exchanger in metastasis. *Nat Rev Cancer* **5**:786–795.
Carmeliet P (2005) VEGF as a key mediator of angiogenesis in cancer. *Oncology* **69** (Suppl 3):4–10.
Carpenter G and Cohen S (1979) Epidermal growth factor. *Annu Rev Biochem* **48**: 193–216.
Castle MC, Margileth DA, and Oliverio VT (1976) Distribution and excretion of ($^3$H)vincristine in the rat and the dog. *Cancer Res* **36**:3684–3689.
Cattaneo AG, Gornati R, Sabbioni E, Chiriva-Internati M, Cobos E, Jenkins MR, and Bernardini G (2010) Nanotechnology and human health: risks and benefits. *J Appl Toxicol* **30**:730–744.
Catterall JB, Jones LM, and Turner GA (1999) Membrane protein glycosylation and CD44 content in the adhesion of human ovarian cancer cells to hyaluronan. *Clin Exp Metastasis* **17**:583–591.
Cavalli R, Caputo O, and Gasco MR (1993) Solid lipospheres of doxorubicin and idarubicin. *Int J Pharm* **89**:9–12.
Cavalli R, Caputo O, and Gasco MR (2000) Preparation and characterization of solid lipid nanospheres containing paclitaxel. *Eur J Pharm Sci* **10**:305–309.
Chamberlain MC and Corey-Bloom J (1991) Leptomeningeal metastases: 111indium-DTPA CSF flow studies. *Neurology* **41**:1765–1769.
Chamberlain MC, Khatibi S, Kim JC, Howell SB, Chatelut E, and Kim S (1993) Treatment of leptomeningeal metastasis with intraventricular administration of depot cytarabine (DTC 101). A phase I study. *Arch Neurol* **50**: 261–264.
Chan S, Davidson N, Juozaityte E, Erdkamp F, Pluzanska A, Azarnia N, and Lee LW (2004) Phase III trial of liposomal doxorubicin and cyclophosphamide compared with epirubicin and cyclophosphamide as first-line therapy for metastatic breast cancer. *Ann Oncol* **15**:1527–1534.
Chan JM, Rhee JW, Drum CL, Bronson RT, Golomb G, Langer R, and Farokhzad OC (2011) In vivo prevention of arterial restenosis with paclitaxel-encapsulated targeted lipid-polymeric nanoparticles. *Proc Natl Acad Sci USA* **108**:19347–19352.
Chan JM, Zhang L, Tong R, Ghosh D, Gao W, Liao G, Yuet KP, Gray D, Rhee J-W, and Cheng J, et al. (2010) Spatiotemporal controlled delivery of nanoparticles to injured vasculature. *Proc Natl Acad Sci USA* **107**:2213–2218.
Chan JM, Zhang L, Yuet KP, Liao G, Rhee J-W, Langer R, and Farokhzad OC (2009) PLGA-lecithin-PEG core-shell nanoparticles for controlled drug delivery. *Biomaterials* **30**:1627–1634.
Chandaroy P, Sen A, and Hui SW (2001) Temperature-controlled content release from liposomes encapsulating Pluronic F127. *J Control Release* **76**:27–37.
Chang J, Jallouli Y, Kroubi M, Yuan XB, Feng W, Kang CS, Pu PY, and Betbeder D (2009) Characterization of endocytosis of transferrin-coated PLGA nanoparticles by the blood-brain barrier. *Int J Pharm* **379**:285–292.

Chanturiya A, Chernomordik LV, and Zimmerberg J (1997) Flickering fusion pores comparable with initial exocytotic pores occur in protein-free phospholipid bilayers. *Proc Natl Acad Sci USA* **94**:14423–14428.
Charcosset C, El-Harati A, and Fessi H (2005) Preparation of solid lipid nanoparticles using a membrane contactor. *J Control Release* **108**:112–120.
Cheng WW and Allen TM (2008) Targeted delivery of anti-CD19 liposomal doxorubicin in B-cell lymphoma: a comparison of whole monoclonal antibody, Fab' fragments and single chain Fv. *J Control Release* **126**:50–58.
Cheow WS and Hadinoto K (2011) Factors affecting drug encapsulation and stability of lipid-polymer hybrid nanoparticles. *Colloids Surf B Biointerfaces* **85**:214–220.
Chernomordik LV and Kozlov MM (2003) Protein-lipid interplay in fusion and fission of biological membranes. *Annu Rev Biochem* **72**:175–207.
Chernomordik LV and Kozlov MM (2008) Mechanics of membrane fusion. *Nat Struct Mol Biol* **15**:675–683.
Chernomordik LV, Melikyan GB, and Chizmadzhev YA (1987) Biomembrane fusion: a new concept derived from model studies using two interacting planar lipid bilayers. *Biochim Biophys Acta* **906**:309–352.
Chithrani BD, Ghazani AA, and Chan WC (2006) Determining the size and shape dependence of gold nanoparticle uptake into mammalian cells. *Nano Lett* **6**: 662–668.
Cho K, Wang X, Nie S, Chen ZG, and Shin DM (2008) Therapeutic nanoparticles for drug delivery in cancer. *Clin Cancer Res* **14**:1310–1316.
Choi HS, Liu W, Misra P, Tanaka E, Zimmer JP, Itty Ipe B, Bawendi MG, and Frangioni JV (2007) Renal clearance of quantum dots. *Nat Biotechnol* **25**: 1165–1170.
Choi W-J, Kim J-K, Choi S-H, Park J-S, Ahn WS, and Kim C-K (2004) Low toxicity of cationic lipid-based emulsion for gene transfer. *Biomaterials* **25**:5893–5903.
Chou H-H, Wang K-L, Chen C-A, Wei L-H, Lai C-H, Hsieh C-Y, Yang Y-C, Twu N-F, Chang T-C, and Yen M-S; Taiwanese Gynecologic Oncology Group (2006) Pegylated liposomal doxorubicin (Lipo-Dox) for platinum-resistant or refractory epithelial ovarian carcinoma: a Taiwanese gynecologic oncology group study with long-term follow-up. *Gynecol Oncol* **101**:423–428.
Chu C-J, Dijkstra J, Lai M-Z, Hong K, and Szoka FC (1990) Efficiency of cytoplasmic delivery by pH-sensitive liposomes to cells in culture. *Pharm Res* **7**:824–834.
Chu C-J and Szoka FC (1994) pH-sensitive liposomes. *J Liposome Res* **4**:361–395.
Chu C-H, Wang Y-C, Huang H-Y, Wu L-C, and Yang C-S (2011) Ultrafine PEG-coated poly(lactic-co-glycolic acid) nanoparticles formulated by hydrophobic surfactant-assisted one-pot synthesis for biomedical applications. *Nanotechnology* **22**:185601.
Clague MJ, Urbé S, Aniento F, and Gruenberg J (1994) Vacuolar ATPase activity is required for endosomal carrier vesicle formation. *J Biol Chem* **269**:21–24.
Clarke SJ and Rivory LP (1999) Clinical pharmacokinetics of docetaxel. *Clin Pharmacokinet* **36**:99–114.
Collins D(1995) pH-sensitive liposomes as tools for cytoplasmic delivery, in *Liposomes as Tools in Basic Research and Industry* (Philippot JR and Schuber F eds) pp 201–214, CRC Press, Boca Raton.
Comiskey SJ and Heath TD (1990) Serum-induced leakage of negatively charged liposomes at nanomolar lipid concentrations. *Biochemistry* **29**:3626–3631.
Cortes JE, Goldberg SL, Feldman EJ, Rizzeri DA, Hogge DE, Larson M, Pigneux A, Recher C, Schiller G, and Warzocha K, et al. (2015) Phase II, multicenter, randomized trial of CPX-351 (cytarabine:daunorubicin) liposome injection versus intensive salvage therapy in adults with first relapse AML. *Cancer* **121**:234–242.
Crom WR, de Graaf SS, Synold T, Uges DR, Bloemhof H, Rivera G, Christensen ML, Mahmoud H, and Evans WE (1994) Pharmacokinetics of vincristine in children and adolescents with acute lymphocytic leukemia. *J Pediatr* **125**:642–649.
Cudd A and Nicolau C (1985) Intracellular fate of liposome-encapsulated DNA in mouse liver. Analysis using electron microscope autoradiography and subcellular fractionation. *Biochim Biophys Acta* **845**:477–491.
Cullis PR, Chonn A, and Semple SC (1998) Interactions of liposomes and lipid-based carrier systems with blood proteins: Relation to clearance behaviour in vivo. *Adv Drug Deliv Rev* **32**:3–17.
Cullis PR and de Kruijff B (1979) Lipid polymorphism and the functional roles of lipids in biological membranes. *Biochim Biophys Acta* **559**:399–420.
Daemen T, Velinova M, Regts J, de Jager M, Kalicharan R, Donga J, van der Want JJ, and Scherphof GL (1997) Different intrahepatic distribution of phosphatidylglycerol and phosphatidylserine liposomes in the rat. *Hepatology* **26**:416–423.
Dagher R, Johnson J, Williams G, Keegan P, and Pazdur R (2004) Accelerated approval of oncology products: a decade of experience. *J Natl Cancer Inst* **96**: 1500–1509.
Damen J, Regts J, and Scherphof G (1981) Transfer and exchange of phospholipid between small unilamellar liposomes and rat plasma high density lipoproteins. Dependence on cholesterol content and phospholipid composition. *Biochim Biophys Acta* **665**:538–545.
Damodar G, Smitha T, Gopinath S, Vijayakumar S, and Rao Y (2014) An evaluation of hepatotoxicity in breast cancer patients receiving injection Doxorubicin. *Ann Med Health Sci Res* **4**:74–79.
Damoiseau X, Schuitmaker HJ, Lagerberg JW, and Hoebeke M (2001) Increase of the photosensitizing efficiency of the Bacteriochlorin a by liposome-incorporation. *J Photochem Photobiol B* **60**:50–60.
Dandamudi S and Campbell RB (2007) The drug loading, cytotoxicty and tumor vascular targeting characteristics of magnetite in magnetic drug targeting. *Biomaterials* **28**:4673–4683.
Danhier F, Feron O, and Préat V (2010) To exploit the tumor microenvironment: Passive and active tumor targeting of nanocarriers for anti-cancer drug delivery. *J Control Release* **148**:135–146.
Daniels TR, Delgado T, Helguera G, and Penichet ML (2006) The transferrin receptor part II: targeted delivery of therapeutic agents into cancer cells. *Clin Immunol* **121**: 159–176.
Das S and Chaudhury A (2011) Recent advances in lipid nanoparticle formulations with solid matrix for oral drug delivery. *AAPS PharmSciTech* **12**:62–76.
Dautry-Varsat A, Ciechanover A, and Lodish HF (1983) pH and the recycling of transferrin during receptor-mediated endocytosis. *Proc Natl Acad Sci USA* **80**: 2258–2262.
Davies EJ, Blackhall FH, Shanks JH, David G, McGown AT, Swindell R, Slade RJ, Martin-Hirsch P, Gallagher JT, and Jayson GC (2004) Distribution and clinical significance of heparan sulfate proteoglycans in ovarian cancer. *Clin Cancer Res* **10**:5178–5186.
Davis ME, Chen ZG, and Shin DM (2008) Nanoparticle therapeutics: an emerging treatment modality for cancer. *Nat Rev Drug Discov* **7**:771–782.
De Gennes P (1987) Polymers at an interface; a simplified view. *Adv Colloid Interface Sci* **27**:189–209.
De Miguel D, Basáñez G, Sánchez D, Malo PG, Marzo I, Larrad L, Naval J, Pardo J, Anel A, and Martinez-Lostao L (2013) Liposomes decorated with Apo2L/TRAIL overcome chemoresistance of human hematologic tumor cells. *Mol Pharm* **10**: 893–904.
De Miguel I, Imbertie L, Rieumajou V, Major M, Kravtzoff R, and Betbeder D (2000) Proofs of the structure of lipid coated nanoparticles (SMBV) used as drug carriers. *Pharm Res* **17**:817–824.
Deamer D and Bangham AD (1976) Large volume liposomes by an ether vaporization method. *Biochim Biophys Acta* **443**:629–634.
Deckers R, Rome C, and Moonen CT (2008) The role of ultrasound and magnetic resonance in local drug delivery. *J Magn Reson Imaging* **27**:400–409.
Demirgöz D, Garg A, and Kokkoli E (2008) PR_b-targeted PEGylated liposomes for prostate cancer therapy. *Langmuir* **24**:13518–13524.
Denekamp J (1984) Vasculature as a target for tumour therapy. *Prog Appl Microcirc* **4**:28–38.
Denekamp J and Hobson B (1982) Endothelial-cell proliferation in experimental tumours. *Br J Cancer* **46**:711–720.
Derksen JT, Morselt HW, Kalicharan D, Hulstaert CE, and Scherphof GL (1987) Interaction of immunoglobulin-coupled liposomes with rat liver macrophages in vitro. *Exp Cell Res* **168**:105–115.
Derycke AS and de Witte PA (2004) Liposomes for photodynamic therapy. *Adv Drug Deliv Rev* **56**:17–30.
Desgrosellier JS and Cheresh DA (2010) Integrins in cancer: biological implications and therapeutic opportunities. *Nat Rev Cancer* **10**:9–22.
Deshpande PP, Biswas S, and Torchilin VP (2013) Current trends in the use of liposomes for tumor targeting. *Nanomedicine (Lond)* **8**:1509–1528.
Devine DV, Wong K, Serrano K, Chonn A, and Cullis PR (1994) Liposome-complement interactions in rat serum: implications for liposome survival studies. *Biochim Biophys Acta* **1191**:43–51.
Dhami S and Phillips D (1996) Comparison of the photophysics of an aggregating and non-aggregating aluminium phthalocyanine system incorporated into unilamellar vesicles. *J Photochem Photobiol Chem* **100**:77–84.
Diaz SL, Padler-Karavani V, Ghaderi D, Hurtado-Ziola N, Yu H, Chen X, Brinkman-Van der Linden EC, Varki A, and Varki NM (2009) Sensitive and specific detection of the non-human sialic Acid N-glycolylneuraminic acid in human tissues and biotherapeutic products. *PLoS One* **4**:e4241.
Dienst A, Grunow A, Unruh M, Rabausch B, Nör JE, Fries JW, and Gottstein C (2005) Specific occlusion of murine and human tumor vasculature by VCAM-1-targeted recombinant fusion proteins. *J Natl Cancer Inst* **97**:733–747.
Dijkstra J, van Galen WJ, Hulstaert CE, Kalicharan D, Roerdink FH, and Scherphof GL (1984) Interaction of liposomes with Kupffer cells in vitro. *Exp Cell Res* **150**: 161–176.
Dimmer KS, Friedrich B, Lang F, Deitmer JW, and Bröer S (2000) The low-affinity monocarboxylate transporter MCT4 is adapted to the export of lactate in highly glycolytic cells. *Biochem J* **350**:219–227.
DiResta GR, Lee J, Larson SM, and Arbit E (1993) Characterization of neuroblastoma xenograft in rat flank. I. Growth, interstitial fluid pressure, and interstitial fluid velocity distribution profiles. *Microvasc Res* **46**:158–177.
Doktorovová S, Araújo J, Garcia ML, Rakovský E, and Souto EB (2010) Formulating fluticasone propionate in novel PEG-containing nanostructured lipid carriers (PEG-NLC). *Colloids Surf B Biointerfaces* **75**:538–542.
Dos Santos N, Allen C, Doppen A-M, Anantha M, Cox KA, Gallagher RC, Karlsson G, Edwards K, Kenner G, and Samuels L, et al. (2007) Influence of poly(ethylene glycol) grafting density and polymer length on liposomes: relating plasma circulation lifetimes to protein binding. *Biochim Biophys Acta* **1768**:1367–1377.
Dragovich T, Mendelson D, Kurtin S, Richardson K, Von Hoff D, and Hoos A (2006) A Phase 2 trial of the liposomal DACH platinum L-NDDP in patients with therapy-refractory advanced colorectal cancer. *Cancer Chemother Pharmacol* **58**: 759–764.
Drummond DC, Noble CO, Guo Z, Hong K, Park JW, and Kirpotin DB (2006) Development of a highly active nanoliposomal irinotecan using a novel intraliposomal stabilization strategy. *Cancer Res* **66**:3271–3277.
Dubey PK, Mishra V, Jain S, Mahor S, and Vyas SP (2004) Liposomes modified with cyclic RGD peptide for tumor targeting. *J Drug Target* **12**:257–264.
du Bois A, Burges A, Meier W, Pfisterer J, Schmalfeldt B, Richter B, Jackisch C, Staehle A, Kimmig R, and Elser G; Arbeitsgemeinschaft Gynaekologische Onkologie Studiengruppe Ovarialkarzinom (2006) Pegylated liposomal doxorubicin and carboplatin in advanced gynecologic tumors: a prospective phase I/II study of the Arbeitsgemeinschaft Gynaekologische Onkologie Studiengruppe Ovarialkarzinom (AGO-OVAR). *Ann Oncol* **17**:93–96.
Duffaud F, Borner M, Chollet P, Vermorken JB, Bloch J, Degardin M, Rolland F, Dittrich C, Baron B, and Lacombe D, et al.; EORTC-New Drug Development Group/New Drug Development Program (2004) Phase II study of OSI-211 (liposomal lurtotecan) in patients with metastatic or loco-regional recurrent squamous cell carcinoma of the head and neck. An EORTC New Drug Development Group study. *Eur J Cancer* **40**:2748–2752.
Düzgünes N, Simões S, Slepushkin V, Pretzer E, Rossi JJ, De Clercq E, Antao VP, Collins ML, and de Lima MC (2001) Enhanced inhibition of HIV-1 replication in macrophages by antisense oligonucleotides, ribozymes and acyclic nucleoside

phosphonate analogs delivered in pH-sensitive liposomes. *Nucleosides Nucleotides Nucleic Acids* **20**:515–523.
Düzgüneş N, Straubinger RM, Baldwin PA, Friend DS, and Papahadjopoulos D (1985) Proton-induced fusion of oleic acid-phosphatidylethanolamine liposomes. *Biochemistry* **24**:3091–3098.
Düzgüneş N, Wilschut J, Fraley R, and Papahadjopoulos D (1981) Studies on the mechanism of membrane fusion. Role of head-group composition in calcium- and magnesium-induced fusion of mixed phospholipid vesicles. *Biochim Biophys Acta* **642**:182–195.
Dvorak HF, Nagy JA, Dvorak JT, and Dvorak AM (1988) Identification and characterization of the blood vessels of solid tumors that are leaky to circulating macromolecules. *Am J Pathol* **133**:95–109.
Easson EC and Pointon RCS (1985) *The radiotherapy of malignant disease*, 1st ed, Springer-Verlag London, London.
Edwards K, Johnsson M, Karlsson G, and Silvander M (1997) Effect of polyethyleneglycol-phospholipids on aggregate structure in preparations of small unilamellar liposomes. *Biophys J* **73**:258–266.
Eichhorn ME, Luedemann S, Strieth S, Papyan A, Ruhstorfer H, Haas H, Michaelis U, Sauer B, Teifel M, and Enders G, et al. (2007) Cationic lipid complexed camptothecin (EndoTAG-2) improves antitumoral efficacy by tumor vascular targeting. *Cancer Biol Ther* **6**:920–929.
Eliaz RE and Szoka FC Jr (2001) Liposome-encapsulated doxorubicin targeted to CD44: a strategy to kill CD44-overexpressing tumor cells. *Cancer Res* **61**: 2592–2601.
Ellens H, Bentz J, and Szoka FC (1985) $H^+$- and $Ca^{2+}$-induced fusion and destabilization of liposomes. *Biochemistry* **24**:3099–3106.
Ellens H, Bentz J, and Szoka FC (1986) Destabilization of phosphatidylethanolamine liposomes at the hexagonal phase transition temperature. *Biochemistry* **25**: 285–294.
Enoch HG and Strittmatter P (1979) Formation and properties of 1000-A-diameter, single-bilayer phospholipid vesicles. *Proc Natl Acad Sci USA* **76**:145–149.
Fang RH, Aryal S, Hu C-MJ, and Zhang L (2010) Quick synthesis of lipid-polymer hybrid nanoparticles with low polydispersity using a single-step sonication method. *Langmuir* **26**:16958–16962.
Fang RH, Chen KN, Aryal S, Hu C-MJ, Zhang K, and Zhang L (2012) Large-scale synthesis of lipid-polymer hybrid nanoparticles using a multi-inlet vortex reactor. *Langmuir* **28**:13824–13829.
Fasol U, Frost A, Büchert M, Arends J, Fiedler U, Scharr D, Scheuenpflug J, and Mross K (2012) Vascular and pharmacokinetic effects of EndoTAG-1 in patients with advanced cancer and liver metastasis. *Ann Oncol* **23**:1030–1036.
Fears CY, Gladson CL, and Woods A (2006) Syndecan-2 is expressed in the microvasculature of gliomas and regulates angiogenic processes in microvascular endothelial cells. *J Biol Chem* **281**:14533–14536.
Feldman EJ, Lancet JE, Kolitz JE, Ritchie EK, Roboz GJ, List AF, Allen SL, Asatiani E, Mayer LD, and Swenson C, et al. (2011) First-in-man study of CPX-351: a liposomal carrier containing cytarabine and daunorubicin in a fixed 5:1 molar ratio for the treatment of relapsed and refractory acute myeloid leukemia. *J Clin Oncol* **29**:979–985.
Felgner PL, Gadek TR, Holm M, Roman R, Chan HW, Wenz M, Northrop JP, Ringold GM, and Danielsen M (1987) Lipofection: a highly efficient, lipid-mediated DNA-transfection procedure. *Proc Natl Acad Sci USA* **84**:7413–7417.
Fenart L, Casanova A, Dehouck B, Duhem C, Slupek S, Cecchelli R, and Betbeder D (1999) Evaluation of effect of charge and lipid coating on ability of 60-nm nanoparticles to cross an in vitro model of the blood-brain barrier. *J Pharmacol Exp Ther* **291**:1017–1022.
Feron O (2009) Pyruvate into lactate and back: from the Warburg effect to symbiotic energy fuel exchange in cancer cells. *Radiother Oncol* **92**:329–333.
Ferrari M (2005) Cancer nanotechnology: Opportunities and challenges. *Nat Rev Cancer* **5**:161–171.
Ferrati S, Nicolov E, Bansal S, Hosali S, Landis M, and Grattoni A (2015) Docetaxel/2-Hydroxypropyl β -Cyclodextrin Inclusion Complex Increases Docetaxel Solubility and Release from a Nanochannel Drug Delivery System. *Curr Drug Targets* **16**: 1645–1649.
Filipović-Grcić J, Skalko-Basnet N, and Jalsenjak I (2001) Mucoadhesive chitosan-coated liposomes: characteristics and stability. *J Microencapsul* **18**:3–12.
Fischer V, Rodríguez-Gascón A, Heitz F, Tynes R, Hauck C, Cohen D, and Vickers AE (1998) The multidrug resistance modulator valspodar (PSC 833) is metabolized by human cytochrome P450 3A. Implications for drug-drug interactions and pharmacological activity of the main metabolite. *Drug Metab Dispos* **26**: 802–811.
Folkman J (1971) Transplacental carcinogenesis by stilbestrol. *N Engl J Med* **285**: 404–405.
Forrest ML, Won C-Y, Malick AW, and Kwon GS (2006) In vitro release of the mTOR inhibitor rapamycin from poly(ethylene glycol)-b-poly(ε-caprolactone) micelles. *J Control Release* **110**:370–377.
Forssen EA (1997) The design and development of DaunoXome® for solid tumor targeting in vivo. *Adv Drug Deliv Rev* **24**:133–150.
Forssen EA, Coulter DM, and Proffitt RT (1992) Selective in vivo localization of daunorubicin small unilamellar vesicles in solid tumors. *Cancer Res* **52**:3255–3261.
Forssen EA, Malé-Brune R, Adler-Moore JP, Lee MJ, Schmidt PG, Krasieva TB, Shimizu S, and Tromberg BJ (1996) Fluorescence imaging studies for the disposition of daunorubicin liposomes (DaunoXome) within tumor tissue. *Cancer Res* **56**: 2066–2075.
Forssen EA and Ross ME (1994) Daunoxome® treatment of solid tumors: preclinical and clinical investigations. *J Liposome Res* **4**:481–512.
Frenkel V (2008) Ultrasound mediated delivery of drugs and genes to solid tumors. *Adv Drug Deliv Rev* **60**:1193–1208.
Friend DS, Papahadjopoulos D, and Debs RJ (1996) Endocytosis and intracellular processing accompanying transfection mediated by cationic liposomes. *Biochim Biophys Acta* **1278**:41–50.
Funato K, Yoda R, and Kiwada H (1992) Contribution of complement system on destabilization of liposomes composed of hydrogenated egg phosphatidylcholine in rat fresh plasma. *Biochim Biophys Acta* **1103**:198–204.
Fundarò A, Cavalli R, Bargoni A, Vighetto D, Zara GP, and Gasco MR (2000) Non-stealth and stealth solid lipid nanoparticles (SLN) carrying doxorubicin: pharmacokinetics and tissue distribution after i.v. administration to rats. *Pharmacol Res* **42**:337–343.
Fuster MM and Esko JD (2005) The sweet and sour of cancer: glycans as novel therapeutic targets. *Nat Rev Cancer* **5**:526–542.
Gabizon A, Catane R, Uziely B, Kaufman B, Safra T, Cohen R, Martin F, Huang A, and Barenholz Y (1994) Prolonged circulation time and enhanced accumulation in malignant exudates of doxorubicin encapsulated in polyethylene-glycol coated liposomes. *Cancer Res* **54**:987–992.
Gabizon A, Chisin R, Amselem S, Druckmann S, Cohen R, Goren D, Fromer I, Peretz T, Sulkes A, and Barenholz Y (1991) Pharmacokinetic and imaging studies in patients receiving a formulation of liposome-associated adriamycin. *Br J Cancer* **64**:1125–1132.
Gabizon A, Horowitz AT, Goren D, Tzemach D, Shmeeda H, and Zalipsky S (2003a) In vivo fate of folate-targeted polyethylene-glycol liposomes in tumor-bearing mice. *Clin Cancer Res* **9**:6551–6559.
Gabizon A and Martin F (1997) Polyethylene glycol-coated (pegylated) liposomal doxorubicin. Rationale for use in solid tumours. *Drugs* **54** (Suppl 4):15–21.
Gabizon AA and Muggia FM (1998) Initial clinical evaluation of pegylated-liposomal doxorubicin in solid tumors, in *Long Circulating Liposomes: Old drugs, New Therapeutics* (Woodle MC and Storm G, eds, ed) pp 165–174, Springer, Berlin.
Gabizon A and Papahadjopoulos D (1988) Liposome formulations with prolonged circulation time in blood and enhanced uptake by tumors. *Proc Natl Acad Sci USA* **85**:6949–6953.
Gabizon A, Peretz T, Sulkes A, Amselem S, Ben-Yosef R, Ben-Baruch N, Catane R, Biran S, and Barenholz Y (1989) Systemic administration of doxorubicin-containing liposomes in cancer patients: a phase I study. *Eur J Cancer Clin Oncol* **25**:1795–1803.
Gabizon A, Shmeeda H, and Barenholz Y (2003b) Pharmacokinetics of pegylated liposomal Doxorubicin: review of animal and human studies. *Clin Pharmacokinet* **42**:419–436.
Gamucci T, Paridaens R, Heinrich B, Schellens JH, Pavlidis N, Verweij J, Sessa C, Kaye S, Roelvink M, and Wanders J, et al. (2000) Activity and toxicity of GI147211 in breast, colorectal and non-small-cell lung cancer patients: an EORTC-ECSG phase II clinical study. *Ann Oncol* **11**:793–797.
Ganta S, Devalapally H, Shahiwala A, and Amiji M (2008) A review of stimuli-responsive nanocarriers for drug and gene delivery. *J Control Release* **126**: 187–204.
Gao Z, Lukyanov AN, Chakilam AR, and Torchilin VP (2003) PEG-PE/phosphatidylcholine mixed immunomicelles specifically deliver encapsulated taxol to tumor cells of different origin and promote their efficient killing. *J Drug Target* **11**:87–92.
Gao Z, Lukyanov AN, Singhal A, and Torchilin VP (2002) Diacyllipid-polymer micelles as nanocarriers for poorly soluble anticancer drugs. *Nano Lett* **2**:979–982.
Garbuzenko O, Barenholz Y, and Priev A (2005) Effect of grafted PEG on liposome size and on compressibility and packing of lipid bilayer. *Chem Phys Lipids* **135**: 117–129.
Garcia AM, Alarcon E, Muñoz M, Scaiano JC, Edwards AM, and Lissi E (2011) Photophysical behaviour and photodynamic activity of zinc phthalocyanines associated to liposomes. *Photochem Photobiol Sci* **10**:507–514.
Garg A, Tisdale AW, Haidari E, and Kokkoli E (2009) Targeting colon cancer cells using PEGylated liposomes modified with a fibronectin-mimetic peptide. *Int J Pharm* **366**:201–210.
Gasco M (1997) Solid lipid nanospheres from warm micro-emulsions. *Pharm Techn Eur* **9**:52–58.
Gasco MR (1993), inventors, Gasco MR, assignee. Method for producing solid lipid microspheres having a narrow size distribution. U.S. Patent US5250236. 1991 Aug 2.
Gaspani S and Milani B (2013) Access to liposomal generic formulations: beyond AmBisome and Doxil/Caelyx. *GaBi J* **2**:60–62.
Gbadamosi JK, Hunter AC, and Moghimi SM (2002) PEGylation of microspheres generates a heterogeneous population of particles with differential surface characteristics and biological performance. *FEBS Lett* **532**:338–344.
Gelmon KA, Tolcher A, Diab AR, Bally MB, Embree L, Hudon N, Dedhar C, Ayers D, Eisen A, and Melosky B, et al. (1999) Phase I study of liposomal vincristine. *J Clin Oncol* **17**:697–705.
Geng Y, Dalhaimer P, Cai S, Tsai R, Tewari M, Minko T, and Discher DE (2007) Shape effects of filaments versus spherical particles in flow and drug delivery. *Nat Nanotechnol* **2**:249–255.
Genís L, Gálvez BG, Gonzalo P, and Arroyo AG (2006) MT1-MMP: universal or particular player in angiogenesis? *Cancer Metastasis Rev* **25**:77–86.
Gerritsen WJ, Verkley AJ, Zwaal RF, and Van Deenen LL (1978) Freeze-fracture appearance and disposition of band 3 protein from the human erythrocyte membrane in lipid vesicles. *Eur J Biochem* **85**:255–261.
Gewirtz DA (1999) A critical evaluation of the mechanisms of action proposed for the antitumor effects of the anthracycline antibiotics adriamycin and daunorubicin. *Biochem Pharmacol* **57**:727–741.
Ghanbarzadeh S, Arami S, Pourmoazzen Z, and Khorrami A (2014) Improvement of the antiproliferative effect of rapamycin on tumor cell lines by poly (monomethylitaconate)-based pH-sensitive, plasma stable liposomes. *Colloids Surf B Biointerfaces* **115**:323–330.
Ghinea N and Simionescu N (1985) Anionized and cationized hemeundecapeptides as probes for cell surface charge and permeability studies: differentiated labeling of endothelial plasmalemmal vesicles. *J Cell Biol* **100**:606–612.
Gill PS, Espina BM, Muggia F, Cabriales S, Tulpule A, Esplin JA, Liebman HA, Forssen E, Ross ME, and Levine AM (1995) Phase I/II clinical and pharmacokinetic evaluation of liposomal daunorubicin. *J Clin Oncol* **13**:996–1003.

Gill PS, Wernz J, Scadden DT, Cohen P, Mukwaya GM, von Roenn JH, Jacobs M, Kempin S, Silverberg I, and Gonzales G, et al. (1996) Randomized phase III trial of liposomal daunorubicin versus doxorubicin, bleomycin, and vincristine in AIDS-related Kaposi's sarcoma. *J Clin Oncol* **14**:2353–2364.

Glantz MJ, Jaeckle KA, Chamberlain MC, Phuphanich S, Recht L, Swinnen LJ, Maria B, LaFollette S, Schumann GB, and Cole BF, et al. (1999a) A randomized controlled trial comparing intrathecal sustained-release cytarabine (DepoCyt) to intrathecal methotrexate in patients with neoplastic meningitis from solid tumors. *Clin Cancer Res* **5**:3394–3402.

Glantz MJ, LaFollette S, Jaeckle KA, Shapiro W, Swinnen L, Rozental JR, Phuphanich S, Rogers LR, Gutheil JC, and Batchelor T, et al. (1999b) Randomized trial of a slow-release versus a standard formulation of cytarabine for the intrathecal treatment of lymphomatous meningitis. *J Clin Oncol* **17**:3110–3116.

Goldstein JL, Brown MS, Anderson RG, Russell DW, and Schneider WJ (1985) Receptor-mediated endocytosis: concepts emerging from the LDL receptor system. *Annu Rev Cell Biol* **1**:1–39.

Gomme PT, McCann KB, and Bertolini J (2005) Transferrin: structure, function and potential therapeutic actions. *Drug Discov Today* **10**:267–273.

Goormaghtigh E, Chatelain P, Caspers J, and Ruysschaert JM (1980) Evidence of a specific complex between adriamycin and negatively-charged phospholipids. *Biochim Biophys Acta* **597**:1–14.

Gordon AN, Fleagle JT, Guthrie D, Parkin DE, Gore ME, and Lacave AJ (2001) Recurrent epithelial ovarian carcinoma: a randomized phase III study of pegylated liposomal doxorubicin versus topotecan. *J Clin Oncol* **19**:3312–3322.

Gordon KB, Tajuddin A, Guitart J, Kuzel TM, Eramo LR, and VonRoenn J (1995) Hand-foot syndrome associated with liposome-encapsulated doxorubicin therapy. *Cancer* **75**:2169–2173.

Gordon AN, Tonda M, Sun S, and Rackoff W; Doxil Study 30-49 Investigators (2004) Long-term survival advantage for women treated with pegylated liposomal doxorubicin compared with topotecan in a phase 3 randomized study of recurrent and refractory epithelial ovarian cancer. *Gynecol Oncol* **95**:1–8.

Goren D, Horowitz AT, Tzemach D, Tarshish M, Zalipsky S, and Gabizon A (2000) Nuclear delivery of doxorubicin via folate-targeted liposomes with bypass of multidrug-resistance efflux pump. *Clin Cancer Res* **6**:1949–1957.

Gosk S, Moos T, Gottstein C, and Bendas G (2008) VCAM-1 directed immunoliposomes selectively target tumor vasculature in vivo. *Biochim Biophys Acta* **1778**:854–863.

Graham FL and Whitmore GF (1970) The effect of-beta-D-arabinofuranosylcytosine on growth, viability, and DNA synthesis of mouse L-cells. *Cancer Res* **30**: 2627–2635.

Gratton SE, Ropp PA, Pohlhaus PD, Luft JC, Madden VJ, Napier ME, and DeSimone JM (2008) The effect of particle design on cellular internalization pathways. *Proc Natl Acad Sci USA* **105**:11613–11618.

Gregoriadis G (1976a) The carrier potential of liposomes in biology and medicine (first of two parts). *N Engl J Med* **295**:704–710.

Gregoriadis G (1976b) The carrier potential of liposomes in biology and medicine (second of two parts). *N Engl J Med* **295**:765–770.

Gregoriadis G (1988) *Liposomes as drug carriers: Recent trends and progress*, 1st ed, John Wiley & Sons, Chichester, UK.

Gregoriadis G (1995) Engineering liposomes for drug delivery: progress and problems. *Trends Biotechnol* **13**:527–537.

Grüll H and Langereis S (2012) Hyperthermia-triggered drug delivery from temperature-sensitive liposomes using MRI-guided high intensity focused ultrasound. *J Control Release* **161**:317–327.

Gruner SM, Lenk RP, Janoff AS, and Ostro MJ (1985) Novel multilayered lipid vesicles: comparison of physical characteristics of multilamellar liposomes and stable plurilamellar vesicles. *Biochemistry* **24**:2833–2842.

Gubernator J (2011) Active methods of drug loading into liposomes: recent strategies for stable drug entrapment and increased in vivo activity. *Expert Opin Drug Deliv* **8**:565–580.

Guo LS, Hamilton RL, Goerke J, Weinstein JN, and Havel RJ (1980) Interaction of unilamellar liposomes with serum lipoproteins and apolipoproteins. *J Lipid Res* **21**:993–1003.

Guo J, Ping Q, Jiang G, Huang L, and Tong Y (2003) Chitosan-coated liposomes: characterization and interaction with leuprolide. *Int J Pharm* **260**:167–173.

Hadinoto K, Sundaresan A, and Cheow WS (2013) Lipid-polymer hybrid nanoparticles as a new generation therapeutic delivery platform: a review. *Eur J Pharm Biopharm* **85** (3 Pt A):427–443.

Hagemeister F, Rodriguez MA, Deitcher SR, Younes A, Fayad L, Goy A, Dang NH, Forman A, McLaughlin P, and Medeiros LJ, et al. (2013) Long term results of a phase 2 study of vincristine sulfate liposome injection (Marqibo(®) ) substituted for non-liposomal vincristine in cyclophosphamide, doxorubicin, vincristine, prednisone with or without rituximab for patients with untreated aggressive non-Hodgkin lymphomas. *Br J Haematol* **162**:631–638.

Haim N, Epelbaum R, Ben-Shahar M, Yarnitsky D, Simri W, and Robinson E (1994) Full dose vincristine (without 2-mg dose limit) in the treatment of lymphomas. *Cancer* **73**:2515–2519.

Hamaguchi T, Matsumura Y, Nakanishi Y, Muro K, Yamada Y, Shimada Y, Shirao K, Niki H, Hosokawa S, and Tagawa T, et al. (2004) Antitumor effect of MCC-465, pegylated liposomal doxorubicin tagged with newly developed monoclonal antibody GAH, in colorectal cancer xenografts. *Cancer Sci* **95**:608–613.

Hamilton RL Jr, Goerke J, Guo LS, Williams MC, and Havel RJ (1980) Unilamellar liposomes made with the French pressure cell: a simple preparative and semi-quantitative technique. *J Lipid Res* **21**:981–992.

Han HD, Shin BC, and Choi HS (2006) Doxorubicin-encapsulated thermosensitive liposomes modified with poly(N-isopropylacrylamide-co-acrylamide): drug release behavior and stability in the presence of serum. *Eur J Pharm Biopharm* **62**: 110–116.

Haran G, Cohen R, Bar LK, and Barenholz Y (1993) Transmembrane ammonium sulfate gradients in liposomes produce efficient and stable entrapment of amphipathic weak bases. *Biochim Biophys Acta* **1151**:201–215.

Harding CV, Collins DS, Slot JW, Geuze HJ, and Unanue ER (1991) Liposome-encapsulated antigens are processed in lysosomes, recycled, and presented to T cells. *Cell* **64**:393–401.

Harivardhan Reddy L, Sharma RK, Chuttani K, Mishra AK, and Murthy RS (2005) Influence of administration route on tumor uptake and biodistribution of etoposide loaded solid lipid nanoparticles in Dalton's lymphoma tumor bearing mice. *J Control Release* **105**:185–198.

Harris L, Batist G, Belt R, Rovira D, Navari R, Azarnia N, Welles L, and Winer E; TLC D-99 Study Group (2002) Liposome-encapsulated doxorubicin compared with conventional doxorubicin in a randomized multicenter trial as first-line therapy of metastatic breast carcinoma. *Cancer* **94**:25–36.

Hasan W, Chu K, Gullapalli A, Dunn SS, Enlow EM, Luft JC, Tian S, Napier ME, Pohlhaus PD, and Rolland JP, et al. (2012) Delivery of multiple siRNAs using lipid-coated PLGA nanoparticles for treatment of prostate cancer. *Nano Lett* **12**: 287–292.

Hashizume H, Baluk P, Morikawa S, McLean JW, Thurston G, Roberge S, Jain RK, and McDonald DM (2000) Openings between defective endothelial cells explain tumor vessel leakiness. *Am J Pathol* **156**:1363–1380.

Hatakeyama H, Akita H, Ishida E, Hashimoto K, Kobayashi H, Aoki T, Yasuda J, Obata K, Kikuchi H, and Ishida T, et al. (2007) Tumor targeting of doxorubicin by anti-MT1-MMP antibody-modified PEG liposomes. *Int J Pharm* **342**:194–200.

Hauck ML, LaRue SM, Petros WP, Poulson JM, Yu D, Spasojevic I, Pruitt AF, Klein A, Case B, and Thrall DE, et al. (2006) Phase I trial of doxorubicin-containing low temperature sensitive liposomes in spontaneous canine tumors. *Clin Cancer Res* **12**:4004–4010.

Hauser H (1982) Methods of preparation of lipid vesicles: assessment of their suitability for drug encapsulation. *Trends Pharmacol Sci* **3**:274–277.

He C, Hu Y, Yin L, Tang C, and Yin C (2010) Effects of particle size and surface charge on cellular uptake and biodistribution of polymeric nanoparticles. *Biomaterials* **31**:3657–3666.

He X, Li L, Su H, Zhou D, Song H, Wang L, and Jiang X (2015) Poly(ethylene glycol)-block-poly(ε-caprolactone)-and phospholipid-based stealth nanoparticles with enhanced therapeutic efficacy on murine breast cancer by improved intracellular drug delivery. *Int J Nanomedicine* **10**:1791–1804.

Heath TD (1988) Liposome dependent drugs, in *Liposomes As Drug Carriers: Recent Trends and Progress* (Gregoriadis G ed) Wiley, New York.

Heldin C-H, Rubin K, Pietras K, and Ostman A (2004) High interstitial fluid pressure - an obstacle in cancer therapy. *Nat Rev Cancer* **4**:806–813.

Hirschfeld S, Ho PT, Smith M, and Pazdur R (2003) Regulatory approvals of pediatric oncology drugs: previous experience and new initiatives. *J Clin Oncol* **21**: 1066–1073.

Hittelet A, Legendre H, Nagy N, Bronckart Y, Pector JC, Salmon I, Yeaton P, Gabius HJ, Kiss R, and Camby I (2003) Upregulation of galectins-1 and -3 in human colon cancer and their role in regulating cell migration. *Int J Cancer* **103**:370–379.

Hitzman CJ, Elmquist WF, Wattenberg LW, and Wiedmann TS (2006) Development of a respirable, sustained release microcarrier for 5-fluorouracil I: In vitro assessment of liposomes, microspheres, and lipid coated nanoparticles. *J Pharm Sci* **95**:1114–1126.

Hoarau D, Delmas P, David S, Roux E, and Leroux JC (2004) Novel long-circulating lipid nanocapsules. *Pharm Res* **21**:1783–1789.

Hobbs SK, Monsky WL, Yuan F, Roberts WG, Griffith L, Torchilin VP, and Jain RK (1998) Regulation of transport pathways in tumor vessels: role of tumor type and microenvironment. *Proc Natl Acad Sci USA* **95**:4607–4612.

Hood JD, Bednarski M, Frausto R, Guccione S, Reisfeld RA, Xiang R, and Cheresh DA (2002) Tumor regression by targeted gene delivery to the neovasculature. *Science* **296**:2404–2407.

Hopkins CR and Trowbridge IS (1983) Internalization and processing of transferrin and the transferrin receptor in human carcinoma A431 cells. *J Cell Biol* **97**: 508–521.

Hortobágyi GN (1997) Anthracyclines in the treatment of cancer. An overview. *Drugs* **54** (Suppl 4):1–7.

Hu C-MJ, Kaushal S, Tran Cao HS, Aryal S, Sartor M, Esener S, Bouvet M, and Zhang L (2010) Half-antibody functionalized lipid-polymer hybrid nanoparticles for targeted drug delivery to carcinoembryonic antigen presenting pancreatic cancer cells. *Mol Pharm* **7**:914–920.

Huang C (1969) Studies on phosphatidylcholine vesicles. Formation and physical characteristics. *Biochemistry* **8**:344–352.

Huang Z-R, Hua SC, Yang YL, and Fang JY (2008) Development and evaluation of lipid nanoparticles for camptothecin delivery: a comparison of solid lipid nanoparticles, nanostructured lipid carriers, and lipid emulsion. *Acta Pharmacol Sin* **29**:1094–1102.

Huang SK, Lee KD, Hong K, Friend DS, and Papahadjopoulos D (1992) Microscopic localization of sterically stabilized liposomes in colon carcinoma-bearing mice. *Cancer Res* **52**:5135–5143.

Huang SK, Martin FJ, Jay G, Vogel J, Papahadjopoulos D, and Friend DS (1993) Extravasation and transcytosis of liposomes in Kaposi's sarcoma-like dermal lesions of transgenic mice bearing the HIV tat gene. *Am J Pathol* **143**: 10–14.

Huber PE, Jenne JW, Rastert R, Simiantonakis I, Sinn H-P, Strittmatter H-J, von Fournier D, Wannenmacher MF, and Debus J (2001) A new noninvasive approach in breast cancer therapy using magnetic resonance imaging-guided focused ultrasound surgery. *Cancer Res* **61**:8441–8447.

Hunter RJ (1981) *Zeta Potential in Colloid Science: Principles and Applications*, 1st ed, Academic Press Limited, London.

Hwang KJ (1987) Liposome pharmacokinetics, in *Liposomes: From biophysics to therapeutics* (Ostro M ed) pp 247–262, Marcel Dekker, New York.

Hwang KJ, Luk K-FS, and Beaumier PL (1982) Volume of distribution and transcapillary passage of small unilamellar vesicles. *Life Sci* **31**:949–955.

Hwang KJ and Mauk MR (1977) Fate of lipid vesicles in vivo: a gamma-ray perturbed angular correlation study. *Proc Natl Acad Sci USA* **74**:4991–4995.

Ichikawa K, Takeuchi Y, Yonezawa S, Hikita T, Kurohane K, Namba Y, and Oku N (2004) Antiangiogenic photodynamic therapy (PDT) using Visudyne causes effective suppression of tumor growth. *Cancer Lett* **205**:39–48.
Igarashi A, Konno H, Tanaka T, Nakamura S, Sadzuka Y, Hirano T, and Fujise Y (2003) Liposomal photofrin enhances therapeutic efficacy of photodynamic therapy against the human gastric cancer. *Toxicol Lett* **145**:133–141.
Iinuma H, Maruyama K, Okinaga K, Sasaki K, Sekine T, Ishida O, Ogiwara N, Johkura K, and Yonemura Y (2002) Intracellular targeting therapy of cisplatin-encapsulated transferrin-polyethylene glycol liposome on peritoneal dissemination of gastric cancer. *Int J Cancer* **99**:130–137.
Immordino ML, Brusa P, Arpicco S, Stella B, Dosio F, and Cattel L (2003) Preparation, characterization, cytotoxicity and pharmacokinetics of liposomes containing docetaxel. *J Control Release* **91**:417–429.
Iqbal MA, Md S, Sahni JK, Baboota S, Dang S, and Ali J (2012) Nanostructured lipid carriers system: recent advances in drug delivery. *J Drug Target* **20**:813–830.
Ishida O, Maruyama K, Tanahashi H, Iwatsuru M, Sasaki K, Eriguchi M, and Yanagie H (2001a) Liposomes bearing polyethyleneglycol-coupled transferrin with intracellular targeting property to the solid tumors in vivo. *Pharm Res* **18**: 1042–1048.
Ishida T, Atobe K, Wang X, and Kiwada H (2006) Accelerated blood clearance of PEGylated liposomes upon repeated injections: effect of doxorubicin-encapsulation and high-dose first injection. *J Control Release* **115**:251–258.
Ishida T, Harada M, Wang XY, Ichihara M, Irimura K, and Kiwada H (2005) Accelerated blood clearance of PEGylated liposomes following preceding liposome injection: effects of lipid dose and PEG surface-density and chain length of the first-dose liposomes. *J Control Release* **105**:305–317.
Ishida T, Harashima H, and Kiwada H (2002) Liposome clearance. *Biosci Rep* **22**: 197–224.
Ishida T, Kashima S, and Kiwada H (2008) The contribution of phagocytic activity of liver macrophages to the accelerated blood clearance (ABC) phenomenon of PEGylated liposomes in rats. *J Control Release* **126**:162–165.
Ishida T, Kirchmeier MJ, Moase EH, Zalipsky S, and Allen TM (2001b) Targeted delivery and triggered release of liposomal doxorubicin enhances cytotoxicity against human B lymphoma cells. *Biochim Biophys Acta* **1515**:144–158.
Ishida T and Kiwada H (2008) Accelerated blood clearance (ABC) phenomenon upon repeated injection of PEGylated liposomes. *Int J Pharm* **354**:56–62.
Itano N and Kimata K (2008) Altered hyaluronan biosynthesis in cancer progression. *Semin Cancer Biol* **18**:268–274.
Iwasaki H, Liu YP, Nojyo Y, Ueda T, and Nakamura T (1995) Quantitative description of morphologic changes effected by antileukemic agents in L1210 leukemia cells. *Anticancer Res* **15**:133–139.
Jaeckle KA, Batchelor T, O'Day SJ, Phuphanich S, New P, Lesser G, Cohn A, Gilbert M, Aiken R, and Heros D, et al. (2002) An open label trial of sustained-release cytarabine (DepoCyt) for the intrathecal treatment of solid tumor neoplastic meningitis. *J Neurooncol* **57**:231–239.
Jaeckle KA, Phuphanich S, Bent MJ, Aiken R, Batchelor T, Campbell T, Fulton D, Gilbert M, Heros D, and Rogers L, et al. (2001) Intrathecal treatment of neoplastic meningitis due to breast cancer with a slow-release formulation of cytarabine. *Br J Cancer* **84**:157–163.
Jaffrézou J-P, Levade T, Bettaïeb A, Andrieu N, Bezombes C, Maestre N, Vermeersch S, Rousse A, and Laurent G (1996) Daunorubicin-induced apoptosis: triggering of ceramide generation through sphingomyelin hydrolysis. *EMBO J* **15**:2417–2424.
Jain RK (1987) Transport of molecules in the tumor interstitium: a review. *Cancer Res* **47**:3039–3051.
Jain RK and Gerlowski LE (1986) Extravascular transport in normal and tumor tissues. *Crit Rev Oncol Hematol* **5**:115–170.
Jain RK, Tong RT, and Munn LL (2007) Effect of vascular normalization by anti-angiogenic therapy on interstitial hypertension, peritumor edema, and lymphatic metastasis: insights from a mathematical model. *Cancer Res* **67**:2729–2735.
Jansons VK, Weis P, Chen T, and Redwood WR (1978) In vitro interaction of L1210 cells with phospholipid vesicles. *Cancer Res* **38**:530–535.
Javadi M, Pitt WG, Belnap DM, Tsosie NH, and Hartley JM (2012) Encapsulating nanoemulsions inside eLiposomes for ultrasonic drug delivery. *Langmuir* **28**: 14720–14729.
Javadi M, Pitt WG, Tracy CM, Barrow JR, Willardson BM, Hartley JM, and Tsosie NH (2013) Ultrasonic gene and drug delivery using eLiposomes. *J Control Release* **167**:92–100.
Jeon S, Lee J, Andrade J, and De Gennes P (1991) Protein-surface interactions in the presence of polyethylene oxide: I. Simplified theory. *J Colloid Interface Sci* **142**: 149–158.
Jeong S-Y, Yi SL, Lim S-K, Park S-J, Jung J, Woo HN, Song SY, Kim J-S, Lee JS, and Lee JS, et al. (2009) Enhancement of radiotherapeutic effectiveness by temperature-sensitive liposomal 1-methylxanthine. *Int J Pharm* **372**:132–139.
Jian B, de la Llera-Moya M, Royer L, Rothblat G, Francone O, and Swaney JB (1997) Modification of the cholesterol efflux properties of human serum by enrichment with phospholipid. *J Lipid Res* **38**:734–744.
Johnston MJ, Semple SC, Klimuk SK, Edwards K, Eisenhardt ML, Leng EC, Karlsson G, Yanko D, and Cullis PR (2006) Therapeutically optimized rates of drug release can be achieved by varying the drug-to-lipid ratio in liposomal vincristine formulations. *Biochim Biophys Acta* **1758**:55–64.
Johnstone SA, Masin D, Mayer L, and Bally MB (2001) Surface-associated serum proteins inhibit the uptake of phosphatidylserine and poly(ethylene glycol) liposomes by mouse macrophages. *Biochim Biophys Acta* **1513**:25–37.
Jones M and Leroux J (1999) Polymeric micelles - a new generation of colloidal drug carriers. *Eur J Pharm Biopharm* **48**:101–111.
Jores K, Haberland A, Wartewig S, Mäder K, and Mehnert W (2005) Solid lipid nanoparticles (SLN) and oil-loaded SLN studied by spectrofluorometry and Raman spectroscopy. *Pharm Res* **22**:1887–1897.
Jores K, Mehnert W, Drechsler M, Bunjes H, Johann C, and Mäder K (2004) Investigations on the structure of solid lipid nanoparticles (SLN) and oil-loaded solid lipid nanoparticles by photon correlation spectroscopy, field-flow fractionation and transmission electron microscopy. *J Control Release* **95**:217–227.
Jori G (1990) Factors controlling the selectivity and efficiency of tumour damage in photodynamic therapy. *Lasers Med Sci* **5**:115–120.
Judge A, McClintock K, Phelps JR, and Maclachlan I (2006) Hypersensitivity and loss of disease site targeting caused by antibody responses to PEGylated liposomes. *Mol Ther* **13**:328–337.
Juliano RL and Stamp D (1975) The effect of particle size and charge on the clearance rates of liposomes and liposome encapsulated drugs. *Biochem Biophys Res Commun* **63**:651–658.
Jung SH, Jung SH, Seong H, Cho SH, Jeong K-S, and Shin BC (2009) Polyethylene glycol-complexed cationic liposome for enhanced cellular uptake and anticancer activity. *Int J Pharm* **382**:254–261.
Kagawa Y and Racker E (1971) Partial resolution of the enzymes catalyzing oxidative phosphorylation XXV. Reconstitution of vesicles catalyzing 32Pi-adenosine triphosphate exchange. *J Biol Chem* **246**:5477–5487.
Kale AA and Torchilin VP (2007) "Smart" drug carriers: PEGylated TATp-modified pH-sensitive liposomes. *J Liposome Res* **17**:197–203.
Kalender Y, Yel M, and Kalender S (2005) Doxorubicin hepatotoxicity and hepatic free radical metabolism in rats. The effects of vitamin E and catechin. *Toxicology* **209**:39–45.
Kalinowski DS and Richardson DR (2005) The evolution of iron chelators for the treatment of iron overload disease and cancer. *Pharmacol Rev* **57**:547–583.
Kamen BA and Capdevila A (1986) Receptor-mediated folate accumulation is regulated by the cellular folate content. *Proc Natl Acad Sci USA* **83**:5983–5987.
Kamen BA and Smith AK (2004) A review of folate receptor alpha cycling and 5-methyltetrahydrofolate accumulation with an emphasis on cell models in vitro. *Adv Drug Deliv Rev* **56**:1085–1097.
Kandel PK, Fernando LP, Ackroyd PC, and Christensen KA (2011) Incorporating functionalized polyethylene glycol lipids into reprecipitated conjugated polymer nanoparticles for bioconjugation and targeted labeling of cells. *Nanoscale* **3**: 1037–1045.
Kang H, O'Donoghue MB, Liu H, and Tan W (2010) A liposome-based nanostructure for aptamer directed delivery. *Chem Commun (Camb)* **46**:249–251.
Kang MH, Wang J, Makena MR, Lee JS, Paz N, Hall CP, Song MM, Calderon RI, Cruz RE, and Hindle A, et al. (2015) Activity of MM-398, nanoliposomal irinotecan (nal-IRI), in Ewing's family tumor xenografts is associated with high exposure of tumor to drug and high SLFN11 expression. *Clin Cancer Res* **21**:1139–1150.
Kanter PM, Bullard GA, Ginsberg RA, Pilkiewicz FG, Mayer LD, Cullis PR, and Pavelic ZP (1993) Comparison of the cardiotoxic effects of liposomal doxorubicin (TLC D-99) versus free doxorubicin in beagle dogs. *In Vivo* **7**:17–26.
Kanter PM, Klaich GM, Bullard GA, King JM, Bally MB, and Mayer LD (1994) Liposome encapsulated vincristine: preclinical toxicologic and pharmacologic comparison with free vincristine and empty liposomes in mice, rats and dogs. *Anticancer Drugs* **5**:579–590.
Kaplan JG, DeSouza TG, Farkash A, Shafran B, Pack D, Rehman F, Fuks J, and Portenoy R (1990) Leptomeningeal metastases: comparison of clinical features and laboratory data of solid tumors, lymphomas and leukemias. *J Neurooncol* **9**:225–229.
Karanth H and Murthy RS (2007) pH-sensitive liposomes–principle and application in cancer therapy. *J Pharm Pharmacol* **59**:469–483.
Karukstis KK, Thompson EH, Whiles JA, and Rosenfeld RJ (1998) Deciphering the fluorescence signature of daunomycin and doxorubicin. *Biophys Chem* **73**:249–263.
Kashchiev D and Exerowa D (1983) Bilayer lipid membrane permeation and rupture due to hole formation. *Biochim Biophys Acta* **732**:133–145.
Kayser K, Hauck E, André S, Bovin NV, Kaltner H, Banach L, Lancaster E, and Gabius H-J (2001) Expression of endogenous lectins (galectins, receptors for ABH-epitopes) and the MIB-1 antigen in esophageal carcinomas and their syntactic structure analysis in relation to post-surgical tumor stage and lymph node involvement. *Anticancer Res* **21** (2B):1439–1444.
Kayser K, Zink S, André S, Schüring M-P, Hecker E, Klar E, Bovin NV, Kaltner H, and Gabius H-J (2002) Primary colorectal carcinomas and their intrapulmonary metastases: clinical, glyco-, immuno- and lectin histochemical, nuclear and syntactic structure analysis with emphasis on correlation with period of occurrence of metastases and survival. *APMIS* **110**:435–446.
Keizer HG, Pinedo HM, Schuurhuis GJ, and Joenje H (1990) Doxorubicin (adriamycin): a critical review of free radical-dependent mechanisms of cytotoxicity. *Pharmacol Ther* **47**:219–231.
Kelland L (2007) Broadening the clinical use of platinum drug-based chemotherapy with new analogues. Satraplatin and picoplatin. *Expert Opin Investig Drugs* **16**: 1009–1021.
Kenworthy AK, Hristova K, Needham D, and McIntosh TJ (1995a) Range and magnitude of the steric pressure between bilayers containing phospholipids with covalently attached poly(ethylene glycol). *Biophys J* **68**:1921–1936.
Kenworthy AK, Simon SA, and McIntosh TJ (1995b) Structure and phase behavior of lipid suspensions containing phospholipids with covalently attached poly(ethylene glycol). *Biophys J* **68**:1903–1920.
Kim S, Chatelut E, Kim JC, Howell SB, Cates C, Kormanik PA, and Chamberlain MC (1993a) Extended CSF cytarabine exposure following intrathecal administration of DTC 101. *J Clin Oncol* **11**:2186–2193.
Kim S and Howell SB (1987a) Multivesicular liposomes containing cytarabine entrapped in the presence of hydrochloric acid for intracavitary chemotherapy. *Cancer Treat Rep* **71**:705–711.
Kim S and Howell SB (1987b) Multivesicular liposomes containing cytarabine for slow-release Sc administration. *Cancer Treat Rep* **71**:447–450.
Kim S, Khatibi S, Howell SB, McCully C, Balis FM, and Poplack DG (1993b) Prolongation of drug exposure in cerebrospinal fluid by encapsulation into DepoFoam. *Cancer Res* **53**:1596–1598.
Kim S, Kim DJ, Geyer MA, and Howell SB (1987a) Multivesicular liposomes containing 1-beta-D-arabinofuranosylcytosine for slow-release intrathecal therapy. *Cancer Res* **47**:3935–3937.

Kim S, Kim DJ, and Howell SB (1987b) Modulation of the peritoneal clearance of liposomal cytosine arabinoside by blank liposomes. *Cancer Chemother Pharmacol* **19**:307–310.

Kim Y, Lee Chung B, Ma M, Mulder WJ, Fayad ZA, Farokhzad OC, and Langer R (2012) Mass production and size control of lipid-polymer hybrid nanoparticles through controlled microvortices. *Nano Lett* **12**:3587–3591.

Kim SS, Rait A, Kim E, Pirollo KF, and Chang EH (2015) A tumor-targeting p53 nanodelivery system limits chemoresistance to temozolomide prolonging survival in a mouse model of glioblastoma multiforme. *Nanomedicine (Lond)* **11**:301–311.

Kirby C and Gregoriadis G (1980) The effect of the cholesterol content of small unilamellar liposomes on the fate of their lipid components in vitro. *Life Sci* **27**: 2223–2230.

Kirby CJ and Gregoriadis G (1984) A simple procedure for preparing liposomes capable of high encapsulation efficiency under mild conditions, in *Liposome technology* (Gregoriadis G ed) pp 19–27, CRC Press, Boca Raton.

Kirpotin DB, Drummond DC, Shao Y, Shalaby MR, Hong K, Nielsen UB, Marks JD, Benz CC, and Park JW (2006) Antibody targeting of long-circulating lipidic nanoparticles does not increase tumor localization but does increase internalization in animal models. *Cancer Res* **66**:6732–6740.

Kirpotin D, Hong K, Mullah N, Papahadjopoulos D, and Zalipsky S (1996) Liposomes with detachable polymer coating: destabilization and fusion of dioleoylphosphatidylethanolamine vesicles triggered by cleavage of surface-grafted poly(ethylene glycol). *FEBS Lett* **388**:115–118.

Kiziltepe T, Ashley JD, Stefanick JF, Qi YM, Alves NJ, Handlogten MW, Suckow MA, Navari RM, and Bilgicer B (2012) Rationally engineered nanoparticles target multiple myeloma cells, overcome cell-adhesion-mediated drug resistance, and show enhanced efficacy in vivo. *Blood Cancer J* **2**:e64.

Klausner RD, Kleinfeld AM, Hoover RL, and Karnovsky MJ (1980) Lipid domains in membranes. Evidence derived from structural perturbations induced by free fatty acids and lifetime heterogeneity analysis. *J Biol Chem* **255**:1286–1295.

Klibanov AL, Maruyama K, Beckerleg AM, Torchilin VP, and Huang L (1991) Activity of amphipathic poly(ethylene glycol) 5000 to prolong the circulation time of liposomes depends on the liposome size and is unfavorable for immunoliposome binding to target. *Biochim Biophys Acta* **1062**:142–148.

Kobayashi T, Ishida T, Okada Y, Ise S, Harashima H, and Kiwada H (2007) Effect of transferrin receptor-targeted liposomal doxorubicin in P-glycoprotein-mediated drug resistant tumor cells. *Int J Pharm* **329**:94–102.

Kommareddy S and Amiji M (2005) Preparation and evaluation of thiol-modified gelatin nanoparticles for intracellular DNA delivery in response to glutathione. *Bioconjug Chem* **16**:1423–1432.

Kong G, Braun RD, and Dewhirst MW (2000) Hyperthermia enables tumor-specific nanoparticle delivery: effect of particle size. *Cancer Res* **60**:4440–4445.

Kong G, Braun RD, and Dewhirst MW (2001) Characterization of the effect of hyperthermia on nanoparticle extravasation from tumor vasculature. *Cancer Res* **61**: 3027–3032.

Kong G and Dewhirst MW (1999) Hyperthermia and liposomes. *Int J Hyperthermia* **15**:345–370.

Kong SD, Sartor M, Hu C-MJ, Zhang W, Zhang L, and Jin S (2013) Magnetic field activated lipid-polymer hybrid nanoparticles for stimuli-responsive drug release. *Acta Biomater* **9**:5447–5452.

Kono K (2001) Thermosensitive polymer-modified liposomes. *Adv Drug Deliv Rev* **53**: 307–319.

Kono K, Igawa T, and Takagishi T (1997) Cytoplasmic delivery of calcein mediated by liposomes modified with a pH-sensitive poly(ethylene glycol) derivative. *Biochim Biophys Acta* **1325**:143–154.

Kono K, Yoshino K, and Takagishi T (2002) Effect of poly(ethylene glycol) grafts on temperature-sensitivity of thermosensitive polymer-modified liposomes. *J Control Release* **80**:321–332.

Kono K, Zenitani K, and Takagishi T (1994) Novel pH-sensitive liposomes: liposomes bearing a poly(ethylene glycol) derivative with carboxyl groups. *Biochim Biophys Acta* **1193**:1–9.

Kostarelos K and Miller AD (2005) Synthetic, self-assembly ABCD nanoparticles; a structural paradigm for viable synthetic non-viral vectors. *Chem Soc Rev* **34**: 970–994.

Krasnici S, Werner A, Eichhorn ME, Schmitt-Sody M, Pahernik SA, Sauer B, Schulze B, Teifel M, Michaelis U, and Naujoks K, et al. (2003) Effect of the surface charge of liposomes on their uptake by angiogenic tumor vessels. *Int J Cancer* **105**:561–567.

Kreder K and Dmochowski R (2007) *The Overactive Bladder: Evaluation and Management*, 1st ed, CRC Press, Boca Raton.

Kreuter J (1994) Drug targeting with nanoparticles. *Eur J Drug Metab Pharmacokinet* **19**:253–256.

Kreuter J (2007) Nanoparticles–a historical perspective. *Int J Pharm* **331**:1–10.

Krishna R and Mayer LD (2000) Multidrug resistance (MDR) in cancer. Mechanisms, reversal using modulators of MDR and the role of MDR modulators in influencing the pharmacokinetics of anticancer drugs. *Eur J Pharm Sci* **11**:265–283.

Krishna R, Webb MS, St Onge G, and Mayer LD (2001) Liposomal and nonliposomal drug pharmacokinetics after administration of liposome-encapsulated vincristine and their contribution to drug tissue distribution properties. *J Pharmacol Exp Ther* **298**:1206–1212.

Krishnadas A, Rubinstein I, and Onyüksel H (2003) Sterically stabilized phospholipid mixed micelles: in vitro evaluation as a novel carrier for water-insoluble drugs. *Pharm Res* **20**:297–302.

Krown SE, Northfelt DW, Osoba D, and Stewart JS (2004) Use of liposomal anthracyclines in Kaposi's sarcoma. *Semin Oncol* **31**(6, Suppl 13)36–52.

Kubo T, Sugita T, Shimose S, Nitta Y, Ikuta Y, and Murakami T (2001) Targeted systemic chemotherapy using magnetic liposomes with incorporated adriamycin for osteosarcoma in hamsters. *Int J Oncol* **18**:121–125.

Kwon GS and Kataoka K (1995) Block copolymer micelles as long-circulating drug vehicles. *Adv Drug Deliv Rev* **16**:295–309.

Laginha K, Mumbengegwi D, and Allen T (2005a) Liposomes targeted via two different antibodies: assay, B-cell binding and cytotoxicity. *Biochim Biophys Acta* **1711**:25–32.

Laginha KM, Verwoert S, Charrois GJ, and Allen TM (2005b) Determination of doxorubicin levels in whole tumor and tumor nuclei in murine breast cancer tumors. *Clin Cancer Res* **11**:6944–6949.

Lai MZ, Düzgüneş N, and Szoka FC (1985) Effects of replacement of the hydroxyl group of cholesterol and tocopherol on the thermotropic behavior of phospholipid membranes. *Biochemistry* **24**:1646–1653.

Lakadamyali M, Rust MJ, and Zhuang X (2006) Ligands for clathrin-mediated endocytosis are differentially sorted into distinct populations of early endosomes. *Cell* **124**:997–1009.

Lammers T, Hennink WE, and Storm G (2008) Tumour-targeted nanomedicines: principles and practice. *Br J Cancer* **99**:392–397.

Langer K, Balthasar S, Vogel V, Dinauer N, von Briesen H, and Schubert D (2003) Optimization of the preparation process for human serum albumin (HSA) nanoparticles. *Int J Pharm* **257**:169–180.

Lasic DD (1982) A molecular model for vesicle formation. *Biochim Biophys Acta* **692**: 501–502.

Lasic D, Ceh B, Stuart M, Guo L, Frederik P, and Barenholz Y (1995) Transmembrane gradient driven phase transitions within vesicles: Lessons for drug delivery. *Biochim Biophys Acta* **1239**:145–156.

Lasic DD, Frederik PM, Stuart MC, Barenholz Y, and McIntosh TJ (1992) Gelation of liposome interior. A novel method for drug encapsulation. *FEBS Lett* **312**: 255–258.

Lasic DD, Martin FJ, Gabizon A, Huang SK, and Papahadjopoulos D (1991) Sterically stabilized liposomes: a hypothesis on the molecular origin of the extended circulation times. *Biochim Biophys Acta* **1070**:187–192.

Latagliata R, Breccia M, Fazi P, Iacobelli S, Martinelli G, Di Raimondo F, Sborgia M, Fabbiano F, Pirrotta MT, and Zaccaria A, et al. (2008) Liposomal daunorubicin versus standard daunorubicin: long term follow-up of the GIMEMA GSI 103 AMLE randomized trial in patients older than 60 years with acute myelogenous leukaemia. *Br J Haematol* **143**:681–689.

Lattin JR, Belnap DM, and Pitt WG (2012) Formation of eLiposomes as a drug delivery vehicle. *Colloids Surf B Biointerfaces* **89**:93–100.

Lee CM, Tanaka T, Murai T, Kondo M, Kimura J, Su W, Kitagawa T, Ito T, Matsuda H, and Miyasaka M (2002) Novel chondroitin sulfate-binding cationic liposomes loaded with cisplatin efficiently suppress the local growth and liver metastasis of tumor cells in vivo. *Cancer Res* **62**:4282–4288.

Lee RJ, Wang S, and Low PS (1996) Measurement of endosome pH following folate receptor-mediated endocytosis. *Biochim Biophys Acta* **1312**:237–242.

Leighton TG (2007) What is ultrasound? *Prog Biophys Mol Biol* **93**:3–83.

Lentacker I, Geers B, Demeester J, De Smedt SC, and Sanders NN (2010) Design and evaluation of doxorubicin-containing microbubbles for ultrasound-triggered doxorubicin delivery: cytotoxicity and mechanisms involved. *Mol Ther* **18**: 101–108.

Lentz BR, Malinin V, Haque ME, and Evans K (2000) Protein machines and lipid assemblies: current views of cell membrane fusion. *Curr Opin Struct Biol* **10**: 607–615.

Lenz H-J (2007) Management and preparedness for infusion and hypersensitivity reactions. *Oncologist* **12**:601–609.

Leonard RC, Williams S, Tulpule A, Levine AM, and Oliveros S (2009) Improving the therapeutic index of anthracycline chemotherapy: focus on liposomal doxorubicin (Myocet). *Breast* **18**:218–224.

Leung AK, Tam YY, and Cullis PR (2014) Lipid nanoparticles for short interfering RNA delivery. *Adv Genet* **88**:71–110.

Levchenko TS, Rammohan R, Lukyanov AN, Whiteman KR, and Torchilin VP (2002) Liposome clearance in mice: the effect of a separate and combined presence of surface charge and polymer coating. *Int J Pharm* **240**:95–102.

Li X, Anton N, Arpagaus C, Belleteix F, and Vandamme TF (2010b) Nanoparticles by spray drying using innovative new technology: the Büchi nano spray dryer B-90. *J Control Release* **147**:304–310.

Li X, Cabral-Lilly D, Janoff A, and Perkins W (2000) Complexation of internalized doxorubicin into fiber bundles affects its release rate from liposomes. *J Liposome Res* **10**:15–27.

Li X, Ding L, Xu Y, Wang Y, and Ping Q (2009) Targeted delivery of doxorubicin using stealth liposomes modified with transferrin. *Int J Pharm* **373**:116–123.

Li J, He Y-Z, Li W, Shen Y-Z, Li Y-R, and Wang Y-F (2010a) A novel polymer-lipid hybrid nanoparticle for efficient nonviral gene delivery. *Acta Pharmacol Sin* **31**: 509–514.

Li X, Hirsh DJ, Cabral-Lilly D, Zirkel A, Gruner SM, Janoff AS, and Perkins WR (1998) Doxorubicin physical state in solution and inside liposomes loaded via a pH gradient. *Biochim Biophys Acta* **1415**:23–40.

Li Y, Taulier N, Rauth AM, and Wu XY (2006) Screening of lipid carriers and characterization of drug-polymer-lipid interactions for the rational design of polymer-lipid hybrid nanoparticles (PLN). *Pharm Res* **23**:1877–1887.

Lim S-J, Lee M-K, and Kim C-K (2004) Altered chemical and biological activities of all-trans retinoic acid incorporated in solid lipid nanoparticle powders. *J Control Release* **100**:53–61.

Lin Y-K, Huang Z-R, Zhuo R-Z, and Fang J-Y (2010) Combination of calcipotriol and methotrexate in nanostructured lipid carriers for topical delivery. *Int J Nanomedicine* **5**:117–128.

Lin YY, Kao HW, Li JJ, Hwang JJ, Tseng YL, Lin WJ, Lin MH, Ting G, and Wang HE (2013) Tumor burden talks in cancer treatment with PEGylated liposomal drugs. *PLoS One* **8**:e63078.

Little JR, Dale AJ, and Okazaki H (1974) Meningeal carcinomatosis. Clinical manifestations. *Arch Neurol* **30**:138–143.

Litzinger DC, Buiting AM, van Rooijen N, and Huang L (1994) Effect of liposome size on the circulation time and intraorgan distribution of amphipathic poly(ethylene glycol)-containing liposomes. *Biochim Biophys Acta* **1190**:99–107.

Liu DX and Huang L (1989) Small, but not large, unilamellar liposomes composed of dioleoylphosphatidylethanolamine and oleic acid can be stabilized by human plasma. *Biochemistry* **28**:7700–7707.
Liu Z, Jiao Y, Wang Y, Zhou C, and Zhang Z (2008) Polysaccharides-based nanoparticles as drug delivery systems. *Adv Drug Deliv Rev* **60**:1650–1662.
Liu Y, Li K, Pan J, Liu B, and Feng S-S (2010a) Folic acid conjugated nanoparticles of mixed lipid monolayer shell and biodegradable polymer core for targeted delivery of Docetaxel. *Biomaterials* **31**:330–338.
Liu D, Liu Z, Wang L, Zhang C, and Zhang N (2011) Nanostructured lipid carriers as novel carrier for parenteral delivery of docetaxel. *Colloids Surf B Biointerfaces* **85**: 262–269.
Liu Y, Pan J, and Feng S-S (2010b) Nanoparticles of lipid monolayer shell and biodegradable polymer core for controlled release of paclitaxel: effects of surfactants on particles size, characteristics and in vitro performance. *Int J Pharm* **395**: 243–250.
Lobert S, Fahy J, Hill BT, Duflos A, Etievant C, and Correia JJ (2000) Vinca alkaloid-induced tubulin spiral formation correlates with cytotoxicity in the leukemic L1210 cell line. *Biochemistry* **39**:12053–12062.
Löhr JM, Haas SL, Bechstein WO, Bodoky G, Cwiertka K, Fischbach W, Fölsch UR, Jäger D, Osinsky D, and Prausova J, et al.; CT4001 Study Group (2012) Cationic liposomal paclitaxel plus gemcitabine or gemcitabine alone in patients with advanced pancreatic cancer: a randomized controlled phase II trial. *Ann Oncol* **23**: 1214–1222.
Lopez-Berestein G, Kasi L, Rosenblum MG, Haynie T, Jahns M, Glenn H, Mehta R, Mavligit GM, and Hersh EM (1984) Clinical pharmacology of 99mTc-labeled liposomes in patients with cancer. *Cancer Res* **44**:375–378.
Lopes de Menezes DE, Pilarski LM, and Allen TM (1998) In vitro and in vivo targeting of immunoliposomal doxorubicin to human B-cell lymphoma. *Cancer Res* **58**: 3320–3330.
Lotan R, Matsushita Y, Ohannesian D, Carralero D, Ota DM, Cleary KR, Nicolson GL, and Irimura T (1991) Lactose-binding lectin expression in human colorectal carcinomas. Relation to tumor progression. *Carbohydr Res* **213**:47–57.
Low PS and Kularatne SA (2009) Folate-targeted therapeutic and imaging agents for cancer. *Curr Opin Chem Biol* **13**:256–262.
Lu XQ, Burdette EC, Bornstein BA, Hansen JL, and Svensson GK (1996) Design of an ultrasonic therapy system for breast cancer treatment. *Int J Hyperthermia* **12**: 375–399.
Lu C, Perez-Soler R, Piperdi B, Walsh GL, Swisher SG, Smythe WR, Shin HJ, Ro JY, Feng L, and Truong M, et al. (2005) Phase II study of a liposome-entrapped cisplatin analog (L-NDDP) administered intrapleurally and pathologic response rates in patients with malignant pleural mesothelioma. *J Clin Oncol* **23**:3495–3501.
Lu WL, Qi XR, Zhang Q, Li RY, Wang GL, Zhang RJ, and Wei SL (2004) A pegylated liposomal platform: pharmacokinetics, pharmacodynamics, and toxicity in mice using doxorubicin as a model drug. *J Pharmacol Sci* **95**:381–389.
Lukyanov AN, Gao Z, Mazzola L, and Torchilin VP (2002) Polyethylene glycol-diacyllipid micelles demonstrate increased acculumation in subcutaneous tumors in mice. *Pharm Res* **19**:1424–1429.
Lukyanov AN, Gao Z, and Torchilin VP (2003) Micelles from polyethylene glycol/phosphatidylethanolamine conjugates for tumor drug delivery. *J Control Release* **91**:97–102.
Lukyanov AN and Torchilin VP (2004) Micelles from lipid derivatives of water-soluble polymers as delivery systems for poorly soluble drugs. *Adv Drug Deliv Rev* **56**:1273–1289.
Lundberg BB, Griffiths G, and Hansen HJ (2004) Cellular association and cytotoxicity of anti-CD74-targeted lipid drug-carriers in B lymphoma cells. *J Control Release* **94**:155–161.
Luo Q, Zhao J, Zhang X, and Pan W (2011) Nanostructured lipid carrier (NLC) coated with Chitosan Oligosaccharides and its potential use in ocular drug delivery system. *Int J Pharm* **403**:185–191.
Luo Y, Bernshaw NJ, Lu Z-R, Kopecek J, and Prestwich GD (2002) Targeted delivery of doxorubicin by HPMA copolymer-hyaluronan bioconjugates. *Pharm Res* **19**: 396–402.
Lurje G and Lenz H-J (2009) EGFR signaling and drug discovery. *Oncology* **77**: 400–410.
Lyass O, Hubert A, and Gabizon AA (2001) Phase I study of doxil-cisplatin combination chemotherapy in patients with advanced malignancies. *Clin Cancer Res* **7**: 3040–3046.
Maeda H, Bharate GY, and Daruwalla J (2009) Polymeric drugs for efficient tumor-targeted drug delivery based on EPR-effect. *Eur J Pharm Biopharm* **71**: 409–419.
Maeda H, Sawa T, and Konno T (2001) Mechanism of tumor-targeted delivery of macromolecular drugs, including the EPR effect in solid tumor and clinical overview of the prototype polymeric drug SMANCS. *J Control Release* **74**:47–61.
Maestrelli F, González-Rodríguez ML, Rabasco AM, and Mura P (2006) Effect of preparation technique on the properties of liposomes encapsulating ketoprofen-cyclodextrin complexes aimed for transdermal delivery. *Int J Pharm* **312**:53–60.
Mahalingam D, Nemunaitis JJ, Malik L, Sarantopoulos J, Weitman S, Sankhala K, Hart J, Kousba A, Gallegos NS, and Anderson G, et al. (2014) Phase I study of intravenously administered ATI-1123, a liposomal docetaxel formulation in patients with advanced solid tumors. *Cancer Chemother Pharmacol* **74**:1241–1250.
Mamidi RN, Weng S, Stellar S, Wang C, Yu N, Huang T, Tonelli AP, Kelley MF, Angiuoli A, and Fung M-C (2010) Pharmacokinetics, efficacy and toxicity of different pegylated liposomal doxorubicin formulations in preclinical models: is a conventional bioequivalence approach sufficient to ensure therapeutic equivalence of pegylated liposomal doxorubicin products? *Cancer Chemother Pharmacol* **66**: 1173–1184.
Mamot C, Drummond DC, Noble CO, Kallab V, Guo Z, Hong K, Kirpotin DB, and Park JW (2005) Epidermal growth factor receptor-targeted immunoliposomes significantly enhance the efficacy of multiple anticancer drugs in vivo. *Cancer Res* **65**:11631–11638.
Mantripragada S (2002) A lipid based depot (DepoFoam technology) for sustained release drug delivery. *Prog Lipid Res* **41**:392–406.
Mao Y, Triantafillou G, Hertlein E, Towns W, Stefanovski M, Mo X, Jarjoura D, Phelps M, Marcucci G, and Lee LJ, et al. (2013) Milatuzumab-conjugated liposomes as targeted dexamethasone carriers for therapeutic delivery in CD74+ B-cell malignancies. *Clin Cancer Res* **19**:347–356.
Marsh D (2013) *Handbook of Lipid Bilayers*, 2nd ed, CRC Press, Boca Raton.
Mastrobattista E, Koning GA, van Bloois L, Filipe AC, Jiskoot W, and Storm G (2002) Functional characterization of an endosome-disruptive peptide and its application in cytosolic delivery of immunoliposome-entrapped proteins. *J Biol Chem* **277**: 27135–27143.
Matsubara Y, Katoh S, Taniguchii H, Oka M, Kadota J, and Kohno S (2000) Expression of CD44 variants in lung cancer and its relationship to hyaluronan binding. *J Int Med Res* **28**:78–90.
Matsumura Y, Gotoh M, Muro K, Yamada Y, Shirao K, Shimada Y, Okuwa M, Matsumoto S, Miyata Y, and Ohkura H, et al. (2004) Phase I and pharmacokinetic study of MCC-465, a doxorubicin (DXR) encapsulated in PEG immunoliposome, in patients with metastatic stomach cancer. *Ann Oncol* **15**:517–525.
Matsumura Y and Maeda H (1986) A new concept for macromolecular therapeutics in cancer chemotherapy: mechanism of tumoritropic accumulation of proteins and the antitumor agent smancs. *Cancer Res* **46**:6387–6392.
Matteucci ML, Anyarambhatla G, Rosner G, Azuma C, Fisher PE, Dewhirst MW, Needham D, and Thrall DE (2000) Hyperthermia increases accumulation of technetium-99m-labeled liposomes in feline sarcomas. *Clin Cancer Res* **6**: 3748–3755.
Mauk MR and Gamble RC (1979a) Preparation of lipid vesicles containing high levels of entrapped radioactive cations. *Anal Biochem* **94**:302–307.
Mauk MR and Gamble RC (1979b) Stability of lipid vesicles in tissues of the mouse: a gamma-ray perturbed angular correlation study. *Proc Natl Acad Sci USA* **76**: 765–769.
Mauk MR, Gamble RC, and Baldeschwieler JD (1980) Vesicle targeting: timed release and specificity for leukocytes in mice by subcutaneous injection. *Science* **207**: 309–311.
May JP and Li S-D (2013) Hyperthermia-induced drug targeting. *Expert Opin Drug Deliv* **10**:511–527.
Mayer LD, Bally MB, Cullis PR, Wilson SL, and Emerman JT (1990a) Comparison of free and liposome encapsulated doxorubicin tumor drug uptake and antitumor efficacy in the SC115 murine mammary tumor. *Cancer Lett* **53**:183–190.
Mayer LD, Bally MB, Loughrey H, Masin D, and Cullis PR (1990b) Liposomal vincristine preparations which exhibit decreased drug toxicity and increased activity against murine L1210 and P388 tumors. *Cancer Res* **50**:575–579.
Mayer LD, Nayar R, Thies RL, Boman NL, Cullis PR, and Bally MB (1993) Identification of vesicle properties that enhance the antitumour activity of liposomal vincristine against murine L1210 leukemia. *Cancer Chemother Pharmacol* **33**: 17–24.
Mehnert W and Mäder K (2001) Solid lipid nanoparticles: production, characterization and applications. *Adv Drug Deliv Rev* **47**:165–196.
Messerschmidt SK, Musyanovych A, Altvater M, Scheurich P, Pfizenmaier K, Landfester K, and Kontermann RE (2009) Targeted lipid-coated nanoparticles: delivery of tumor necrosis factor-functionalized particles to tumor cells. *J Control Release* **137**:69–77.
Michieli M, Michelutti A, Damiani D, Pipan C, Raspadori D, Lauria F, and Baccarani M (1993) A comparative analysis of the sensitivity of multidrug resistant (MDR) and non-MDR cells to different anthracycline derivatives. *Leuk Lymphoma* **9**: 255–264.
Mieszawska AJ, Gianella A, Cormode DP, Zhao Y, Meijerink A, Langer R, Farokhzad OC, Fayad ZA, and Mulder WJ (2012) Engineering of lipid-coated PLGA nanoparticles with a tunable payload of diagnostically active nanocrystals for medical imaging. *Chem Commun (Camb)* **48**:5835–5837.
Miller CR, Bondurant B, McLean SD, McGovern KA, and O'Brien DF (1998) Liposome-cell interactions in vitro: effect of liposome surface charge on the binding and endocytosis of conventional and sterically stabilized liposomes. *Biochemistry* **37**:12875–12883.
Mills JK and Needham D (2005) Lysolipid incorporation in dipalmitoylphosphatidylcholine bilayer membranes enhances the ion permeability and drug release rates at the membrane phase transition. *Biochim Biophys Acta* **1716**:77–96.
Milsmann MH, Schwendener RA, and Weder H-G (1978) The preparation of large single bilayer liposomes by a fast and controlled dialysis. *Biochim Biophys Acta* **512**:147–155.
Minko T (2004) Drug targeting to the colon with lectins and neoglycoconjugates. *Adv Drug Deliv Rev* **56**:491–509.
Mitchell MJ and King MR (2014) Physical biology in cancer. 3. The role of cell glycocalyx in vascular transport of circulating tumor cells. *Am J Physiol Cell Physiol* **306**:C89–C97.
Miyata H and Hotani H (1992) Morphological changes in liposomes caused by polymerization of encapsulated actin and spontaneous formation of actin bundles. *Proc Natl Acad Sci USA* **89**:11547–11551.
Moghimi SM, Hedeman H, Christy NM, Illum L, and Davis SS (1993a) Enhanced hepatic clearance of intravenously administered sterically stabilized microspheres in zymosan-stimulated rats. *J Leukoc Biol* **54**:513–517.
Moghimi SM, Hedeman H, Muir IS, Illum L, and Davis SS (1993b) An investigation of the filtration capacity and the fate of large filtered sterically-stabilized microspheres in rat spleen. *Biochim Biophys Acta* **1157**:233–240.
Money-Kyrle JF, Bates F, Ready J, Gazzard BG, Phillips RH, and Boag FC (1993) Liposomal daunorubicin in advanced Kaposi's sarcoma: a phase II study. *Clin Oncol (R Coll Radiol)* **5**:367–371.
Moore A and Pinkerton R (2009) Vincristine: Can its therapeutic index be enhanced? *Pediatr Blood Cancer* **53**:1180–1187.
Morgan E (1981) Transferrin, biochemistry, physiology and clinical significance. *Mol Aspects Med* **4**:1–123.

Mouritsen OG and Jørgensen K (1998) A new look at lipid-membrane structure in relation to drug research. *Pharm Res* **15**:1507–1519.
Muller R, Dingier A, Schneppe T, and Gohla S (2000a) Large-scale production of solid lipid nanoparticles (SLN) and nanosuspensions (DissoCubes), in *Handbook of Pharmaceutical Controlled Release Technology* (Wise D ed) pp 359–376, CRC Press, Boca Raton.
Muller R, Maaßen S, Weyhers H, Specht F, and Lucks J (1996) Cytotoxicity of magnetite-loaded polylactide, polylactide/glycolide particles and solid lipid nanoparticles. *Int J Pharm* **138**:85–94.
Müller RH, Mäder K, and Gohla S (2000b) Solid lipid nanoparticles (SLN) for controlled drug delivery - a review of the state of the art. *Eur J Pharm Biopharm* **50**: 161–177.
Müller RH, Radtke M, and Wissing SA (2002) Solid lipid nanoparticles (SLN) and nanostructured lipid carriers (NLC) in cosmetic and dermatological preparations. *Adv Drug Deliv Rev* **54** (Suppl 1):S131–S155.
Murry DJ and Blaney SM (2000) Clinical pharmacology of encapsulated sustained-release cytarabine. *Ann Pharmacother* **34**:1173–1178.
Nagasawa K, Natazuka T, Chihara K, Kitazawa F, Tsumura A, Takara K, Nomiyama M, Ohnishi N, and Yokoyama T (1996) Transport mechanism of anthracycline derivatives in human leukemia cell lines: uptake and efflux of pirarubicin in HL60 and pirarubicin-resistant HL60 cells. *Cancer Chemother Pharmacol* **37**:297–304.
Nagayasu A, Uchiyama K, and Kiwada H (1999) The size of liposomes: a factor which affects their targeting efficiency to tumors and therapeutic activity of liposomal antitumor drugs. *Adv Drug Deliv Rev* **40**:75–87.
Naito M, Nagai H, Kawano S, Umezu H, Zhu H, Moriyama H, Yamamoto T, Takatsuka H, and Takei Y (1996) Liposome-encapsulated dichloromethylene diphosphonate induces macrophage apoptosis in vivo and in vitro. *J Leukoc Biol* **60**:337–344.
Nam HY, Kwon SM, Chung H, Lee S-Y, Kwon S-H, Jeon H, Kim Y, Park JH, Kim J, and Her S, et al. (2009) Cellular uptake mechanism and intracellular fate of hydrophobically modified glycol chitosan nanoparticles. *J Control Release* **135**: 259–267.
Needham D, Anyarambhatla G, Kong G, and Dewhirst MW (2000) A new temperature-sensitive liposome for use with mild hyperthermia: characterization and testing in a human tumor xenograft model. *Cancer Res* **60**:1197–1201.
Needham D, Park J-Y, Wright AM, and Tong J (2013) Materials characterization of the low temperature sensitive liposome (LTSL): effects of the lipid composition (lysolipid and DSPE-PEG2000) on the thermal transition and release of doxorubicin. *Faraday Discuss* **161**:515–534, discussion 563–589.
Needham D, Stoicheva N, and Zhelev DV (1997) Exchange of monooleoylphosphatidylcholine as monomer and micelle with membranes containing poly(ethylene glycol)-lipid. *Biophys J* **73**:2615–2629.
Nicholas AR, Scott MJ, Kennedy NI, and Jones MN (2000) Effect of grafted polyethylene glycol (PEG) on the size, encapsulation efficiency and permeability of vesicles. *Biochim Biophys Acta* **1463**:167–178.
Nickels J and Palmer AF (2003) Changes in liposome morphology induced by actin polymerization in submicrometer liposomes. *Langmuir* **19**:10581–10587.
Nie S, Xing Y, Kim GJ, and Simons JW (2007) Nanotechnology applications in cancer. *Annu Rev Biomed Eng* **9**:257–288.
Nikolova AN and Jones MN (1996) Effect of grafted PEG-2000 on the size and permeability of vesicles. *Biochim Biophys Acta* **1304**:120–128.
Nirmalanandhan VS, Hurren R, Cameron WD, Gronda M, Shamas-Din A, You L, Minden MD, Rocheleau JV, and Schimmer AD (2015) Increased pressure alters plasma membrane dynamics and renders acute myeloid leukemia cells resistant to daunorubicin. *Haematologica* **100**:e406–e408.
Nisato RE, Tille JC, Jonczyk A, Goodman SL, and Pepper MS (2003) alphav β 3 and alphav β 5 integrin antagonists inhibit angiogenesis in vitro. *Angiogenesis* **6**: 105–119.
Nishi T and Forgac M (2002) The vacuolar ($H^+$)-ATPases–nature's most versatile proton pumps. *Nat Rev Mol Cell Biol* **3**:94–103.
Noble CO, Kirpotin DB, Hayes ME, Mamot C, Hong K, Park JW, Benz CC, Marks JD, and Drummond DC (2004) Development of ligand-targeted liposomes for cancer therapy. *Expert Opin Ther Targets* **8**:335–353.
Nobuto H, Sugita T, Kubo T, Shimose S, Yasunaga Y, Murakami T, and Ochi M (2004) Evaluation of systemic chemotherapy with magnetic liposomal doxorubicin and a dipole external electromagnet. *Int J Cancer* **109**:627–635.
Noguchi A, Furuno T, Kawaura C, and Nakanishi M (1998) Membrane fusion plays an important role in gene transfection mediated by cationic liposomes. *FEBS Lett* **433**:169–173.
Nohl H and Jordan W (1983) OH.-generation by adriamycin semiquinone and H2O2; an explanation for the cardiotoxicity of anthracycline antibiotics. *Biochem Biophys Res Commun* **114**:197–205.
Northfelt DW, Dezube BJ, Thommes JA, Miller BJ, Fischl MA, Friedman-Kien A, Kaplan LD, Du Mond C, Mamelok RD, and Henry DH (1998) Pegylated-liposomal doxorubicin versus doxorubicin, bleomycin, and vincristine in the treatment of AIDS-related Kaposi's sarcoma: results of a randomized phase III clinical trial. *J Clin Oncol* **16**:2445–2451.
Northfelt DW, Martin FJ, Working P, Volberding PA, Russell J, Newman M, Amantea MA, and Kaplan LD (1996) Doxorubicin encapsulated in liposomes containing surface-bound polyethylene glycol: pharmacokinetics, tumor localization, and safety in patients with AIDS-related Kaposi's sarcoma. *J Clin Pharmacol* **36**: 55–63.
Nyborg WL (2001) Biological effects of ultrasound: development of safety guidelines. Part II: general review. *Ultrasound Med Biol* **27**:301–333.
Oberoi HS, Nukolova NV, Kabanov AV, and Bronich TK (2013) Nanocarriers for delivery of platinum anticancer drugs. *Adv Drug Deliv Rev* **65**:1667–1685.
O'Brien ME, Wigler N, Inbar M, Rosso R, Grischke E, Santoro A, Catane R, Kieback DG, Tomczak P, and Ackland SP, et al.; CAELYX Breast Cancer Study Group (2004) Reduced cardiotoxicity and comparable efficacy in a phase III trial of pegylated liposomal doxorubicin HCl (CAELYX/Doxil) versus conventional doxorubicin for first-line treatment of metastatic breast cancer. *Ann Oncol* **15**: 440–449.
O'Brien S, Schiller G, Lister J, Damon L, Goldberg S, Aulitzky W, Ben-Yehuda D, Stock W, Coutre S, and Douer D, et al. (2013) High-dose vincristine sulfate liposome injection for advanced, relapsed, and refractory adult Philadelphia chromosome-negative acute lymphoblastic leukemia. *J Clin Oncol* **31**:676–683.
Ohannesian DW, Lotan D, and Lotan R (1994) Concomitant increases in galectin-1 and its glycoconjugate ligands (carcinoembryonic antigen, lamp-1, and lamp-2) in cultured human colon carcinoma cells by sodium butyrate. *Cancer Res* **54**: 5992–6000.
Ohsawa T, Miura H, and Harada K (1984) A novel method for preparing liposome with a high capacity to encapsulate proteinous drugs: freeze-drying method. *Chem Pharm Bull (Tokyo)* **32**:2442–2445.
Oja CD, Semple SC, Chonn A, and Cullis PR (1996) Influence of dose on liposome clearance: critical role of blood proteins. *Biochim Biophys Acta* **1281**:31–37.
Olson F, Hunt CA, Szoka FC, Vail WJ, and Papahadjopoulos D (1979) Preparation of liposomes of defined size distribution by extrusion through polycarbonate membranes. *Biochim Biophys Acta* **557**:9–23.
Olson ME, Chernik NL, and Posner JB (1974) Infiltration of the leptomeninges by systemic cancer. A clinical and pathologic study. *Arch Neurol* **30**:122–137.
Orlowski RZ, Nagler A, Sonneveld P, Bladé J, Hajek R, Spencer A, San Miguel J, Robak T, Dmoszynska A, and Horvath N, et al. (2007) Randomized phase III study of pegylated liposomal doxorubicin plus bortezomib compared with bortezomib alone in relapsed or refractory multiple myeloma: combination therapy improves time to progression. *J Clin Oncol* **25**:3892–3901.
Owens DE 3rd and Peppas NA (2006) Opsonization, biodistribution, and pharmacokinetics of polymeric nanoparticles. *Int J Pharm* **307**:93–102.
Pagano RE, Huang L, and Wey C (1974) Interaction of phospholipid vesicles with cultured mammalian cells. *Nature* **252**:166–167.
Pagano RE and Takeichi M (1977) Adhesion of phospholipid vesicles to Chinese hamster fibroblasts. Role of cell surface proteins. *J Cell Biol* **74**:531–546.
Pan XQ, Wang H, and Lee RJ (2003) Antitumor activity of folate receptor-targeted liposomal doxorubicin in a KB oral carcinoma murine xenograft model. *Pharm Res* **20**:417–422.
Papahadjopoulos D, Allen TM, Gabizon A, Mayhew E, Matthay K, Huang SK, Lee KD, Woodle MC, Lasic DD, and Redemann C, et al. (1991) Sterically stabilized liposomes: improvements in pharmacokinetics and antitumor therapeutic efficacy. *Proc Natl Acad Sci USA* **88**:11460–11464.
Papahadjopoulos D, Poste G, and Schaeffer BE (1973) Fusion of mammalian cells by unilamellar lipid vesicles: inflluence of lipid surface charge, fluidity and cholesterol. *Biochim Biophys Acta* **323**:23–42.
Papahadjopoulos D and Watkins JC (1967) Phospholipid model membranes. II. Permeability properties of hydrated liquid crystals. *Biochim Biophys Acta* **135**: 639–652.
Park H, Kim Y, Lim Y, Han I, and Oh E-S (2002) Syndecan-2 mediates adhesion and proliferation of colon carcinoma cells. *J Biol Chem* **277**:29730–29736.
Pasqualini R, Koivunen E, Kain R, Lahdenranta J, Sakamoto M, Stryhn A, Ashmun RA, Shapiro LH, Arap W, and Ruoslahti E (2000) Aminopeptidase N is a receptor for tumor-homing peptides and a target for inhibiting angiogenesis. *Cancer Res* **60**: 722–727.
Pastorino F, Brignole C, Di Paolo D, Nico B, Pezzolo A, Marimpietri D, Pagnan G, Piccardi F, Cilli M, and Longhi R, et al. (2006) Targeting liposomal chemotherapy via both tumor cell-specific and tumor vasculature-specific ligands potentiates therapeutic efficacy. *Cancer Res* **66**:10073–10082.
Pastorino F, Brignole C, Marimpietri D, Cilli M, Gambini C, Ribatti D, Longhi R, Allen TM, Corti A, and Ponzoni M (2003) Vascular damage and anti-angiogenic effects of tumor vessel-targeted liposomal chemotherapy. *Cancer Res* **63**: 7400–7409.
Patel KR, Tin GW, Williams LE, and Baldeschwieler JD (1985) Biodistribution of phospholipid vesicles in mice bearing Lewis lung carcinoma and granuloma. *J Nucl Med* **26**:1048–1055.
Paulos CM, Reddy JA, Leamon CP, Turk MJ, and Low PS (2004) Ligand binding and kinetics of folate receptor recycling in vivo: impact on receptor-mediated drug delivery. *Mol Pharmacol* **66**:1406–1414.
Peer D and Margalit R (2004a) Loading mitomycin C inside long circulating hyaluronan targeted nano-liposomes increases its antitumor activity in three mice tumor models. *Int J Cancer* **108**:780–789.
Peer D and Margalit R (2004b) Tumor-targeted hyaluronan nanoliposomes increase the antitumor activity of liposomal Doxorubicin in syngeneic and human xenograft mouse tumor models. *Neoplasia* **6**:343–353.
Peixoto Júnior AA, Teles BC, Castro EF, Santos AA, de Oliveira GR, Ribeiro RA, Rola FH, and Gondim FA (2009) Vincristine delays gastric emptying and gastrointestinal transit of liquid in awake rats. *Braz J Med Biol Res* **42**:567–573.
Pencer J and Hallett FR (2003) Effects of vesicle size and shape on static and dynamic light scattering measurements. *Langmuir* **19**:7488–7497.
Peng X, Chen B, Lim CC, and Sawyer DB (2005) The cardiotoxicology of anthracycline chemotherapeutics: translating molecular mechanism into preventative medicine. *Mol Interv* **5**:163–171.
Perez-Soler R, Lopez-Berestein G, Lautersztain J, al-Baker S, Francis K, Macias-Kiger D, Raber MN, and Khokhar AR (1990) Phase I clinical and pharmacological study of liposome-entrapped cis-bis-neodecanoato-trans-R,R-1,2-diaminocyclohexane platinum(II). *Cancer Res* **50**:4254–4259.
Perillo NL, Marcus ME, and Baum LG (1998) Galectins: versatile modulators of cell adhesion, cell proliferation, and cell death. *J Mol Med (Berl)* **76**:402–412.
Pignatello R, Musumeci T, Graziano AC, Lo Furno D, Varamini P, Mansfeld FM, Cardile V, and Toth I (2015) A study on liposomal encapsulation of a lipophilic prodrug of LHRH. *Pharm Dev Technol* 1–8.
Pires P, Simões S, Nir S, Gaspar R, Düzgünes N, and Pedroso de Lima MC (1999) Interaction of cationic liposomes and their DNA complexes with monocytic leukemia cells. *Biochim Biophys Acta* **1418**:71–84.

Planting AS, Sonneveld P, van der Gaast A, Sparreboom A, van der Burg ME, Luyten GP, de Leeuw K, de Boer-Dennert M, Wissel PS, and Jewell RC, et al. (2005) A phase I and pharmacologic study of the MDR converter GF120918 in combination with doxorubicin in patients with advanced solid tumors. *Cancer Chemother Pharmacol* **55**:91–99.

Pommier Y (2006) Topoisomerase I inhibitors: camptothecins and beyond. *Nat Rev Cancer* **6**:789–802.

Ponce AM, Viglianti BL, Yu D, Yarmolenko PS, Michelich CR, Woo J, Bally MB, and Dewhirst MW (2007) Magnetic resonance imaging of temperature-sensitive liposome release: drug dose painting and antitumor effects. *J Natl Cancer Inst* **99**: 53–63.

Ponce AM, Vujaskovic Z, Yuan F, Needham D, and Dewhirst MW (2006) Hyperthermia mediated liposomal drug delivery. *Int J Hyperthermia* **22**:205–213.

Porter CJ, Moghimi SM, Illum L, and Davis SS (1992) The polyoxyethylene/polyoxypropylene block co-polymer poloxamer-407 selectively redirects intravenously injected microspheres to sinusoidal endothelial cells of rabbit bone marrow. *FEBS Lett* **305**:62–66.

Poste G and Papahadjopoulos D (1976) Lipid vesicles as carriers for introducing materials into cultured cells: influence of vesicle lipid composition on mechanism(s) of vesicle incorporation into cells. *Proc Natl Acad Sci USA* **73**:1603–1607.

Potchoiba M, West M, Smolarek T, Macaione G, Santacroce E, and Lundeen G (1996) Tissue distribution of doxorubicin in the free and liposomal forms in male Beagles. *Proc Am Assoc Cancer Res* **37**:A2675.

Pownall HJ, Massey JB, Kusserow SK, and Gotto AM Jr (1978) Kinetics of lipid–protein interactions: interaction of apolipoprotein A-I from human plasma high density lipoproteins with phosphatidylcholines. *Biochemistry* **17**:1183–1188.

Pozzi D, Colapicchioni V, Caracciolo G, Piovesana S, Capriotti AL, Palchetti S, De Grossi S, Riccioli A, Amenitsch H, and Laganà A (2014) Effect of polyethyleneglycol (PEG) chain length on the bio-nano-interactions between PEGylated lipid nanoparticles and biological fluids: from nanostructure to uptake in cancer cells. *Nanoscale* **6**:2782–2792.

Pradhan P, Giri J, Rieken F, Koch C, Mykhaylyk O, Döblinger M, Banerjee R, Bahadur D, and Plank C (2010) Targeted temperature sensitive magnetic liposomes for thermo-chemotherapy. *J Control Release* **142**:108–121.

Presant CA, Blayney D, Proffitt RT, Turner AF, Williams LE, Nadel HI, Kennedy P, Wiseman C, Gala K, and Crossley RJ, et al. (1990) Preliminary report: imaging of Kaposi sarcoma and lymphoma in AIDS with indium-111-labelled liposomes. *Lancet* **335**:1307–1309.

Presant CA, Proffitt RT, Turner AF, Williams LE, Winsor D, Werner JL, Kennedy P, Wiseman C, Gala K, and McKenna RJ, et al. (1988) Successful imaging of human cancer with indium-111-labeled phospholipid vesicles. *Cancer* **62**:905–911.

Presant CA, Scolaro M, Kennedy P, Blayney DW, Flanagan B, Lisak J, and Presant J (1993) Liposomal daunorubicin treatment of HIV-associated Kaposi's sarcoma. *Lancet* **341**:1242–1243.

Proffitt RT, Williams LE, Presant CA, Tin GW, Uliana JA, Gamble RC, and Baldeschwieler JD (1983a) Liposomal blockade of the reticuloendothelial system: improved tumor imaging with small unilamellar vesicles. *Science* **220**:502–505.

Proffitt RT, Williams LE, Presant CA, Tin GW, Uliana JA, Gamble RC, and Baldeschwieler JD (1983b) Tumor-imaging potential of liposomes loaded with In-111-NTA: biodistribution in mice. *J Nucl Med* **24**:45–51.

Prost AC, Ménégaux F, Langlois P, Vidal J-M, Koulibaly M, Jost J-L, Duron J-J, Chigot J-P, Vayre P, and Aurengo A, et al. (1998) Differential transferrin receptor density in human colorectal cancer: A potential probe for diagnosis and therapy. *Int J Oncol* **13**:871–875.

Raj TAS, Smith AM, and Moore AS (2013) Vincristine sulfate liposomal injection for acute lymphoblastic leukemia. *Int J Nanomedicine* **8**:4361–4369.

Ranjan A, Jacobs GC, Woods DL, Negussie AH, Partanen A, Yarmolenko PS, Gacchina CE, Sharma KV, Frenkel V, and Wood BJ, et al. (2012) Image-guided drug delivery with magnetic resonance guided high intensity focused ultrasound and temperature sensitive liposomes in a rabbit Vx2 tumor model. *J Control Release* **158**:487–494.

Reitsma S, Slaaf DW, Vink H, van Zandvoort MA, and oude Egbrink MG (2007) The endothelial glycocalyx: composition, functions, and visualization. *Pflugers Arch* **454**:345–359.

Richardson DR and Baker E (1990) The uptake of iron and transferrin by the human malignant melanoma cell. *Biochim Biophys Acta* **1053**:1–12.

Richardson D and Baker E (1992) Two mechanisms of iron uptake from transferrin by melanoma cells. The effect of desferrioxamine and ferric ammonium citrate. *J Biol Chem* **267**:13972–13979.

Richardson DR and Ponka P (1997) The molecular mechanisms of the metabolism and transport of iron in normal and neoplastic cells. *Biochim Biophys Acta* **1331**: 1–40.

Rifkin RM, Gregory SA, Mohrbacher A, and Hussein MA (2006) Pegylated liposomal doxorubicin, vincristine, and dexamethasone provide significant reduction in toxicity compared with doxorubicin, vincristine, and dexamethasone in patients with newly diagnosed multiple myeloma: a Phase III multicenter randomized trial. *Cancer* **106**:848–858.

Roerdink F, Wassef NM, Richardson EC, and Alving CR (1983) Effects of negatively charged lipids on phagocytosis of liposomes opsonized by complement. *Biochim Biophys Acta* **734**:33–39.

Ropert C, Malvy C, and Couvreur P(1996) pH sensitive liposomes as efficient carriers for intracellular delivery of oligonucleotides, in *Targeting of Drugs 5. Strategies for Oligonucleotide and Gene Delivery in Therapy* (Gregoriadis G and McCormack B eds) pp 151–162, Springer, New York.

Rosen MJ and Kunjappu JT (2012) *Surfactants and Interfacial Phenomena*, 4th ed, John Wiley & Sons, Hoboken.

Ross Hallett F (1994) Particle size analysis by dynamic light scattering. *Food Res Int* **27**:195–198.

Roy AC, Park SR, Cunningham D, Kang YK, Chao Y, Chen LT, Rees C, Lim HY, Tabernero J, and Ramos FJ, et al. (2013) A randomized phase II study of PEP02 (MM-398), irinotecan or docetaxel as a second-line therapy in patients with locally advanced or metastatic gastric or gastro-oesophageal junction adenocarcinoma. *Ann Oncol* **24**:1567–1573.

Rubino OP, Kowalsky R, and Swarbrick J (1993) Albumin microspheres as a drug delivery system: relation among turbidity ratio, degree of cross-linking, and drug release. *Pharm Res* **10**:1059–1065.

Rudenko G, Henry L, Henderson K, Ichtchenko K, Brown MS, Goldstein JL, and Deisenhofer J (2002) Structure of the LDL receptor extracellular domain at endosomal pH. *Science* **298**:2353–2358.

Ruktanonchai U, Bejrapha P, Sakulkhu U, Opanasopit P, Bunyapraphatsara N, Junyaprasert V, and Puttipipatkhachorn S (2009) Physicochemical characteristics, cytotoxicity, and antioxidant activity of three lipid nanoparticulate formulations of alpha-lipoic acid. *AAPS PharmSciTech* **10**:227–234.

Saari H, Lázaro-Ibáñez E, Viitala T, Vuorimaa-Laukkanen E, Siljander P, and Yliperttula M (2015) Microvesicle- and exosome-mediated drug delivery enhances the cytotoxicity of Paclitaxel in autologous prostate cancer cells. *J Control Release* **220** (Pt B):727–737.

Saba NF, Wang X, Müller S, Tighiouart M, Cho K, Nie S, Chen Z, and Shin DM (2009) Examining expression of folate receptor in squamous cell carcinoma of the head and neck as a target for a novel nanotherapeutic drug. *Head Neck* **31**: 475–481.

Sabín J, Prieto G, Ruso JM, Messina PV, Salgado FJ, Nogueira M, Costas M, and Sarmiento F (2009) Interactions between DMPC liposomes and the serum blood proteins HSA and IgG. *J Phys Chem B* **113**:1655–1661.

Sahin S, Selek H, Ponchel G, Ercan MT, Sargon M, Hincal AA, and Kas HS (2002) Preparation, characterization and in vivo distribution of terbutaline sulfate loaded albumin microspheres. *J Control Release* **82**:345–358.

Saif MW (2014) MM-398 achieves primary endpoint of overall survival in phase III study in patients with gemcitabine refractory metastatic pancreatic cancer. *JOP* **15**:278–279.

Saiki I, Fujii H, Yoneda J, Abe F, Nakajima M, Tsuruo T, and Azuma I (1993) Role of aminopeptidase N (CD13) in tumor-cell invasion and extracellular matrix degradation. *Int J Cancer* **54**:137–143.

Saito G, Swanson JA, and Lee K-D (2003) Drug delivery strategy utilizing conjugation via reversible disulfide linkages: role and site of cellular reducing activities. *Adv Drug Deliv Rev* **55**:199–215.

Salomir R, Palussière J, Fossheim SL, Rogstad A, Wiggen UN, Grenier N, and Moonen CT (2005) Local delivery of magnetic resonance (MR) contrast agent in kidney using thermosensitive liposomes and MR imaging-guided local hyperthermia: a feasibility study in vivo. *J Magn Reson Imaging* **22**:534–540.

Sapra P and Allen TM (2004) Improved outcome when B-cell lymphoma is treated with combinations of immunoliposomal anticancer drugs targeted to both the CD19 and CD20 epitopes. *Clin Cancer Res* **10**:2530–2537.

Saunders L, Perrin J, and Gammack D (1962) Ultrasonic irradiation of some phospholipid sols. *J Pharm Pharmacol* **14**:567–572.

Saupe A, Gordon KC, and Rades T (2006) Structural investigations on nanoemulsions, solid lipid nanoparticles and nanostructured lipid carriers by cryo-field emission scanning electron microscopy and Raman spectroscopy. *Int J Pharm* **314**: 56–62.

Sawant RM, Hurley JP, Salmaso S, Kale A, Tolcheva E, Levchenko TS, and Torchilin VP (2006) "SMART" drug delivery systems: double-targeted pH-responsive pharmaceutical nanocarriers. *Bioconjug Chem* **17**:943–949.

Sawant RR and Torchilin VP (2010) Liposomes as 'smart' pharmaceutical nanocarriers. *Soft Matter* **6**:4026–4044.

Scaltriti M and Baselga J (2006) The epidermal growth factor receptor pathway: a model for targeted therapy. *Clin Cancer Res* **12**:5268–5272.

Schafer FQ and Buettner GR (2001) Redox environment of the cell as viewed through the redox state of the glutathione disulfide/glutathione couple. *Free Radic Biol Med* **30**:1191–1212.

Schiffelers RM, Koning GA, ten Hagen TL, Fens MH, Schraa AJ, Janssen AP, Kok RJ, Molema G, and Storm G (2003) Anti-tumor efficacy of tumor vasculature-targeted liposomal doxorubicin. *J Control Release* **91**:115–122.

Schoeppner HL, Raz A, Ho SB, and Bresalier RS (1995) Expression of an endogenous galactose-binding lectin correlates with neoplastic progression in the colon. *Cancer* **75**:2818–2826.

Schroeder A, Honen R, Turjeman K, Gabizon A, Kost J, and Barenholz Y (2009a) Ultrasound triggered release of cisplatin from liposomes in murine tumors. *J Control Release* **137**:63–68.

Schroeder A, Kost J, and Barenholz Y (2009b) Ultrasound, liposomes, and drug delivery: principles for using ultrasound to control the release of drugs from liposomes. *Chem Phys Lipids* **162**:1–16.

Schroit AJ, Madsen J, and Nayar R (1986) Liposome-cell interactions: in vitro discrimination of uptake mechanism and in vivo targeting strategies to mononuclear phagocytes. *Chem Phys Lipids* **40**:373–393.

Schubert MA and Müller-Goymann CC (2003) Solvent injection as a new approach for manufacturing lipid nanoparticles–evaluation of the method and process parameters. *Eur J Pharm Biopharm* **55**:125–131.

Schwarz C, Mehnert W, Lucks J, and Muller R (1994) Solid lipid nanoparticles (SLN) for controlled drug delivery. I. Production, characterization and sterilization. *J Control Release* **30**:83–96.

Screnci D, McKeage MJ, Galettis P, Hambley TW, Palmer BD, and Baguley BC (2000) Relationships between hydrophobicity, reactivity, accumulation and peripheral nerve toxicity of a series of platinum drugs. *Br J Cancer* **82**:966–972.

Seddon JM, Cevc G, and Marsh D (1983) Calorimetric studies of the gel-fluid (L beta-L alpha) and lamellar-inverted hexagonal (L alpha-HII) phase transitions in dialkyl- and diacylphosphatidylethanolamines. *Biochemistry* **22**: 1280–1289.

Seiden MV, Muggia F, Astrow A, Matulonis U, Campos S, Roche M, Sivret J, Rusk J, and Barrett E (2004) A phase II study of liposomal lurtotecan (OSI-211) in patients with topotecan resistant ovarian cancer. *Gynecol Oncol* **93**:229–232.

Semple SC, Leone R, Wang J, Leng EC, Klimuk SK, Eisenhardt ML, Yuan ZN, Edwards K, Maurer N, and Hope MJ, et al. (2005) Optimization and characterization of a sphingomyelin/cholesterol liposome formulation of vinorelbine with promising antitumor activity. *J Pharm Sci* **94**:1024–1038.

Sengupta S, Eavarone D, Capila I, Zhao G, Watson N, Kiziltepe T, and Sasisekharan R (2005) Temporal targeting of tumour cells and neovasculature with a nanoscale delivery system. *Nature* **436**:568–572.

Senior JH, Trimble KR, and Maskiewicz R (1991) Interaction of positively-charged liposomes with blood: implications for their application in vivo. *Biochim Biophys Acta* **1070**:173–179.

Serpe L, Catalano MG, Cavalli R, Ugazio E, Bosco O, Canaparo R, Muntoni E, Frairia R, Gasco MR, and Eandi M, et al. (2004) Cytotoxicity of anticancer drugs incorporated in solid lipid nanoparticles on HT-29 colorectal cancer cell line. *Eur J Pharm Biopharm* **58**:673–680.

Sessa G and Weissmann G (1968) Phospholipid spherules (liposomes) as a model for biological membranes. *J Lipid Res* **9**:310–318.

Shadidi M and Sioud M (2003) Selective targeting of cancer cells using synthetic peptides. *Drug Resist Updat* **6**:363–371.

Shan S, Flowers C, Peltz CD, Sweet H, Maurer N, Kwon E-JG, Krol A, Yuan F, and Dewhirst MW (2006) Preferential extravasation and accumulation of liposomal vincristine in tumor comparing to normal tissue enhances antitumor activity. *Cancer Chemother Pharmacol* **58**:245–255.

Shangguan D, Cao ZC, Li Y, and Tan W (2007a) Aptamers evolved from cultured cancer cells reveal molecular differences of cancer cells in patient samples. *Clin Chem* **53**:1153–1155.

Shangguan D, Tang Z, Mallikaratchy P, Xiao Z, and Tan W (2007b) Optimization and modifications of aptamers selected from live cancer cell lines. *ChemBioChem* **8**: 603–606.

Shapiro WR, Posner JB, Ushio Y, Chemik NL, and Young DF (1977) Treatment of meningeal neoplasms. *Cancer Treat Rep* **61**:733–743.

Sharma A and Sharma US (1997) Liposomes in drug delivery: progress and limitations. *Int J Pharm* **154**:123–140.

Shaw DJ and Costello B(1993) *Introduction to colloid and surface chemistry: Butterworth-Heinemann*, Elsevier, Oxford.

Shenoy D, Little S, Langer R, and Amiji M (2005a) Poly(ethylene oxide)-modified poly(β-amino ester) nanoparticles as a pH-sensitive system for tumor-targeted delivery of hydrophobic drugs. 1. In vitro evaluations. *Mol Pharm* **2**:357–366.

Shenoy D, Little S, Langer R, and Amiji M (2005b) Poly(ethylene oxide)-modified poly(β-amino ester) nanoparticles as a pH-sensitive system for tumor-targeted delivery of hydrophobic drugs: part 2. In vivo distribution and tumor localization studies. *Pharm Res* **22**:2107–2114.

Shenoy DB and Amiji MM (2005) Poly(ethylene oxide)-modified poly(ε-caprolactone) nanoparticles for targeted delivery of tamoxifen in breast cancer. *Int J Pharm* **293**: 261–270.

Shi G, Guo W, Stephenson SM, and Lee RJ (2002) Efficient intracellular drug and gene delivery using folate receptor-targeted pH-sensitive liposomes composed of cationic/anionic lipid combinations. *J Control Release* **80**:309–319.

Shi J, Xiao Z, Votruba AR, Vilos C, and Farokhzad OC (2011) Differentially charged hollow core/shell lipid-polymer-lipid hybrid nanoparticles for small interfering RNA delivery. *Angew Chem Int Ed Engl* **50**:7027–7031.

Shinohara H, Fan D, Ozawa S, Yano S, Van Arsdell M, Viner JL, Beers R, Pastan I, and Fidler IJ (2000) Site-specific expression of transferrin receptor by human colon cancer cells directly correlates with eradication by antitransferrin recombinant immunotoxin. *Int J Oncol* **17**:643–651.

Shmeeda H, Mak L, Tzemach D, Astrahan P, Tarshish M, and Gabizon A (2006) Intracellular uptake and intracavitary targeting of folate-conjugated liposomes in a mouse lymphoma model with up-regulated folate receptors. *Mol Cancer Ther* **5**: 818–824.

Shmeeda H, Tzemach D, Mak L, and Gabizon A (2009) Her2-targeted pegylated liposomal doxorubicin: retention of target-specific binding and cytotoxicity after in vivo passage. *J Control Release* **136**:155–160.

Siekmann B and Westesen K (1994) Thermoanalysis of the recrystallization process of melt-homogenized glyceride nanoparticles. *Colloids Surf B Biointerfaces* **3**: 159–175.

Siekmann B and Westesen K (1996) Investigations on solid lipid nanoparticles prepared by precipitation in o/w emulsions. *Eur J Pharm Biopharm* **42**: 104–109.

Silverman L and Barenholz Y (2015) In vitro experiments showing enhanced release of doxorubicin from Doxil® in the presence of ammonia may explain drug release at tumor site. *Nanomedicine (Lond)* **11**:1841–1850.

Silverman JA and Deitcher SR (2013) Marqibo® (vincristine sulfate liposome injection) improves the pharmacokinetics and pharmacodynamics of vincristine. *Cancer Chemother Pharmacol* **71**:555–564.

Simard P and Leroux J-C (2010) In vivo evaluation of pH-sensitive polymer-based immunoliposomes targeting the CD33 antigen. *Mol Pharm* **7**:1098–1107.

Simionescu M, Simionescu N, Santoro F, and Palade GE (1985) Differentiated microdomains of the luminal plasmalemma of murine muscle capillaries: segmental variations in young and old animals. *J Cell Biol* **100**:1396–1407.

Simionescu M, Simionescu N, Silbert JE, and Palade GE (1981) Differentiated microdomains on the luminal surface of the capillary endothelium. II. Partial characterization of their anionic sites. *J Cell Biol* **90**:614–621.

Simões S, Slepushkin V, Düzgünes N, and Pedroso de Lima MC (2001) On the mechanisms of internalization and intracellular delivery mediated by pH-sensitive liposomes. *Biochim Biophys Acta* **1515**:23–37.

Sjostrom B and Bergenstahl B (1992) Preparation of submicron drug particles in lecithin-stabilized o/w emulsions I. Model studies of the precipitation of cholesteryl acetate. *Int J Pharm* **88**:53–62.

Sjostrom B, Westesen K, and Bergenstahl B (1993) Preparation of submicron drug particles in lecithin-stabilized o/w emulsions: II. Characterization of cholesteryl acetate particles. *Int J Pharm* **94**:89–101.

Skeel RT and Khleif SN (2011) *Handbook of Cancer Chemotherapy*, 8th ed, Lippincott Williams & Wilkins, Philadelphia.

Slepushkin VA, Simões S, Dazin P, Newman MS, Guo LS, Pedroso de Lima MC, and Düzgüneş N (1997) Sterically stabilized pH-sensitive liposomes. Intracellular delivery of aqueous contents and prolonged circulation in vivo. *J Biol Chem* **272**: 2382–2388.

Slingerland M, Guchelaar H-J, and Gelderblom H (2012) Liposomal drug formulations in cancer therapy: 15 years along the road. *Drug Discov Today* **17**:160–166.

Slingerland M, Guchelaar HJ, Rosing H, Scheulen ME, van Warmerdam LJ, Beijnen JH, and Gelderblom H (2013) Bioequivalence of Liposome-Entrapped Paclitaxel Easy-To-Use (LEP-ETU) formulation and paclitaxel in polyethoxylated castor oil: a randomized, two-period crossover study in patients with advanced cancer. *Clin Ther* **35**:1946–1954.

Smith A (1986) Evaluation of poly (lactic acid) as a biodegradable drug delivery system for parenteral administration. *Int J Pharm* **30**:215–220.

Smith JA, Costales AB, Jaffari M, Urbauer DL, Frumovitz M, Kutac CK, Tran H, and Coleman RL (2015) Is it equivalent? Evaluation of the clinical activity of single agent Lipodox® compared to single agent Doxil® in ovarian cancer treatment. *J Oncol Pharm Pract*, in press.

Smith JA, Mathew L, Burney M, Nyshadham P, and Coleman RL (2016) Equivalency challenge: Evaluation of Lipodox® as the generic equivalent for Doxil® in a human ovarian cancer orthotropic mouse model. *Gynecol Oncol* **141**:357–363.

Solomon R and Gabizon AA (2008) Clinical pharmacology of liposomal anthracyclines: focus on pegylated liposomal Doxorubicin. *Clin Lymphoma Myeloma* **8**: 21–32.

Soni V, Kohli DV, and Jain SK (2005) Transferrin coupled liposomes as drug delivery carriers for brain targeting of 5-florouracil. *J Drug Target* **13**:245–250.

Souto E, Almeida A, and Muller R (2007) Lipid nanoparticles (SLN®, NLC®) for cutaneous drug delivery: structure, protection and skin effects. *J Biomed Nanotechnol* **3**:317–331.

Souza LG, Silva EJ, Martins AL, Mota MF, Braga RC, Lima EM, Valadares MC, Taveira SF, and Marreto RN (2011) Development of topotecan loaded lipid nanoparticles for chemical stabilization and prolonged release. *Eur J Pharm Biopharm* **79**:189–196.

Sparano JA and Winer EP (2001) Liposomal anthracyclines for breast cancer. *Semin Oncol* **28**(4, Suppl 12)32–40.

Srinivas PR, Barker P, and Srivastava S (2002) Nanotechnology in early detection of cancer. *Lab Invest* **82**:657–662.

Staruch R, Chopra R, and Hynynen K (2012) Hyperthermia in bone generated with MR imaging-controlled focused ultrasound: control strategies and drug delivery. *Radiology* **263**:117–127.

Stathopoulos GP, Antoniou D, Dimitroulis J, Michalopoulou P, Bastas A, Marosis K, Stathopoulos J, Provata A, Yiamboudakis P, and Veldekis D, et al. (2010) Liposomal cisplatin combined with paclitaxel versus cisplatin and paclitaxel in non-small-cell lung cancer: a randomized phase III multicenter trial. *Ann Oncol* **21**: 2227–2232.

Stathopoulos GP, Boulikas T, Kourvetaris A, and Stathopoulos J (2006) Liposomal oxaliplatin in the treatment of advanced cancer: a phase I study. *Anticancer Res* **26** (2B):1489–1493.

Stecová J, Mehnert W, Blaschke T, Kleuser B, Sivaramakrishnan R, Zouboulis CC, Seltmann H, Korting HC, Kramer KD, and Schäfer-Korting M (2007) Cyproterone acetate loading to lipid nanoparticles for topical acne treatment: particle characterisation and skin uptake. *Pharm Res* **24**:991–1000.

Stevens PJ, Sekido M, and Lee RJ (2004) A folate receptor-targeted lipid nanoparticle formulation for a lipophilic paclitaxel prodrug. *Pharm Res* **21**:2153–2157.

Straubinger RM, Hong K, Friend DS, and Papahadjopoulos D (1983) Endocytosis of liposomes and intracellular fate of encapsulated molecules: encounter with a low pH compartment after internalization in coated vesicles. *Cell* **32**:1069–1079.

Strieth S, Eichhorn ME, Sauer B, Schulze B, Teifel M, Michaelis U, and Dellian M (2004) Neovascular targeting chemotherapy: encapsulation of paclitaxel in cationic liposomes impairs functional tumor microvasculature. *Int J Cancer* **110**:117–124.

Su X, Fricke J, Kavanagh DG, and Irvine DJ (2011) In vitro and in vivo mRNA delivery using lipid-enveloped pH-responsive polymer nanoparticles. *Mol Pharm* **8**: 774–787.

Sudimack JJ, Guo W, Tjarks W, and Lee RJ (2002) A novel pH-sensitive liposome formulation containing oleyl alcohol. *Biochim Biophys Acta* **1564**:31–37.

Surapaneni MS, Das SK, and Das NG (2012) Designing Paclitaxel drug delivery systems aimed at improved patient outcomes: current status and challenges. *ISRN Pharmacol* **2012**:623139.

Surewicz WK, Epand RM, Pownall HJ, and Hui SW (1986) Human apolipoprotein A-I forms thermally stable complexes with anionic but not with zwitterionic phospholipids. *J Biol Chem* **261**:16191–16197.

Suzuki R, Takizawa T, Kuwata Y, Mutoh M, Ishiguro N, Utoguchi N, Shinohara A, Eriguchi M, Yanagie H, and Maruyama K (2008) Effective anti-tumor activity of oxaliplatin encapsulated in transferrin-PEG-liposome. *Int J Pharm* **346**:143–150.

Swenson C, Perkins W, Roberts P, and Janoff A (2001) Liposome technology and the development of Myocet (liposomal doxorubicin citrate). *Breast* **10**:1–7.

Szebeni J (1998) The interaction of liposomes with the complement system. *Crit Rev Ther Drug Carrier Syst* **15**:57–88.

Szebeni J (2001) Complement activation-related pseudoallergy caused by liposomes, micellar carriers of intravenous drugs, and radiocontrast agents. *Crit Rev Ther Drug Carrier Syst* **18**:567–606.

Szebeni J (2005) Complement activation-related pseudoallergy: a new class of drug-induced acute immune toxicity. *Toxicology* **216**:106–121.

Szebeni J and Alving CR (1999) Complement-mediated acute effects of liposome-encapsulated hemoglobin. *Artif Cells Blood Substit Immobil Biotechnol* **27**:23–41.

Szebeni J, Alving CR, Rosivall L, Bünger R, Baranyi L, Bedöcs P, Tóth M, and Barenholz Y (2007) Animal models of complement-mediated hypersensitivity reactions to liposomes and other lipid-based nanoparticles. *J Liposome Res* **17**: 107–117.

Szebeni J, Alving CR, Savay S, Barenholz Y, Priev A, Danino D, and Talmon Y (2001) Formation of complement-activating particles in aqueous solutions of Taxol: possible role in hypersensitivity reactions. *Int Immunopharmacol* **1**:721–735.
Szebeni J, Baranyi L, Savay S, Bodo M, Morse DS, Basta M, Stahl GL, Bünger R, and Alving CR (2000) Liposome-induced pulmonary hypertension: properties and mechanism of a complement-mediated pseudoallergic reaction. *Am J Physiol Heart Circ Physiol* **279**:H1319–H1328.
Szebeni J, Baranyi L, Savay S, Milosevits J, Bodo M, Bunger R, and Alving CR (2003) The interaction of liposomes with the complement system: in vitro and in vivo assays. *Methods Enzymol* **373**:136–154.
Szebeni J, Baranyi L, Savay S, Milosevits J, Bunger R, Laverman P, Metselaar JM, Storm G, Chanan-Khan A, and Liebes L, et al. (2002) Role of complement activation in hypersensitivity reactions to doxil and hynic PEG liposomes: experimental and clinical studies. *J Liposome Res* **12**:165–172.
Szebeni J, Fontana JL, Wassef NM, Mongan PD, Morse DS, Dobbins DE, Stahl GL, Bünger R, and Alving CR (1999) Hemodynamic changes induced by liposomes and liposome-encapsulated hemoglobin in pigs: a model for pseudoallergic cardiopulmonary reactions to liposomes. Role of complement and inhibition by soluble CR1 and anti-C5a antibody. *Circulation* **99**:2302–2309.
Szebeni J, Muggia FM, and Alving CR (1998) Complement activation by Cremophor EL as a possible contributor to hypersensitivity to paclitaxel: an in vitro study. *J Natl Cancer Inst* **90**:300–306.
Szebeni J, Muggia F, Gabizon A, and Barenholz Y (2011) Activation of complement by therapeutic liposomes and other lipid excipient-based therapeutic products: prediction and prevention. *Adv Drug Deliv Rev* **63**:1020–1030.
Szebeni J, Wassef NM, Spielberg H, Rudolph AS, and Alving CR (1994) Complement activation in rats by liposomes and liposome-encapsulated hemoglobin: evidence for anti-lipid antibodies and alternative pathway activation. *Biochem Biophys Res Commun* **205**:255–263.
Szleifer I (1997) Polymers and proteins: interactions at interfaces. *Curr Opin Solid State Mater Sci* **2**:337–344.
Szoka F Jr and Papahadjopoulos D (1978) Procedure for preparation of liposomes with large internal aqueous space and high capture by reverse-phase evaporation. *Proc Natl Acad Sci USA* **75**:4194–4198.
Tabatt K, Kneuer C, Sameti M, Olbrich C, Müller RH, Lehr C-M, and Bakowsky U (2004a) Transfection with different colloidal systems: comparison of solid lipid nanoparticles and liposomes. *J Control Release* **97**:321–332.
Tabatt K, Sameti M, Olbrich C, Müller RH, and Lehr C-M (2004b) Effect of cationic lipid and matrix lipid composition on solid lipid nanoparticle-mediated gene transfer. *Eur J Pharm Biopharm* **57**:155–162.
Tabernero J, Shapiro GI, LoRusso PM, Cervantes A, Schwartz GK, Weiss GJ, Paz-Ares L, Cho DC, Infante JR, and Alsina M, et al. (2013) First-in-humans trial of an RNA interference therapeutic targeting VEGF and KSP in cancer patients with liver involvement. *Cancer Discov* **3**:406–417.
Tagami T, Nakamura K, Shimizu T, Ishida T, and Kiwada H (2009) Effect of siRNA in PEG-coated siRNA-lipoplex on anti-PEG IgM production. *J Control Release* **137**: 234–240.
Takeuchi H, Yamamoto H, Niwa T, Hino T, and Kawashima Y (1996) Enteral absorption of insulin in rats from mucoadhesive chitosan-coated liposomes. *Pharm Res* **13**:896–901.
Takeuchi Y, Ichikawa K, Yonezawa S, Kurohane K, Koishi T, Nango M, Namba Y, and Oku N (2004) Intracellular target for photosensitization in cancer anti-angiogenic photodynamic therapy mediated by polycation liposome. *J Control Release* **97**:231–240.
Takimoto CH and Calvo E (2008) Principles of oncologic pharmacotherapy, in *Cancer Management: A Multidisciplinary Approach* (Pazdur R, Camphausen K, Hoskins WJ, and Wagma LD ed) CMP Health Care Media, New York.
Tam YY, Chen S, and Cullis PR (2013) Advances in lipid nanoparticles for siRNA delivery. *Pharmaceutics* **5**:498–507.
Tardi P, Choice E, Masin D, Redelmeier T, Bally M, and Madden TD (2000) Liposomal encapsulation of topotecan enhances anticancer efficacy in murine and human xenograft models. *Cancer Res* **60**:3389–3393.
Tayebi L, Vashaee D, and Parikh AN (2012) Stability of uni- and multillamellar spherical vesicles. *ChemPhysChem* **13**:314–322.
Theodore WH and Gendelman S (1981) Meningeal carcinomatosis. *Arch Neurol* **38**: 696–699.
Thevenot J, Troutier A-L, David L, Delair T, and Ladavière C (2007) Steric stabilization of lipid/polymer particle assemblies by poly(ethylene glycol)-lipids. *Biomacromolecules* **8**:3651–3660.
Thigpen JT, Aghajanian CA, Alberts DS, Campos SM, Gordon AN, Markman M, McMeekin DS, Monk BJ, and Rose PG (2005) Role of pegylated liposomal doxorubicin in ovarian cancer. *Gynecol Oncol* **96**:10–18.
Thomas DA, Kantarjian HM, Stock W, Heffner LT, Faderl S, Garcia-Manero G, Ferrajoli A, Wierda W, Pierce S, and Lu B, et al. (2009) Phase 1 multicenter study of vincristine sulfate liposomes injection and dexamethasone in adults with relapsed or refractory acute lymphoblastic leukemia. *Cancer* **115**:5490–5498.
Thomas DA, Sarris AH, Cortes J, Faderl S, O'Brien S, Giles FJ, Garcia-Manero G, Rodriguez MA, Cabanillas F, and Kantarjian H (2006) Phase II study of sphingosomal vincristine in patients with recurrent or refractory adult acute lymphocytic leukemia. *Cancer* **106**:120–127.
Thurston G, McLean JW, Rizen M, Baluk P, Haskell A, Murphy TJ, Hanahan D, and McDonald DM (1998) Cationic liposomes target angiogenic endothelial cells in tumors and chronic inflammation in mice. *J Clin Invest* **101**:1401–1413.
Torchilin VP (2000) Drug targeting. *Eur J Pharm Sci* **11** (Suppl 2):S81–S91.
Torchilin VP (2001) Structure and design of polymeric surfactant-based drug delivery systems. *J Control Release* **73**:137–172.
Torchilin VP (2005) Recent advances with liposomes as pharmaceutical carriers. *Nat Rev Drug Discov* **4**:145–160.
Torchilin VP (2007a) Micellar nanocarriers: pharmaceutical perspectives. *Pharm Res* **24**:1–16.
Torchilin VP (2007b) Targeted pharmaceutical nanocarriers for cancer therapy and imaging. *AAPS J* **9**:E128–E147.
Torchilin VP, Lukyanov AN, Gao Z, and Papahadjopoulos-Sternberg B (2003) Immunomicelles: targeted pharmaceutical carriers for poorly soluble drugs. *Proc Natl Acad Sci USA* **100**:6039–6044.
Torchilin VP, Omelyanenko VG, Papisov MI, Bogdanov AA Jr, Trubetskoy VS, Herron JN, and Gentry CA (1994) Poly(ethylene glycol) on the liposome surface: on the mechanism of polymer-coated liposome longevity. *Biochim Biophys Acta* **1195**: 11–20.
Torchilin VP and Trubetskoy VS (1995) Which polymers can make nanoparticulate drug carriers long-circulating? *Adv Drug Deliv Rev* **16**:141–155.
Torchilin VP, Zhou F, and Huang L (1993) pH-sensitive liposomes. *J Liposome Res* **3**: 201–255.
Trinder D, Zak O, and Aisen P (1996) Transferrin receptor-independent uptake of differic transferrin by human hepatoma cells with antisense inhibition of receptor expression. *Hepatology* **23**:1512–1520.
Tripathy N, Ahmad R, Ko HA, Khang G, and Hahn Y-B (2015) Enhanced anticancer potency using an acid-responsive ZnO-incorporated liposomal drug-delivery system. *Nanoscale* **7**:4088–4096.
Troutier A-L, Delair T, Pichot C, and Ladavière C (2005) Physicochemical and interfacial investigation of lipid/polymer particle assemblies. *Langmuir* **21**: 1305–1313.
Tsou KC, Lo KW, Ledis SL, and Miller EE (1972) Indigogenic phosphodiesters as potential chromogenic cancer chemotherapeutic agents. *J Med Chem* **15**:1221–1225.
Turek JJ, Leamon CP, and Low PS (1993) Endocytosis of folate-protein conjugates: ultrastructural localization in KB cells. *J Cell Sci* **106**:423–430.
Turner AF, Presant CA, Proffitt RT, Williams LE, Winsor DW, and Werner JL (1988) In-111-labeled liposomes: dosimetry and tumor depiction. *Radiology* **166**:761–765.
Tyrrell DA, Heath TD, Colley CM, and Ryman BE (1976) New aspects of liposomes. *Biochim Biophys Acta* **457**:259–302.
Uchiyama K, Nagayasu A, Yamagiwa Y, Nishida T, Harashima H, and Kiwada H (1995) Effects of the size and fluidity of liposomes on their accumulation in tumors: A presumption of their interaction with tumors. *Int J Pharm* **121**:195–203.
Ugazio E, Cavalli R, and Gasco MR (2002) Incorporation of cyclosporin A in solid lipid nanoparticles (SLN). *Int J Pharm* **241**:341–344.
Ulbrich K, Hekmatara T, Herbert E, and Kreuter J (2009) Transferrin- and transferrin-receptor-antibody-modified nanoparticles enable drug delivery across the blood-brain barrier (BBB). *Eur J Pharm Biopharm* **71**:251–256.
Vaage J, Donovan D, Uster P, and Working P (1997) Tumour uptake of doxorubicin in polyethylene glycol-coated liposomes and therapeutic effect against a xenografted human pancreatic carcinoma. *Br J Cancer* **75**:482–486.
Valencia PM, Basto PA, Zhang L, Rhee M, Langer R, Farokhzad OC, and Karnik R (2010) Single-step assembly of homogenous lipid-polymeric and lipid-quantum dot nanoparticles enabled by microfluidic rapid mixing. *ACS Nano* **4**:1671–1679.
van der Meel R, Vehmeijer LJ, Kok RJ, Storm G, and van Gaal EV (2013) Ligand-targeted particulate nanomedicines undergoing clinical evaluation: current status. *Adv Drug Deliv Rev* **65**:1284–1298.
van der Zee J, González González D, van Rhoon GC, van Dijk JD, van Putten WL, and Hart AA; Dutch Deep Hyperthermia Group (2000) Comparison of radiotherapy alone with radiotherapy plus hyperthermia in locally advanced pelvic tumours: a prospective, randomised, multicentre trial. *Lancet* **355**:1119–1125.
van Golen RF, van Gulik TM, and Heger M (2012) Mechanistic overview of reactive species-induced degradation of the endothelial glycocalyx during hepatic ischemia/reperfusion injury. *Free Radic Biol Med* **52**:1382–1402.
Van Leuven F, Cassiman J-J, and Van Den Berghe H (1980) Primary amines inhibit recycling of α 2M receptors in fibroblasts. *Cell* **20**:37–43.
van Sluis R, Bhujwalla ZM, Raghunand N, Ballesteros P, Alvarez J, Cerdán S, Galons J-P, and Gillies RJ (1999) In vivo imaging of extracellular pH using 1H MRSI. *Magn Reson Med* **41**:743–750.
van Vlerken LE, Duan Z, Seiden MV, and Amiji MM (2007) Modulation of intracellular ceramide using polymeric nanoparticles to overcome multidrug resistance in cancer. *Cancer Res* **67**:4843–4850.
Vandelli MA, Rivasi F, Guerra P, Forni F, and Arletti R (2001) Gelatin microspheres crosslinked with D,L-glyceraldehyde as a potential drug delivery system: preparation, characterisation, in vitro and in vivo studies. *Int J Pharm* **215**:175–184.
Vemuri S and Rhodes CT (1995) Preparation and characterization of liposomes as therapeutic delivery systems: a review. *Pharm Acta Helv* **70**:95–111.
Veronese FM (2001) Peptide and protein PEGylation: a review of problems and solutions. *Biomaterials* **22**:405–417.
Veronese FM and Pasut G (2005) PEGylation, successful approach to drug delivery. *Drug Discov Today* **10**:1451–1458.
Verschraegen CF, Kumagai S, Davidson R, Feig B, Mansfield P, Lee SJ, Maclean DS, Hu W, Khokhar AR, and Siddik ZH (2003) Phase I clinical and pharmacological study of intraperitoneal cis-bis-neodecanoato( trans- R, R-1, 2-diaminocyclohexane)-platinum II entrapped in multilamellar liposome vesicles. *J Cancer Res Clin Oncol* **129**:549–555.
Vertut-Doï A, Ishiwata H, and Miyajima K (1996) Binding and uptake of liposomes containing a poly(ethylene glycol) derivative of cholesterol (stealth liposomes) by the macrophage cell line J774: influence of PEG content and its molecular weight. *Biochim Biophys Acta* **1278**:19–28.
Vidal M and Hoekstra D (1995) In vitro fusion of reticulocyte endocytic vesicles with liposomes. *J Biol Chem* **270**:17823–17829.
Vihinen P, Ala-aho R, and Kähäri V-M (2005) Matrix metalloproteinases as therapeutic targets in cancer. *Curr Cancer Drug Targets* **5**:203–220.
Vijayagopal P, Figueroa JE, and Levine EA (1998) Altered composition and increased endothelial cell proliferative activity of proteoglycans isolated from breast carcinoma. *J Surg Oncol* **68**:250–254.
Vincent S, DePace D, and Finkelstein S (1988) Distribution of anionic sites on the capillary endothelium in an experimental brain tumor model. *Microcirc Endothelium Lymphatics* **4**:45–67.

Vonarbourg A, Passirani C, Saulnier P, and Benoit J-P (2006) Parameters influencing the stealthiness of colloidal drug delivery systems. *Biomaterials* **27**: 4356–4373.
Wacker M (2013) Nanocarriers for intravenous injection–the long hard road to the market. *Int J Pharm* **457**:50–62.
Wall ME and Wani MC (1995) Camptothecin and taxol: discovery to clinic–thirteenth Bruce F. Cain Memorial Award Lecture. *Cancer Res* **55**:753–760.
Wang AZ, Yuet K, Zhang L, Gu FX, Huynh-Le M, Radovic-Moreno AF, Kantoff PW, Bander NH, Langer R, and Farokhzad OC (2010a) ChemoRad nanoparticles: a novel multifunctional nanoparticle platform for targeted delivery of concurrent chemoradiation. *Nanomedicine (Lond)* **5**:361–368.
Wang J, Byrne JD, Napier ME, and DeSimone JM (2011) More effective nanomedicines through particle design. *Small* **7**:1919–1931.
Wang L, Geng D, and Su H (2014) Safe and efficient pH sensitive tumor targeting modified liposomes with minimal cytotoxicity. *Colloids Surf B Biointerfaces* **123**: 395–402.
Wang X, Ishida T, and Kiwada H (2007a) Anti-PEG IgM elicited by injection of liposomes is involved in the enhanced blood clearance of a subsequent dose of PEGylated liposomes. *J Control Release* **119**:236–244.
Wang J, Mongayt D, and Torchilin VP (2005) Polymeric micelles for delivery of poorly soluble drugs: preparation and anticancer activity in vitro of paclitaxel incorporated into mixed micelles based on poly(ethylene glycol)-lipid conjugate and positively charged lipids. *J Drug Target* **13**:73–80.
Wang MD, Shin DM, Simons JW, and Nie S (2007b) Nanotechnology for targeted cancer therapy. *Expert Rev Anticancer Ther* **7**:833–837.
Wang J-X, Sun X, and Zhang Z-R (2002) Enhanced brain targeting by synthesis of 3′,5′-dioctanoyl-5-fluoro-2′-deoxyuridine and incorporation into solid lipid nanoparticles. *Eur J Pharm Biopharm* **54**:285–290.
Wang M and Thanou M (2010) Targeting nanoparticles to cancer. *Pharmacol Res* **62**: 90–99.
Wang H, Zhao P, Su W, Wang S, Liao Z, Niu R, and Chang J (2010b) PLGA/polymeric liposome for targeted drug and gene co-delivery. *Biomaterials* **31**: 8741–8748.
Warburg O (1956a) On respiratory impairment in cancer cells. *Science* **124**:269–270.
Warburg O (1956b) On the origin of cancer cells. *Science* **123**:309–314.
Wassef NM and Alving CR (1993) Complement-dependent phagocytosis of liposomes. *Chem Phys Lipids* **64**:239–248.
Waterhouse DN, Madden TD, Cullis PR, Bally MB, Mayer LD, and Webb MS (2005) Preparation, characterization, and biological analysis of liposomal formulations of vincristine. *Methods Enzymol* **391**:40–57.
Webb MS, Harasym TO, Masin D, Bally MB, and Mayer LD (1995) Sphingomyelin-cholesterol liposomes significantly enhance the pharmacokinetic and therapeutic properties of vincristine in murine and human tumour models. *Br J Cancer* **72**: 896–904.
Webb MS, Logan P, Kanter PM, St-Onge G, Gelmon K, Harasym T, Mayer LD, and Bally MB (1998) Preclinical pharmacology, toxicology and efficacy of sphingomyelin/cholesterol liposomal vincristine for therapeutic treatment of cancer. *Cancer Chemother Pharmacol* **42**:461–470.
Weijer R, Broekgaarden M, Kos M, van Vught R, Rauws EA, Breukink E, van Gulik TM, Storm G, and Heger M (2015) Enhancing photodynamic therapy of refractory solid cancers: combining second-generation photosensitizers with multi-targeted liposomal delivery. *J Photochem Photobiol Chem* **23**:103–131.
Weiss RB (1992) The anthracyclines: will we ever find a better doxorubicin? *Semin Oncol* **19**:670–686.
Weissig V, Whiteman KR, and Torchilin VP (1998) Accumulation of protein-loaded long-circulating micelles and liposomes in subcutaneous Lewis lung carcinoma in mice. *Pharm Res* **15**:1552–1556.
Westesen K, Bunjes H, and Koch M (1997) Physicochemical characterization of lipid nanoparticles and evaluation of their drug loading capacity and sustained release potential. *J Control Release* **48**:223–236.
Westesen K, Siekmann B, and Koch MH (1993) Investigations on the physical state of lipid nanoparticles by synchrotron radiation X-ray diffraction. *Int J Pharm* **93**: 189–199.
Wicki A, Witzigmann D, Balasubramanian V, and Huwyler J (2015) Nanomedicine in cancer therapy: challenges, opportunities, and clinical applications. *J Control Release* **200**:138–157.
Williams LE, Duda RB, Proffitt RT, Beatty BG, Beatty JD, Wong JY, Shively JE, and Paxton RJ (1988) Tumor uptake as a function of tumor mass: a mathematic model. *J Nucl Med* **29**:103–109.
Williams KJ, Phillips MC, and Rodrigueza WV (1998) Structural and metabolic consequences of liposome-lipoprotein interactions. *Adv Drug Deliv Rev* **32**:31–43.
Wilschut J and Hoekstra D (1986) Membrane fusion: lipid vesicles as a model system. *Chem Phys Lipids* **40**:145–166.
Wilson JJ and Lippard SJ (2012) In vitro anticancer activity of cis-diammineplatinum(II) complexes with β-diketonate leaving group ligands. *J Med Chem* **55**:5326–5336.
Wirth M, Fuchs A, Wolf M, Ertl B, and Gabor F (1998) Lectin-mediated drug targeting: preparation, binding characteristics, and antiproliferative activity of wheat germ agglutinin conjugated doxorubicin on Caco-2 cells. *Pharm Res* **15**: 1031–1037.
Wisse E, Jacobs F, Topal B, Frederik P, and De Geest B (2008) The size of endothelial fenestrae in human liver sinusoids: implications for hepatocyte-directed gene transfer. *Gene Ther* **15**:1193–1199.
Wissing SA, Kayser O, and Müller RH (2004) Solid lipid nanoparticles for parenteral drug delivery. *Adv Drug Deliv Rev* **56**:1257–1272.
Witton CJ, Reeves JR, Going JJ, Cooke TG, and Bartlett JM (2003) Expression of the HER1-4 family of receptor tyrosine kinases in breast cancer. *J Pathol* **200**:290–297.
Wong HL, Bendayan R, Rauth AM, Li Y, and Wu XY (2007) Chemotherapy with anticancer drugs encapsulated in solid lipid nanoparticles. *Adv Drug Deliv Rev* **59**: 491–504.
Wong HL, Bendayan R, Rauth AM, and Wu XY (2004) Development of solid lipid nanoparticles containing ionically complexed chemotherapeutic drugs and chemosensitizers. *J Pharm Sci* **93**:1993–2008.
Wong HL, Bendayan R, Rauth AM, Xue HY, Babakhanian K, and Wu XY (2006) A mechanistic study of enhanced doxorubicin uptake and retention in multidrug resistant breast cancer cells using a polymer-lipid hybrid nanoparticle system. *J Pharmacol Exp Ther* **317**:1372–1381.
Wood BJ, Poon RT, Locklin JK, Dreher MR, Ng KK, Eugeni M, Seidel G, Dromi S, Neeman Z, and Kolf M, et al. (2012) Phase I study of heat-deployed liposomal doxorubicin during radiofrequency ablation for hepatic malignancies. *J Vasc Interv Radiol* **23**:248–55.e7.
Woodle MC (1995) Sterically stabilized liposome therapeutics. *Adv Drug Deliv Rev* **16**:249–265.
Woodle MC (1998) Controlling liposome blood clearance by surface-grafted polymers. *Adv Drug Deliv Rev* **32**:139–152.
Working P, Newman M, Huang S, Mayhew E, Vaage J, and Lasic D (1994) Pharmacokinetics, biodistribution and therapeutic efficacy of doxorubicin encapsulated in Stealth® liposomes (Doxil®). *J Liposome Res* **4**:667–687.
Wrobel I and Collins D (1995) Fusion of cationic liposomes with mammalian cells occurs after endocytosis. *Biochim Biophys Acta* **1235**:296–304.
Wu NZ, Klitzman B, Rosner G, Needham D, and Dewhirst MW (1993) Measurement of material extravasation in microvascular networks using fluorescence video-microscopy. *Microvasc Res* **46**:231–253.
Wu S-C, Yu C-H, Lin C-W, and Chu I-M (2003) The domain III fragment of Japanese encephalitis virus envelope protein: mouse immunogenicity and liposome adjuvanticity. *Vaccine* **21**:2516–2522.
Xing H, Tang L, Yang X, Hwang K, Wang W, Yin Q, Wong NY, Dobrucki LW, Yasui N, and Katzenellenbogen JA, et al. (2013) Selective delivery of an anticancer drug with aptamer-functionalized liposomes to breast cancer cells in vitro and in vivo. *J Mater Chem B Mater Biol Med* **1**:5288–5297.
Xu L, Huang CC, Huang W, Tang WH, Rait A, Yin YZ, Cruz I, Xiang LM, Pirollo KF, and Chang EH (2002) Systemic tumor-targeted gene delivery by anti-transferrin receptor scFv-immunoliposomes. *Mol Cancer Ther* **1**:337–346.
Xu L, Tang WH, Huang CC, Alexander W, Xiang LM, Pirollo KF, Rait A, and Chang EH (2001) Systemic p53 gene therapy of cancer with immunolipoplexes targeted by anti-transferrin receptor scFv. *Mol Med* **7**:723–734.
Yadav DK and Khan F (2013) QSAR, docking and ADMET studies of camptothecin derivatives as inhibitors of DNA topoisomerase-I. *J Chemometr* **27**:21–33.
Yamada Y, Itano N, Narimatsu H, Kudo T, Hirohashi S, Ochiai A, Niimi A, Ueda M, and Kimata K (1999) Receptor for hyaluronan-mediated motility and CD44 expressions in colon cancer assessed by quantitative analysis using real-time reverse transcriptase-polymerase chain reaction. *Jpn J Cancer Res* **90**:987–992.
Yan Z, Zhu ZL, Qian ZZ, Hu G, Wang HQ, Liu WH, and Cheng G (2012) Pharmacokinetic characteristics of vincristine sulfate liposomes in patients with advanced solid tumors. *Acta Pharmacol Sin* **33**:852–858.
Yang X-Z, Dou S, Wang Y-C, Long H-Y, Xiong M-H, Mao C-Q, Yao Y-D, and Wang J (2012a) Single-step assembly of cationic lipid-polymer hybrid nanoparticles for systemic delivery of siRNA. *ACS Nano* **6**:4955–4965.
Yang X-X, Hu Z-P, Xu A-L, Duan W, Zhu Y-Z, Huang M, Sheu F-S, Zhang Q, Bian J-S, and Chan E, et al. (2006) A mechanistic study on reduced toxicity of irinotecan by coadministered thalidomide, a tumor necrosis factor-α inhibitor. *J Pharmacol Exp Ther* **319**:82–104.
Yang L and Huang HW (2003) A rhombohedral phase of lipid containing a membrane fusion intermediate structure. *Biophys J* **84**:1808–1817.
Yang XY, Li YX, Li M, Zhang L, Feng LX, and Zhang N (2013) Hyaluronic acid-coated nanostructured lipid carriers for targeting paclitaxel to cancer. *Cancer Lett* **334**: 338–345.
Yang SH, Lin CC, Lin ZZ, Tseng YL, and Hong RL (2012b) A phase I and pharmacokinetic study of liposomal vinorelbine in patients with advanced solid tumor. *Invest New Drugs* **30**:282–289.
Yang SC, Lu LF, Cai Y, Zhu JB, Liang BW, and Yang CZ (1999) Body distribution in mice of intravenously injected camptothecin solid lipid nanoparticles and targeting effect on brain. *J Control Release* **59**:299–307.
Yang F, Teves SS, Kemp CJ, and Henikoff S (2014a) Doxorubicin, DNA torsion, and chromatin dynamics. *Biochim Biophys Acta* **1845**:84–89.
Yang G, Yang T, Zhang W, Lu M, Ma X, and Xiang G (2014b) In vitro and in vivo antitumor effects of folate-targeted ursolic acid stealth liposome. *J Agric Food Chem* **62**:2207–2215.
Yatvin MB, Mühlensiepen H, Porschen W, Weinstein JN, and Feinendegen LE (1981) Selective delivery of liposome-associated cis-dichlorodiammineplatinum(II) by heat and its influence on tumor drug uptake and growth. *Cancer Res* **41**:1602–1607.
Yatvin MB, Weinstein JN, Dennis WH, and Blumenthal R (1978) Design of liposomes for enhanced local release of drugs by hyperthermia. *Science* **202**:1290–1293.
Yoshimura T, Shono M, Imai K, and Hong K (1995) Kinetic analysis of endocytosis and intracellular fate of liposomes in single macrophages. *J Biochem* **117**:34–41.
Yuan F, Dellian M, Fukumura D, Leunig M, Berk DA, Torchilin VP, and Jain RK (1995) Vascular permeability in a human tumor xenograft: molecular size dependence and cutoff size. *Cancer Res* **55**:3752–3756.
Yuan F, Leunig M, Huang SK, Berk DA, Papahadjopoulos D, and Jain RK (1994) Microvascular permeability and interstitial penetration of sterically stabilized (stealth) liposomes in a human tumor xenograft. *Cancer Res* **54**:3352–3356.
Zalipsky S, Qazen M, Walker JA 2nd, Mullah N, Quinn YP, and Huang SK (1999) New detachable poly(ethylene glycol) conjugates: cysteine-cleavable lipopolymers regenerating natural phospholipid, diacyl phosphatidylethanolamine. *Bioconjug Chem* **10**:703–707.
Zara GP, Cavalli R, Bargoni A, Fundarò A, Vighetto D, and Gasco MR (2002) Intravenous administration to rabbits of non-stealth and stealth doxorubicin-loaded solid lipid nanoparticles at increasing concentrations of stealth agent: pharmacokinetics and distribution of doxorubicin in brain and other tissues. *J Drug Target* **10**:327–335.

Zara GP, Cavalli R, Fundarò A, Bargoni A, Caputo O, and Gasco MR (1999) Pharmacokinetics of doxorubicin incorporated in solid lipid nanospheres (SLN). *Pharmacol Res* **40**:281–286.

Zhang JA, Anyarambhatla G, Ma L, Ugwu S, Xuan T, Sardone T, and Ahmad I (2005) Development and characterization of a novel Cremophor EL free liposome-based paclitaxel (LEP-ETU) formulation. *Eur J Pharm Biopharm* **59**:177–187.

Zhang L, Chan JM, Gu FX, Rhee J-W, Wang AZ, Radovic-Moreno AF, Alexis F, Langer R, and Farokhzad OC (2008a) Self-assembled lipid–polymer hybrid nanoparticles: a robust drug delivery platform. *ACS Nano* **2**:1696–1702.

Zhang X, Gan Y, Gan L, Nie S, and Pan W (2008c) PEGylated nanostructured lipid carriers loaded with 10-hydroxycamptothecin: an efficient carrier with enhanced anti-tumour effects against lung cancer. *J Pharm Pharmacol* **60**:1077–1087.

Zhang X-G, Miao J, Dai Y-Q, Du Y-Z, Yuan H, and Hu F-Q (2008b) Reversal activity of nanostructured lipid carriers loading cytotoxic drug in multi-drug resistant cancer cells. *Int J Pharm* **361**:239–244.

Zhao P, Wang H, Yu M, Liao Z, Wang X, Zhang F, Ji W, Wu B, Han J, and Zhang H, et al. (2012) Paclitaxel loaded folic acid targeted nanoparticles of mixed lipid-shell and polymer-core: in vitro and in vivo evaluation. *Eur J Pharm Biopharm* **81**:248–256.

Zhelev DV (1998) Material property characteristics for lipid bilayers containing lysolipid. *Biophys J* **75**:321–330.

Zheng Y, Yu B, Weecharangsan W, Piao L, Darby M, Mao Y, Koynova R, Yang X, Li H, and Xu S, et al. (2010) Transferrin-conjugated lipid-coated PLGA nanoparticles for targeted delivery of aromatase inhibitor 7α-APTADD to breast cancer cells. *Int J Pharm* **390**:234–241.

Zhigaltsev IV, Maurer N, Akhong Q-F, Leone R, Leng E, Wang J, Semple SC, and Cullis PR (2005) Liposome-encapsulated vincristine, vinblastine and vinorelbine: a comparative study of drug loading and retention. *J Control Release* **104**: 103–111.

Zhong Q, Chinta DM, Pamujula S, Wang H, Yao X, Mandal TK, and Luftig RB (2010) Optimization of DNA delivery by three classes of hybrid nanoparticle/DNA complexes. *J Nanobiotechnology* **8**:6–15.

Zhu L, Kate P, and Torchilin VP (2012) Matrix metalloprotease 2-responsive multifunctional liposomal nanocarrier for enhanced tumor targeting. *ACS Nano* **6**: 3491–3498.

Zimm S, Collins JM, Miser J, Chatterji D, and Poplack DG (1984) Cytosine arabinoside cerebrospinal fluid kinetics. *Clin Pharmacol Ther* **35**: 826–830.

Zou Y, Ling Y-H, Reddy S, Priebe W, and Perez-Soler R (1995) Effect of vesicle size and lipid composition on the in vivo tumor selectivity and toxicity of the non-cross-resistant anthracycline annamycin incorporated in liposomes. *Int J Cancer* **61**:666–671.

Zou Y, Priebe W, Ling Y-H, and Perez-Soler R (1993) Organ distribution and tumor uptake of annamycin, a new anthracycline derivative with high affinity for lipid membranes, entrapped in multilamellar vesicles. *Cancer Chemother Pharmacol* **32**:190–196.

zur Mühlen A, Schwarz C, and Mehnert W (1998) Solid lipid nanoparticles (SLN) for controlled drug delivery–drug release and release mechanism. *Eur J Pharm Biopharm* **45**:149–155.